Comparative functional analysis of WOX genes during flower development in Petunia and Arabidopsis

Enrico Costanzo

THÈSE

en vue de l'obtention du grade de

Docteur de l'Université de Lyon, délivré par l'École Normale Supérieure de Lyon

En cotutelle avec la Scuola Superiore Sant'Anna, Pisa, ITALIE

Discipline : Sciences de la Vie

& Agrobiodiversity - Plant genetic resources

Laboratoire UMR 5667 Reproduction et Développement des Plantes

& Istituto di Scienze della Vita

École Doctorale 340 Biologie Moléculaire Intégrative et Cellulaire

présentée et soutenue publiquement le 5 novembre 2015

par Monsieur Enrico COSTANZO

Comparative functional analysis of *WOX* genes during flower development in Petunia and Arabidopsis

---

Directeur de thèse : M. Michiel VANDENBUSSCHE

Co-tuteur de thèse : M. Mario Enrico PÈ

Après l'avis de :

Mme Sophie NADOT

M. Martin KATER

Devant le jury composé de :

M. Olivier HAMANT, Institut National de la Recherche Agronomique, Examinateur

M. Martin KATER, Università degli Studi di Milano, Examinateur/Rapporteur

Mme Sophie NADOT, Université Paris XI (Paris-Sud), Examinateur/Rapporteur

M. Mario Enrico PÈ, Scuola Superiore Sant'Anna di Pisa, Co-tuteur

M. Michiel VANDENBUSSCHE, Centre National de la Recherche Scientifique, Directeur

In rebus quibuscumque difficilioribus non expectandum, ut quis simul, et serat, et metat, sed praeparatione opus est, ut per gradus maturescant.

Francis Bacon

Remerciements

Tout d'abord, many thanks to Mme Sophie Nadot and Professor Martin Kater, for accepting to review the manuscript and taking part in the PhD defence.

Many thanks to Michiel Vandenbussche, for the project illustrated in this book, and for the invaluable help with the manuscript.

Merci à Patrice Morel et Pierre Chambrier, pour leur support quotidien dans les « manips ».

Grazie al Prof. Mario Enrico Pè, cui devo la cotutela con la Scuola Superiore Sant'Anna. Grazie anche ad Edoardo Bertolini, per il supporto nell'analisi RNA-Seq.

Merci également à Jeremy Just (RNA-Seq) et Christophe Trehin, Aurélie Vialette, Amélie Robin, Charlie Scutt, Annick Dubois, Massimiliano Sassi, Roberta Galletti, Ursula Abad. Sempre in laboratorio, un grazie particolare a Alessia Armezzani (per le lunghe conversazioni).

From the "past", thanks to Kai Ament, Rita San-Bento, Benoit Landrein, and Naomi Nakayama.

Merci à tous les membres de l'équipe culture, dont Alexis Lacroix, pour avoir pris soins de plantes et, particularly for Petunias, many thanks to Suzanne Rodrigues Bento.

A special thanks to Gwyneth Ingram and Professor Ronald Koes, for taking part in the annual "thesis committees", and their help in pointing out the key issues of the experimental work.

Un grand merci à Olivier Hamant, tout d'abord pour avoir accepté de juger mon travail de thèse, ainsi que pour les précieux conseils et les discussions « anthropocéniques ».

Un merci tout particulier au Professeur Ioan Negrutiu ; je lui suis reconnaissant pour pas mal de choses, dont mon entrée au RDP.

Il dottorato, in fondo, è la conclusione di un percorso che inizia assai prima, nel 2007. La mia passione per la biologia vegetale la devo essenzialmente a due figure ispiratrici, i Prof. Pierdomenico Perata e Amedeo Alpi.

Grazie, infine, alla mia famiglia.

Résumé

Dans le domaine des plantes, la formation de la fleur a été un pas crucial dans la capacité des végétaux à coloniser une grande diversité de niches écologiques sur notre planète. Les deux espèces *Petunia* x *hybrida* et *Arabidopsis thaliana* représentent deux groupes majeurs des plantes à fleur. Nous avons montré que les gènes à homéodomaine d'une famille appelée WOX (Wuschel homeobOX) sont fortement impliqués dans le développement des organes dotés de polarité (dont les feuilles et des organes de la fleur : sépales, pétales, carpelles). Un double mutant (*maw mawb*), chez le Pétunia, développe des pétales en forme de filament, avec disparition du tube floral. De plus, nous avons découvert que ces mêmes gènes interagissent au niveau génétique avec d'autres gènes (appelés gènes à boite MADS) dans la formation des ovules, structures à partir desquelles les graines se forment. Nous avons aussi montré que des gènes de la même famille sont impliqués dans la formation d'autres structures chez le Pétunia : les trichomes ou poils aériens de surface. Ces derniers sont impliqués dans plusieurs taches, qui vont de la protection contre les pathogènes à celles contre les stress abiotiques. Grâce à des études de génétique fonctionnelle nous avons pu montrer un recrutement différentiel des gènes *WOX* ici étudiés, dépendant de l'organe et de l'espèce. Ces travaux de thèse montrent l'importance de cette famille génique pour les études d'evo-devo (Biologie Evolutionniste du Développement). Finalement, une analyse de RNA-Seq (séquençage du transcriptome), dévoile les réseaux génétiques contrôlés par ces gènes *WOX*.

Les deux espèces étudiées, *Petunia* x *hybrida* (nom commun : Pétunia) et *Arabidopsis thaliana* (nom commun : Arabette), représentent bien les deux groupes majeurs des eudicotylédones, auxquels ils appartiennent, respectivement les Asteridae et les Rosidae. A cela il faut ajouter que ces deux espèces montrent deux types d'architecture florale bien distincts : pétales fusionnés (avec formation d'un tube floral) pour le Pétunia, pétales séparés pour l'Arabette. La fusion des pétales représente une barrière pre-zygotique fondamentale dans la séparation entre espèces, du fait que une (seule) espèce de plante peut développer une relation monogamique avec une (seule) espèce de pollinisateur. Le pollinisateur aura une morphologie adaptée à celle de la fleur de l'espèce partenaire. Chez le Pétunia, il a été montré que mutations dans le gène *MAEWEST* (*MAW*) produisent des fleurs à pétales partiellement séparés (Vandenbussche et al. 2009). Cela est dû au fait que l'expansion latérale des pétales est affectée, empêchent leur fusionnement dans la coté distale. Ces défauts d'expansion latérale des organes ne sont pas limités aux pétales, mais ils s'étendent à tous les organes dotés de polarité, tels que les carpelles et les sépales dans la fleur, et aussi les feuilles. Ces observations suggèrent un rôle très large pour *MAW* dans le développement végétal, lié à la capacité de *MAW* de contrôler le développement médiolatéral des organes latéraux des plantes (tels que les feuilles, sépales, pétales, carpelles). *MAW* code pour un facteur de transcription à homéodomaine appartenant à la sous-famille MAW/WOX1 des gènes *WOX* (*Wuschel related homeobOX*), gènes spécifiques des végétaux. Dans la sous-famille MAW/WOX1, deux gènes sont répertoriés chez l'Arabette : *WOX1* et *WOX6*. Toutefois, ni les mutants simples *wox1* et *wox6*, ni le double *wox1 wox6* n'ont montré un phénotype altéré. Par contre, le mutant *wox1 prs* chez l'Arabette (Vandenbussche et al. 2009) montre un phénotype comparable à celui des mutant *maw* chez le Pétunia, à savoir que les pétales et les sépales sont très étroits. Cet observation est plutôt remarquable si on considère que le gène *PRS* (lui aussi un *WOX*), fait partie de la sous-famille WOX3/PRS : Les gènes *WOX3/PRS* n'ont pas la même structure génique que les

gènes de la sous-famille MAW/WOX1. Il faut remarquer que, si pétales et sépales sont sévèrement affectés chez les mutants *wox1 prs* d'Arabette, les carpelles, au contraire, gardent un phénotype sauvage, ce qui marque une différence avec le Pétunia. Ces observations suggèrent un recrutement différentiel des gènes *WOX* au cours du développement des végétaux.

Objectif

Dans ce projet, nous avons adopté à la fois une approche génétique et comparative pour comprendre les différentes relations fonctionnelles des gènes *WOX* entre le Pétunia et l'Arabette, et une approche moléculaire pour cadrer les fonctions géniques dans leurs réseaux géniques respectifs.

Résultats

Afin d'effectuer une analyse comparative des tous les membres des sous-familles MAW/WOX1 et PRS/WOX3 dans les deux espèces, nous avons analysé les fonctions des gènes *Ph-WOX3* et *Ph-WOX3B* (sous-famille PRS/WOX3), et un deuxième membre de la sous-famille MAW/WOX1, *Ph-MAWB*, chez le Pétunia. Nous avons obtenu les correspondants à partir de notre collection des lignées à transposons (collection basée sur le transposon *dTph1*) et nous avons analysé les mutants et combinaisons de mutants suivants : *mawb, maw mawb, wox3, wox3b, wox3 wox3b, maw mawb wox3 wox3b*.

Le mutant *mawb* montre un phénotype sauvage, alors que le double mutant *maw mawb* nous a révélé un phénotype très intéressant : pétales et sépales (mais aussi les feuilles) sont très étroits, ce qui amène à la disparition complète du tube floral. Les carpelles sont raccourcis et non fusionnés, par rapport au WT, avec production de carpelles surnuméraires. Nous avons pu montrer, avec analyse au microscope électronique à balayage (MEB), que ces carpelles surnuméraires dérivent très probablement de la transformation homéotique des ovules.

Une différence remarquable entre les rôles des gènes *MAW/WOX1* chez le Pétunia et chez l'Arabette, est représentée par le fait que chez le Pétunia les mutants *maw* et *maw mawb* sont affectés aussi au niveau des carpelles. A l'opposé, cela n'a pas été observé chez l'Arabette dans les mutants pour les gènes orthologues. Après analyse phénotypique et statistique sur différents mutants pour les gènes *WOX1* et *WOX6* (sous-famille MAW/WOX1), et *PRS* (sous-famille PRS/WOX3), le triple mutant *wox1 prs wox6* s'est révélé affecté au niveau du développement du stigma. Ce fait est donc dans la même direction que les précédents. Néanmoins, seulement un peu moins d'1/4 des fleurs chez les plantes *wox1 prs wox6* montre un phénotype au niveau du stigma. Il faut aussi remarquer que les ovaires et le style restent de phénotype sauvage, ce qui pourrait indiquer que, chez l'Arabette, d'autres gènes sont impliqués avec les *WOX* dans le fusionnement des carpelles au niveau du style et de l'ovaire.

Dans le modèle actuel du développement de la fleur, le développement des différents organes est régulé par des gènes appartenant à différentes classe (A, B, C et D), avec les gènes de classe C et D impliqués dans le développement des ovules. Chez le Pétunia, nous avons montré une interaction entre les gènes de la lignée D et les gènes *MAW/WOX1* avec la production de mutants multiple pour *FB7*, *FBP11*, *MAW* et *MAWB*. Dans ces mutants multiples, nous avons observé la transformation homéotique complète des ovules en carpelles. Ce phénotype est identique à celui des mutants pour les gènes *C* et de la lignée D déjà décrits en littérature (Heijmans et al. 2012a), ce qui suggère pour la première fois l'implication des gènes de la sous-famille WOX1 dans l'identité des ovules. Les mutants multiples obtenus ont été caractérisé au niveau phénotypique (MEB et photographie).

Nous avons aussi testé la capacité de *Ph-MAW* de restaurer le phénotype sauvage dans le mutant *wox1 prs* d'Arabette. Nous avons observé une restauration du phénotype presque complète, ce qui suggère la capacité de *Ph-MAW* d'agir au sein du même réseau de

régulation génique chez l'Arabette, que nous supposons être conservé entre les deux espèces.

Pour identifier les réseaux géniques affectés par la perte de la fonction WOX, ainsi que pour identifier les cibles directes de MAW/MAWB, nous avons adopté une approche transcriptomique. Plus précisément, une analyse RNA-Seq sur le WT, le mutant *maw* et le double mutant *maw mawb* a été effectuée en collaboration avec la Scuola Superiore Sant'Anna de Pise (Italie), dans le cadre de la cotutelle de thèse.

Le nombre des gènes différentiellement exprimés (DEGs) partagé par les trois différentes conditions testées (WT, *maw*, et *maw mawb*) est autour de 2.600. Parmi ces gènes, nous avons sélectionné uniquement les gènes avec un profil d'expression où le mutant *maw* montre clairement un niveau d'expression intermédiaire entre le WT et le double mutant. Nous avons identifié et annoté environ 550 DEGs présentent ces profils. Parmi ceux-ci, nous avons répertorié plusieurs gènes liés à l'auxine, ainsi que des gènes à homéodomaine. Cette analyse, en plus de donner un cadre général des réseaux génétiques contrôlés par MAW et MAWB, pourra permettre des cibler des candidats intéressants pour l'analyse fonctionnelle. Dans cette même démarche, la construction inductible *pMAW::GR-MAW* a été introduite dans le double mutant *maw mawb,* avec l'objectif d'identifier par analyse transcriptomique les cibles directes de MAW après induction de *pMAW::GR-MAW* par dexaméthasone.

Pour compléter l'analyse comparatives des sous-familles WOX1 et WOX3, nous avons analysé les double mutants *wox3 wox3b* de Pétunia, qui se sont révélés affectés au niveau de la production de trichomes, ce qui montre un rôle diffèrent pour les gènes *PRS/WOX3* chez le Pétunia par rapport à l'Arabette. Notamment, les plantes ont révélé un aspect plus glabre, comparés aux sauvages, particulièrement évident au niveau de la tige et sur la face adaxiale des feuilles et des bractées. Au contraire, le développement des trichomes au

niveau de la fleur semble être moins affecté. Ces observations ont été confirmées après caractérisation phénotypique et analyse au MEB. Pour supporter le lien entre le phénotype observé et la mutation dans *PRS* et *WOX3B* chez le Pétunia, nous avons exploité la susceptibilité de notre lignée à l'excision du transposon *dTph1*. Normalement, l'excision va créer une emprunte de 8 pb (« fantôme »). Il peut néanmoins arriver que la taille de cette trace soit différente. Si la taille est 3 pb ou un multiple de trois, le cadre de lecture est restauré. Si la mutation étudiée et le phénotype observé sont liés et le cadre de lecture est restauré, la plante peut potentiellement montrer un phénotype WT (donc, avec restauration du phénotype avec trichomes). Nous sommes en train d'étudier les patrons d'expression de *PRS* et *WOX3B* par hybridation *in situ*.

Publications issues des travaux de recherche

Article dans journal scientifique évalué par les pairs : Costanzo, E., Trehin, C. & Vandenbussche, M. *The role of* WOX *genes in flower development*. **Ann. Bot. (2014)**. doi:10.1093/aob/mcu123.

Présentation dans congrès scientifique : Costanzo, E., Morel, P., Vandenbussche, M. - *Role of WOX genes in Petunia Flower Architecture* - Presentation, 13th **World Petunia Days Congress, Nijmegen, The Netherlands** - September, 2013.

Posters dans congrès scientifiques :

Costanzo, E., Morel, P., Just, J., Bertolini, E., Pé, M.E, & Vandenbussche, M. *Lateral development of floral organs: Unraveling the role of* MAEWEST *and* MAEWESTB *in Petunia*. Poster, **Plant Organ growth Symposium, Ghent University, Belgium** – March 2015.

Costanzo, E., Morel, P., Bertolini, E., Pè, M.E, & Vandenbussche, M. *Petunia* MAEWEST *and* MAEWESTB *functionally overlap in promoting lateral development of floral organs*. **FISV Congress, Pisa, Italy** – September 2014.

Table of contents

REMERCIEMENTS 4

RÉSUMÉ 5

TABLE OF CONTENTS 13

I. INTRODUCTION 20

ANGIOSPERMS' STORY: WHY FLOWERS MATTER 20

Plant evo-devo 21

Fossil flowers, phylogeny and genes 22

The origin of carpels and hermaphrodite flowers 23

Leaf development: A snapshot 25

Petunia: The evolution of a model system 27

II. THE ROLE OF *WOX* GENES IN FLOWER DEVELOPMENT 33

WOX genes are HOMEOBOX genes 34

WOX genes play different roles in plant development 35

At-WUSCHEL is required for stem-cell maintenance in the flower (WUS lineage) 37

The PRS/WOX3 subfamily 42

The MAW/WOX1 subfamily 43

Functional overlap between MAW/WOX1 and PRS/WOX3 subfamilies 44

EVERGREEN in Petunia is involved in inflorescence architecture (WOX9 subfamily) 46

Evolution of WOX gene function: Primarily through changes in expression patterns? 50

WOX genes and Flower development: Concluding remarks 51

UPDATE 52

III. *MAW* AND *MAWB* ARE INVOLVED IN BLADE OUTGROWTH AND OVULE DEVELOPMENT IN PETUNIA **57**

ABSTRACT 57

INTRODUCTION 58

The role of the WOX1 subfamily in blade expansion *58*

Expanding the role of WOX genes in Petunia *59*

RESULTS 60

In silico genome screening for novel WOX genes identifies MAWB as a second member of the WOX1 subfamily in Petunia *60*

Expression pattern of MAWB *65*

mawb mutants display a WT phenotype *67*

MAWB is redundantly involved with MAEWEST in lateral organ development *67*

maw mawb mutants are affected in mediolateral polarity *72*

maw mawb mutants are affected in carpel and ovule development *75*

MAW and MAWB are involved in defining ovule identity along with D lineage genes *76*

DISCUSSION 79

Comparison between the WOX1 and WOX3 subfamilies *81*

Interplay between WOX1 and WOX3 subfamily members in Arabidopsis *81*

The WOX1 subfamily is involved in ovule development in Petunia *82*

ANNEX I: COMPARATIVE ANALYSIS OF *WOX1* GENES IN *ARABIDOPSIS THALIANA* 85

ABSTRACT 85

INTRODUCTION 85

At-WOX6 is involved with WOX1 and PRS in stigma development in Arabidopsis *86*

DISCUSSION 88

Differential roles of WOX1 and WOX3 subfamilies among Asteridae and Rosidae *88*

WOX1 genes only play a minor role in carpel development in Arabidopsis 89

ANNEX II: HETEROLOGOUS EXPRESSION OF *PH-MAW* ON A *WOX1 PRS* ARABIDOPSIS BACKGROUND 90

Ph-MAW partially rescues the mutant phenotype in wox1 prs flowers of Arabidopsis 90

MATERIALS AND METHODS 92

IV. DISSECTING THE MOLECULAR ROLE OF *MAW* AND *MAWB* BY RNA-SEQ ANALYSIS 99

SUMMARY 99

INTRODUCTION 100

RESULTS 102

Experimental set up 102

Two genomes for one analysis 103

DEGs quantification using Cuffdiff 105

Filtering RNA-Seq data 111

GO terms based annotation of transcripts 113

Expression profiles of transcription factors 114

Auxin-related genes are mainly downregulated in maw and maw mawb 117

Cell-proliferation genes are downregulated in maw and maw mawb 118

The miR156/SPL genetic module is progressively affected in maw and maw mawb 119

A method for MAW/MAWB direct targets discovery 123

DISCUSSION 124

General analysis of RNA-Seq data 126

Auxin plays an important role in maw and maw mawb phenotypes 126

Cell-proliferation genes are affected in maw and maw mawb 128

The miR156/SPL genetic module is affected in maw and maw mawb, and it likely accounts for supernumerary organs production *128*

PERSPECTIVES 129

RNA-Seq analysis *129*

Validation of RNA-Seq data *129*

Biological stories *129*

Implementation of a method for MAW/MAWB direct targets discovery *130*

MATERIALS AND METHODS 131

Aknowledgements *134*

V. THE TWO GENES *WOX3* AND *WOX3B* ARE INVOLVED IN TRICHOME DEVELOPMENT IN PETUNIA **138**

ABSTRACT 138

INTRODUCTION 139

RESULTS 144

The WOX3 subfamily is composed of two members in Petunia *144*

wox3 wox3b double mutants display a glabrous phenotype *148*

The glabrous phenotype co-segregate with mutations in WOX3 and WOX3B in the Mitchell background *150*

Phenotypic characterization of wild-type Petunia trichomes *150*

Further phenotypic comparison of WT and prs wox3b mutants *153*

Revertant analysis provides independent proof that trichome development is impaired because of mutations in WOX3 and WOX3B. *155*

The two subfamilies WOX1 and WOX3 are functionally independent in Petunia *161*

DISCUSSION 163

Evo-devo of WOX3 subfamily genes *165*

PERSPECTIVES 168

Investigating the gene regulatory network involved in trichome development in Asteridae *168*

MATERIALS AND METHODS 169

VI. CONCLUSIONS **170**

VII. MATERIALS AND METHODS **176**

Plant material and growth conditions *176*

DNA extraction (Edwards' method) *177*

Polymerase Chain Reactions (PCRs) *178*

Elchrom™ electrophoresis *180*

DNA extraction from agarose gels *181*

Competent cells transformation (heat-shock) *181*

Colony PCRs *181*

Plasmid extraction from bacterial cell cultures (miniprep) *182*

RNA extraction (TRIzol® method) *182*

cDNA synthesis *182*

Phusion® PCR (High-Fidelity) *183*

In situ hybridization *184*

Ph-MAW cloning and Arabidopsis transformation *188*

DEX inducible pMAW::GR-MAW Petunia line *188*

Statistical analysis of Arabidopsis carpels *192*

Statistical analysis of organ number in WT, maw, and maw mawb Petunia plants *194*

ANNEX III: PROTEIN ALIGNMENT OF WOX1 SEQUENCES 196

ANNEX IV: BIOINFORMATICS AND PHYLOGENETIC ANALYSIS 198

RNA-sequencing *200*

Library trimming *201*

Production of a transcriptome assembly for downstream analysis and primer design in P. × hybrida *205*

APPENDIX I 207

Chronostratigraphic Chart *207*

APPENDIX II 208

REFERENCES **211**

I. Introduction

Angiosperms' story: Why flowers matter

Flowering plants have always fascinated biologists and natural philosophers, even before the emergence of biology as a separate and defined discipline. The two ways to understand a flower, *Development* and *Evolution*, have evolved in parallel for a long time before fusing together in modern evo-devo. The integration of genomics into evo-devo has been a major step in recent years (de Bruijn et al. 2012). Taxonomists have been able to quantify part of the diversity of angiosperms: More than 300,000 different species of flowering plants have been identified (304,419 accepted names of different angiosperm species can be found in catalogues ("The Plant List (2013). Version 1.1."). Each of these species is defined by specific morphological characters. Most of these characters are linked to flower structure and organization, partly because flowers are immediately appealing the eye (simplifying the task to researchers), partly because, as reproductive structures, they are extremely important for plant species, and represent a major target for natural selection. However, morphological characters are just the tip of an iceberg, the result of tightly regulated developmental processes. These processes are mostly made possible by underlying gene regulatory networks, in which some genes are more or less dispensable, whereas other genes play a fundamental role. Often, these fundamental genes are called master regulators because they control other genes on their turn involved in other gene regulatory networks. Master regulators genes typically code for transcription factors, proteins able to bind DNA and perform transcription, starting a regulatory cascade.

The core of this doctoral project is the understanding of the functional and evolutionary role of a handful of plant-specific transcription factors, belonging to the WOX (Wuschel homeobOX) family. We focused our attention on these particular *WOX*

genes because of their dramatic effects on plant morphology, in particular at the flower level. The importance of *WOX* genes in the evolutionary process is not fully understood, as well as their role in leading to the astonishing diversity of floral and plant forms that we can observe today. For these reasons, *WOXes* represent an interesting area of research for plant evo-devo.

Plant evo-devo

Goethe, the famous German philosopher, is usually referred to as among the firsts to realize that "*all is leaf*", recognizing that flower organs (*i.e.*, sepals, petals, stamens, and carpels) are different manifestations of leaves. Goethe probably intended the homology among leaves and flower organs only in idealist terms (Friedman and Diggle 2011), meaning that he didn't think in an evolutionary perspective (70 years separate his *Versuch die Metamorphose der Pflanzen zu erklären* from *On the Origin of Species*). This is well illustrated by a famous picture, drawn by the botanist and illustrator Pierre Jean François Turpin (published in 1837), of a primitive, ideal plant (Goethe et al. 1837; Minelli 2009) which was intended as an archetype for all plants. This is distant from our current view of plant development and evolution. However, years before the famous sentence of Goethe, the botanist Caspar Friedrich Wolff already stated that flower organs are transformed leaves (as acknowledged by the same Goethe). Wolff founded his statements not upon an archetypal plant, but from the direct observation of the shoot apex and the fact that leaves and flower organs share a similar way of development. Moreover, Wolff demonstrated that leaf primordia are not miniature leaves that will slowly grow till their final size (in fact, preformationist ideas were still largely spread in the biology of the time) (Friedman and Diggle 2011), in this way setting the basis of modern plant morphology and development.

Accurate morphological analyses of flower development were later performed, in a parallel way to the work of zoologists of the time concerning embryo development in

animals. However, these developmental observations were not concerned with evolution. Only after the birth of the "Theory of evolution by means of natural selection" of Darwin (and Wallace), the problems of morphology and development could be finally seen in the *light of evolution* (Dobzhansky 1973). Charles Darwin, in a famous letter ("Darwin Correspondence Project"), defined the emergence of angiosperms as an "abominable mystery", referring to the apparently abrupt emergence and rapid diversification of flowering plants during the Cretaceous period. This observation was questioning some crucial points of the evolutionary theory: Rapid and possibly saltational *versus* long and gradual evolutionary processes (Friedman 2009). To explain the rapid emergence of angiosperms in the fossil record, Darwin even postulated the existence of a small continent in the Southern hemisphere as a birthplace for angiosperms, suggesting their cryptic evolution in that place before spreading all over the world.

Interestingly, in the same letter Darwin was also reporting an ecological explanation, attributed to botanist Gaston de Saporta: The interaction between flowers and insects (Friedman 2009) which, nowadays, is considered as a major driver of flower evolution (Grimaldi 1999; Barrett and Willis 2001).

Fossil flowers, phylogeny and genes

The direct evidence for the emergence of early flowers is mainly linked to their discovery as fossils or fossil traces. Several mesofossils of early flowers (small fossils of few millimeters in size, still visible at naked eye but requiring some kind of microscopic technique for an accurate analysis) are known from the Cretaceous period; fossil traces, such as fossil pollens, can be dated back till the Hauterivian (early-Cretaceous) about 136 Myr ago (Frohlich and Chase 2007). The presence of flowering plants even much before, in the Jurassic period, has also been suggested, accordingly to recently published phylogenies based on molecular and morphological characters (Zeng et al. 2014) (see also the

International Chronostratigraphic Chart in Chapter VII – Materials and Methods – Appendix I, for further details about geological times nomenclature). If flowering plants really emerged in the Jurassic, then a striking parallel between the emergence of flowering plants and pollinators may explain the rapid diversification of angiosperms (Zeng et al. 2014), confirming the ecological explanation reported by Darwin in his famous letter (Friedman 2009). Recent studies, based upon relaxed clock analyses, provided evidence for phylogenetic proliferation of angiosperms taking place in the Early Cretaceous (Magallon et al., 2015). This do not exclude possible earlier emergence of angiosperms, however, further studies might better compare angiosperm and insect diversification in that period, therefore providing evidence (or not) concerning the "ecological explanation". Although the fossil record might virtually provide excellent tests for different scenarios (for example, by accidental discovering of "missing links" fossils) (Frohlich 2003), the current absence of a clear stem-group fossil flower is problematic (even a famous discovery, the *Archaefructus,* doesn't seem to be a stem-group angiosperm) (Sun et al. 2002; Frohlich and Chase 2007). For these reasons, morphological and phylogenetic analyses (including molecular phylogenies) represent a major way to understand the emergence of angiosperms.

The origin of carpels and hermaphrodite flowers

Modern phylogenies state that extant gymnosperms are monophyletic, and consequently they are all equally distant from flowering plants (Frohlich and Chase 2007; Xi et al. 2013). From a morphological point of view, ovule structure and organization can be considered the main discriminant between gymnosperms and angiosperms. In fact, angiosperm ovules are protected by carpels, whereas Gymnosperms are not always protected by specific structures. This is early observation of botanists was marked in their definition: Gymno- (from Greek γυμνός, *i.e.* "naked") and angio- (from Greek αγγειον, *i.e.* "receptacle"). Plants "bearing naked seeds/ovules" *versus* plants provided with "protected seeds/ovules". Of course, we nowadays know other (and, possibly, more important)

differences between gymnosperms and angiosperms. However, the general absence of protecting structures in gymnosperms marked their etymology in botanical textbooks forever. In angiosperms, carpels provide fundamental facilities for their reproduction, such as mechanisms for pollen recognition (including pollen self-incompatibility), or pollen-capture trough the stigma (the apical part of the carpel) and *papillae* (finger-like structures supported by the same stigma), which represents specific characters of angiosperms. Carpel tissue is transformed into fruit after pollination, ensuring seed dispersal/protection as well as a fundamental source of food for mankind (Scutt et al. 2006). Like other floral organs, carpels are probably derived from leaves. The problem has been how to explain this process from an evolutionary perspective. Different theories have been looking for complex and long-lasting intermediate steps leading to modern angiosperm features (such as hermaphroditism or ovule coating). A more radical view of the origin of carpels and hermaphrodite flowers has recently been developed [supported, among others, by Mathews and Kramer (Mathews and Kramer 2012)]. This view is of interest because it very well frames also the findings, illustrated in this thesis, concerning the evo-devo role of *WOX* genes.

At the core of this view of plant development is the modular organization of plants and the special role played by meristems. The gene *WUSCHEL* (*WUS*) in Arabidopsis plays a central role in organizing the shoot apical meristem, maintaining stem-cell niches there, whereas other genes [such as *CLAVATA3 (CLV3)*] are involved in restricting the role of *WUS*. Interestingly, the same *WUS* is also needed for proper ovule development: *WUS* is expressed in the nucellus (the distal part of the ovule) and *wus* mutants expressing the *CLV1::WUS* construct resulted in naked ovules, without integuments (*CLV1* is expressed in the meristem but not in the ovule) (Gross-Hardt et al. 2002).

The placenta is the meristematic structure from which ovules emerge, and ovules are characterized by being determinate structures. Mathews and Kramer (2012) noticed that ovules display analogies with apical meristems: Ovules express *WUS* and they have their own "lateral organs" (the integuments, expressing adaxial-abaxial sets of genes typical of lateral organs, such as *HDZIPIII* or *KANADI*). A similar genetic module can be found one step back, at the carpel level. Carpels can also be described as structures analogous to lateral organs. In fact, carpels use genetic modules from the peripheral zone of meristems (PZ) in a female reproductive background (Mathews and Kramer 2012). Highlighting the fact that similar genetic modules can be found behind different morphological structures (such as leaves, carpels and ovule integuments) leads to the possibility that, during plant evolution, simple genetic shifts resulted in the rapid and independent emergence of these structures among different lineages.

Leaf development: A snapshot

All the components of the flower derive from leaves. For this reason, it is of interest to rapidly describe what is known about the developmental pathways leading to a leaf.

PRODUCTION OF PRIMORDIA - In Arabidopsis, leaf primordia originate from the shoot apical meristem (SAM), in which auxin maxima form. Production of auxin maxima is associated with proper patterning of PIN1 proteins (auxin efflux carrier) (Reinhardt et al. 2003; Traas and Monéger 2010) and repression of *KNOX* genes (Jackson et al. 1994; Lincoln et al. 1994; Long et al. 1996; Sinha 1999) [N.B., this sequence of events seems not conserved among all plant species (Tomescu 2009)]. The role of auxin is therefore fundamental in leaf and lateral organ development among different species.

CELL PROLIFERATION - When leaf primordia are formed, cell proliferation and proper organ development take place. The final organ derives from the correct interplay between three different axis of leaf polarity: Proximo-distal (from the base to the tip),

adaxial-abaxial (the side before the stem, and its opposite), and mediolateral (from the center to the margins). A genetic basis for the axis of cell proliferation going from the centre of the leaf till the boundary, which is required to explain lamina expansion, was firstly provided by the *phantastica* mutant in snapdragon. *phantastica* displays leaf-phenotypes including needle-like (full abaxialization) and string-like leaves (lamina expansion defects), also depending on temperature (Waites and Hudson 1995).

In Petunia, the *maw* mutant, central to this thesis, is affected in blade expansion in leaves and floral organs, leading to a partial lack of petal fusion in the corolla (Vandenbussche et al. 2009). Among the first mutants for lamina expansion in Arabidopsis, the *ago1* mutant displays narrow leaves, sepals and petals (Bohmert et al. 1998). *AGO1* codes for an ARGONAUTE protein required for *miR165/166* activity. *MiR165/166* a repressor of adaxial-specific *HD-ZIP III* transcripts in the abaxial region of organs (Kidner and Martienssen 2004; Mallory et al. 2004; Bowman 2004). More precisely, *HD-ZIP IIIs* are *HOMEOBOX* genes (*PHABULOSA, PHAVOLUTA, REVOLUTA*), required for adaxial identity (Otsuga et al. 2001; McConnell et al. 2001). AGO10 (also known as ZWILLE/PINHEAD) (Lynn et al. 1999) competes with AGO1, in this way repressing *miR165/166* activity and protecting *HD-ZIP III* transcripts (Zhang and Zhang 2012). Other players of the adaxial side in Arabidopsis include the *TAS3* tasiRNA, regulated by AGO7/ZIP (Hunter et al. 2003, 2006), a repressor of *ETTIN* and *ARF4* (abaxial-specxific) (Garcia et al. 2006; Hunter et al. 2006), and *MYB* genes *AS1 & 2* (Byrne et al. 2000; Semiarti et al. 2001). Additionally, *AGO7* and *AS1* together regulate the abaxial-specific gene *FIL*.

CELL EXPANSION - At the end of leaf development, once organ polarity is established and the final form has been reached, cell proliferation is followed by cell expansion (Dkhar and Pareek 2014). This process is associated with endoreduplication

(D'Amato, F 1952; Beemster et al. 2005), and forecasted by abrupt arrest of the cell cycle along the proximo-distal axis (from the tip to the basis of the leaf) (Donnelly et al. 1999). Since this is a coordinated process, a cell-cycle arrest front moves along the leaf (Andriankaja et al. 2012).

All the previous steps (emergence of primordia, cell proliferation, and cell expansion) are common to leaves but also lateral organs in general, including flower organs.

Petunia: The evolution of a model system

The majority of the experimental work reported in this thesis has been performed using the model species *Petunia* x *hybrida*, characterized by the following floral formula: $Ca_5Co_{(5)}A_5G_{(2)}$. The *genus Petunia* is native of South-America and belongs to the larger group of *Solanaceae*. Interestingly, the name Petunia itself comes from an indigenous appellation given to Tobacco. *Petunia* as a *genus* was described for the first time by Jussieu (1803) and then revised by other authors, including De Candolle, till the large revision of the genus performed by Fries in 1911 (Stehmann et al. 2009). Another landmark in *Petunia* taxonomy is at the end of the '80, the early '90 of the XX Century, when a division between species with 2n = 18 and species with 2n = 14 was eventually adopted by taxonomists. "Petunias" with 2n = 18 formed the *genus Calibrachoa*, and the ones with 2n = 14 formed the *genus Petunia,* as it is known today (Stehmann et al. 2009). This classification was further confirmed by molecular phylogenetic analysis (Ando et al. 2005). *Petunia* x *hybrida* (HooK.) Vilm. (garden Petunia, 2n = 14) is reported as obtained around 1834 on the British Isles, from an intended hybridization event (Stehmann et al. 2009). Wijsman (Wijsman 1982) proposed, based on taxonomic analysis and herbaria inspection, that only two species were involved in originating *P.* x *hybrida*: *P. axillaris*, characterized by white corolla and long petal tube (pollinated by sphyngid hawk moths), and *P. inflata*, characterized by purple corolla and short petal tube (pollinated by diurnal bees) (Stuurman

et al. 2004). Petunia genetic studies were originally developed at the University of Amsterdam (The Netherlands), and the INRA group in Dijon (France). Unfortunately, most of the genetic material developed in these centres was loss when these groups were closed. Along with tomato, and before Arabidopsis, Petunia was originally proposed as an outstanding model system for the community of plant researchers (Gerats and Vandenbussche 2005). In fact, Petunia has a life cycle of ~3-3,5 months from seed to seed; it can be easily reproduced by cutting; it is easy to use for cytogenetic or biochemical analysis, because of its large flowers and leaves; large sets of mutants are available; standard and efficient protocols for stable transformation (van der Meer 2006; Avila and Day 2014) and virus induced gene silencing (VIGS) (Broderick and Jones 2014) have been developed (Gerats and Vandenbussche 2005). Today, an outstanding interest of Petunia relies on the fact that Petunia can be used to address questions that can't be addressed in Arabidopsis: Flower colour; root-mycorrhyza interaction; petal fusion; production of volatile organic compound; or pollination syndromes. For laboratory purposes, three different cultivars of *P.* x *hybrida* are widely used: The W138 line, Mitchell, and V26.

W138 is a Petunia line of which its compact architecture is particularly well adapted to high densitity cultivation in green-house and growth chamber culture. The W138 is an high-copy number transposon line with more than 200 copies of the *dTph1* transposon in each plant and ~20-40 copies moving from one generation to the next one (*dTph1* is a ClassII DNA-DNA transposon, similar to the well known the *Ac*/*Ds*- system) (Gerats et al. 2013). This line has been widely used to create transposon-based mutant collections (Vandenbussche et al. 2008), such as the in-house collection from which the mutants used in this study are derived (Morel et al., unpublished). The *dTph1* transposon has a length of ~284 bp (Gerats et al. 1990) and, depending on in which region the insertion takes places, it can (or not) impair gene functionality. Because of its small size, insertions outside of the CDS/inside intronic regions are unlikely to disrupt gene functionality (unless in some

special cases, in which intronic regions have a regulatory function, or when the insertion impairs correct splicing). Insertions in the promoter +5'UTR or into the exonic region can affect gene functionality. In the first case, another possible effect is a change in the expression pattern of the gene. When the insertion is located in an exon into or upstream of a functional region (*e.g.*, DNA binding domains, functional domains, etc.) it is likely that the resulting mutant will be a full knock-out. Note that, again due to its small size, *dTph1* insertions in coding sequences usually do not lead to changes in transcript levels, with the exception of insertions into the coding sequence of genes coding for autoregulatory transcription factors. Instead the *dTph1* sequence is usually co-transcribed in the mRNA. However, translation results in truncated proteins, since *dTph1* encodes multiple stop codons in all six possible reading frames. As stated before, the *dTph1* transposon can undergo excision and move elsewhere in the genome. In this case, *dTph1* typically leaves an 8 bp footprint at the original insertion site, corresponding to the target site duplication (Levin and Moran 2011) that maintains the mutation because of the frameshift. More rarely, the footprint left behind is a 3 bp sequence (or a multiple), therefore restoring the reading frame and, possibly, gene function. Other events include excision with restoration of the WT sequence (no footprint left), and deletions in which part of the genomic sequence is taken away by the excision process. Also in these cases, gene functionality can be restored along with the correct reading frame. One drawback of the W138 line is that it is virtually not transformable as a pure line. However, F_1 progeny derived from W138 crosses with *e.g.* V26 or Mitchell (see further) displays superior transformation capacity.

The "Mitchell" line is a doubled-haploid derived from the *in vitro* culture of anthers from a plant obtained by crossing *P. axillaris* X (*P. axillaris* X *P.* x *hybrida*, cv. "*Rose du Ciel*"). Mitchell was widely used in the '80 as genetic system because of the high degree of homozygosity (Kole 2011). Nowadays, the Mitchell line is especially useful for its genetic

transformability using *Agrobacterium*. Mitchell retains some aspects of *P. axillaris*, such as longer stems and white, bigger flowers, compared with other cultivars.

The V26 line is also efficiently transformable with *Agrobacterium tumefaciens* (van der Meer 2006), and typically displays dark purple flowers. Although not growing as high as Mitchell, V26 displays also a much less compact growth habit than W138.

Until recently, no sequenced genome was available for the Petunia system. The Petunia Genome Consortium made available, to participating laboratories, including the Evolution & Development of the flower team in the RDP, the draft sequences of *P. axillaris* and *P. inflata* in 2010. The two sequenced genomes are, for the moment, available only as scaffold assemblies (*P. inflata* N50 406 Kb; N90 2,450 Kb - *P. axillaris* N50 309 Kb; N90 1,051 Kb; *Petunia genomes assemblies Status at February 2014* – unpublished presentation), meaning that it is not possible to establish the exact scaffold order, or to map sequences on chromosomes. Additionally, a *consensus* GFF file (coordinate file of the genome) is not currently available for *P. axillaris* and *P. inflata*. Despite of that, we have obtained and implemented different GFF files suitable for RNA-Seq analysis. We also developed a *de novo* transcriptome aimed at helping bio-informatics analysis of gene sequences, for example, by facilitating the identification of upstream and downstream regions of the coding sequence.

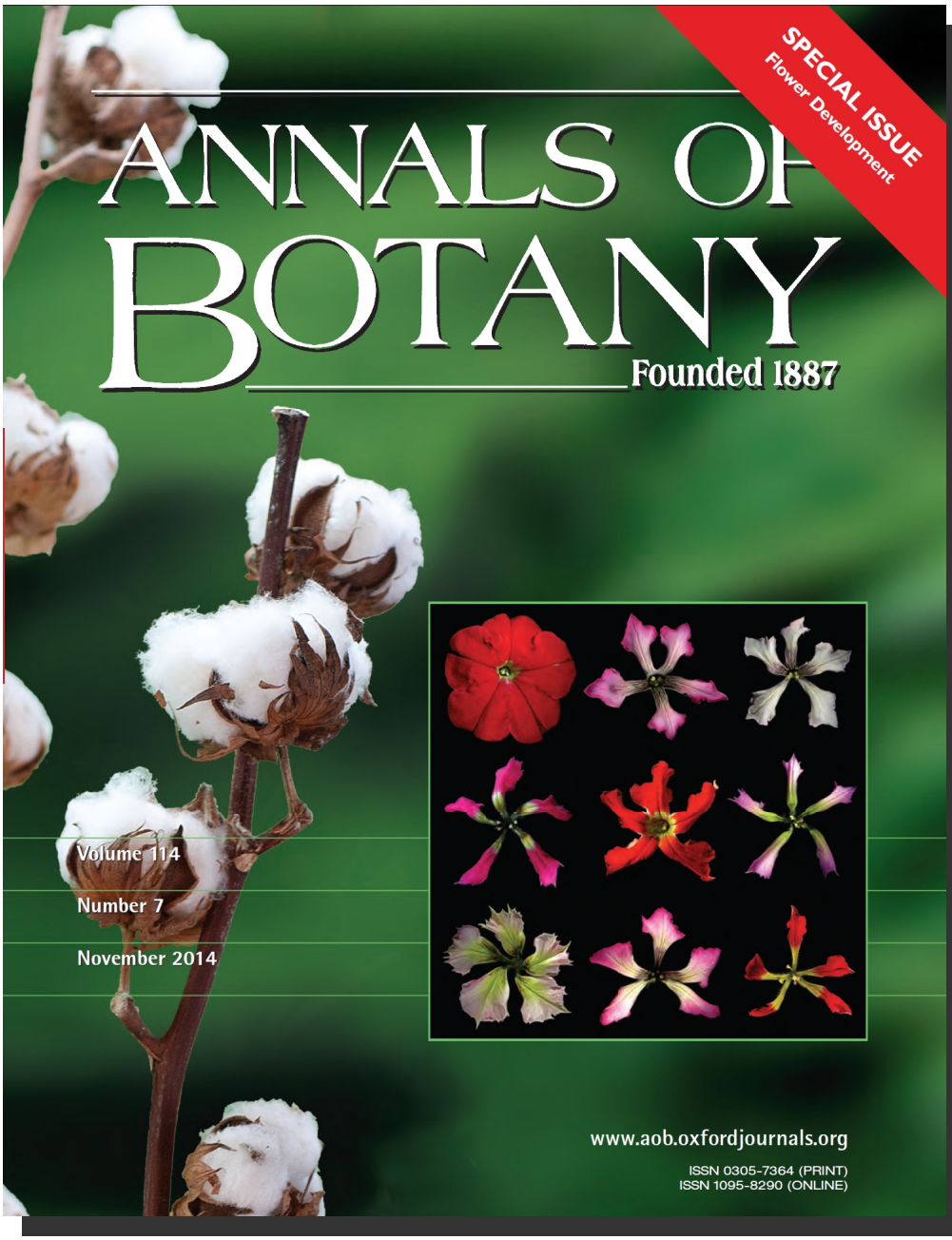

Cover illustration: The inset cover image shows a flower of the Petunia W138 *dTph1* transposon line (upper left corner) in which the original *maewest* mutation (centre) was isolated. The remaining images show *maewest* introgressed into different genetic backgrounds, illustrating the aesthetic and horticultural possibilities of this mutation (images by Michiel Vandenbussche). See Costanzo et al. (pp. 1545–1553).

II. The role of *WOX* genes in flower development

Enrico Costanzo[1,2], Christophe Trehin[1] & Michiel Vandenbussche[1].

The following chapter has been partly published in "Costanzo et al., The Role of *WOX* Genes in Flower Development., *Annals of Botany*, 2014, 114 (7): 1545–53. doi:10.1093/aob/mcu123" by permission of Oxford University Press (license number 3577101105448 – figures –, and license number 3577100998064 – text –).

BACKGROUND:

WOX (*Wuschel-like homeobOX*) genes form a family of plant-specific HOMEODOMAIN transcription factors, the members of which play important developmental roles in a diverse range of processes. *WOX* genes were first identified as determining cell fate during embryo development, as well as playing important roles in maintaining stem cell niches in the plant. In recent years, new roles have been identified in plant architecture and organ development, particularly at the flower level.

SCOPE:

In this review, the role of *WOX* genes in flower development and flower architecture is highlighted, as evidenced from data obtained in the last few years. The roles played by *WOX* genes in different species and different flower organs are compared, and differential functional recruitment of *WOX* genes during flower evolution is considered.

CONCLUSIONS:

This review compares available data concerning the role of *WOX* genes in flower and organ architecture among different species of angiosperms, including representatives of monocots and eudicots (rosids and asterids). These comparative data highlight the usefulness of the WOX gene family for evo-devo studies of floral development.

KEYWORDS:

Arabidopsis thaliana; EVERGREEN/WOX9; HOMEOBOX; MAW/WOX1; PRS/WOX3; Petunia × hybrida; WOX genes; WUSCHEL; eudicots; flower development; monocots; plant evo–devo.

[1]Laboratory of Reproduction and Development of Plants, UMR5667, Ecole Normale Supérieure de Lyon, Lyon, FRANCE

[2]Istituto di Scienze della Vita, Scuola Superiore Sant'Anna, Pisa, ITALY

WOX **genes are** ***HOMEOBOX*** **genes**

The > than 250,000 wild species of flowering plants display an incredible diversity of flower shapes (Krizek and Fletcher 2005), whose architectural traits (such as fused *versus* free-standing petals and large *versus* narrow petals) can be very different from one species to another.

Despite the fact that the genetic basis of organ identity in the flower is well understood nowadays, thanks to the development of the ABCE model of flower development, mainly based of the *MADS BOX* gene family (Smaczniak et al. 2012; Heijmans et al. 2012b; Bowman et al. 2012), little is known about organ shape and the general morphology of the flower, for which such a general model is still lacking. Interestingly, whereas *MADS BOX* genes are involved in organ identity at the flower level in plants, organ identity in animals is based on a completely different class of genes, the *HOMEOTIC BOX* (or *HOMEOBOX*) genes (Holland 2013). First discovered in the fruit fly *Drosophila melanogaster* (Carroll 1995; Castelli-Gair 1998), *HOMEOBOX* genes derive their name from William Bateson's concept of homeosis, since mutations in these genes may led to transformation of one part of the embryo into another one during development (Robert 2001). At the molecular level, HOMEOBOX proteins are characterized by the HOMEODOMAIN, composed of 60 amino acids on average and arranged in space with a *N*-terminal arm plus three α helixes able to bind DNA (Wolberger 1996). At least 14 different classes of *HOMEOBOX* genes (where specific conserved domains, in addition to the shared HOMEODOMAIN, can be found) have been described in plants, from angiosperms to red algae, and many of them have been shown to play a role in plant development (Mukherjee et al. 2009).

Plant *HOMEOBOX* genes sharing sequence identity with the gene *WUSCHEL* (*At-WUS*) from arabidopsis are referred as *WOX* (*Wuschel related homeobOX*) genes. *At-WUS* was identified as a central player in stem cell maintenance in the shoot apical meristem (SAM), although not required for SAM initiation (Laux et al. 1996; Liu et al. 2011). The name

wuschel apparently derives from the bristled and bushy phenotype of the mutants, in which ectopic meristems are repetitively produced and prematurely terminated (Laux et al. 1996).

Since the discovery of *At-WUS*, several *WOX* genes have been characterized in different species. Other members of the WOX family are usually referred as "*WOX*" followed by an Arabic numeral (with few exceptions), and can be grouped in different subfamilies or subfamilies (van der Graaf et al. 2009; Vandenbussche et al. 2009).

***WOX* genes play different roles in plant development**

In arabidopsis, *WOX* genes have been shown to play a broad role in plant development, from stem cell maintenance at the meristem level (*WUSCHEL* in shoot meristem*, WOX4* in cambium*, WOX5* in root meristem) till embryo patterning (Laux et al. 1996; Haecker et al. 2004; Ananda K Sarkar et al. 2007; Ji et al. 2010). We know from *Picea abi*es that all the major *WOX* subfamilies, with the exception of the MAW/WOX1 subfamily, probably originated before the separation of angiosperms from gymnosperms. A relationship between *WOX* gene number and body pattern complexity among different species, all from the 'green lineage' (a grouping of land plants and green algae), has also been proposed (Hedman et al. 2013). In fact, *WOX* genes can be divided into three different lineages that are supposed to reflect their ancestry: an ancient lineage (comprising *At-WOX10, At-WOX13, At-WOX14* and their homologues), an intermediate lineage (comprising *At-WOX8-9-11-12* and their homologs), and a new or "WUS" lineage (other times called "WUS clade", see Nardmann and Werr 2013), comprising *AtWOX1* to *7*, including *WUSCHEL* (Haecker et al. 2004; Nardmann and Werr 2012). Moreover, *WOX* genes from the WUS lineage are absent from green algae, bryophytes and ferns (with the exception of *Leptosporangiatae*). Further diversification, sub-functionalization and recruitment in different stem-cell niches of these genes in angiosperms (but also gymnosperms), has been considered as contributing to the body plan diversity and

evolutionary success of these groups (Nardmann and Werr 2012). At the molecular level, the acquisition of repressive activity by proteins from the modern lineage, mainly due to an aminoacidic domain called the "WUSCHEL box" (see red box on gene pictograms in Fig. 1), has been proposed to play a major role in this process (Lin, Niu, McHale, et al. 2013). In this review we will further focus on the implication of WOX gene function during floral development.

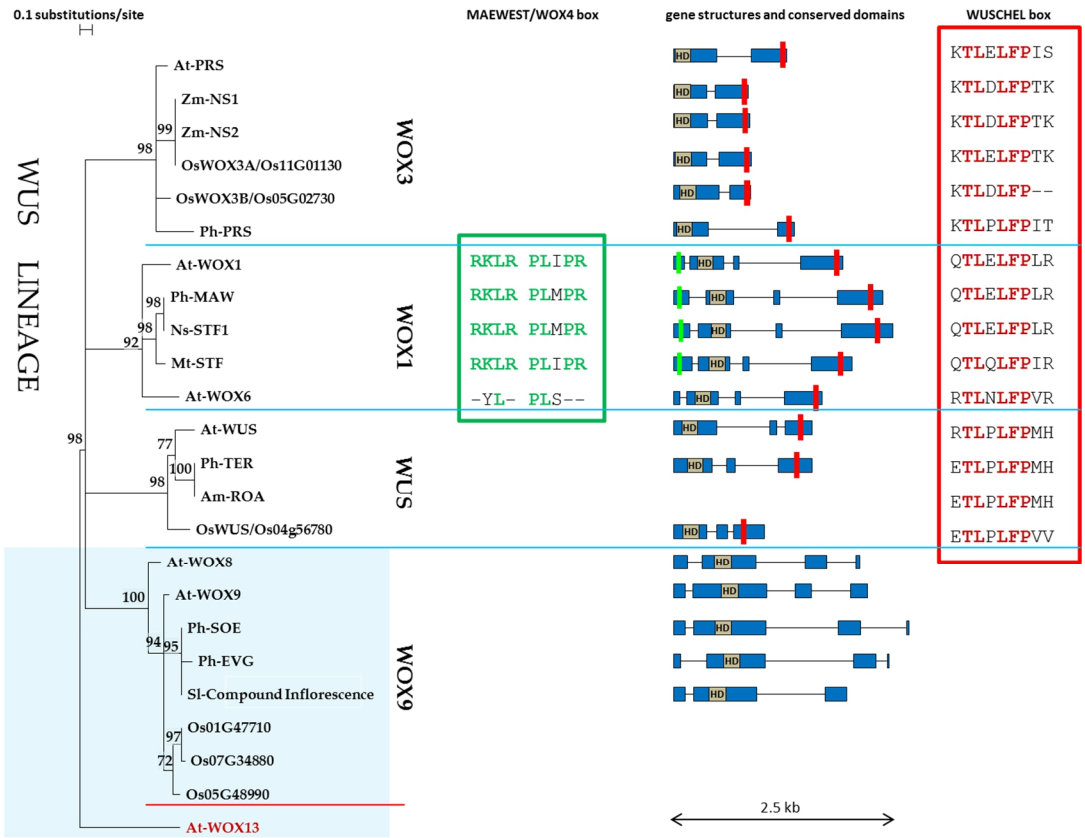

FIG.1 Phylogenetic tree of WOX sequences

WOX sequences from different species (Am, *Antirrhinum majus*; At, *Arabidopsis thaliana*; Mt, *Medicago truncatula*; Ns, *Nicotiana sylvestris*, Ph, *Petunia × hybrida*; Os, *Oryza sativa*; Sl, *Solanum lycopersicum*; Zm, *Zea mays*) are clustered into different subfamilies (WOX3, WOX1, WUS, WOX9) after phylogenetic analysis. The phylogenetic tree is based on the HOMEODOMAIN sequences. The WOX13 sequence

(dark red) from arabidopsis is used as outgroup. To support WOX relationships, 1000 bootstrap samples were obtained using the software TREECON (Van de Peer and De Wachter, 1994). Bootstrap values <65 % are not shown and corresponding branches are displayed as unresolved. On the right of the tree, gene structure is displayed for most of the WOX gene sequences (solid blue bars are used for exons and thin black lines for introns), also depicting conserved amino acidic boxes (HD, HOMEODOMAIN; red rectangle, WUSCHEL box; green rectangle, MAEWEST/WOX4 box, as in Vandenbussche et al., 2009). In addition, conserved amino acid residues are displayed for the MAEWEST/WOX4 box and the WUSCHEL box. Note that WOX sequences also display characteristic C-terminal motifs with functional properties (not shown), as illustrated in Vandenbussche et al. (2009). Where not specified, accession numbers are the same as in Vandenbussche et al. (2009); Mt-STF (AEL30892.1), Nt-STF1 (AEL30893.1) and Sl-Compound Inflorescence (NP_001234072.1) are from GenBank. The WUS LINEAGE (also called WUS clade, see Nardmann and Werr 2013), that is, the modern lineage of *WOX* genes to which the same *WUS* belongs, is highlighted on the left.

At-WUSCHEL **is required for stem-cell maintenance in the flower (WUS lineage)**

WUSCHEL (*WUS*) is the founding member of the WOX family and is also representative of a subfamily, the so called "WUS lineage" (FIG. 1). *WUS* was initially isolated in arabidopsis (Laux et al. 1996) and its function has been thoroughly investigated in this model species.

WUS promotes the identity and maintenance of stem cells, a pool of undifferentiated and continuously dividing cells located in the central zone of both the SAM and the flower meristem (FM) (Laux et al. 1996; Besnard et al. 2011). Thus, on a *wus* genetic background, the SAM, instead of producing new organs throughout the life of the plant, stops functioning prematurely in an aberrant flat morphology. However, *wus* plants are still able to initiate secondary meristem, but it fails to self-maintain, resulting in plants with a highly disorganized, bushy architecture. Similarly, *wus* flowers display many fewer stamens (usually one or two) and no carpels, consistent with precocious FM termination (Laux et al. 1996). *WUS* is therefore necessary for meristem maintenance, but is not required for their initiation. Consistent with this function, *WUS* expression is restricted to a small domain,

the organizing center, located in the basal part of the central zone, beneath the L3 layer in the SAM and beneath the L2 layer in the FM (Mayer et al. 1998). Mechanistically, it is known now that WUS acts non cell-autonomously to both promote stem cell identity and directly activate *CLAVATA3* (*CLV3*) expression within the central zone (Schoof et al. 2000; Yadav et al. 2011). In turn, the CLE peptide CLV3 diffuses outside of the central zone, binds to the CLV1 and CLV2/CORYNE receptor kinases and thus triggers the signaling pathway that eventually leads to the restriction of *WUS* expression within the organizing centre (Schoof et al. 2000; Brand et al. 2000; Lenhard and Laux 2003; Nimchuk et al. 2011; Katsir et al. 2011). Much evidence suggest that POLTERGEIST and POLTERGEIST LIKE1 are signaling intermediates between CLV3 perception and *WUS* regulation (Yu et al. 2000; Song et al. 2006). *WUS* is thus part of a negative genetic feedback loop that ensures the homeostasis of the meristem. Within this loop, it is interesting to note that WUS is also directly repressing *CLV1* expression (Busch et al. 2010).

Identification of additional direct WUS targets, such as the A-type *Arabidopsis Response Regulators7* (*ARR7*), shed light on the way *WUS* specifies stem cell identity (Leibfried et al. 2005). By repressing the expression of *ARR7*, WUS counteracts the inhibitory activity of ARR7 on cytokinin signaling in the center of the SAM (To et al. 2004; Leibfried et al. 2005). WUS can therefore act both as an activator and a repressor of transcription (Ikeda et al. 2009; Busch et al. 2010), and the WUS box has been reported to be absolutely required for these two types of activity (Ikeda et al. 2009). The role of WUS as a transcriptional repressor was further underscored by its interaction with two co-repressors, WSIP1/TOPLESS and WSIP2 (Kieffer et al. 2006; Long et al. 2006).

Under inductive conditions, the vegetative SAM can switch to an inflorescence SAM (iSAM or IM) which, instead of producing leaves on its flanks, generates FM. All the data

gathered on WUS function cannot be generalized to the FM, as exemplified for instance with *TOPLESS RELATED1* and *2,* which are repressed by WUS in the SAM but activated in the FM (Busch et al. 2010), further confirming the complex regulatory interaction reported earlier (Ikeda et al. 2009). However, the majority of data are common to both meristems. This is especially true for the stem cell maintenance process and the WUS/CLV negative feedback loop, with some minor differences, such as reduced sensitivity to changes in CLV signaling in the FM compared with the SAM (Laux et al. 1996; Clark et al. 1997; Mayer et al. 1998; Schoof et al. 2000; Müller et al. 2006; Yadav et al. 2011). In arabidopsis, the WUS/CLV loop is absent in incipient floral primordia but it is rapidly set up, with the activation of *WUS* expression at stage 1, followed by that of *CLV3* at stage 2-2$^{1/2}$. However, and contrary to what happens in the SAM, stem cell maintenance is only transient in the FM (Prunet et al. 2009). Indeed, once all floral organs have been initiated, activity of the FM stops and the flower becomes determinate. The mechanism controlling FM termination has been described mainly in arabidopsis. It has been shown to rely on a second genetic feedback loop that implies *WUS* and *AGAMOUS* (*AG*) (Lenhard et al. 2001; Lohmann et al. 2001). *AG* encodes a C-Class MADS box protein that also controls the identity of stamens and carpels, the male and female reproductive organs, respectively (Yanofsky et al. 1990; Bowman et al. 1991). The feedback loop starts with the activation of *AG* transcription, at stage 3, by WUS together with LEAFY (LFY), which acts in a partially redundant way in this process (Yanofsky et al. 1990; Lohmann et al. 2001), and ends up with the repression of *WUS* in the centre of the FM, at stage 6, concomitantly with or immediately after carpel initiation. This second part of the loop absolutely requires AG, making AG the main developmental switch to FM termination. Thus, on an *ag* genetic background, flowers are indeterminate and keep producing floral organs in their centre, and this phenotype coincides with the maintenance of *WUS* expression within the FM organizing centre (Bowman et al. 1991; Lenhard et al. 2001;

Lohmann et al. 2001). FM termination is therefore closely linked to initiation of carpel development. However, these two processes are not coincident and are uncoupled although both controlled by *AG* (Mizukami and Ma 1995; Ji et al. 2011). Very interestingly, the fact that organizing centre cells retain a molecular identity distinguishable from that of surrounding cells even after the cessation of *WUS* expression further confirms the separation of the two processes but also demonstrate that organizing centre cells persist after FM termination and are not incorporated into carpels (Liu et al. 2011). Recently, two different mechanisms of repression of *WUS* by AG have been reported. They both explain why AG does not repress *WUS* expression right from the stage 3. In the first mechanism, AG represses *WUS* expression indirectly by activating *KNUCKLES* (*KNU*, a C2H2-type zinc finger transcription factor) expression, which in turn represses *WUS* expression directly or indirectly (Sun et al. 2009). In this model, *KNU* expression is blocked by repressive marks that are removed in an AG-dependent manner at stage 6. In the second mechanism, AG also directly represses *WUS* expression by recruiting polycomb group proteins (PcG) to *WUS* earlier than in the first model, at stage 5 (Liu et al. 2011). These two mechanisms are probably coordinated and act in parallel to each other in terminating floral stem cell maintenance.

From this detailed analysis in arabidopsis, it is clear now that to make a flower with a fixed number of floral organs it is of crucial importance that *WUSCHEL* is switched off at very precise moments during development of the floral bud. Not all flowering species display such a rigidly controlled floral organ number within their flowers, which seems to be a character acquired later in angiosperm evolution. It would be interesting to investigate whether changes in the *WUS* regulatory network have occurred during evolution that might have led to an increased robustness of the system, resulting in fully determined flower architectures. Likewise, one can question whether floral meristem termination occurs at the same moment in species with different placentation topologies (Colombo et

al. 2008). For example in *Petunia* and rice, which belong to the central placentation types, the floral meristem remains active after carpel primordia have been produced, because the placenta (and later on the ovules) develops directly from the floral meristem centre between the carpels. By contrast, in parietal placentation types such as arabidopsis, the placenta and ovules differentiate from the medial regions of the carpels after the FM has terminated. Interestingly, in both rice and *Petunia*, it has been shown that both D- and C-subfamily *AG*-like MADS-box proteins participate in floral meristem termination (Dreni et al. 2011; Heijmans et al. 2012b), with the D-lineage proteins being strongly expressed during placenta development, while the D-subfamily gene *STK* in arabidopsis does not seem to be involved at all in determinacy control (Pinyopich et al., 2003). This regulatory difference might be a direct consequence of different placentation topologies.

Besides arabidopsis, loss of function mutants for *WUS* orthologues have been described so far only in *Petunia* (*terminator*) and snapdragon (*rosulata*) (Stuurman et al. 2002; Kieffer et al. 2006), confirming their role in maintenance of the SAM. Unfortunately, *ter* and *roa* mutants never develop flowering branches, and the roles of *TER* and *ROA* in floral meristem control have therefore not yet been analysed. Expression studies of *WUS* orthologues are available for a wider range of species. Perhaps the most remarkable findings have been presented by (Nardmann and Werr 2006), who showed in grasses that, none of the isolated *WUS* orthologues exhibited an organizing centre-type expression pattern in the vegetative SAM, as in arabidopsis. Instead, it has been shown that the *WOX4* orthologue in rice, *Os-WOX4*, is involved in SAM maintenance, along with cytokinins (Ohmori et al. 2013). Moreover, in rice, mutant plants for the *LONELY GUY* gene, which codes for a cytokinin-activasting enzyme, are also affected at the SAM, inflorescence and floral meristems (Kurakawa et al. 2007). Taken together, these facts suggest major differences in *WUS* function in grass species compared with eudicots.

The PRS/WOX3 subfamily

The second *WOX* gene that was found to play a role in flower development is arabidopsis *PRESSED FLOWER* (*At-PRS,* also called *WOX3*). Mutants for this gene have flowers with a flattened appearance (hence the name) because lateral sepal development is affected: they are usually smaller, sometimes with a filamentous appearance, or can be completely absent (Matsumoto and Okada 2001). Although the size of the abaxial and adaxial sepals is normal, marginal regions showed defects. *At-PRS* was shown to act independently of organ identity and meristem size. The expression of *At-PRS* was detected at the lateral regions of all lateral organs at very early stages including leaves, flower primordia and floral organ primordia, despite the fact that phenotypic defects were much more restricted. Because of its expression pattern and mutant phenotype, *At-PRS* was proposed to regulate lateral axis-dependent development of arabidopsis flowers (Matsumoto and Okada 2001). Later, it was reported that arabidopsis *prs* mutants also lacked lateral stamens, and were additionally affected at the leaf level because of the absence of stipules at the leaf base (Nardmann et al. 2004).

Initially, floral mutant phenotypes had not been described for *PRS/WOX3* homologues in species other than arabidopsis. Instead, it was shown that *the NARROW SHEATH 1* and *2* genes in maize are *PRS/WOX3* homologs (Nardmann et al. 2004) and that they perform a crucial role in leaf margin development, with the *ns1 ns2* double mutant displaying a severely reduced leaf blade (Scanlon et al. 1996, 2000; Scanlon 2000). A very similar leaf phenotype was found in *nal2 nal3* double mutants in rice, with *NAL2* and *NAL3* (*OsWOX3A*) being homologous to the maize *NS1`* and *NS2* genes (Ishiwata et al. 2013; Cho et al. 2013). Interestingly, the widths of lemma and palea were also significantly reduced in *nal2 nal3* mutants (Cho et al. 2013). Since lemma and palea are considered the equivalent of the eudicot sepals, it indicates that the function of PRS/WOX3 proteins during floral development is conserved between monocots and eudicots. Rice contains a

third *WOX3* copy, called *OsWOX3B/DEP*, but this functions in the regulation of trichome formation in leaves and glumes (Angeles-Shim et al. 2012). It therefore seems that the *WOX3/PRS* subfamily in rice has further functionally diverged.

The MAW/WOX1 subfamily

The evolutionary invention of petals, the usually brightly coloured organs of the flower, is generally believed to have played a major role in the evolution of pollination syndromes. In many taxa throughout the angiosperms, petals fuse partly or completely to form a tubular structure, thereby creating a protective barrier enclosing the reproductive organs and nectaries in the centre of the flower. The *maewest* (*maw*) mutant in Petunia was isolated in a genetic screen for mutants with defects in petal fusion (Vandenbussche et al. 2009). Morphological analysis of *maw* flowers showed that petal fusion defects were mainly due to a reduced lateral outgrowth of the initially separate petal primordia, which subsequently fail to properly fuse. Similar defects were found in carpels, resulting in partly unfused carpels, and also sepals were narrower than wild-type. In addition, leaf blade outgrowth was considerably reduced along the lateral axis, as observed in floral organs, indicating that *MAW* plays a general role in the lateral outgrowth of organs. *MAW* was shown to encode a member of the *WOX1* subfamily of WOX transcription factors (Vandenbussche et al. 2009). Similar phenotypes in leaf and flower development were found for mutants of *MAW/WOX1* homologues in *Medicago truncatula* and *Nicotiana sylvestris* (Tadege, Lin, Bedair, et al. 2011; Tadege, Lin, Niu, et al. 2011) (McHale and Marcotrigiano 1998; Lin, Niu, McHale, et al. 2013). In addition, mutants for *MAW/WOX1* homologues in two other different species, *narrow organs1* in *Lotus japonicus* and *lathyroides* in *Pisum sativum* (garden pea), have also been shown to be affected in lateral outgrowth of organs such as leaves and petals (Zhuang et al. 2012), further showing a broadly conserved role for *MAW/WOX1* genes among different dicot species. In contrast, the dramatic *maw/wox1* phenotypes found in *Petunia, Medicago, Nicotiana, Lotus* and Pea are absent in arabidopsis

wox1, *wox6*, and *wox1 wox6* double mutants, showing that *WOX1* function is redundant (Vandenbussche et al. 2009), and that other factors can compensate for the loss of *WOX1/6* function in Arabidopsis.

Functional overlap between MAW/WOX1 and PRS/WOX3 subfamilies

Because mutants of members of both the *PRS/WOX3* and *MAW/WOX1* subfamilies in arabidopsis display a much less severe or no phenotypic difference compared with homologous mutants in other species (see the two previous paragraphs), and because *PRS* and *WOX1* overlap in expression pattern, it was hypothesized that Arabidopsis *WOX1* and *PRS* genes might overlap in function. This was indeed confirmed by the phenotype of *wox1 prs* double mutants, consistent with their overlapping expression domains at the adaxial–abaxial boundary layer and at the organ margins (Vandenbussche et al. 2009; Nakata et al. 2012). In contrast to *prs* single mutant flowers, all sepals (not only the lateral ones) in *prs wox1* flowers displayed a reduced blade outgrowth, as was the case also for the petals. This phenotype was also found in leaf development, with *wox1 prs* leaves displaying obvious defects in blade outgrowth, while *prs* mutants were only lacking stipules. These results clearly indicate that, despite the fact that *PRS/WOX3* and *MAW/WOX1* subfamilies are structurally different (FIG. 1), their proteins share a common function in organ development along the lateral axis. However, note that the carpel fusion defects found in *Petunia, Nicotiana* and *Medicago wox1* mutants (Vandenbussche et al. 2009; Tadege, Lin, Bedair, et al. 2011) were not observed in *wox1 prs* mutants (Vandenbussche et al. 2009). So far, functional data for both *PRS/WOX3* and the *MAW/WOX1* subfamily are only available in arabidopsis, and it will be interesting to investigate whether this functional overlap also exists in species in which *maw/wox1* single mutants do already display a strong phenotype on their own. Along the same line, loss of *wox3/prs* function in monocots results in severe leaf blade reduction, but, remarkably, grasses (including wheat, maize, rice, and *Brachypodium*) do not have *WOX1* representatives (Nardmann and Werr 2006;

Nardmann et al. 2007; Vandenbussche et al. 2009) while all other WOX subfamilies are represented in their genomes. It would be very interesting to investigate whether the absence of the *WOX1* subfamily in grasses has developmental implications related to differences in leaf development between monocots and eudicots.

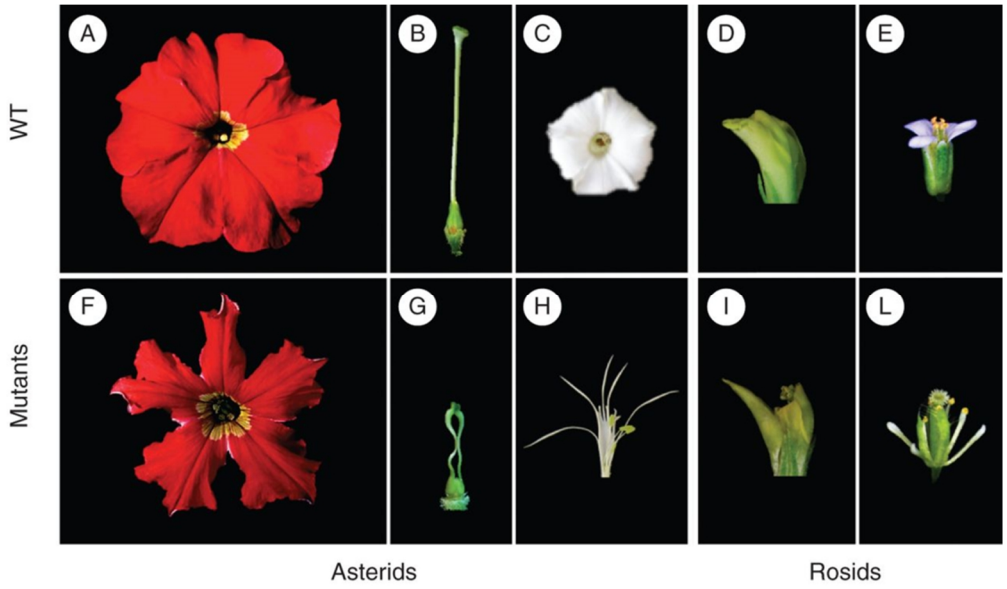

FIG. 2 *wox* mutant flower phenotypes in petunia, *Nicotiana*, *Medicago* and arabidopsis (Vandenbussche *et al.*, 2009; Tadege, Lin, Bedair, *et al.*, 2011*b*; Lin *et al.*, 2013).

A, **C**, **D**, **E** - Wild-type (WT) flower phenotypes for *Petunia* × *hybrida*, *Nicotiana sylvestris*, *Medicago truncatula* and *Arabidopsis thaliana*, respectively. (**B**) A *Petunia* wild-type pistil.

F, **H**, **I**, **L** - Mutant flowers: *maw* in *Petunia* (**F**), *lam1* in *Nicotiana* (**H**), *stf* in *Medicago* (**I**) and *wox1 prs* in arabidopsis (**L**). (**G**) A strongly affected *maw* pistil (carpels unfused). (**C**, **D**, **H**, **I**) Courtesy of M. Tadege.

In arabidopsis, *At-WOX1* and *At-PRS* have recently been proposed to define a so called middle domain in leaf development, different from the classical adaxial and abaxial sides of the leaf, and able to drive blade outgrowth (Nakata et al. 2012). Furthermore, in this model *At-WOX1* and *At-WOX3* would be at the spatial and regulatory interface of adaxial (*HD-*

ZIPIIIs, ASYMETTRIC LEAVES1&2) abaxial (*KANADIs, ARFs),* or middle-abaxial (*FILAMENTOUS FLOWER*) specifying genes (Nakata and Okada 2012; Tsukaya 2013). This may also imply the role of several hormones. For instance, *ASYMMETRIC LEAVES1* and *2* regulate the expression of *ARF3* (in both a direct and an indirect way) (Iwasaki et al. 2013), which probably controls the cytokinin biosynthetic pathway in its turn (Takahashi et al. 2013). At the same time, *KANADI1* is linked to plant hormone pathways and leaf morphology, usually in a way antagonistic to *HD-ZIPIII* genes (Reinhart et al. 2013), such as the auxin pathway (Huang et al. 2014), but probably also the cytokinin pathway, by binding to the *ASYMMETRIC LEAVES2* promoter (Merelo et al. 2013). On the other hand, a study of *stenofolia* (*stf*) mutants in *Medicago* and *Nicotiana* proposes a role in modulating phytohormone homeostasis and sugar metabolism, and in this way playing a role in leaf development (Tadege, Lin, Bedair, et al. 2011). Moreover, a role in cell proliferation along the adaxial-abaxial boundary has been shown for *STF* (Tadege, Lin, Bedair, et al. 2011) and *WOX1&PRS* (Nakata et al. 2012), and a recent paper describes the interaction between *STF* and *ASYMMETRIC LEAVES2* with *TOPLESS* along the leaf margin (Zhang et al. 2014).

EVERGREEN **in Petunia is involved in inflorescence architecture (WOX9 subfamily)**

The WOX9 subfamily is represented by two genes both in arabidopsis and *Petunia* (FIG. 1). The Arabidopsis representatives are named *STIMPY* (*STIP*, *WOX9*) and *STIMPY-LIKE* (*STPL*, *WOX8*) (Haecker et al. 2004; Wu et al. 2005), and in Petunia *EVERGREEN* (*EVG*) and *SISTER OF EVERGREEN* (*SOE*) (Rebocho et al. 2008). *EVG*, in Petunia, and *COMPOUND INFLORESCENCE*, in tomato, are essential for inflorescence development and architecture (Rebocho et al. 2008; Lippman et al. 2008). On an *evg* background, floral identity is not specified and apical floral meristems develop as inflorescence shoots instead. Moreover, *evg* mutations display defects in the physical

separation of the apical and lateral meristem, resulting in the formation of a fasciated meristem. *Petunia* displays a cymose inflorescence in which the apical meristem terminates by forming a FM and growth continues from the lateral or 'sympodial' meristem, which will generate a subsequent sympodial meristem before terminating in a flower. In *Petunia*, FM identity is mainly specified by *ABERRANT LEAF AND FLOWER* (*ALF*) and *DOUBLE TOP* (*DOT*), which are the homologs of *LEAFY* and *UNUSUAL FLORAL ORGANS*, respectively (Souer et al. 1998, 2008). Unexpectedly, *EVG* is not expressed in the apical floral meristem but in the sympodial incipient meristem (Rebocho et al. 2008). Mechanistically, the model assumes *EVG* counteracts the effect of an unknown mobile factor that inhibits *DOT* expression in the FM, possibly indirectly by promoting proliferation of the lateral IM and separation from the apical FM.

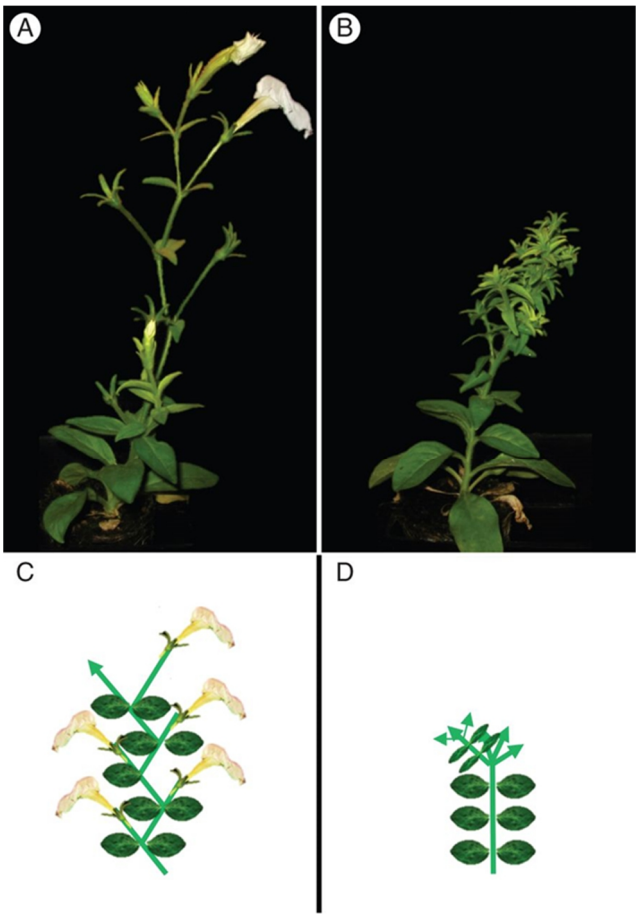

FIG. 3 *evergreen* in *Petunia* (Rebocho *et al.*, 2008).

Petunia wild-type (**A**) and *evg* (**B**) inflorescences - Whereas the wild-type follows a typical zig-zag pattern, making a flower at each node and resulting in a cymose inflorescence (**C**), the *evg* mutant has a fasciated and bushy inflorescence (**D**), flowering only occasionally (terminal flowers).

In contrast, *WOX8/STPL* and *WOX9/STIP* in arabidopsis are required for embryo patterning and vegetative SAM maintenance but not for inflorescence development and architecture. *WOX8/STPL* and *WOX9/STIP* are expressed during early stages of embryo development with overlapping and specific expression domains (Haecker et al. 2004). Briefly, only *WOX8/STPL* is expressed in egg cell and zygote, whereas *WOX8/STPL* and *WOX9/STIP* are both expressed after the division of the zygote. However, their

expression is restricted to the basal daughter cell, which will form the suspensor and the hypophysis (Haecker et al. 2004). Consistent with this expression pattern, weak *wox9/stip* alleles display fewer cells in the basal part of embryo while embryo development of strong alleles stop at the globular stage, both phenotypes being due to a reduction or a complete arrest of the cell cycle (Wu et al. 2005, 2007). Interestingly, the *wox9/stip* phenotype can be rescued by the addition of exogenous sucrose, although developing carpels are not fully rescued, further confirming the role of *WOX9/STIP* in stimulating the cell cycle (Wu et al. 2005). *WOX8/STPL* was shown to functionally overlap with *WOX9/STIP* in promoting embryonic cell division (Wu et al. 2007; Breuninger et al. 2008). Later during development, *WOX9/STIP* promotes the growth of the vegetative SAM and is required for the maintenance of *WUS* expression at the shoot apex. In this regulatory network, *WOX9/STIP* acts downstream of the cytokinin signalling pathways (Skylar et al. 2010). More recently, *WOX8/STPL* has been shown to promote, along with the expression of *WOX2*, *CUC2&3*, the establishment of the cotyledon boundary (Lie et al. 2012).

It therefore seems that *EVG*, *WOX8/STPL* and *WOX9/STIP* have nothing in common. However, it is interesting to note that in both arabidopsis and Petunia the constitutive expression of *WOX9/STIP* and *EVG* causes similar defects, suggesting that the proteins are functionally very similar and that diversification of *EVG* and *WOX9/STIP* might rely on alterations in their expression patterns.

SOE, the second member of the WOX9 subfamily in Petunia, displays an expression pattern very similar to those of *WOX8/STPL* and *WOX9/STIP* in arabidopsis (Rebocho et al. 2008). Furthermore, the constitutive expression of *SOE* in *Petunia* phenocopies the ones of *EVG* and *WOX9/STIP*, further indicating that these proteins are functionally similar. It has therefore been proposed that *SOE* and *WOX8/STPL-WOX9/STIP* represent an ancestral gene and that *EVG* is a duplicated gene that acquired a new function

in inflorescence development and a key role in the evolution of cymes (Rebocho et al. 2008). This example illustrates how genes can be recruited upon duplication to undergo a neo or sub-functionalization process.

Evolution of WOX gene function: Primarily through changes in expression patterns?

Despite the fact that most of the different WOX subfamilies are structurally quite different from each other (differences in exon numbers, conserved peptide motifs specific for each subfamily, see Vandenbussche et al., 2009), proteins in a number of these subfamilies do seem to share some ancestral common function. A first example can be found in members of the WOX1 and PRS subfamilies in arabidopsis (Vandenbussche et al. 2009; Nakata et al. 2012). In this case, *WOX1* and *PRS* expression overlaps and the phenotype of *wox1 prs* double mutants clearly shows that they also functionally overlap. In a series of other examples, it turns out that the protein sequences of different family members have retained similar capacities, even though their expression patterns have completely diverged and do not overlap anymore: For example, *WUS* is able to complement *prs* and *wox5* mutant phenotypes when expressed under their respective promoters (Ananda K Sarkar et al. 2007; Shimizu et al. 2009). More recently, Lin and colleagues (Lin, Niu, McHale, et al. 2013) showed that arabidopsis *WUS, WOX1, WOX2, WOX3, WOX4, WOX5* and *WOX6* were all able to complement leaf blade and floral developmental defects in the *Nicotiana lam1* mutant (*lam1* is the *Nicotiana wox1* homologue mutant) when expressed under the control of *Mt-STF* promoter [promoter of the Medicago *STENOFOLIA* gene (*WOX1* homolog)].

Together, this demonstrates that proteins of the WUS, MAW/WOX1, WOX2, PRS/WOX3, WOX4, and WOX5 subfamilies (together forming the WUS clade) still have some functional properties in common, despite their ancient origin. This further suggests that changes in *cis*-regulatory elements have constituted a major source of functional

diversification within the WUS clade, obviously without excluding the possibility that changes in the protein sequence might have also contributed.

In contrast, *WOX7, WOX9, WOX11* and *WOX13* were not able to complement the *lam1* mutant phenotype. Interestingly, all WOX proteins that were able to complement possess the WUS box (WUS clade), whereas all others lack this motif (Vandenbussche et al. 2009; Lin, Niu, McHale, et al. 2013), highlighting the importance of repressive activity linked to the WUSCHEL box for leaf blade expansion. This was further confirmed by the observation that chimeric WOX7, WOX9, and WOX13 proteins fused with either the WUS-box or an SRDX repressor domain could complement the *lam1* phenotype (Lin, Niu, McHale, et al. 2013). This shows that the acquisition of one or more transcriptional repressor domains in the members of WUS clade compared with the more ancient WOX9 and WOX13 subfamilies has been instrumental in gaining their central function in organizing cell proliferation for meristem maintenance and lateral organ development.

WOX **genes and Flower development: Concluding remarks**

Floral phenotypes thus far described for *wox* mutants include premature floral termination (*wus*), reduced lateral development of floral organs (MAW/WOX1 and PRS/WOX3 subfamilies), resulting in narrow organs with petal and carpel fusion defects, or the complete absence of flowering due to a defect in inflorescence meristem identity (*evergreen*, WOX9 subfamily). Except for the latter, the developmental defects found in the flower are part of a more general phenotype, which also includes defects in leaf blade expansion. Goethe (Goethe 1790; Coen 2001) proposed a long time ago that floral organs are in fact modified leaves, so it is perhaps not very surprising to find that *WOX* mutants are affected in both vegetative and floral development. Yet it is clear that nature has exploited *WOX* gene function during evolution for shaping floral architecture. Therefore, while the homeotic function of animal *HOX* genes is fulfilled in plant flowers by MADS-box

transcription factors, *WOX* genes contribute to general aspects of floral architecture and morphology. Classically, plant developmental biology has focused mainly on *Arabidopsis thaliana* as a model organism. Nevertheless, much of the progress made in our understanding of the function of different *WOX* genes comes from studies in different species. We consider this to be a strong argument in favour of the idea that plant developmental biology in general would benefit from a reorientation towards a more multi-model approach.

Acknowledgments

M.V. is funded by an ATIP-AVENIR grant (Centre National de la Recherche Scientifique). We are grateful to Million Tadege (Oklahoma State University) and his team for providing pictures of *lam1* and *stf* mutants in *Nicotiana* and *Medicago*. We would also like to thank the two anonymous reviewers, as well as the editor, for very helpful suggestions to improve the manuscript.

Update

Since the publication of this Review, some new papers have appeared concerning the role of *WOX* genes in plant and flower development. In Rice, the *DWT1* gene has been shown to code for a *WOX8/9* gene and to be involved in tiller development in this species: *DWT1* controls uniformity of multiple-tillers development and *dwt1* mutants display lateral tillers characterized by shorter internodes (W Wang et al. 2014). Uniformity of multiple tillers (reaching the same size of the main shoot) is an agronomical important trait that can be found in species like Rice, Barley, and Wheat (W Wang et al. 2014). This shows that another *WOX8/9* gene is involved in inflorescence architecture, similarly to *EVG* and *SOE* in Petunia. Interestingly, a *WOX8/9* orthologue has also been characterized outside

angiosperms (Zhu et al. 2014) in Norway spruce (*Picea abies*, gymnosperms), in which it is involved in embryo development (a role performed also in Arabidopsis). In Medicago, another member of the Rosidae, the *WOX3* gene *LFL* has been recently shown to play a role in flower development (Niu et al. 2015). The *lfl* flower is characterized by fusion defects of petals and sepals, and LFL acts as a transcriptional repressor also by interacting with the corepressor TOPLESS. Moreover, the genetic interaction with *STF* (a WOX1 subfamily gene) has been tested. However, with the possible exception of carpel development, no synergistic phenotype has been observed in the *stf lfl* double mutant (Niu et al. 2015). This is marking a difference with the synergistic interaction of *WOX1* and *PRS* in Arabidopsis. Here, genetic interactions look like the "negative" of Medicago, because *WOX1* and *WOX3* genes genetically interact in floral organs but not at the carpel level (Vandenbussche et al. 2009; Nakata et al. 2012).

Chapter III cover - SEM pictures of two Petunia floral buds. WT (up), and *maw mawb* mutant (bottom). Different structures are highlighted: Petals (red), carpels (green), anthers (yellow), ovules (blue).

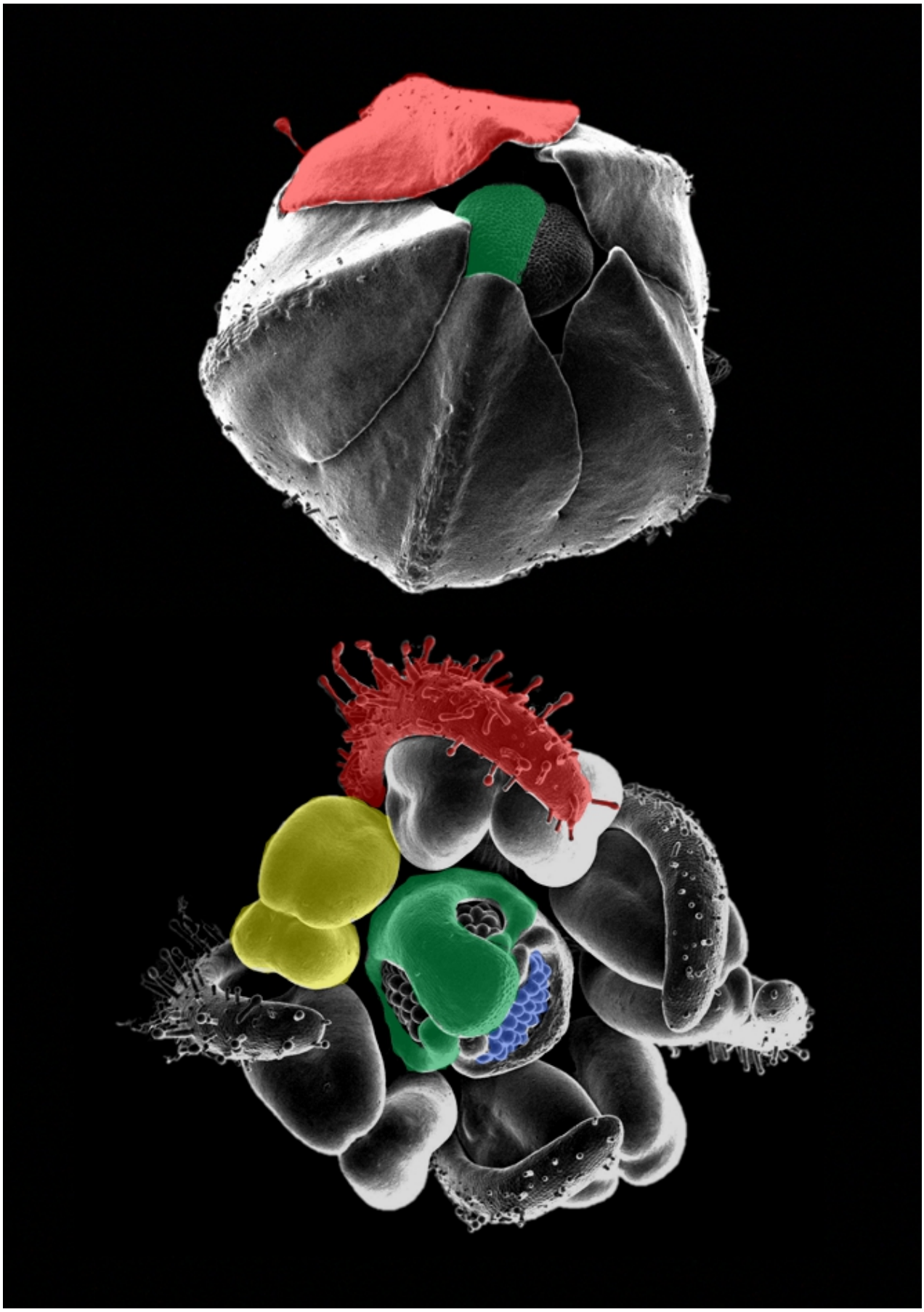

III. *MAW* and *MAWB* are involved in blade outgrowth and ovule development in Petunia

Enrico Costanzo[1,2], Patrice Morel[1], Pierre Chambrier[1] & Michiel Vandenbussche[1].

Abstract

WOX genes are involved in several aspects of plant development. The *MAW* gene has been previously shown as required for blade outgrowth in lateral organs in Petunia (Vandenbussche et al. 2009). Here, we report a second *WOX* gene from the same MAW/WOX1 subfamily, *MAWB*, and its functional interplay with *MAW* in blade expansion. We found that *MAWB* is expressed is a very similar pattern as *MAW*, suggesting a similar function in blade development. While *mawb* mutants display a WT phenotype, interestingly, we observed a gene dosage effect, along the gradient WT > *maw* > *maw MAWB* +/- > *maw mawb*, characterized by progressive reduction of the blade in all lateral organs. The *maw mawb* double mutant exhibits a severe impairment in blade outgrowth in all lateral organs, leading to complete disruption of the petal tube in the flower. Carpel fusion was also severely affected in the double mutant.

In addition, we found that the *maw mawb* mutant displays partial homeotic conversion of ovules into carpels. By means of different mutant combinations for *WOX1* and D lineage genes, we show full conversion of ovules into carpels in Petunia, similarly to the previously described *pMADS3 RNAi fbp7 fbp11* and *fbp6 fbp7 fbp11* mutants (Heijmans et al. 2012a). These findings identify *WOX1* genes as novel regulators of ovule identity.

[1]*Laboratory of Reproduction and Development of Plants, UMR5667, Ecole Normale Supérieure de Lyon, Lyon, FRANCE*

[2]*Istituto di Scienze della Vita, Scuola Superiore Sant'Anna, Pisa, ITALY*

Introduction

Several plant species, mainly belonging to the angiosperms, are characterized by an expanded leaf lamina, and several molecular players required for this process have been identified in Arabidopsis. However, little is known about the molecular mechanisms behind blade outgrowth in other species. Understanding the molecular mechanisms behind organs' architecture in different species is of key importance in plant evo-devo.

The role of the WOX1 subfamily in blade expansion

The *MAEWEST* (*MAW*) gene in Petunia was identified in a forward genetics screen for mutants displaying defects in petal fusion, and was shown to encode a member of the WOX1 subfamily of *WOX* genes (*Wuschel homeobOX*) (Vandenbussche et al. 2009). The *maw* mutant displays a partially disrupted petal tube, which is due to the failing ability of petals to expand laterally and consequently to fuse together in their distal region. A similar reduction in blade expansion is found in all lateral organs (leaves, sepals, petals, and carpels) in *maw*, therefore broadly affecting the plant phenotype (Vandenbussche et al. 2009). Such a phenotype is greatly enhanced in the double mutant *maw chsu*, which displays an almost complete disruption of the petal tube because of the extreme narrowing of petals (Vandenbussche et al. 2009).

Here, we show that the close homolog of *MAW* in Petunia, *MAEWESTB* (*MAWB*), is cooperating with *MAW* in blade expansion in lateral organs, producing dramatic defects in the double mutant *maw mawb*. In addition to defects in blade expansion in leaves, sepals, and petals, we observed that carpel and ovule development is also affected. *MAW* and *MAWB* are the two Petunia members of the WOX1 subfamily of *WOX* (*Wuschel-related HomeobOX*) genes, a plant specific branch of the homeodomain transcription factor family involved in variety of developmental processes (Costanzo et al. 2014). A similar phenotype in blade expansion had been previously described in the *lamiata1* (*lam1*) mutant (McHale

and Marcotrigiano 1998) in *Nicotiana sylvestris*. More recently the *LAM1* gene has also been identified as a member of the WOX1 subfamily (Tadege, Lin, Bedair, et al. 2011). Moreover, the *STENOFOLIA* (*STF*) gene in Medicago (orthologue of *MAW* and *LAM1*), has been shown to display narrow lateral organs (Tadege, Lin, Niu, et al. 2011; Zhang et al. 2014), indicating a strongly conserved role for *WOX1* genes in these species. Similarly, a classical *locus* in Pea, *LATHYROIDES* (*LATH*), known to affect lateral organ development, has also been shown to code for a WOX1 member (Zhuang et al. 2012). In Arabidopsis, the two genes in the WOX1 subfamily (*WOX1* and *WOX6*) do not display any phenotype in blade outgrowth neither as single or double mutants (Vandenbussche et al. 2009). Instead, the *wox1 prs* mutant, in which *PRS* (*PRESSED FLOWER*) is the only member of the WOX3 clade in Arabidopsis, display narrow leaves, petals, and sepals, showing that both the WOX1 and WOX3 subfamilies are involved in blade outgrowth in this species (Vandenbussche et al. 2009; Nakata et al. 2012). Blade expansion takes place thanks to proper cell proliferation along the axis going from the midrib to the margin (the mediolateral axis). Moreover, proper interaction of the adaxial and abaxial side of the leaf at the leaf margin is essential for blade expansion, to the point that a new domain of the leaf between the adaxial and the abaxial side, the so called "middle domain", has been proposed in that region (Nakata et al. 2012; Nakata and Okada 2012). In Arabidopsis, the expression domains of *WOX1* and *PRS* would define this third domain of the leaf, placed at a molecular "crossing point" between adaxial factors (*e.g.*, *HDZIP III, AS2*), abaxial factors (*e.g.*, *KANADI*), and middle abaxial factors such as *FILAMENTOUS FLOWER* (Nakata et al. 2012; Nakata and Okada 2012).

Expanding the role of *WOX* genes in Petunia

In addition to defects in blade expansion in floral organs and leaves, we also identified a new role for WOX1 subfamily genes in ovule development in Petunia. In Petunia, the D lineage genes *FBP7* and *FBP11* are involved in ovule identity redundantly with the *C* genes

FBP6 and *pMADS3* (Heijmans et al. 2012a). So called "*spaghetti*" mutants, displaying ovule to carpel conversion (hence the name, because of supernumerary, *spaghetti*-like carpels in the ovary), were obtained in co-suppression experiments of *FBP7* and *FBP*11 in Petunia, and overexpression of *FBP11* resulted in ectopic production of ovule-like structures (Angenent et al. 1995; Colombo et al. 1995). This was later analyzed in more detail, showing that "*spaghetti*" mutants are obtained when mutations in either one the two *C* genes are combined with the *fbp7 fbp11* double mutant (Heijmans et al. 2012a). Here we report that carpel-like structures partially replace ovules in *maw mawb* mutants. This phenotype is further enhanced when D lineage genes are also mutated. This identifies *WOX1* genes as a novel class of transcription factors involved in ovule identity determination.

Results

In silico **genome screening for novel *WOX* genes identifies *MAWB* as a second member of the WOX1 subfamily in Petunia**

Taking advantage of the availability of two parental genomes of *Petunia* x *hybrida* (*P. inflata* and *P. axillaris*), we searched all the *WUSCHEL* related sequences in these genomes. We identified seven new members of the family in Petunia (*MAWB, WOX2B, WOX3B, WOX5, WOX11, WOX13A, WOX13B*), raising the total number of WOX sequences to 14, a number comparable with Arabidopsis (15 WOX members in this species). Based on the alignment of the homeodomain (the highly conserved region responsible for DNA binding), we performed a phylogenetic analysis of the Petunia WOX family including sequences from other plant species (*Arabidopsis thaliana, Oryza sativa, Petunia* spp., *Populus trichocarpa, Sorghum bicolor, Vitis vinifera, Zea mays*). We observed that all sequences group into 9 different subfamilies (WOX3, WUS, WOX4, WOX2, WOX5, WOX1, WOX9, WOX11, WOX13), as also shown by previous studies (Nardmann et al. 2007; van der

Graaf et al. 2009; Vandenbussche et al. 2009) (FIG. 1). To further support the phylogenetic tree, at the level of lowly supported branches, we analyzed gene structure, since exon/intron number is highly conserved inside each subfamily (FIG. 1) (Vandenbussche et al. 2009).

MAWB groups with the WOX1/MAW subfamily, but similar to some other members of this subfamily, with bootstrap values below 65%, possibly due to the limited resolution power of the short homeodomain region used for the alignment. However, *MAWB* displays all structural characteristics of the WOX1 subfamily: Four exons, and conservation of all peptide motifs that are unique to *WOX1* genes (FIG. 1). We conclude therefore that Petunia contains in addition to *MAW* (hence the name *MAWB*), a second member of the WOX1 subfamily. For a full sequence alignment of MAEWESTB protein with other WOX1 sequences, see Annex III in Chapter VII (Materials and Methods).

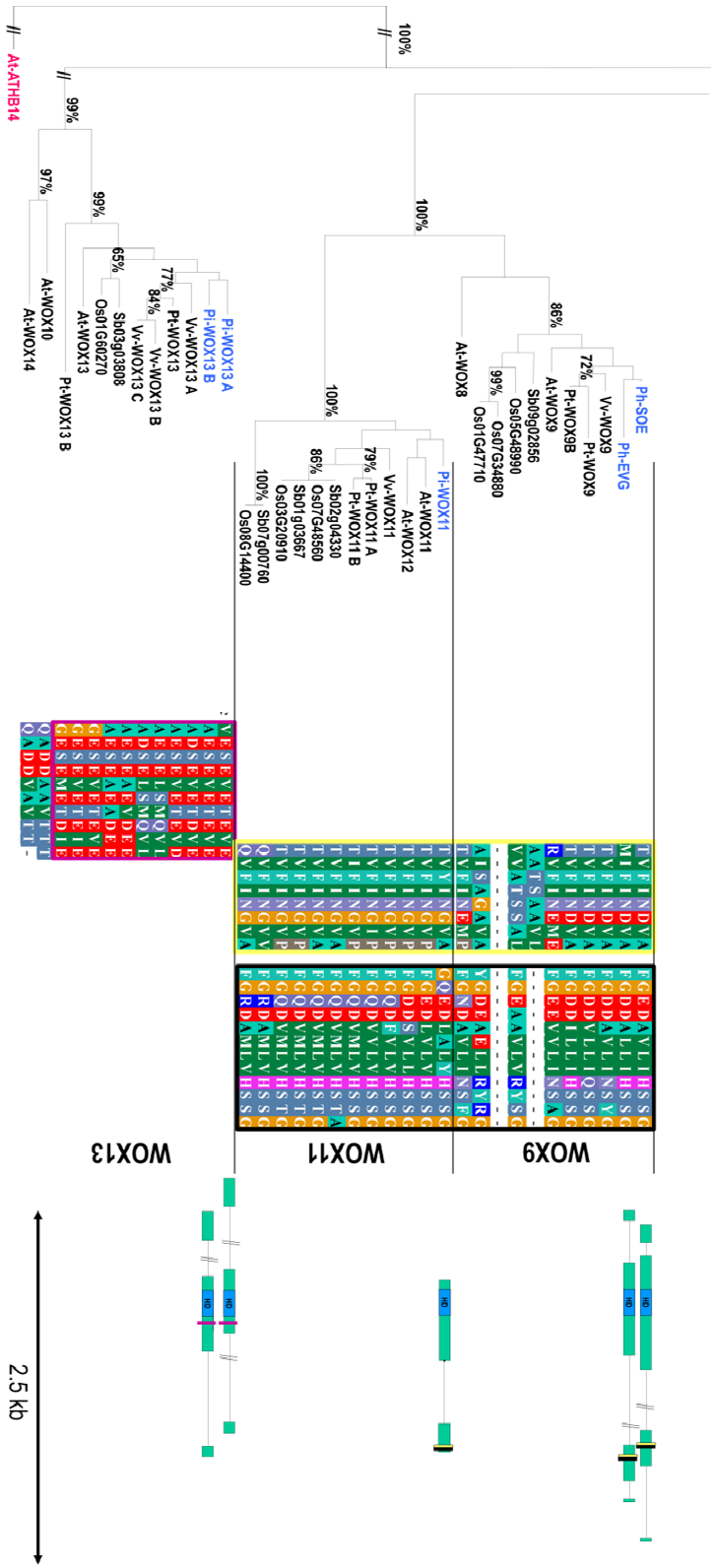
At-ATHB14
100%
99%
97%
At-WOX10
At-WOX14
99%
65%
Sb03g013808
Os01G60270
At-WOX13
Pt-WOX13 B
77%
Pt-WOX13
84%
Vv-WOX13 B
Vv-WOX13 C
Vv-WOX13 A
Pt-WOX13 A
Pt-WOX13 B
100%
100%
86%
At-WOX8
99%
Os05G48990
Sb09g02856
At-WOX9
72%
Pt-WOX9B
Vv-WOX9
Pt-WOX9
Ph-SOE
Ph-EVG
100%
Os08G14400
100%
Sb07g00760
Os03G20910
86%
Os07G48560
Sb01g03667
Sb02g04330
79%
Pt-WOX11 B
Pt-WOX11 A
Vv-WOX11
At-WOX12
At-WOX11
Pt-WOX11
Os01G47710
Os07G34880
WOX13
WOX11
WOX9
2.5 kb

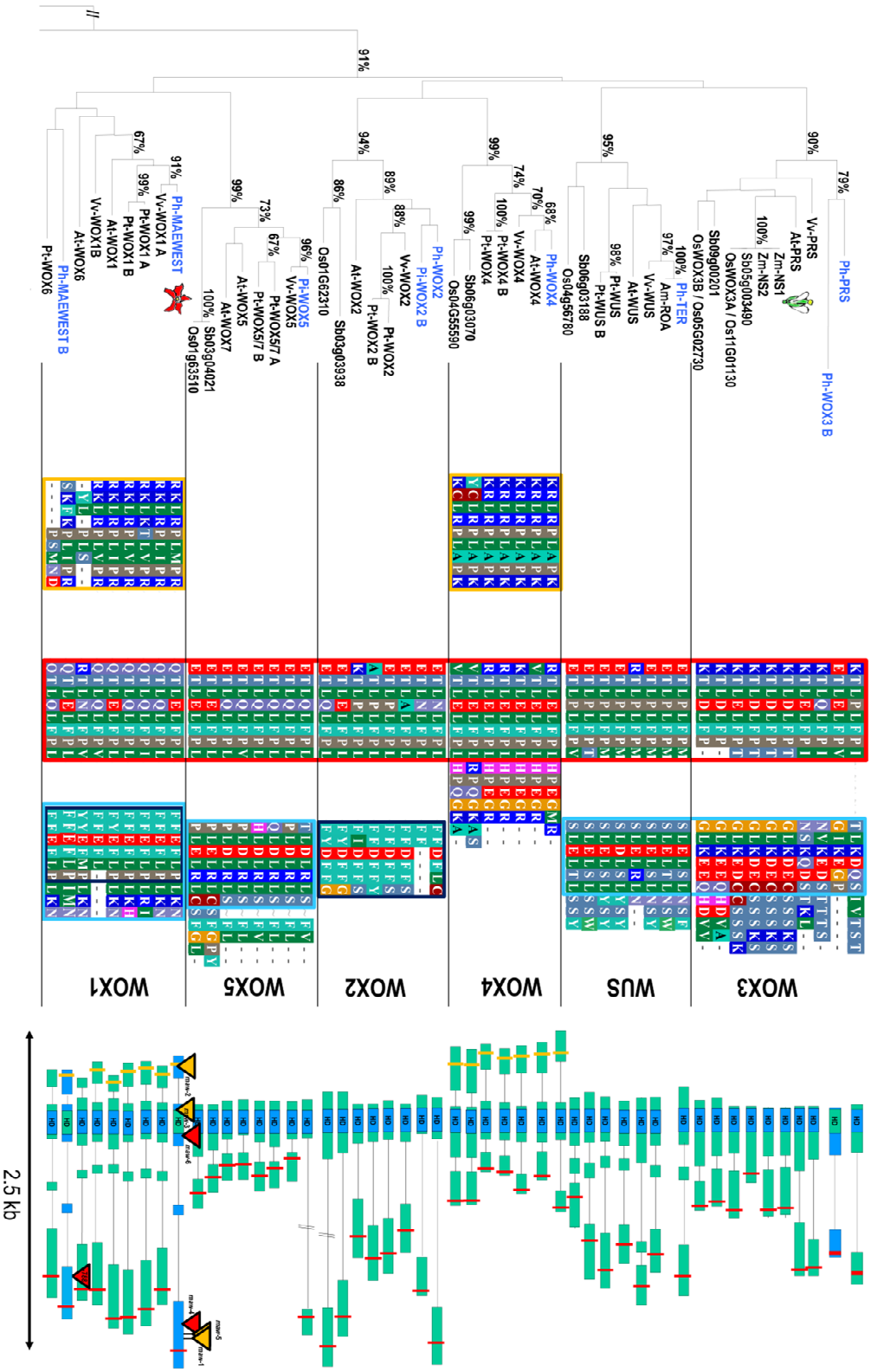
WUS box
WOX3
WUS
WOX4
WOX2
WOX5
WOX1
Ph-PRS
Ph-WOX3 B
Vv-PRS
At-PRS
Zm-NS1
Zm-NS2
Sb05g003490
OsWOX3A / Os11G01130
Sb09g002010
OsWOX3B / Os05G02730
Ph-TER
Am-ROA
Vv-WUS
At-WUS
Pt-WUS
Pt-WUS B
Sb06g03188
Os04g56780
Ph-WOX4
At-WOX4
Vv-WOX4
Pt-WOX4 B
Pt-WOX4
Sb06g03070
Os04G55590
Ph-WOX2
Pt-WOX2 B
Vv-WOX2
Pt-WOX2
At-WOX2
Sb03g03938
Os01G62310
Pt-WOX5
Vv-WOX5
Pt-WOX5/7 A
Pt-WOX5/7 B
At-WOX5
At-WOX7
Sb03g04021
Os01g63510
Ph-MAEWEST
Vv-WOX1 A
Pt-WOX1 B
Pt-WOX1
At-WOX1
Vv-WOX1B
At-WOX6
Ph-MAEWEST B
Pt-WOX6
2.5 kb

FIG. 1 Neighbor joining tree of the WOX family

The tree (left), is based on the highly conserved homeodomain region from WOX proteins from the following species: At, *Arabidopsis thaliana*; Os, *Oryza sativa*; Petunia spp. (Ph, *Petunia x hybrida* and Pi, *Petunia inflata*); Pt, *Populus trichocarpa*; Sb, *Sorghum bicolor*; Vv, *Vitis vinifera*; Zm, *Zea mays*. Only bootstrap values above 65% are shown. To further support the phylogenetic analysis, gene structures (right) are represented for some of the analyzed sequences, as shown in (Vandenbussche et al. 2009).

Petunia sequences were either cloned from *P.* x *hybrida*, or *in silico* identified in the *Petunia* x *hybrida* parental genomes (*P. inflata* and *P. axillaris*). In this case, the newly identified *WOX* genes were found in both the *P. inflata* and *P. axillaris* genome (strongly suggesting that they have also been retained in *P.* x *hybrida*). Only the *P. inflata* sequence is shown in the phylogenetic tree.

Inside each subfamily, gene structure is conserved in terms of exons/introns number. Well conserved short peptide motifs are also displayed (centre – conserved sequences, and right – position on gene cartoons). The WUSCHEL box is displayed in **red**; the *WOX1/4* -5' subfamily-specific box is displayed in **orange** (Vandenbussche et al. 2009).

Other conserved regions already described in (Vandenbussche et al. 2009) are shown, including the *3'c WOX1* / STF box (Vandenbussche et al. 2009) (**light blue**) (Zhang et al. 2014). *Loci* of *dTph1* insertions are displayed for mutant alleles used in this study (red triangles), and for other mutant alleles available from the in-house collection (orange triangles). Scale bar is 2.5 Kb.

Because of the important role played by *MAW* in blade expansion and petal fusion, and the close phylogenetic relationship of *MAWB* with *MAW*, we considered *MAWB* as an interesting target for functional analysis in Petunia.

Expression pattern of *MAWB*

By means of *in situ* hybridization, we analyzed the expression pattern of *MAW*B in floral and shoot apical meristems (FIG. 2). *MAWB* is expressed in the middle region of young polar organs at the flower (FIG. 2A) and shoot level (FIG. 2C). This expression pattern is very similar to *MAW* (FIG. 2B), as described in (Vandenbussche et al. 2009). Like *MAW* expression pattern, two expression *foci* are visible in the margins of young polar organs in *MAWB in situs* (FIG. 2B, arrow). We also detected expression of *MAWB* in developing carpels and in the above part of the placenta tissue (FIG. 2D, E).

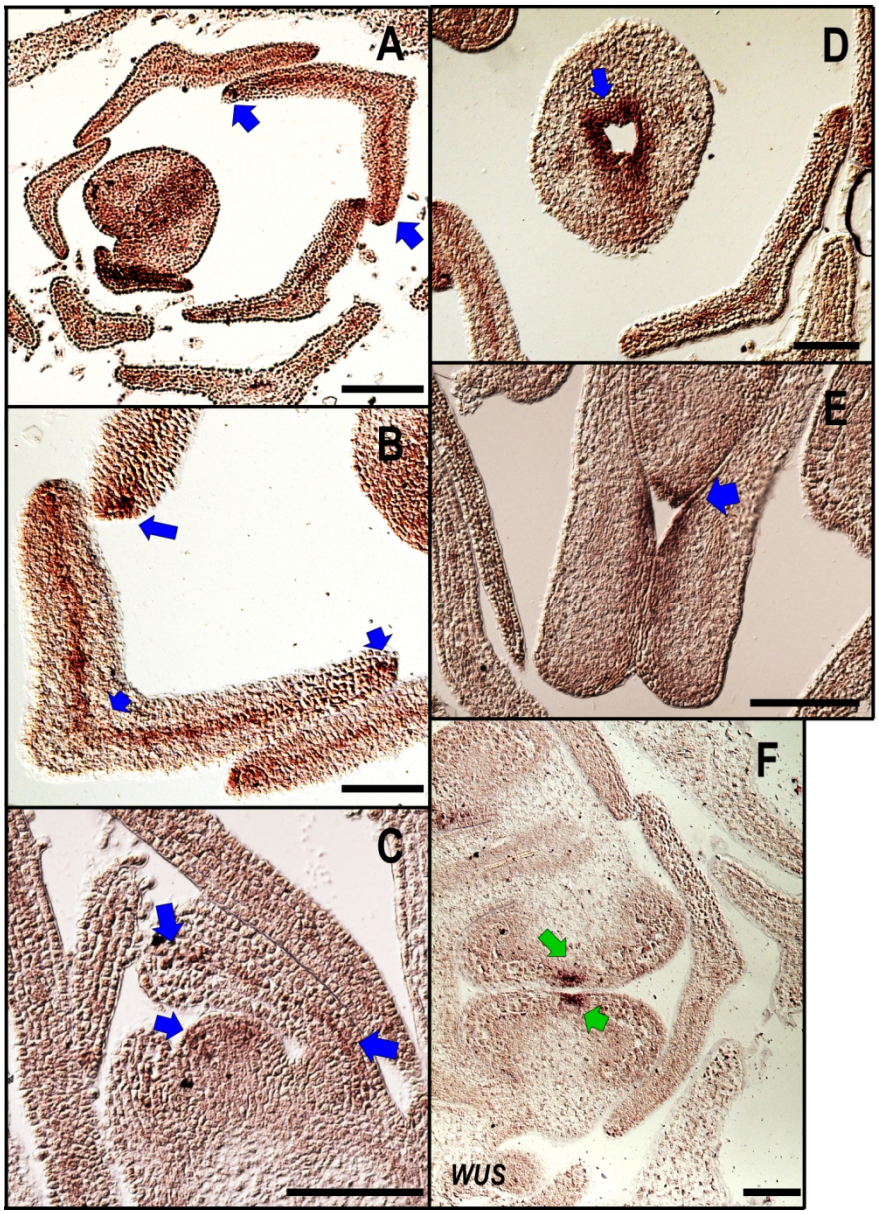

FIG. 2 *MAWB in situ* hybridization

In situ hybridization for *MAWB* showing its expression pattern on flower and shoot apical meristems. **A** – Lateral section of a flower primordium. *MAWB* is expressed in the middle domain of young floral organs, with two expression *foci* along the margin (arrows). **B** – Lateral section of young petal, showing *MAWB* expression domain in the middle zone of the organ and in lateral *foci* (arrow). **C** – Shoot apical meristem, longitudinal section. *MAWB* is expressed along the middle domain of young primordia and at the site of primordia origin

(arrows). **D** – Lateral section of young pistil. *MAWB* is expressed in a ring on the internal side (arrow) of the upper part of the pistil, corresponding to the style region. **E** – Longitudinal section of a developing gynoecium. In addition to the expression pattern on the internal side of carpels, a peak of expression is also visible at the top of the placental tissue (arrow). **F** – *WUS* expressed in the *stomium* of anthers is shown as control. Scale bars: 200 μm (**A**), and 100 μm (**B**, **C**, **D**, **E**, and **F**).

mawb mutants display a WT phenotype

To analyze the function of *MAWB*, we screened our sequence-indexed *dTph1* transposon collection for insertions into *MAWB*. We identified a single candidate insertion, and were able to confirm *in planta* a *dTph1* insertion located in the fourth exon of *MAWB* (*mawb*-788 allele, see gene cartoon in FIG. 1), 788 bp downstream of the ATG in the coding sequence. This insertion is located upstream of the WUS box, previously shown as fundamental for proper *WOX* activity. This suggests that the resulting mutant may be a full knock-out. However, we didn't observe any phenotype different from WT, in *mawb* mutants (FIG. 3), suggesting functional redundancy with other genes. Alternatively, the *mawb* mutant obtained from the transposon collection is not a real knock-out. We considered this second hypothesis unlikely because of the position of the insertion, which eliminates the functionally important WUS box.

MAWB is redundantly involved with *MAEWEST* in lateral organ development

The expression patterns of *MAW* (Vandenbussche et al. 2009) and *MAWB* are extremely similar, since both are expressed in the middle region of lateral organs and in two *foci* at the margins (FIG. 2). Moreover, *MAWB* is the only other member of the WOX1 subfamily in Petunia, along with *MAW* (see FIG. 1). When looking for possible redundancy, it is logical to test closely related genes as possible candidates in a first attempt. Therefore, we tested genetic interaction with *MAW* by obtaining double mutant plants for *MAW* and *MAWB*. We used two different, independent alleles of *MAW*: *maw*-4 and *maw*-6 (FIG. 1), already described in (Vandenbussche et al. 2009). Interestingly, we observed an

increased *maewest* phenotype already in *maw MAWB* +/- plants (FIG. 3 to 6), and a dramatic phenotype in the double, homozygous mutant (FIG. 3 to 6). A gradual phenotype can be observed in both leaves and floral organs, suggesting gene dosage effect.

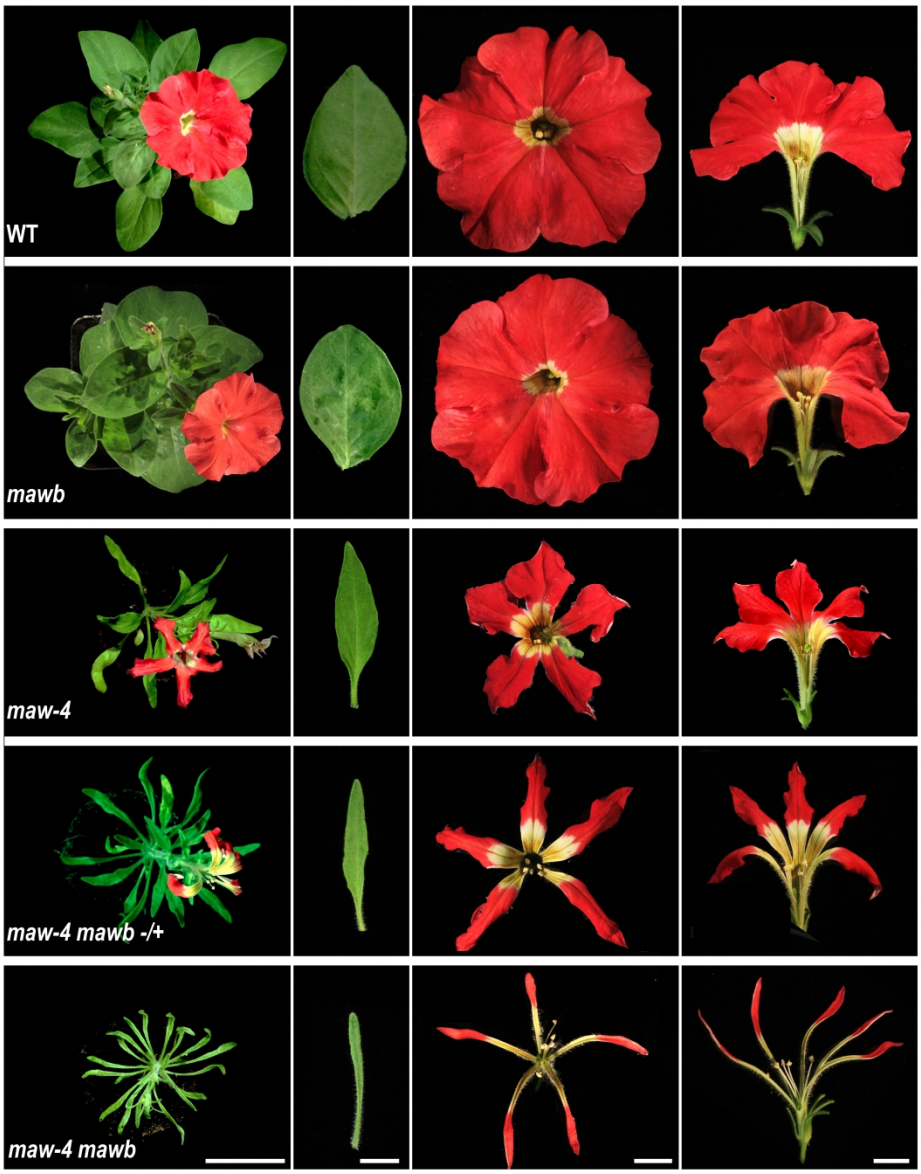

FIG. 3 Mutant flowers and leaves on *Petunia* x *hybrida* W138 background

Rosettes, leaves, flowers (top and lateral view) are shown from WT*, mawb, maw*-4*, maw*-4 *mawb* -/+*, maw*-4 *mawb* W138 plants. Progressive increase of the mutant phenotype can be observed along the gradient WT > *maw* > *maw MAWB* +/- > *maw mawb*. Scale bars: Rosettes 5 cm, leaves 1 cm, flowers 1 cm.

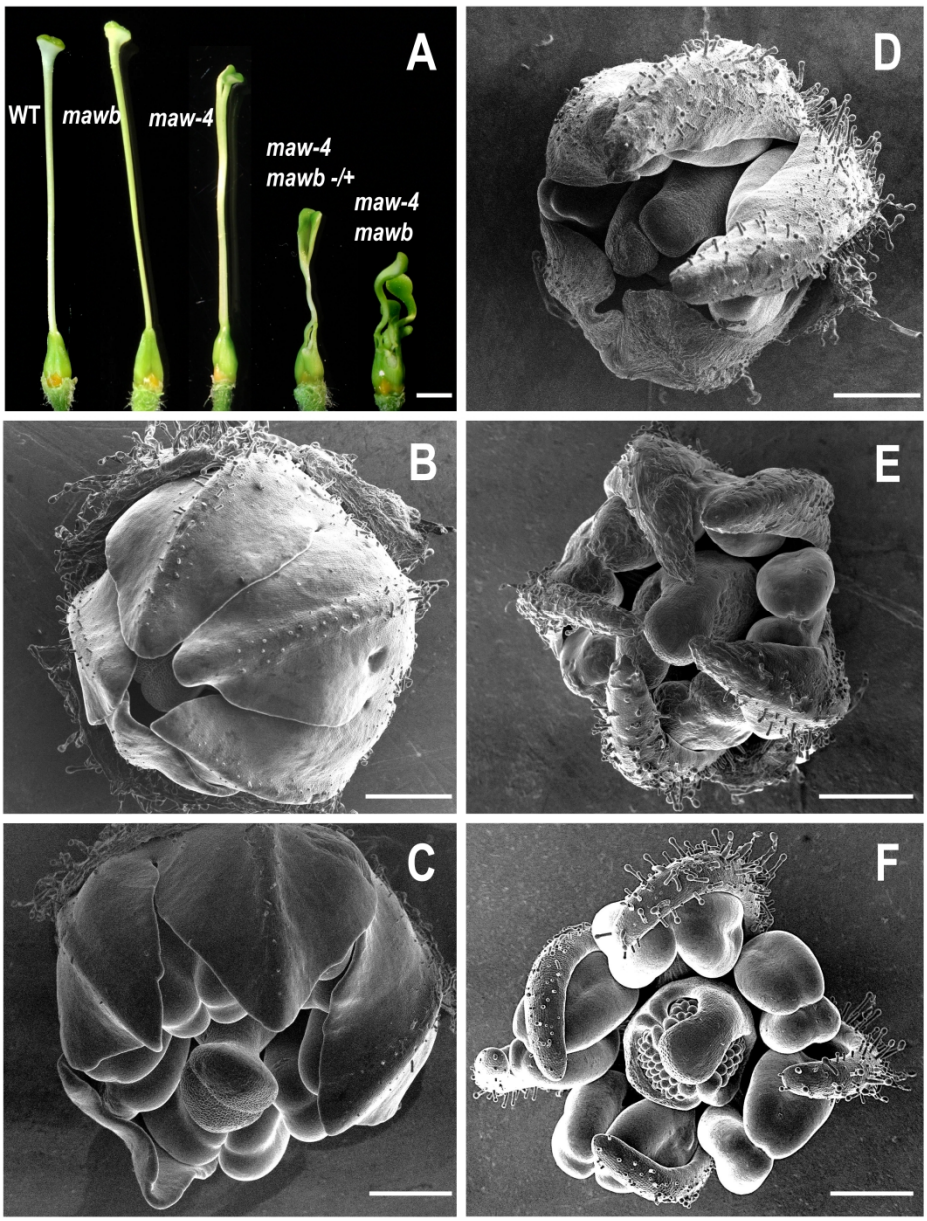

FIG. 4 Mutant carpels and floral buds on *Petunia* x *hybrida* W138 background

A – Carpels from WT*, mawb, maw*-4*, maw*-4 *mawb* -/+*, maw*-4 *mawb* W138 plants are shown (from left to right), displaying progressive shortening and separation of

carpels. Scale bar: 25 mm. **B** – SEM picture of a WT floral bud. **C** – SEM picture of a *mawb* floral bud. **D** – SEM picture of a *maw*-4 floral bud. **E** – SEM picture of a *maw*-4 *maw* -/+ floral bud. **F** – SEM picture of a *maw*-4 *mawb* floral bud. Scale bars for SEM pictures: 250 μm. Sepals have been removed in B-F prior to analysis.

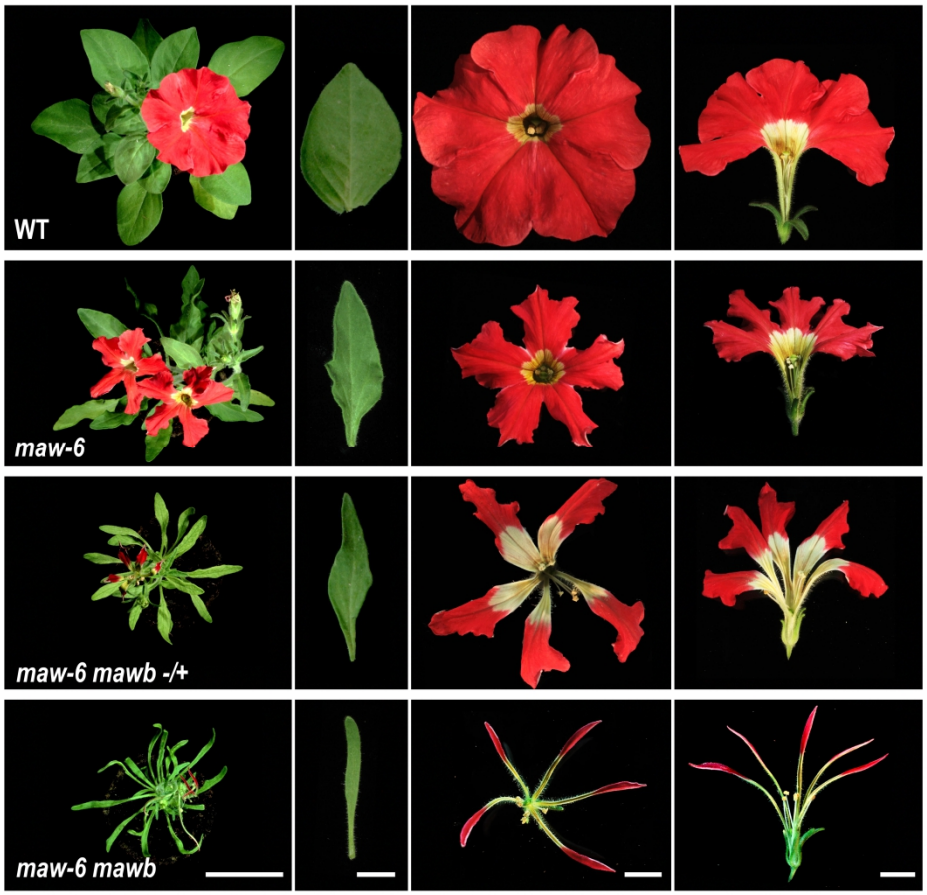

FIG. 5 Additional phenotypes of mutant flowers and leaves on *Petunia* x *hybrida* W138 background

Rosettes, leaves, flowers (top and lateral view) from WT*, maw*-6*, maw*-6 *mawb* -/+*, maw*-6 *mawb* W138 plants are shown. Progressive increase of the mutant phenotype can be observed along the gradient WT > *maw* > *maw MAWB* +/- > *maw mawb*. Scale bars: Rosettes 5 cm, leaves 1 cm, flowers 1 cm.

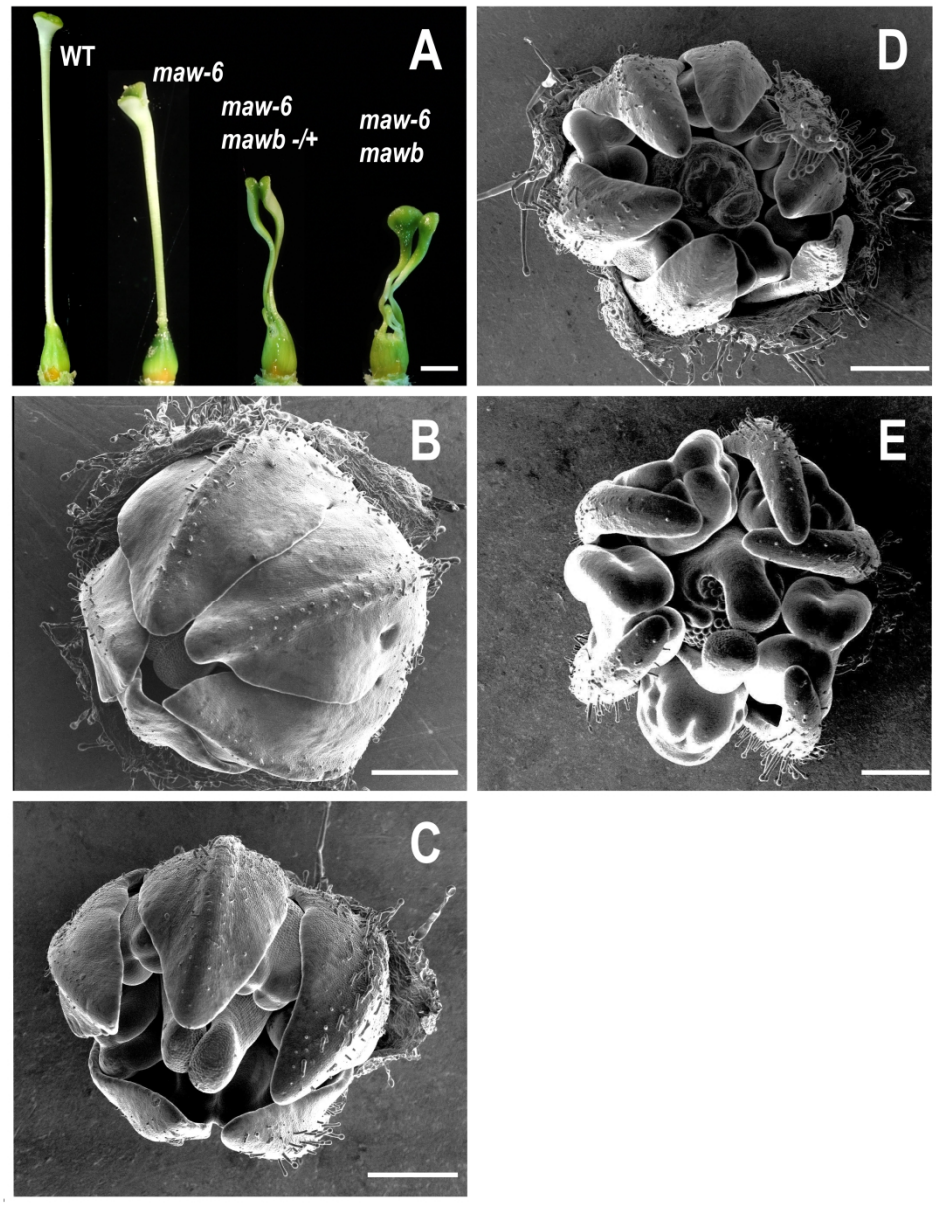

FIG. 6 Additional phenotypes of mutant carpels and floral buds on *Petunia* x *hybrida* W138 background

A – Carpels from WT, *maw*-6, *maw*-6 *mawb* -/+, *maw*-6 *mawb* shown (from left to right) W138 plants are shown, displaying progressive shortening and separation of

carpels. Scale bar: 25 mm. **B** – SEM picture of a WT floral bud. **C** – SEM picture of a *maw*-6 floral bud. **D** – SEM picture of a *maw*-6 *maw* -/+ floral bud. Scale bars for SEM pictures: 250 μm. **E** – SEM picture of a *maw*-6 *mawb* floral bud. Sepals have been removed in B-E prior to analysis.

We found that a phenotypic gradient can be observed in WT > *maw* > *maw MAWB* +/- > *maw mawb* plants. For instance, leaf lamina is progressively smaller till almost disappearing in the homozygous double mutant (FIG. 3 and 5). The same can be observed for petals and sepals (FIG. 3 to 6). This dosage effect of *MAW/MAWB* is interesting, since mutations often affect gene functionality in a yes/no fashion. Moreover, the fact that the *mawb* mutant is phenotypically WT while *maw* mutants display already a phenotype, indicates that upon duplication of the *MAW/MAWB* ancestor, an asymmetric sub-functionalization process took place, resulting in functional differences among the two duplicated genes. A phenotypic gradient can equally be observed in carpels from WT > *maw* > *maw MAWB* +/- > *maw mawb* plants, since carpels are progressively shorter and unfused. In *maw mawb,* carpels are extremely short and completely unfused, displaying naked ovules (FIG. 4F, and FIG. 6E).

maw mawb **mutants are affected in mediolateral polarity**

The phenotype observed in *maw mawb* mutants is very similar to the *lam1* mutant in Tobacco (McHale and Marcotrigiano 1998). In both *maw mawb* and *lam1*, leaf blade is virtually absent, meaning that *LAM1* in *N. sylvestris*, and *MAW* and *MAWB* in Petunia are required for blade dorso-ventrality or, which is the same, for the mediolateral polarity of the entire leaf. In fact, only the medial region of lateral organs develops properly (FIG. 7 and FIG. 8). In this region, adaxial-abaxial polarity is locally conserved. This is confirmed by the persistence of trichomes on the abaxial side of petals (FIG. 4, F, H) and their absence on the adaxial side (FIG. 7, E, G), exactly as in WT organs (FIG. 7A, C and B, D).

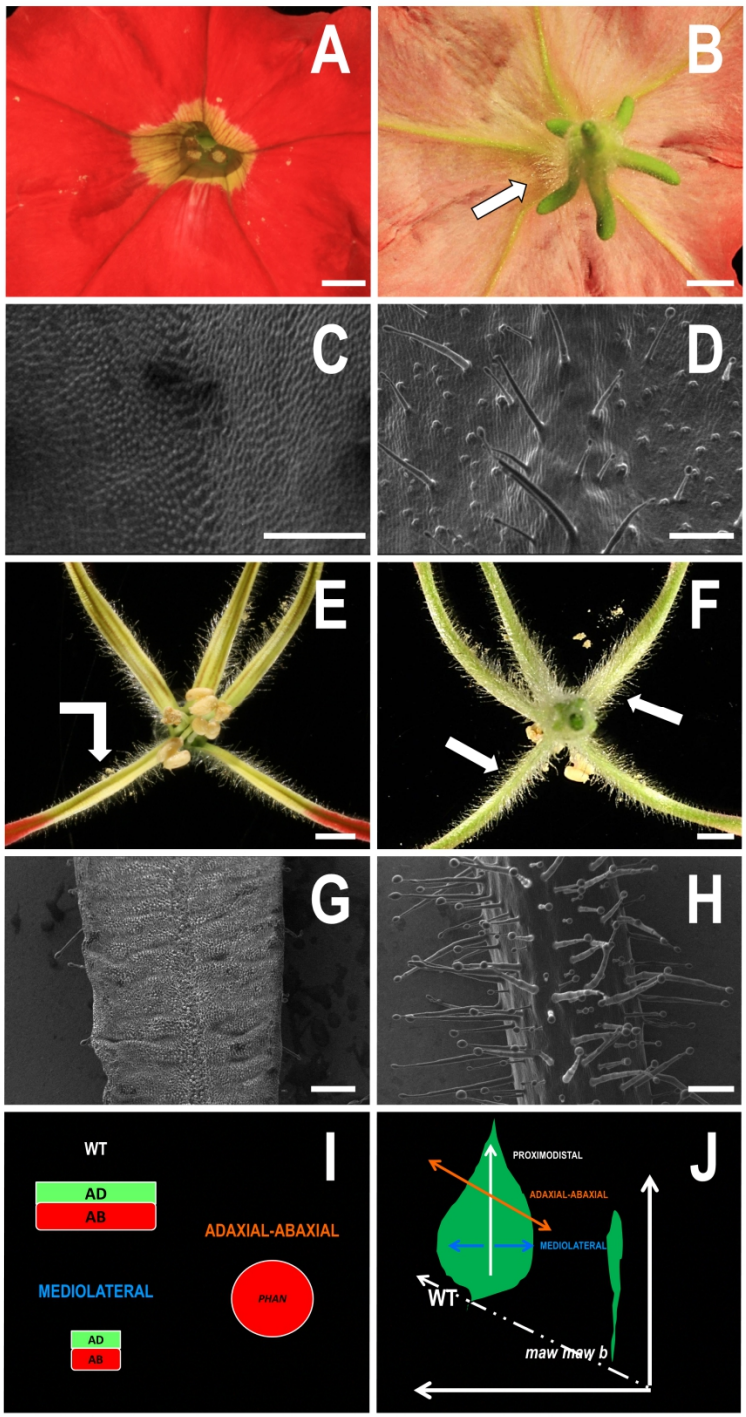

FIG. 7 Comparison of WT and *maw mawb* organs

Only the medial region develops in *maw mawb* mutants, in which adaxial-abaxial polarity is locally conserved. WT petals, adaxial (**A**, **C**) and abaxial sides (**B**, **D**) are shown in pictures (**A**, **B**) and SEM images (**C**, **D**) are shown for comparison with *maw mawb* petals, adaxial (**E**, **G**) and abaxial sides (**F**, **H**); photographic pictures (**E**, **F**) and SEM images (**G**, **H**). Scale bars: 50 mm photographs, 250 µm SEM pictures. **I** – Cartoon sections illustrating WT lateral organs, and organs affected in adaxial-abaxial (extreme *phantastica* phenotype) and mediolateral polarity (*e.g.*, *lam1*), are shown. WT lateral organs, such as leaves, are characterized by an expanded lamina composed by an adaxial an abaxial side. Fully abaxialized (or adaxialized) organs tend to be round, because of the absence of the other layer. Blade mutants (mediolateral polarity mutants) display a central part in which adaxial-abaxial polarity is locally conserved. However, the blade itself has disappeared. **J** – Relative position in the space of the three different types of polarity axes, with reference to WT and *maw mawb* leaves. The proximodistal axis extends from the tip to the base of the leaf. The adaxial-abaxial axis goes from the side up (close to the meristem) to the side down (opposed to the meristem) (equivalent to the dorsoventral axis in animals). The mediolateral axis extends from the mid region of the leaf to the leaf margins.

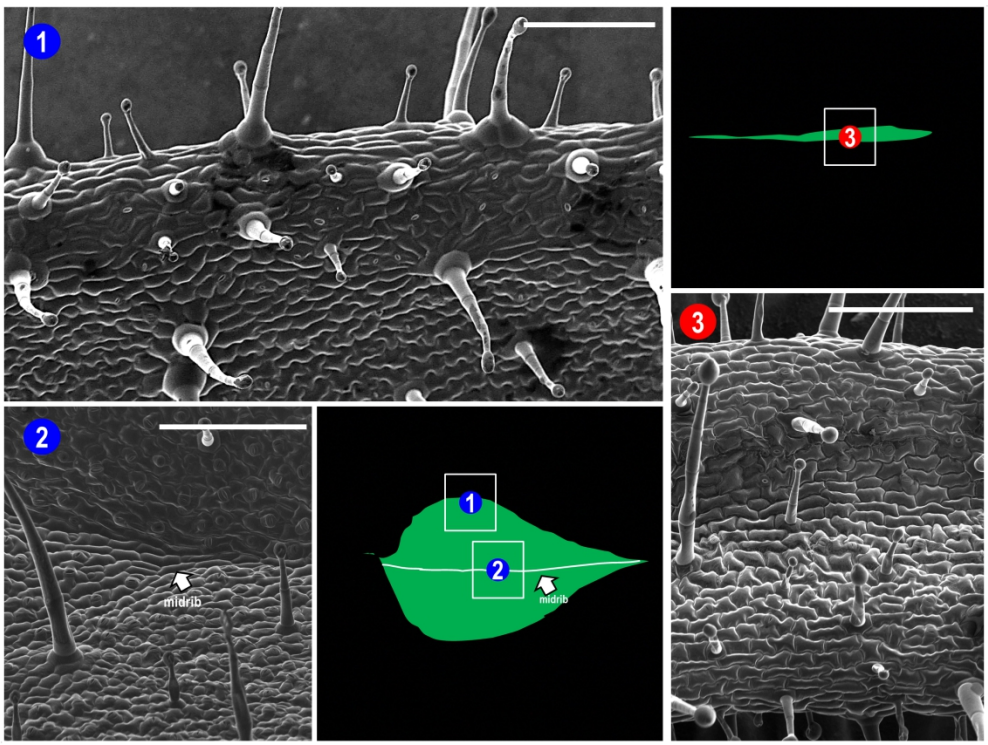

FIG. 8 Cell shape of leaf surface in WT and *maw mawb*

Cell types at the leaf margin (1) of WT leaves are elongated. Elongated cells are also visible in the midrib of WT leaves (2). Between the margin and the midrib, jigsaw cells cover the blade surface. In *maw mawb* (3) mainly one kind of cells is visible: Irregular cells partly elongated along the proximo-distal axis.

maw mawb **mutants are affected in carpel and ovule development**

We also observed supernumerary, small carpels in *maw mawb* mutants (FIG. 8E and F, white arrows). This is consistent with the observed expression pattern of *MAWB*, which expressed also in the marginal region of the *placenta*, from which ovules normally develop (FIG. 2E). We analysed these structures more in detail, finding small carpels emerging from the centre of the ovary (FIG. 8F and G). This suggests homeotic conversion of ovules into carpels. This phenotype has already been described in Petunia, and plants displaying ovule-to-carpel conversion had been called "*spaghetti*-mutants" because of the shape of converted structures (Angenent et al. 1995; Colombo et al. 1995; Heijmans et al. 2012a). Further observation of ovules using electron microscopy showed phenotypical differences between WT (FIG. 8D) and mutant (Fig. 8H) ovules. In fact, intermediate, hybrid structures between ovules and carpels can be observed (FIG. 8H, white arrow). Notably, abnormal ovules were mostly found at the tip of the ovary, whereas most of the ovules at the base of the ovary were WT-looking (FIG. 8C and G).

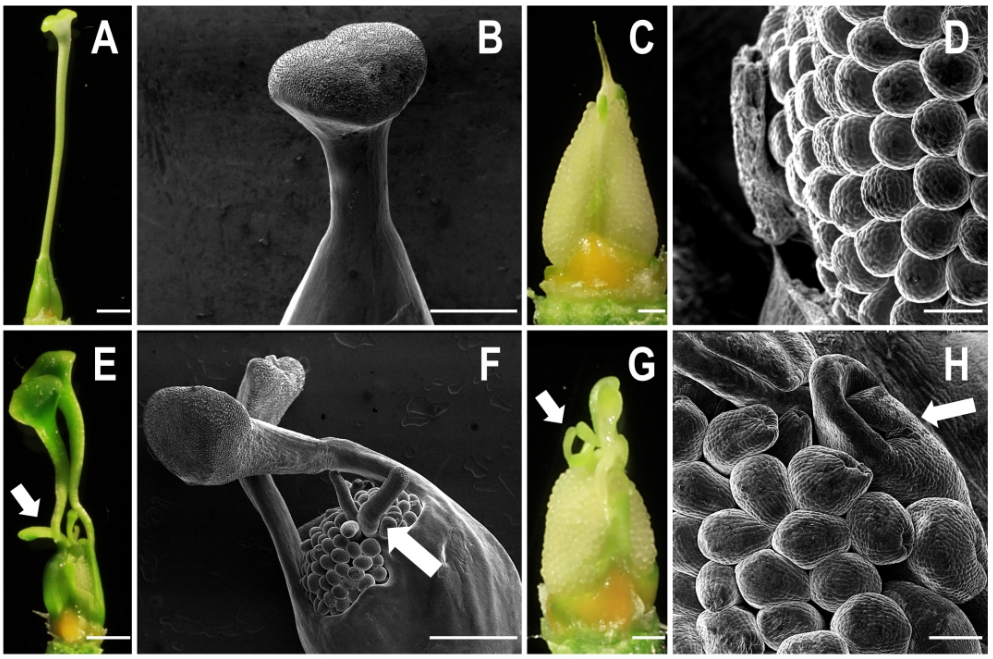

FIG. 8 Phenotypes of WT and *maw mawb* ovules and carpels

WT carpels (**A**) and close up of the WT stigma at the SEM (**B**) are compared with *maw mawb* carpels (**E**) and close up at the SEM (**F**). Note the splitting and shortening of carpels in **E** and **F**. Scale bars: **A**, **E** – 2.5 mm; **B**, **F** – 500 μm. Mutant ovaries display small supernumerary carpels (white arrows in **B** and **F**). These structures likely derive from ovules (**F**, and **G**, white arrows), and are absent in WT ovaries (**C**). SEM analysis of WT (**D**) and *maw mawb* ovules (**H**). Morphological differences between the two, including intermediate structures resembling "carpelloid ovules" are highlighted (**H**, white arrow). Scale bars: **C**, **G** – 500 μM; **D**, **H** – 100 μm.

***MAW* and *MAWB* are involved in defining ovule identity along with D lineage genes**

In Petunia, D lineage genes (*FBP7* and *FBP11*) are involved in ovule development together with *C* genes (*FBP6* and *PMADS3*). In fact, *fbp7 fbp11* double mutants are not impaired in ovule identity, with the exception of rarely converted ovules usually found at the top of the *placenta*. At the same time, both *pMADS3-RNAi fbp7 fbp11* and *fbp6 fbp7 fbp11* mutants display full ovule-to-carpel conversion (Heijmans et al. 2012a). Since *maw mawb* also displays ovules converted into carpels, we looked for possible genetic

interactions between WOX1 subfamily genes (*MAW* and *MAWB*) and D lineage genes (*FBP7* and *FBP11*). To further support our analysis, we used the two *MAW* alleles *maw*-4 and *maw*-6 and crossed *maw mawb* with *fbp7 fbp11* double mutants. We analysed the F_2 progeny, in which mutations for the four genes were segregating, observing different phenotypes. A selection of informative genotypes/phenotypes is shown in FIG. 9. Although we didn't obtain a quadruple mutant in the F_2 population analyzed, we already observed full ovule-to-carpel conversion ("*spaghetti* mutants") in *maw*-4 *fbp7 fbp11* (FIG. 9D) and *maw*-6 *MAWB* +/- *fbp7 fbp11* (FIG. 9E). This phenotype is identical to the one previously described in *pMADS3-RNAi fbp7 fbp11* mutants (FIG. 9F) (Heijmans et al. 2012a). Although we observed converted carpelloid structures in *maw*-6 *mawb fbp7* (FIG. 9C), we didn't observe a phenotype different from the one of *maw mawb* double mutants (FIG. 8G). *fbp7 fbp11* mutants display a WT phenotype in ovules (Heijmans et al. 2012a), similarly to *MAW*-6 +/- *mawb fbp7 fbp11* mutants (FIG. 9B), which also display a WT phenotype (FIG. 9A). Moreover, this shows that even in ovules, the role of *MAWB* is probably less relevant than *MAW*, as previously found for other lateral organs.

We further noticed that carpelloid structures are phenotypically identical to functional carpels. This is suggested by the observation that phenotypically normal *papillae* are visible on the stigmatic side of converted carpels (FIG. 9G).

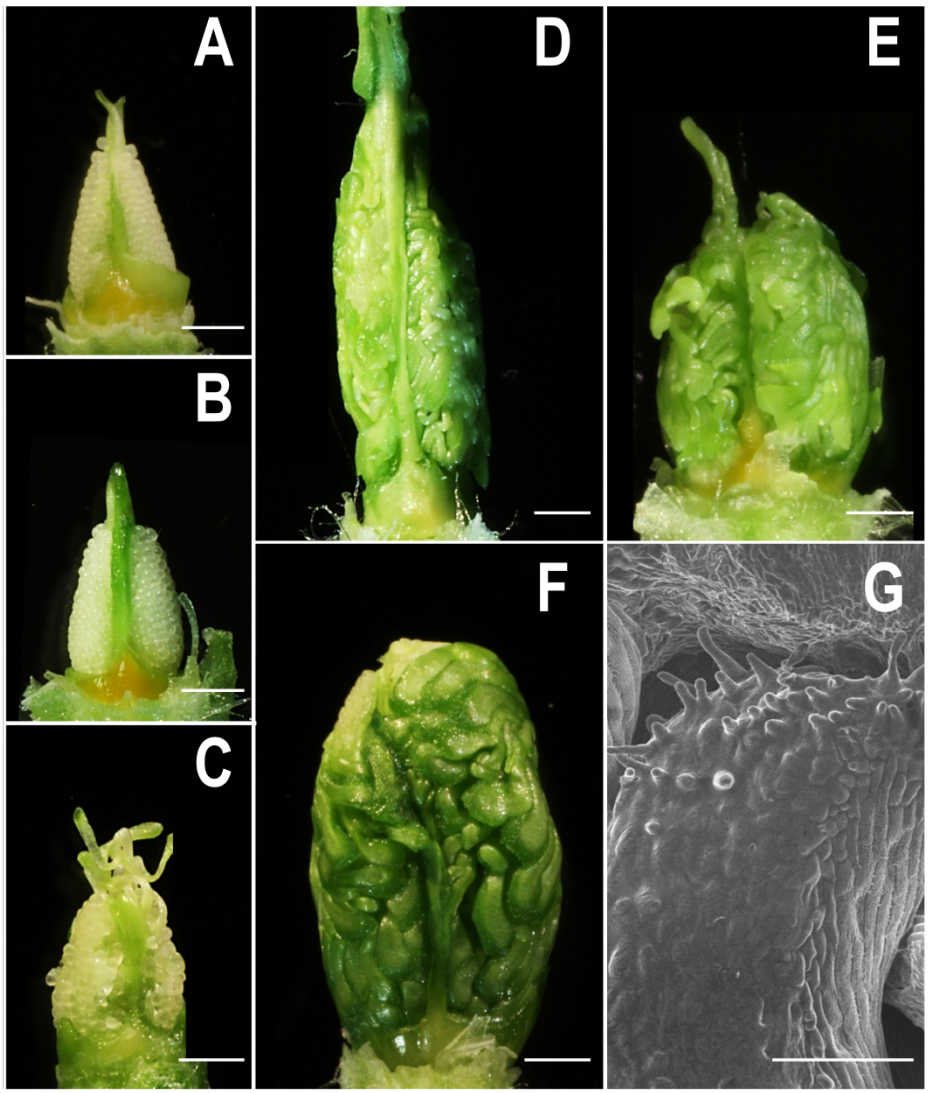

FIG. 9 Selection of informative genotypes/phenotypes from *WOX1/MAW* and D lineage genes mutant combinations (ovaries)

A to **F** – Ovary phenotypes in relevant mutant backgrounds. Scale bars: 1 mm. **A** – WT phenotype (quadruple heterozygous, displaying WT phenotype). **B** – *MAW*-6 +/- *mawb fbp7 fbp11* (Mitchell background). **C** – *maw*-6 *mawb fbp7* **D** – *maw*-4 *fbp7 fbp11* (Mitchell background). **E** – *maw*-6 *MAWB* +/- *fbp7 fbp11* (Mitchell background). **F** – *pMADS3*-RNAi *fbp7 fbp11* mutant (Mitchell background) [as in (Heijmans et al. 2012a)]. **G** – SEM picture of *papillae* on converted carpels. Scale bar: 100 μm.

Discussion

WOX genes are nowadays considered as major players in plant organ growth and development, from stem cells maintenance in various organs and tissues (shoot, root, cambium), till architecture in inflorescence and flower organs [see (Nardmann and Werr 2006; Costanzo et al. 2014)]. In this paper, we have characterized the role of a new member of the WOX1 subfamily in Petunia, *MAWB*, and discovered a new role for *WOX1* genes in ovule identity.

We first performed an *in silico* screening, searching all the *WOX* representatives in the Petunia genomes and discovering new members, raising their total number to 14 (comparable to Arabidopsis). We then confirmed that WOX sequences from different and distant-related eudicots can be clustered into 9 different subfamilies (FIG. 1), as shown by previous studies (Nardmann et al. 2007; van der Graaf et al. 2009; Vandenbussche et al. 2009). We focused our attention on *MAWB*, the second member of the WOX1 subfamily in Petunia, investigating its functional role by means of transposon-based mutagenesis. Although the *mawb* single mutant does not display any evident phenotype, its expression pattern (FIG. 2) was overlapping with the one previously described for *MAW* (Vandenbussche et al. 2009), suggesting a possible functional overlap between these two genes. In this direction was also the fact that the WOX1 subfamily in Petunia is composed only by two members, *MAW* and *MAWB* (FIG. 1). The expression patterns of *MAW*/*MAWB* indeed are close to the previously described expression domains of *PRS* and *WOX1* in Arabidopsis. In fact, *PRS* is specifically expressed in two lateral *foci* at the margin of young organs, and *WOX1* is more widely expressed along the middle zone of young polar organs (Nakata et al. 2012). Similarly, *MAW* and *MAWB* are expressed in the middle zone of lateral organs and in their margins as specific spots (FIG. 2). We additionally found a defined *MAWB* expression domain in developing carpels and gynoecia. Altogether, these data were strongly suggesting a similar role for *MAW* and

MAWB. We proceeded obtaining the double mutant *maw mawb* that displayed extreme narrowing of lateral organs, with completely unfused, string-like petals. A phenotypic gradient could be observed in WT > *maw* > *maw MAWB* +/- > *maw mawb* plants (FIG. 3 and FIG. 5), illustrating the importance of *MAW*/*MAWB* gene dosage in the control of blade outgrowth.

We reasoned that the extreme narrowing of organs in the double mutant was due to a defect in polarity. In lateral organs, three axis of polarity can be described: Proximo-distal (from the base to the tip), adaxial-abaxial (the back and the front), and mediolateral (from midrib to the margins). Since blade outgrowth is clearly affected, defects in mediolateral polarity (or, which is the same, in blade dorso-ventrality) were probably responsible for the narrowing of the lamina, in a similar way to what previously described in the *lam1* mutant in *N. sylvestris* (McHale and Marcotrigiano 1998), not known to be a *WOX1* gene when it was discovered. Accordingly, we observed that recognizable adaxial and abaxial sides were still present in narrow organs, such as petals (FIG. 7), showing that the midrib develops properly on the basis of an adaxial and abaxial orientation. *lam1* represents a much stronger phenotype than the *maw* single mutant in Petunia, but very comparable with *maw mawb*. In accordance with this observation, *LAM1* is the only WOX1 sequence in the *N. silvestris* genome and cds database. Therefore, *LAM1* in *N. sylvestris* probably still retains functions that in Petunia have sub-functionalized among *MAW* and *MAWB*. Several *WOX* genes are involved in flower and inflorescence development [see (Costanzo et al. 2014)], and the lacking of petal blade expansion in *WOX* mutants results in partial disruption of flower architecture among different species (Arabidopsis, Medicago, Petunia, *Pisum sativum*, *N. sylvestris*). Consequently, defects in petal tube (because of the failing ability of petals to fuse together), can be observed among *wox* mutants in species in which the petal tube is present (McHale and Marcotrigiano 1998; Vandenbussche et al. 2009; Zhuang et al. 2012; Niu et al. 2015).

Comparison between the WOX1 and WOX3 subfamilies

Genes from the WOX3 subfamily (different from the WOX1 subfamily of *MAW*, *LAM1* and *STF*), play also a role in lamina expansion, in particular in Poaceae, in which the WOX1 subfamily is absent. The *narrow sheat (ns)* mutant (Scanlon et al. 1996) in maize is specifically affected in lamina expansion, displaying narrow leaves, and a similar phenotype has been described in the *nal2 nal3* double mutants in rice (Cho et al. 2013). The two subfamilies WOX1 and WOX3 display different features. Genes belonging to the WOX1 subfamily are characterized by four exons. Moreover, the first exon displays a specific conserved box (5'-*WOX1/4*) and it is placed upstream of the exon carrying the homeodomain, which is therefore the second exon (FIG. 1) (Vandenbussche et al. 2009). Additionally, the subfamily-specific 3'c *WOX1/STF* box also represents a special feature of these genes (Vandenbussche et al. 2009; Zhang et al. 2014). In contrast, members of the WOX3 subfamily contain only two exons (the firs exon carrying the homeodomain), and are characterized by a conserved subfamily specific 3'c *WOX3* box (Vandenbussche et al. 2009).

Interplay between WOX1 and WOX3 subfamily members in Arabidopsis

Similar to Petunia, Arabidopsis displays two members of the WOX1 subfamily: *WOX1* and *WOX6*. However, no special phenotype can be observed in *wox1* single mutants in Arabidopsis (Vandenbussche et al. 2009), with the exception of deeper leaf serration (Nakata et al. 2012). Also *wox6* mutants do not display a phenotype different from WT, as was found also for *wox1 wox6* double mutants (Vandenbussche et al. 2009). Interestingly, the *prs* mutant in Arabidopsis (*PRS* is the only member of the WOX3 subfamily in this species) is affected in development of lateral sepals (Matsumoto and Okada 2001). When the *PRS* gene is mutated along with *WOX1*, the *wox1 prs* double mutants clearly display narrow leaves and floral organs, showing the involvement of both the WOX1 and WOX3 subfamily in blade outgrowth in lateral organs in Arabidopsis (Vandenbussche et al. 2009;

Nakata et al. 2012). Further analysis of the *wox1 prs* double mutant led to a developmental model where a middle domain, different from the adaxial and abaxial sides, and located at the leaf margin, is responsible for organization of lamina expansion in Arabidopsis (Nakata et al. 2012; Nakata and Okada 2012). This model was based on the fact that mixed adaxial/abaxial characters have been observed in leaf margins of *wox1 prs* mutants as well as overlapping expression of *AS2* (adaxial factor) and *FIL* (abaxial factor) in that region (Nakata et al. 2012). Additionally, *WOX1* and *PRS* control the expression of *mi*R*165/166* in the leaf margin and genetically interact with the *HD-ZIP III REVOLUTA* (Nakata et al. 2012; Nakata and Okada 2012). So far, such an overlapping role between the WOX1 and the WOX3 subfamily in blade expansion in lateral organs seems specific to Arabidopsis. In Medicago, the *WOX3* orthologue *LFL* plays a role in lateral fusion of petals, and LFL interacts with the corepressor TOPLESS (Niu et al. 2015), similarly to STF in the same species (Zhang et al. 2014). However, leaves are not affected in *lfl* mutants of Medicago (whereas *stf* mutants display narrow leaves) and, differently from Arabidopsis, no synergistic effects in leaf or flower phenotype have been observed in *lfl stf* double mutants, with the possible exception of carpel development (Niu et al. 2015).

The WOX1 subfamily is involved in ovule development in Petunia

We additionally observed supernumerary carpels emerging from the tip of the ovary in *maw mawb* mutants (FIG. 9F and G), suggesting homeotic conversion of carpels into ovules. By means of SEM microscopy, we observed abnormal ovules and intermediate structures displaying carpel features (FIG. 9H). Carpel-to-ovule conversion had been previously described in Petunia, in so called "*spaghetti*-mutants" (Angenent et al. 1995; Colombo et al. 1995; Heijmans et al. 2012a). In fact, *fbp7 fbp11* mutants do not display abnormal ovules (excepted rare conversion usually observed at the top of the *placenta*, the same region from which converted ovules emerge in *maw mawb* mutants). Plants in which at least one of the two *C* genes has been mutated along with the two D lineage genes (*FBP7* and *FBP11*)

display full ovule-to-carpel conversion (Heijmans et al. 2012a). Because of the previously established role co-played by D lineage genes in such a phenotype, we looked for possible genetic interactions between *WOX1* and D lineage genes (FIG. 9). We observed full ovule-to-carpel conversion in various *d/wox1* mutant combinations, displaying the so called "*spaghetti*" phenotype (FIG. 9). In conclusion, *WOX1* genes can be considered as novel regulators of ovule development in Petunia. This is raising two questions. First, the identity of targets and protein interacting partners of WOX1 genes, involved in ovule identity. Second, if the role played by *WOX1* genes in ovule identity is specific to Petunia or shared with other species.

It would be interesting to see if a similar "*spaghetti*" phenotype can be obtained by combining *WOX1* mutations with C-function mutants. Moreover, it will be interesting to analyze the expression levels of C- and D-class MADS-box proteins and of *MAW/MAWB* in the various mutant backgrounds by means of qPCR.

In Arabidopsis, carpel-structures replace ovules in the triple mutant *shp1 shp2 stk,* and overexpression of these genes produces ectopic carpels or ovules on sepals and bracts (Liljegren et al. 2000; Pinyopich et al. 2003; Favaro et al. 2003; Colombo, Battaglia, and Martin M Kater 2008). In addition to *C* genes and D lineage genes, other genes, such as *E* genes, are also involved in ovule development. This is highlighted by *SEP1 +/- sep2 sep3* mutants in Arabidopsis (conversion of ovule integuments into carpelloid structures) (Favaro et al. 2003; Colombo, Battaglia, and Martin M Kater 2008) and *fbp2 fbp5* in Petunia, in which ovules are replaced by leaf-like structures (Vandenbussche et al. 2003). Therefore, *E* genes might represent other possible targets for qPCR analysis in the various mutant backgrounds. The *bel1* mutant in Arabidopsis displays ovule integuments converted into carpel structures (Reiser et al. 1995; Brambilla et al. 2007, 2008), and a similar phenotype has been observed in Arabidopsis (*Landsberg* ecotype) overexpressing *KNAT2* (Lincoln et

al. 1994b). In both cases, ovule-to-carpel conversion is associated with ectopic expression of *AG* in ovules (Robinson-Beers et al. 1992; Modrusan et al. 1994; Pautot et al. 2001). Further analyses are required to investigate possible relationship between these genes and *WOX1* genes in ovule identity. BEL1 interacts with the AG-SEP complex in Arabidopsis (Brambilla et al. 2007, 2008). Interestingly, BEL1 is also a homeodomain transcription factor, although belonging to a different class. It is therefore conceivable that MAW/MAWB proteins also directly interact with the MADS-complex involved in conferring ovule identity. This can be tested by means of yeast three- and four-hybrid interactions. We also noticed that *maw mawb* mutants in Petunia are extremely similar to *maw chsu* mutants (Vandenbussche et al. 2009). Therefore, it will be interesting to further investigate the relationships between *MAW*, *MAWB*, and *CHSU*.

In conclusion, we have characterized the role of *WOX1* genes in Petunia. However, in Arabidopsis, the WOX3 subfamily is also involved, with WOX1 subfamily, in blade outgrowth in lateral organs (Vandenbussche et al. 2009; Nakata et al. 2012). Further studies will elucidate the role played by the WOX3 subfamily in Petunia. To date, some molecular properties of *WOX* genes carrying the WUS box have been elucidated (*e.g.*, the requirement of repression activity for lamina expansion (Lin, Niu, McHale, et al. 2013)) and some downstream targets and genetic interactions allowing lamina expansion have been identified in different species (Nakata et al. 2012; Zhang et al. 2014; Zhang and Tadege 2015). Despite of such progresses, the downstream genetic networks, including the direct targets of MAW/MAWB, are still unknown. More efforts are required to elucidate these aspects.

Annex I: Comparative analysis of *WOX1* genes in *Arabidopsis thaliana*

Abstract

In Petunia, WOX1 members are absolutely required for fusion of the two carpels. In Arabidopsis, the *wox1 prs* mutant has been previously shown to be impaired in blade outgrowth in leaves, sepals and petals, in a similar way to *maw* in Petunia, but remarkably carpel fusion was not affected, despite the severity of the phenotype in other organs. This implies that, differently from Petunia, a *WOX* gene from the WOX3 subfamily, *PRS*, is involved in blade outgrowth in this species. Here we have further investigated in more detail if members of the WOX1 subfamily in Arabidopsis play a role in carpel fusion, and found that the *wox1 prs wox6* triple mutant is partially affected in stigma development. This suggests a conserved role for *WOX1* genes in carpel development in Petunia and Arabidopsis, despite the role also played by the WOX3 subfamily in Arabidopsis. In conclusion, we identified novel roles for *WOX* genes in plant development in Petunia and Arabidopsis, paving the way to further analysis of the corresponding gene regulatory networks.

Introduction

Petunia and Arabidopsis belong to two different, major eu-dicot groups: Asteridae and Rosidae, respectively. In Arabidopsis, members of the WOX3 and WOX1 subfamily are involved in lamina outgrowth in leaves and and floral organs (Vandenbussche et al. 2009; Nakata et al. 2012), but not in carpel development. In fact, *wox1 prs* mutants display very narrow lateral organs, including in flower organs (Vandenbussche et al. 2009; Nakata et al. 2012). However, beside the failure to expand laterally observed in leaves, sepals, and petals, no special phenotype was observed at the carpel level in *wox1 prs* in Arabidopsis. This marks an interesting difference compared with Petunia, where we have previously shown that the WOX1 subfamily is strongly involved in carpel development, also playing a role in ovule identity. We have further investigated the role of these two subfamilies (WOX1 and WOX3) in carpel development in Arabidopsis.

At-WOX6 **is involved with** ***WOX1*** **and** ***PRS*** **in stigma development in Arabidopsis**

Previous analyses of the triple mutant *wox1 prs wox6*, in which all the representatives of the WOX1 and WOX3 subfamily in Arabidopsis are mutated, didn't reveal any evident phenotype at the carpel level (Vandenbussche et al. 2009). We wanted to carefully analyze different *wox1*/*wox3* mutant combinations, by means of a statistically relevant number of plants, in order to discard the hypothesis of a subtle phenotype, previously overlooked. We analyzed carpels and stigmas of WT, *prs, wox1 prs, wox1 wox6, prs wox-*, and *wox1 prs wox6* plants (FIG. 10), grown under similar conditions, to uncover possible phenotypes, previously missed.

Interestingly, about 21% of *wox1 prs wox6* flowers were significantly affected in stigmas (FIG. 10). The range of the observed phenotypes is quite variable, from stigma shape alteration and enlargement, till full splitting of the stigma, which is characterized by the production of two separate stigmas provided with *papillae* (FIG. 8C, white arrow). In the three possible double mutant combinations, very few to none abnormal pistils were found, showing that mutations in all three genes *WOX1*, *WOX6* and *PRS* contribute to this phenotype. This is showing that *WOX1* genes in Arabidopsis play a similar role to the ones in Petunia: Genes from the two species are both involved in blade outgrowth in lateral organs and in carpel development. In addition, in Arabidopsis, *PRS* is also implicated in carpel development, similarly to overlapping role with *WOX1* in blade outgrowth. Despite of that, the low penetrance of the *wox1 prs wox6* stigma phenotype in Arabidopsis, and the reduced portion of the carpel which is affected (only the stigma in Arabidopsis, whereas in Petunia the mutant phenotype extends till the ovary) suggests that other genes may largely rescue carpel fusion in Arabidopsis *wox1 wox6 prs* mutants.

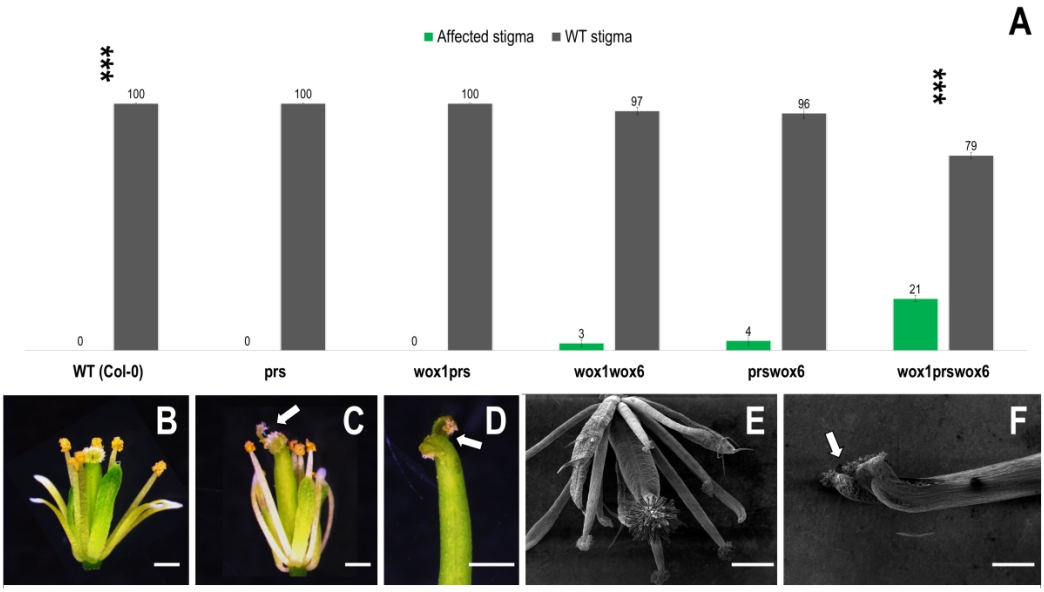

FIG. 10 *WOX6* is involved in stigma development in Arabidopsis, along with *WOX1* and *PRS*.

A – Statistical analysis of different mutant combinations. From left to right: WT, *prs, wox1 prs, wox1 wox6, wox1 prs, wox6* flowers were analyzed for possible defects at the carpel level. Although the finding of some abnormal stigmas in *wox1 wox6* and *prs wox6* mutants, only *wox1 prs wox6* plants displayed a statistically significant number of altered stigmas, compared with all other combinations. Only T test for WT and *wox1 prs wox6* plants is shown – see Chapter VII, Materials and Methods for full dataset. **B** – Picture of *wox1 prs wox6* flower showing WT stigma. **C** – Picture of *wox1 prs wox6* flower showing affected stigma. **D** – Developing silique from a *wox1 prs wox6* affected stigma. **E** – SEM picture of *wox1 prs wox6* flower with WT stigma. **F** – SEM picture of *wox1 prs wox6* silique developing from affected stigma. Scale bars: **B**, **C**, **D** – 1 mm; **E**, **F** – 250 μm.

Discussion

Differential roles of WOX1 and WOX3 subfamilies among Asteridae and Rosidae

WOX1 genes play a major role in blade outgrowth in lateral organs in Asteridae (McHale and Marcotrigiano 1998; Vandenbussche et al. 2009)(this study), whereas an important role in leaf lamina expansion is played by the WOX3 subfamily in monocots (Scanlon et al. 1996; Nardmann et al. 2004; Cho et al. 2013). This fact is probably linked to the remarkable absence of the WOX1 subfamily in this group (see FIG. 1).

Arabidopsis (Rosidae) instead, involves both the WOX1 and WOX3 subfamily for blade outgrowth (Vandenbussche et al. 2009; Nakata et al. 2012). However, the fact that leaf blade development is not affected in *wox1* and *prs* single mutants shows that their function is genetically interchangeable. On the basis of the expression pattern of *WOX1* and *PRS* in Arabidopsis, a 'middle-domain model' of lamina expansion has been proposed (Nakata and Okada 2012). This raises the question of the general value of this model in different species. We found that overexpression of *pMAW::Ph-MAW* in Arabidopsis *wox1 prs* can rescue mutant phenotype to a large extent (FIG. 11), suggesting the ability of *Ph-MAW* to activate the same genetic modules controlled by *At-WOX1* and *At-PRS*. As a consequence, heterologous expression of *Ph-MAW* in Arabidopsis probably overlaps with the previously described middle-domain (Nakata and Okada 2012) (FIG. 11). Moreover, the different role of *WOX1/WOX3* genes in Petunia and Arabidopsis probably is not due to different downstream genetic networks (which appeared quite conserved, as shown by the heterologous expression), but probably resides in the progressive differentiation of their *cis* or *trans* (or both) elements among the two species. Previous studies have shown the interchangeability of WUS and WOX5 in Arabidopsis (Ananda K. Sarkar et al. 2007), complementation of *prs* mutants by overexpression of *pPRS::WUS* in Arabidopsis [reported in (Shimizu et al. 2009)], and complementation of *stf* by *pSTF::LFL* and *lfl* by *pLFL::STF* in Medicago (in which *STF* is a WOX1 subfamily gene and *LFL* a WOX3

subfamily member) (Niu et al. 2015). All these data point to a major role for *cis* elements compared with *trans* elements. However, in the *trans* side, the WUS box has been reported as inducing repressor activity in *WOX* genes (from the WUS clade) and required for blade expansion in lateral organs, as shown by promoter-swapping experiments (Lin, Niu, McHale, et al. 2013).

WOX1 genes only play a minor role in carpel development in Arabidopsis

Although carpels are severely affected in Petunia *wox1* mutants, a similar phenotype had not been previously observed in *wox1/wox3* mutants in Arabidopsis. By means of statistical analysis of different *wox1/wox3* mutant combinations (FIG. 10), we found that on *wox1 prs wox6* plants 21% of flowers are affected in stigma development (FIG. 10), suggesting that *WOX1* genes in Arabidopsis have conserved a role in carpel development. However, differently from Petunia, the WOX3 subfamily gene *PRS* is also involved. In conclusion, in Arabidopsis the function of *WOX6* is apparently restricted to carpel development.

Annex II: Heterologous expression of *Ph-MAW* on a *wox1 prs* Arabidopsis background

Given the phenotypic similarity between the *wox1 prs* double mutant in Arabidopsis, and the *maw* mutant in Petunia, we tested the ability of *Ph-MAW* to rescue the *wox1 prs* phenotype by means of heterologous expression.

Ph-MAW partially rescues the mutant phenotype in *wox1 prs* flowers of Arabidopsis

As previously shown, WOX1 genes play major roles in floral organ development in Petunia, whereas in Arabidopsis, *PRS* also plays a major role in this process. Divergent functional roles for these two subfamilies among Petunia (Asteridae) and Arabidopsis (Rosidae) are evident. To analyze functional conservation among different species and subfamilies, we tested the ability of *Ph-MAEWEST* to restore the *wox1 prs* phenotype in Arabidopsis. To this aim, *wox1 prs* mutants were transformed with the full genomic sequence of *Ph-MAW* (including its own promoter). We observed an important restoration of the WT phenotype in *wox1 prs* flowers and leaves (FIG. 11), suggesting the ability of *Ph-MAW* to control the same genetic modules involved in lamina expansion of lateral organs in a species belonging to a different core-eudicot group, in which similar processes are performed by two different WOX subfamilies.

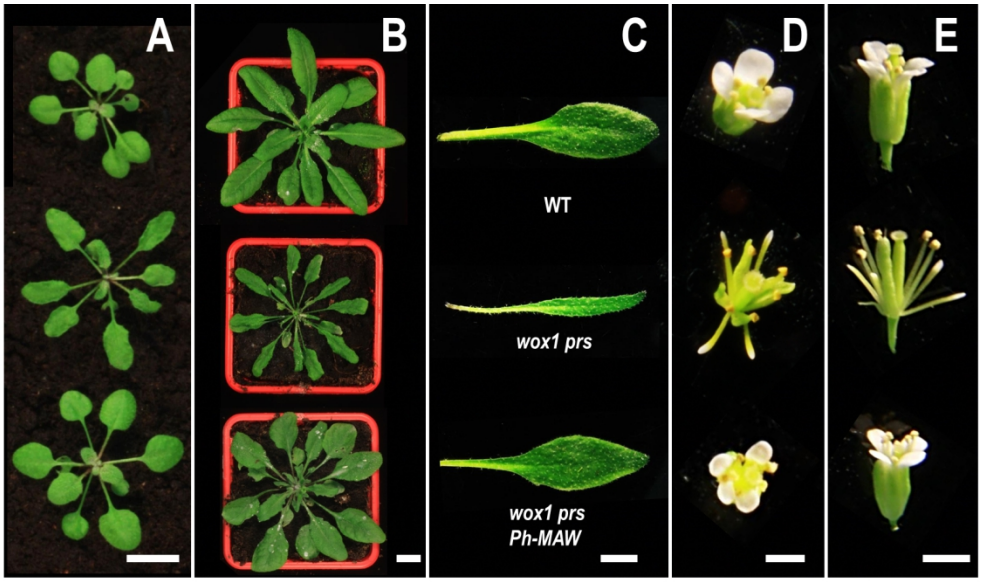

FIG. 11 *Ph-MAW* partly restores the WT phenotype in *wox1 prs* mutants in Arabidopsis

Rosettes from WT, *wox1 prs*, and *wox1 prs* plants complemented with *Ph-MAW::Ph-MAW* genomic sequence at young (**A**), and at a later stage (full developed rosette) (**B**). Scale bars: **A** – 1 mm; **B** – 50 mm**A**

C – Leaves from WT, *wox1 prs*, and *wox1 prs* plants complemented with *Ph-MAW::Ph-MAW* genomic sequence. Scale bar: 50 mm.

Top (**D**) and side view (**E**) of flowers from WT, *wox1 prs*, and *wox1 prs* plants complemented with *Ph-MAW::Ph-MAW* genomic sequence. Scale bars: **D**, **E** – 1 mm.

Materials and methods

Plant material and growth conditions - Petunia mutants were obtained from in-house mutant collection of *dTph1* high-copy number transposon line W138, as described in (Vandenbussche et al. 2008, 2013a; b). Plants were grown in pots (compost ARGIL 10 - FAVORIT®) under green-house conditions. Mutant alleles used in this study are: *maw*-4, *maw*-6 (Vandenbussche et al. 2009), *mawb* (this study). Plants were genotyped by PCR using primers specific for the *dTph1* insertion flanking sequence taken into account, allowing mutant-allele specificity. Primer combinations for Petunia genotyping are listed below.

Mutant allele	Transposon insertion	Primer fw	Primer rv	WT fragment size	Footprint
maw-4	2054 bp after ATG genomi**c sequence**	MLY0158	MLY0159	110 bp	ft analysis: EL300: 110 min
maw-6	601 bp after ATG on genomique	MLY0780	MLY0781	138 bp	
mawb-788	788 bp after ATG on cDNA	MLY0491	MLY0492	120 bp	ft analysis: EL300: 125 min

Primer sequences for mutant screening in *Petunia* x *hybrida*

Primer	Sequence (5'-3')
MLY0158	AGAAAGATGGATACCATTCGATGAG
MLY0159	GTGGTGAACAAGACAAATGCATCA
MLY0780	TGAACAAATTCAGCACATTACTGC
MLY0781	AGCGGCATTGGATTCAAGTTGAC

MLY0491 TCTTCGAACATGCCTCTCAATCAG

MLY0492 CCTTTCATTTTCAACATTTCTTGCTAG

Arabidopsis (Col-0) plants were sown in pots (compost ARGIL 10 - FAVORIT®) and cold-treated at 4°C for 24 h before transferring to short-day conditions for at least 3 weeks. Plants were moved to long-day conditions before bolting. Multiple mutant plants were obtained by crossings the following mutant lines: *wox1* line 8AAJ85 (En205 transposon); *prs* line SALK_127850; *wox6* - pfs2-2 line SALK_033323, as in (Vandenbussche et al. 2009). Plants were genotyped by PCR using the following primer combinations.

Primer	Original name*	Sequence (5'-3')	Notes
MLY0089	*At-WOX1-2* fw	CACAGCAGTGGTGACGATGACG	segregation analysis, 8AAJ85
MLY0090	*At-WOX1-2* rv	CTTCAAGAACCCTTAACTGATCTGGTG	segregation analysis, 8AAJ85
MLY0097	En205 Transposon	AGAAGCACGACGGCTGTAGAATAGGA	For *At-WOX1-2* screening
MLY0093	*At-PRS* fw	GGGAACTGGAGTAGGAGAAGCTC	For *At-PRS* screening
MLY0094	*At-PRS* rv	CATCCAATCTCGACCGTACGATGAG	For *At-PRS* screening
MLY0091	*At-WOX6* fw	TAAAGACGTCAAGGATTCATCATCAG	For *At-WOX6* screening
MLY0092	*At-WOX6* rv	GAGCTTTGTCTGATCAACTCGATG	For *At-WOX6* screening
MLY0099	T-DNA LEFT border	GAACAACACTCAACCCTATCTCG	For mutant screening in lines *prs* SALK_127850 and *wox6* - *pfs2-2* line SALK_033323

DNA extraction and Polymerase Chain Reaction - Extraction of DNA from young tissue was performed accordingly to (Edwards et al. 1991).

PCRs were performed using the GoTaq® PCR kit (Promega), following producer's instructions. For Petunia genotyping, touchdown PCR thermal profiles were also adopted in order to increase PCR specificity and yield (see (Korbie and Mattick 2008)). For mutants screening in Petunia was typically used the following thermal profile:

95 °C x 2'; {95 °C x 30"; 60°C x 30"; 72°C x 30" x $kb_{product}$} x 40; 72 °C x 7'; 18 °C x ∞.

Sequence search and bio-informatics - For sequence search, gene prediction, and annotation, the following softwares and databases were used: The BioEdit package (Hall 1999), the Wise2 tool ("WISE2 Online Tool"), the NCBI databases ("NCBI database"), and the Sol Genomics database ("Sol Genomics Network Database").

Phylogenetic analysis - The homeodomain regions from predicted WOX proteins, as well as sequences from (Vandenbussche et al. 2009), were used. Phylogenetic analysis was performed using Treecon (Van de Peer and De Wachter 1994), as in (Vandenbussche et al. 2009). To support inferred phylogeny, 1000 bootstrap samples were generated.

SEM microscopy and digital images - Samples were analysed using a SEM SH-3000 (HIROX), typically at -20°C and 10 kV. Digital pictures were taken using a Canon EOS 450D camera (SIGMA 50 mm F2.8 and 18-50 mm F2.8 EX DG MACRO lenses).

***In situ* hybridization -** *In situ* hybridization on *MAWB* was performed using the following primers for producing the probe:

CTGATGAATTTAATTCATATGCATGCTC (forward)

TGTAATACGACTCACTATAGGGCAACACAGATCAGAAGACTCATCTATAC (reverse + T7) on the full *MAWB* coding sequence amplified from *Petunia* x *hybrida* cDNA collection, as described in Chapter VII.

Control probe for *Ph-WUS* was obtained using the following primers:

ACCACTGATAACACTAACCTCCCC (forward)

TGTAATACGACTCACTATAGGGCAGAGAAGCTCTAGCAGCAGCCAAG (reverse + T7).

Probes were then hydrolysed in small fragments (a few hundred bp). Sections (10 μm) of Petunia young floral buds and shoot apical meristem in Paraplast Plus® (Sigma-Aldrich®) were obtained using a microtome HM355S (Microm/Zeiss). Probe hybridization and detection was performed as described in Chapter VII. Pictures were taken using an Imager M2 microscope provided with an AxioCam MRc (Zeiss).

Statistical analysis of stigma phenotypes - 4 plants per genotype were grown under the same conditions. From each plant, 25 flowers were visually screened at the microscope for defects in carpel and stigma development. T-test was used to assess statistical significance.

Materials and Methods are reported in full in Chapter VII (Materials and Methods).

Chapter IV cover - Transgenic Petunia carrying the *pMAW::GR-MAW* construct.

IV. Dissecting the molecular role of *MAW* and *MAWB* by RNA-Seq analysis

E. Costanzo[♦♣], E. Bertolini[♣], J.Just[♦], P. Morel[♦], M.E. Pè[♣] & M. Vandenbussche[♦]

Summary

We have previously reported that *maw mawb* mutants in Petunia are severely affected in blade outgrowth in lateral organs (Chapter III). Here, we report results from an RNA-Seq analysis aimed at comparing the transcriptomes of WT, *maw* and *maw mawb* mutants. We performed our analysis on shoot apexes and processed RNA-Seq data following the Tuxedo package, developed by (Trapnell et al. 2012).

We performed comparisons in pairs among conditions, identifying 4,836 DEGs in *maw vs.* WT, 9,641 DEGs in *maw mawb vs. maw*, and 10,421 DEGs in *maw mawb vs.* WT. After selecting DEGs displaying a minimum of 2 fold change, we analyzed general trends among the three conditions.

To identify genes involved in relevant biological processes, affected in both the single and the double mutant, we first identified all the differentially expressed genes (DEGs) shared by the three conditions (~2600). From this pool we selected only DEGs in which the expression level of *maw* was intermediate between WTs and the double mutant, reducing the pool to ~550 DEGs.

The resulting data set was enriched for specific classes of transcription factors (*HOMEOBOX, bHLH, ARF*). This data set displays a different composition from a WT plant genome, such as the Arabidopsis genome.

We found a clear link between auxin related pathways and defects in lamina expansion in *maw* and in the double mutant. Cell-proliferation genes were also differentially expressed among the three conditions. GIF and GRF sequences were consistently affected in *maw* and *maw mawb*, and had been shown to be involved in lamina expansion in Arabidopsis leaves. Interestingly, we identified the genetic module *ARF5/ATHB8*, involved in vein formation, as a target of MAW/MAWB.

Finally, we identified the *miR156/SPL* module as a target of MAW/MAWB, providing a possible explanation for the supernumerary organs displayed by single and double mutants. Eventually, we set up a strategy aimed at identifying the direct targets of MAW/MAWB through DEX activation of *MAW* and subsequent RNA-Seq analysis.

♦*Laboratory of Reproduction and Development of Plants, UMR5667, Ecole Normale Supèrieure de Lyon, Lyon, FRANCE*

♣*Istituto di Scienze della Vita, Scuola Superiore Sant'Anna, Pisa, ITALY*

Introduction

RNA-Seq is a powerful method for transcriptome analysis. Made possible by Next Generation Sequencing (NGS) technologies, it is replacing previous technology for RNA analysis, such as microarrays (based on hybridization methods), in many fields of biology. In fact, microarrays are limited by the previous knowledge of the RNA to be tested, different experiments proved difficult to compare, and were typically affected by problems of signal saturation. Instead, RNA-Seq methods allow new transcripts discovery, do not require the previous knowledge of the genome (that is, RNA-Seq can be easily applied to non-model/non-sequenced organisms) and, compared to microarrays, are more sensible in detecting lowly expressed transcripts and more accurate in measuring absolute expression levels (Fu et al. 2009; Wang et al. 2009; Mutz et al. 2013; C Wang et al. 2014). Probably not surprisingly, methods for studying the transcriptome evolved in parallel with our vision of the transcriptome. In the early 2000, the transcriptome was supposed divided into these components: A low percentage of mRNA (2 - 4 %), tRNA (5 – 15 %), rRNA (80 – 90 %), and noncoding RNA at very low levels (1 %) and, consequently, of relative importance (Costa et al. 2010; Lindberg and Lundeberg 2010). However, the discovery that high amounts of mammalian transcribed RNA is not protein coding, started to reshape the perception of transcriptome landscape, allocating more and more importance to non-coding RNAs (Okazaki, Furuno, et al., FANTOM Consortium and RIKEN Genome Exploration Research Group Phase I & II Team 2002; Lindberg and Lundeberg 2010). Moreover, this part of the transcriptome was designed as "dark matter", a term aimed at highlighting both the gained (supposed) importance and the lack of knowledge associated with these transcripts, a term probably inspired by other disciplines (Johnson et al. 2005; Ponting and Belgard 2010).

RNA-Seq experiments allowed in depth and reliable analysis of this "dark matter"; for instance, in first RNA-Seq experiments a non-negligible percentage of reads appeared as

non-assignable to known gene models, and therefore considered as background or technical artifacts (van Bakel et al. 2010; Mercer et al. 2012). Instead, later NGS analyses provided evidence for the biological significance of these reads: Rare isoforms, alternative splicing variants, unannotated exons and intergenic long non coding RNAs have been shown to account for about 15 % of the sequenced reads in the human transcriptome (Mercer et al. 2012). Interestingly, the complexity of the transcriptome is not only related to its "spatial" landscape, but even to the "time" landscape, as shown by transcriptome oscillations linked to the circadian clock in Arabidopsis (Nolte and Staiger 2015).

In recent years, a straightforward protocol for RNA-Seq data analysis (based on the Linux interface) has emerged as a reference among the biological community: The Tuxedo package (Trapnell et al. 2012). Through the read aligner TopHat2 (incorporating Bowtie2) (Kim et al. 2013) and Cufflinks2, able to assemble transcripts, discovering new isoforms, and calculate abundances.

A major challenge was given by the absence of a *P.* x *hybrid*a sequenced genome. In fact, only the genomes of the two parental species were available (as non-ordered scaffold assemblies). The two parental genomes were merged in a single file. In this way, we obtained a synthetic basis for expression levels calculation of differentially expressed genes (DEGs), which was the aim and goal of the whole analysis. We obtained and analyzed Differentially Expressed genes (DEGs) among three biological conditions already described in the previous Chapter: WT, *maw*, and *maw mawb* double mutants. These data shed light on the downstream genetic pathways and pave the way to further functional analysis.

Finally, we also implemented an inducible system in Petunia, aimed at being coupled with RNA-Seq analysis to MAW/MAB direct-targets discovery.

Results

Experimental set up

RNA was extracted from biological samples belonging to WT, *maw*, and *maw mawb* plants. We opted for *bona fide* vegetative apexes as biological samples, instead of floral buds. In this way, we wanted to avoid the regulatory complexity linked to flower induction and flower development, in order to focus on some basic aspect of the phenotype, in particular, the lack of lamina expansion (organ primordia emerge from the vegetative apex).

Each biological sample (3 biological samples per condition), was itself the result of a pooling of vegetative apexes from individual plants (between ten and seven), to further support the biological reliability of our results.

Sequencing was performed on two lanes on a HiSeq 2500 System (Illumina) by IGA Technologies Inc., resulting in single-end 100 bp reads. In the end, 18 libraries (two per sample) of 20 M fragments each were obtained. By means of the ERNE-FILTER package, libraries were quality trimmed (phred number 33, minimum size 90) and trimmed libraries derived from the same sample were fused together.

For the whole analysis, we relied on the classic Tuxedo package (Trapnell et al. 2012; Kim et al. 2013). However, we adapted this protocol to the peculiarity of the Petunia system, similar to the ones of non-model species (Strickler et al. 2012):

- *Petunia* x *hybrida* is lacking a sequenced genome; only the parental genomes (*P. inflata* and *P. axillaris*) are available.
- The sequenced genomes are lacking a consensus GFF (genome coordinates), as they are available only as unassembled scaffold collections.

Two genomes for one analysis

The main challenge to be solved was the lacking of a genome for *P.* x *hybrida*. Two separate genomes for *P. inflata* and *P. axillaris* (*Petunia Genome Consortium, unpublished genomes*), the two parental species of *P.* x *hybrida*, were available as unassembled scaffolds (*P. inflata* N50 406 Kb; N90 2,450 Kb - *P. axillaris* N50 309 Kb; N90 1,051 Kb; *Petunia genomes assemblies Status at February 2014* – unpublished presentation), therefore lacking a GFF file.

Additionally, no reliable annotation was available when we performed RNA-Seq. Therefore, our challenge was to implement a *pseudo de novo* RNA-Seq analysis on *P.* x *hybrida*. As a first step, a partially annotated GFF file based on sequences from the Tomato protein database was produced for the two separated genomes. This provided a baseline for library assembly and a starting point for the annotation. The two genomes (*P. axillaris* and *P. inflata*) were fused together, obtaining a "synthetic" *P.* x *hybrida* genome. The two GFF files (for *P. axillaris* and *P. inflata*) were also fused together. Technically, this means that in the "synthetic" *P.* x *hybrida* genome, all genes were (virtually) in double compared to the real *P.* x *hybrida* genome. This also makes the genome length double compared to the real one. However, for our purposes (measuring expression levels of differentially expressed genes) this is not affecting the result as we were interested in relative expression levels among conditions.

Quality trimming of reads was performed using ERNE-Filter (Del Fabbro et al. 2013), keeping a mean phred quality of 33 and a minimum read length of 90 bp. On average, ~88 % of the raw reads where kept as good quality reads from each library (see Material and Methods for full data set). Trimmed reads from the same biological samples were merged together, therefore largely reaching the minimum reads number required for robust gene expression profiling (Y Wang et al. 2011). Following the Tuxedo package, Bowtie2 was first used to create a genome index, and the alignment of reads from each biological sample to the genome was subsequently performed by Tophat2, taking advantage of the Tomato-

based GFF file. The parameters used for Bowtie2 are the default ones ("sensitive" parameters). Bowtie2 is an efficient alignment program for short reads to the genome. In practice, the aligner makes a guess concerning the origin of a read from the provided genome. Bowtie2 extracts substrings from each read and from the reverse complement (called "seeds"). This also means that single seed alignments from a single read are not valid (mismatches or gaps for each seed), whereas the overall alignment of the read is valid (Langmead et al. 2009). TopHat2 is a spliced aligner, in our case relying on Bowtie2, for efficient mapping of reads through a genome (Kim et al. 2013). On average, 85.5 % of reads from each sample was successfully mapped by TopHat2. Of these mapped reads, 66.2 % had multiple alignments through the genome. This high rate of multiple alignments was expected, since the "synthetic genome" is working as two genomes at one time. Since reads are just 100 bp in length, if no polymorphism is present in that region, then reads will be equally mapped among the two genomes.

Cufflinks2 was then run on the alignment files (.bam files) derived from each biological sample after running Tophat2. Cufflinks2 is a powerful tool for transcripts assembly and discovery of gene/splice variants not taken into account by the genome aligner. The resulting assembly files were merged together using Cuffmerge (a sub-tool of Cufflinks2). In this way, the software can derive a baseline for calculating transcript expression levels among different conditions. At this point of the analysis, we were able to compare expression patterns from the different libraries (FIG. 1). A map of the Euclidean distances of the different libraries clearly shows that transcript expression levels behave coherently inside each condition (WT, *maw*, *maw mawb*), supporting the validity of our biological sampling.

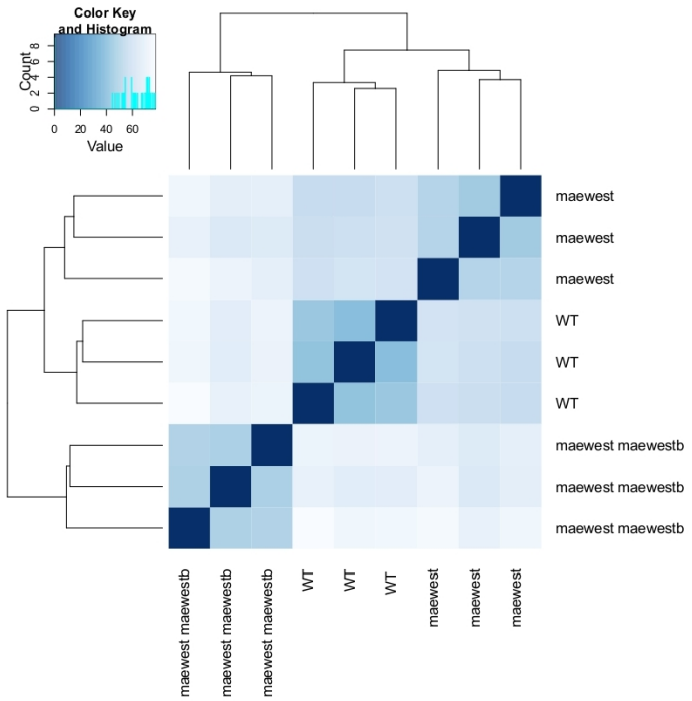

FIG. 1 Euclidean distances of libraries

Libraries from the same sample behave in the same way (Credit: E. Bertolini).
Dendrograms show the relationship among different libraries. As expected, libraries from the same background (WT, *maw*, or *maw mawb*), are more closely related with themselves than with other libraries, confirming the soundness of experimental design.

DEGs quantification using Cuffdiff

The resulting DEGs were quantified in FPKM (Fragments Per Kilobase of exon per Million fragments mapped) (Mortazavi et al. 2008) using Cuffdiff2 (which also is a tool incorporated into Cufflinks2). Results from Cuffdiff2 are consistent with count-based schemes only if isoforms are not differentially regulated in a substantial way [from recent studies, it appears that alternative splicing is widespread among different genomes, including plant genomes (Reddy et al. 2013)], otherwise fold change counts are considered as a poor approximation leading to higher levels of false positives. Cuffdiff2 works using a beta negative binomial distribution implemented in its model for counting fragments in

which the uncertainty of reads ambiguously mapped (widespread in transcriptomes where alternative splicing is present) is combined with fragment-counts across replicates for each transcript and the fragment-counts for each isoform inside each replicate (Trapnell et al. 2013). In this way, the variability among replicates and the effects of reads ambiguously mapped causing uncertainty on the expression levels are both taken into account at the same time (Trapnell et al. 2013). Practically, DEGs passing the statistical validation of Cuddiff2 are labelled as "YES" in the final report. Since Cuffdiff2 performs comparisons in pairs, we performed differential expression analysis among the following conditions: *maw* vs. WT, *maw* vs. *maw mawb*, *maw mawb* vs. WT.

We took considered only DEGs labeled as "YES" for further analysis, after exporting data in Excel. The subsets of statistically significant DEGs were the following ones: *maw* vs. WT – 4,836 DEGs; *maw mawb* vs. *maw* – 9,641 DEGs, *maw mawb* vs. WT – 10,421 DEGs. Roughly speaking, the Cuffdiff software, based upon the beta negative binomial model, labels as statistically relevant also genes displaying very low fold change difference (for example, as low as ~1.2 fold change), because in that model the statistical relevance is depending also upon the distribution among the samples. It remains to be seen if also these low fold change differences have a biological relevance, or not.

Different strategies can then be applied to these data sets to extract relevant information concerning the genes and biological processes controlled by MAW and MAWB. The strategies illustrated below are therefore complementary to each other, and do not exclude further and different analyses in the future. All the main steps of RNA-Seq data processing (ERNE-Filter trimming and Tuxedo package) are illustrated in FIG. 2.

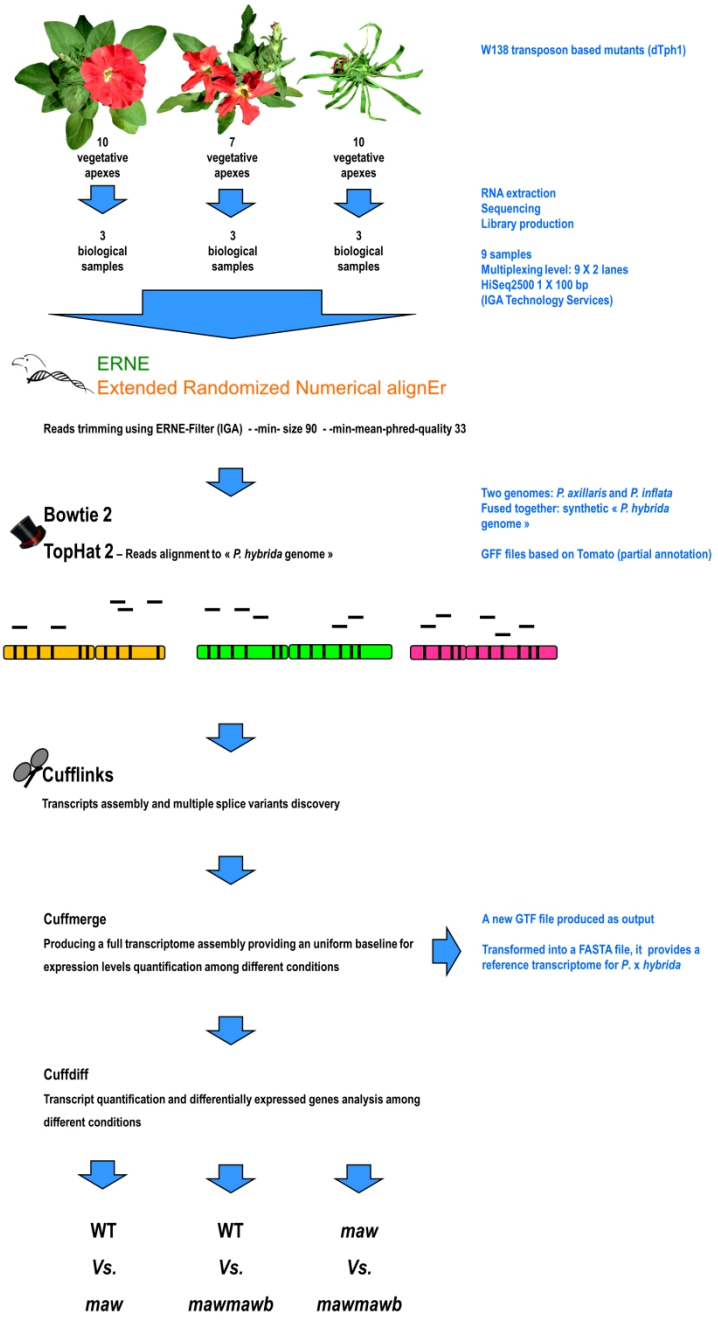

FIG. 2 Scheme of the RNA-Seq analysis performed on *P.* x *hybrida* samples (WT, *maw*, and *maw mawb*)

The main steps from sample extraction till analysis of differentially expressed genes (Tuxedo package) are illustrated.

In order to analyze general trends among the three conditions, we selected DEGs displaying a *minimum* of 2 fold change (considering a minimum of 2 fold change as biologically relevant) from the previous pools. We obtained the following subsets: *maw* vs. WT – 1,205 DEGs; *maw mawb* vs. *maw* – 2,303 DEGs; *maw mawb* vs. WT – 2,932 DEGs. Observing the three comparisons, the lower number of DEGs between WT and the single mutant is probably due to the fact that the *maw* phenotype still retains several WT aspects (for example, leaf lamina is reduced, but not disappeared as in the double mutant).For this reason, we can expect that several genes from the pool *maw* vs. WT will be found also in the data set from *maw mawb* vs. WT. Accordingly, ~43% of upregulated DEGs and ~49% of downregulated DEGs from the pool *maw* vs. WT are in common between the two datasets. Taking into account the subset of DEGs with a minimum of 2 fold change from the comparison *maw mawb* vs. WT (*i.e.*, the comparison between the two extreme conditions), then ~73% of DEGs are upregulated and ~27% are downregulated in the double mutant. A different way to observe this "transcriptomic landscape" is to look at genes which are both differentially expressed between the WT and the double mutant and between *maw* and the double mutant. These genes might be relevant because they show a profile where the trend of the expression level is virtually linear from WT to *maw*, whereas displaying a dramatic change in the double mutant. From the comparison of data sets from *maw* vs. *maw mawb* and *maw mawb* vs. WT we found that 1,032 DEGs over a 2 fold change threshold, upregulated in the double mutant, are shared between the two data sets. In a similar way, only 230 DEGs over a 2 fold change threshold, downregulated in the double mutant, are shared between the two data sets. In TABLE 1, the numbers of DEGs over different fold change thresholds from the three comparisons are summarized.

TABLE 1 – Analysis of fold change ratios of differentially expressed genes among the three comparisons. The ~% over the dataset taken into account (>2 fold change, >5 fold change, or >10 fold change) is also provided.

UPREGULATED	>2 fold change	~%	>5 fold change	~%	>10 fold change	~%
maw vs. WT	723	60%	96	55.5%	21	41%
maw mawb vs. *maw*	1,611	70%	246	83%	86	90.5%
maw mawb vs. WT	2,129	73%	415	85%	109	88%
DOWNREGULATED	>2 fold change	~%	>5 fold change	~%	>10 fold change	~%
maw vs. WT	482	40%	77	44.5%	30	59%
maw mawb vs. *maw*	692	30%	50	17%	9	9.5%
maw mawb vs. WT	803	27%	72	15%	15	12%

These data further support the biological soundness of the analysis. In fact, as shown in Chapter3, the *maw* mutant is more similar to WT than to *maw mawb*; the "true" intermediate condition (taking into account characters such as expansion of leaf lamina or carpel fusion) is provided by the *maw mawb* -/+ mutant. Accordingly, the number of relevant DEGs (displaying high fold change) is relatively low in the comparison WT vs. *maw*, but higher in the other two. Moreover, the number of relevant DEGs between these two is not extremely different, which is in accordance with the fact that the *maw* phenotype still retains several WT characters, in particular, the leaf lamina is still present, although reduced. Inside each subset, we analyzed how many genes are upregulated and downregulated in the most extreme condition (*i.e.*, either *maw* or *maw mawb*), to draw a general scheme among the three conditions. As shown in TABLE 1, the majority of DEGs are upregulated in the most extreme condition, which is in line with previous findings about the repressive activity of the Medicago *MAW* orthologue, *STF* (Tadege, Lin, Bedair,

et al. 2011; Lin, Niu, McHale, et al. 2013; Lin, Niu, and Tadege 2013). A general conclusion that can be drawn from TABLE 1 is that *MAW* and *MAWB* act in a very quantitative manner, affecting plant phenotype in a consequent way. This in accordance, for example, with the progressive reduction of leaf lamina, or the progressive splitting and shortening of carpels, along the gradient WT > *maw* > *maw mawb* -/+ > *maw mawb*.

To exemplify the kind of results obtained in this preliminary analysis, in FIG. 3 are reported the expression profiles (in FPKM, actual values) for a few genes from the subset *maw mawb* vs. WT, displaying a minimum of 10 fold change difference (bot up and downregulated).

Identifier	WT	*maw mawb*	Putative annotation
XLOC_011169	0.20	5.80	bidirectional sugar transporter sweet7. mediates both low-affinity uptake and efflux of sugar across the plasma membrane
XLOC_007375	0.34	8.32	auxin efflux carrier family protein. transporter C5D6.04-like [Solanum lycopersicum]
XLOC_026002	3.81	74.70	transcription factor BHLH51
XLOC_049744	1.11	14.31	1-aminocyclopropane-1-carboxylate oxidase. involved in the ethylene biosynthesis
XLOC_057187	0.90	10.67	P2A13-like. component of SCF(ASK-cullin-F-box) E3 ubiquitin ligase complexes
XLOC_049243	0.58	6.56	wrky transcription factor 50
XLOC_011995	4.68	49.47	lob domain-containing protein 38
XLOC_041435	10.85	0.54	myb family transcription factor

Figure 3 Example of data set derived from the comparison *maw mawb* vs. WT, displaying up and downregulated genes with a minimum fold change threshold of 10. Expression values are in FPKM (Fragments Per Kilobase of exon per Million fragments mapped).

A sugar transporter (sweet7) appears strongly upregulated in the double mutant. Sugar sensing and sugar metabolisms play important roles in organ growth and development, even though interaction with hormone signalling. For instance, an auxin efflux carrier is largely upregulated and also an enzyme involved in ethylene biosynthesis, which has been linked to cell elongation (Qin et al. 2007). We also found a *LOB* sequence in our data set of *maw mawb* vs. WT, which was strongly upregulated in the double mutant. This might be of interest for further functional analysis, because it is known that LOB proteins can play a role in organ development in Arabidopsis. For example, overexpression of a *LOB* gene

resulted in needle-like leaves (Sun et al. 2013), and the *LOB* gene *AS2* is repressed by the *MAW* and *MAW*B orthologue *STF* in Medicago, through recruitment of the corepressor TOPLESS (Zhang et al. 2014; Zhang and Tadege 2015). In FIG. 3 are exemplified the kind of targets that is possible to obtain from the analysis of the single gene sets previously shown (*maw* vs. WT; *maw mawb* vs. *maw*; *maw mawb* vs. WT). However, our principal aim is to identify DEGs relevant for specific biological processes taking place in the single and double mutant following a gradient. For this, we adopted a different strategy from the one briefly illustrated above, as shown in the next section.

Filtering RNA-Seq data

RNA-Seq analyses are high sensitive to external factors and, therefore, reproducibility is affected. In fact, the transcriptome is highly exposed to plant external conditions (both biotic and abiotic), including sampling, resulting in so called "batch effects" that might led to erroneous conclusions (Leek et al. 2010). This can mean a trade-off between information kept and reproducibility of results. Therefore, it is possible to approach the problem selecting data which are likely to be biologically significant and to be reproducible, and then to broad the analysis to the remaining data, to avoid loss of information.

In practice, the use of 3 different conditions (WT, *maw*, and *maw mawb*), in which *maw* is an intermediate phenotype between WT and *maw mawb*, allowed us to apply two sequential, strong filters to our dataset. These filters, taken together, are intended to highlight genes involved in biological processes shared by both the single and the double mutant (for example, lamina outgrowth). The first filter consisted in selecting only DEGs shared by all the three conditions. Since the differential expression analysis was performed in pairs, FPKM values from each pair comparison were plot on Excel tables and merged in a single file. In the end, we obtained 2650 DEGs shared by WT, *maw* and *maw mawb*.

We applied a second strong filter, consisting in selecting only DEGs where the *maw* expression was intermediate (either going up or down) between WTs and double mutants, as expected from making the *a priori* assumption that *maw* mutants have an intermediate phenotype between the other two (FIG. 4). In this way, we considered biologically relevant, and likely involved in biological processes shared by the single and the double mutant, only DEGs where *maw* levels were fitting either the red or the blue expression profiles represented in FIG. 4. After applying this second filter, we reduced the number of DEGs from 2650 to 556, meaning that about 1/5 of the previously selected DEGs were fitting the requirements from our second filter. Interestingly, in this small subset, 133 DEGs had downregulated profiles (~24%), and 423 DEGs had an upregulated profile (~76), where the expression profile is intended from WT to *maw mawb,* as in FIG. 3. In this way, we also obtained a pool of 490 (88%) DEGs displaying a minimum of 2 fold change.

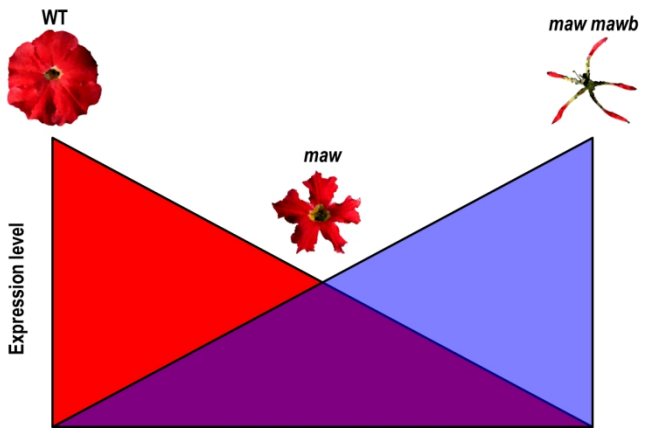

FIG. 4 Biological significance of selected DEGs

DEGs were selected on the basis of their expression profile. Only DEGs where expression in *maw* was intermediate between WT and the double mutant were selected. Therefore, only DEGs displaying a downregulating (red) profile or an upregulating (blue) profile from WT to *maw mawb* were selected.

We plotted DEGs expression levels using a *log2* fold-based heat map and performed sequence annotation based on *Arabidopsis thaliana* proteome (TAIR10-pep) by means of

BioEdit (Hall 1999). The remaining unannotated DEGs were annotated manually using Blast. These transcripts were coding for transposons and for a microRNA precursor.

GO terms based annotation of transcripts

In order to obtain a broad, preliminary view of transcripts significance and involvement in biological processes, we performed a GO terms analysis on the previously filtered dataset, by means of the Blast2GO software (Conesa et al. 2005) based on Viridiplantae Blast database, as well as on InterProScan analysis. From this analysis, ~half of the differentially expressed transcripts were involved in metabolic processes (FIG. 5), and less than 50 DEGs were automatically classified as directly involved in developmental processes (FIG. 5).

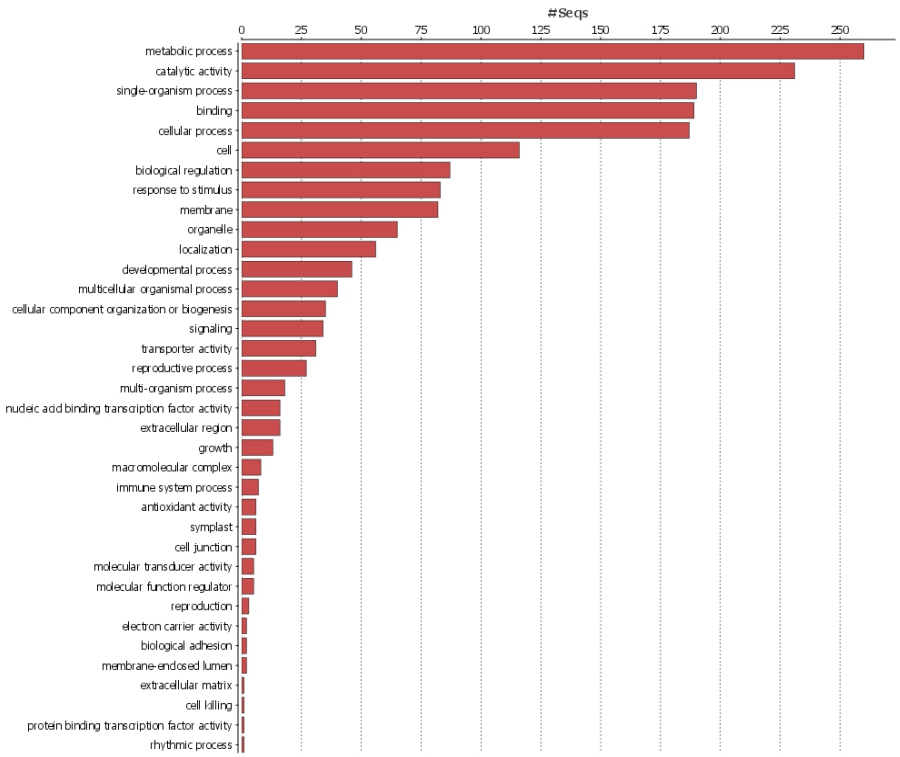

FIG. 5 Bar chart of GO terms classification

GO terms analysis of transcripts from the filtered dataset performed with Blast2GO. Transcript classification is redundant: The same transcripts can be assigned to different GO terms.

Expression profiles of transcription factors

WOX genes are homeobox transcription factors, a large family of genes involved in several aspects of plant development (Mukherjee et al. 2009). As master regulators of gene expression, *WOX* genes likely control the expression of other downstream transcription factors (or co-factors involved in transcriptional complexes), characterized by their own downstream targets. To answer this question, we searched for all DEGs involved in transcription in our dataset (either as direct-DNA binding proteins or as co-factors) identifying 36 transcripts putatively involved in DNA transcription (FIG. 6). The resulting data set is strongly enriched in transcription factors belonging to the homeodomain family, to bHLH, and the ARF family (see pie chart in FIG. 6). This composition is quite different from the general distribution of transcription factors in the Arabidopsis genome, as shown in FIG. 6 [pie chart bottom-left; data are from The Database of Arabidopsis Transcription Factors, (Jin et al. 2014)]. Altogether, the different enrichment compared to the genome of a WT plant is suggesting that the adopted strategy for DEGs filtering likely resulted in enrichment of DEGs involved in relevant biological processes.

Among the selected transcription factors, an orthologue of *At-HB13*, was significantly increased in single and double mutants (FIG. 6). In Arabidopsis, *athb13* mutants displayed faster growth rates of the stem (a phenotype due to higher cell divisions), but also defects in ovule development, with shorter siliques, less seeds, and more unfertilized ovules than WTs (Ribone et al. 2015). The *At-HB8* orthologue was progressively downregulated in single and double mutants (FIG. 6). *At-HB8* is involved in vein formation in Arabidopsis and, interestingly, it is positively controlled by the auxin-response transcription factor 5 (*ARF5*), also called *MONOPTEROS* (Donner et al. 2009). Interestingly, we have found the *ARF5* orthologue in our dataset (FIG. 6), which also is progressively downregulated in the

single and the double mutants, therefore matching with the expression profile of *At-HB8* and previous findings in Arabidopsis. Two *BLH1* like orthologues was instead upregulated in *maw* and *maw mawb* (FIG. 6). Interestingly, in Arabidopsis two *BLH1* like genes are expressed in lateral organs and in leaf margins (Kumar et al. 2007). Moreover, *BLH1* like have been shown to interact with *KNOX* genes in leaf margins (Kumar et al. 2007). In our dataset we found only one *KNOX* gene, an orthologue of *KNATM*, a *KNOX* gene lacking the homeodomain and expressed at the boundary of lateral organs, which also able to interact with BLH1 protein through the meinox domain (Magnani and Hake 2008).

In Arabidopsis, *KNATM* overexpressors displayed elongated and narrower leaves than WTs, because of defects in leaf lamina expansion (Magnani and Hake 2008). The expression profile of *Ph-KNATM* was progressively upregulated in the single and double mutant (FIG. 6), therefore matching with previous observations in Arabidopsis and the phenotypes of *maw* and *maw mawb* in Petunia.

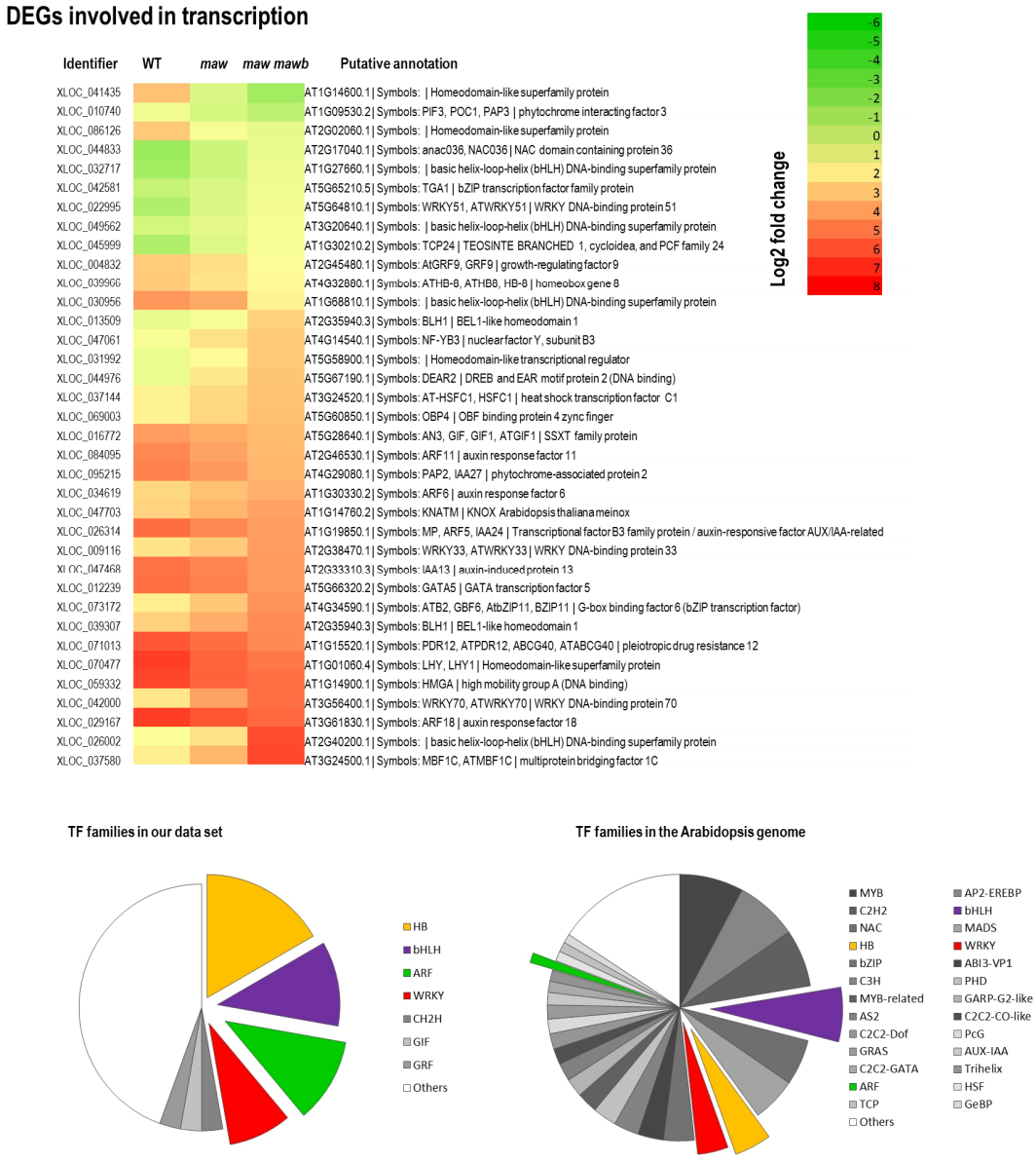

FIG. 6 Expression levels of DEGs involved in transcription

36 DEGs putatively involved in transcription were identified in our dataset. Expression levels are expressed in log2 fold change.

Bottom – Pie chart of TF families in our data set (left) and as distributed in the Arabidopsis genome [data from (Jin et al. 2014)].

For details concerning *At-HB13, At-HB8, ARF5, BLH1* and *KNAT,* see text.

Auxin-related genes are mainly downregulated in *maw* and *maw mawb*

We found several auxin-related DEGs, most of them downregulated in *maw* and in *maw mawb* (FIG. 7). This is interesting for two reasons. First, as only ~24 % of the total DEGs we selected were downregulated, the majority of auxin-related DEGs belong to this subgroup. Second, auxin plays a central role in several aspects of plant development. Although not only auxin quantity, but also auxin distribution should be taken into account, the observed progressive reduction of auxin-related genes well correlates with the progressively reduced blade expansion in the single and in the double mutant. In fact, auxin maxima arise in the shoot meristem at sites of origins of organs. In a similar way, auxin maxima also determine lateral roots emergence (Benková et al. 2003). Moreover, auxin fluxes pattern veins formation (Marcos and Berleth 2014), and auxin has also been shown to be involved in polarity establishment in lateral organs (Qi et al. 2014). Among the auxin-related DEGs, we found three *At-PIN1*-like sequences. We verified that these transcripts were coding for 3 different proteins, and aligned them to Arabidopsis PIN1 sequences, finding high sequence identity. It is well described that PIN1 orientation in Arabidopsis cells is responsible for auxin fluxes and, therefore, for auxin maxima (Benková et al. 2003). Additionally, our findings are in accordance with previous evidence concerning the interplay between auxin and WOX1 subfamily genes in Medicago and *N. sylvestris*, as shown by (Tadege, Lin, Bedair, et al. 2011).

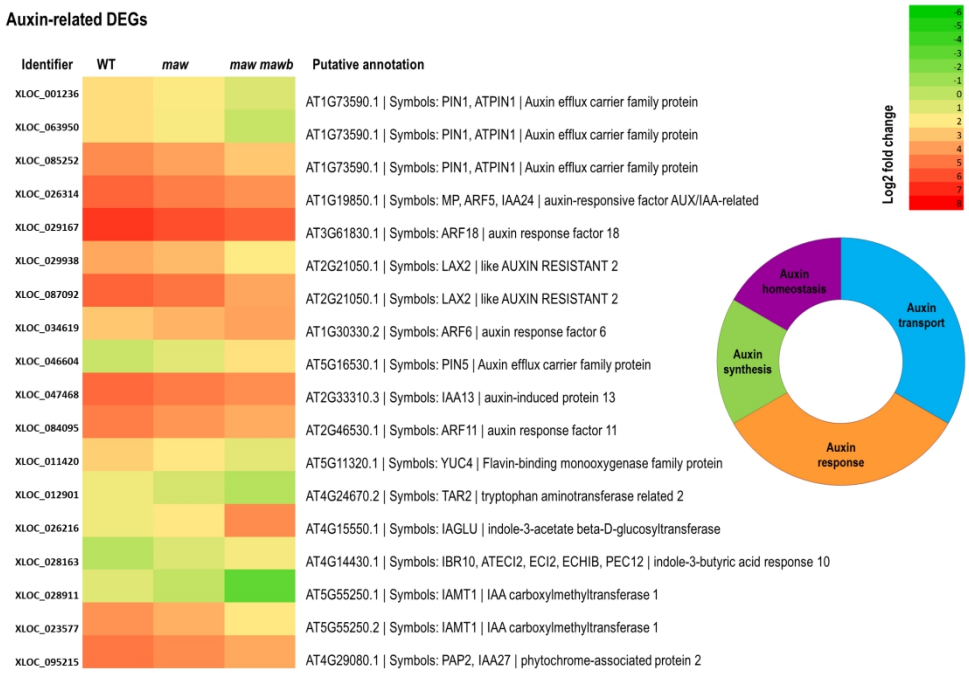

FIG. 7 Expression profiles of auxin-related DEGs

Heat-map for expression profiles of different auxin-related genes from our dataset. Expression levels are in *log2* fold change.

Cell-proliferation genes are downregulated in *maw* and *maw mawb*

Additionally, key cell-proliferation genes were progressively downregulated in the single and the double mutant, matching with the progressive reduction in blade outgrowth (FIG. 8). Among them are two orthologues of *CYCD3;1* in Arabidopsis, involved in cell number determination in developing leaves and lateral organs (Dewitte et al. 2007). Additionally, we also found that an At-*GRF9* and At-*GIF1*/*AN3* orthologues are also downregulated in *maw* and *maw mawb* (FIG. 8). *GRFs* are transcription factors comprising nine members in Arabidopsis, which are involved in organ size determination (Kim et al. 2003). *GRFs* positively control cell proliferation, and they have been shown to interact with the co-interactors called *GIFs*. Single mutants for *GRFs* or *GIFs* display narrower lateral organs than WTs, and multiple mutants combining these two classes of genes display a synergistic effect, with reduced cell number in lateral organs and less palisade cells at the

leaf level and GRFs and GIFs can physically interact, as shown by yeast two-hybrid and in vitro binding assays (Kim and Kende 2004). In particular, *gif1/an3* mutants have been well characterized in Arabidopsis, displaying narrower leaves than WTs, and direct interaction between GIF1/AN3 and GRF9 has also been shown by the yeast-two hybrid system (Horiguchi et al. 2005). Additionally, in previous studies, *CYCD3;1* levels were reduced in *gif* multiple mutants (Lee et al. 2009), which is matching with the DEGs profiles we found in Petunia (FIG. 8).

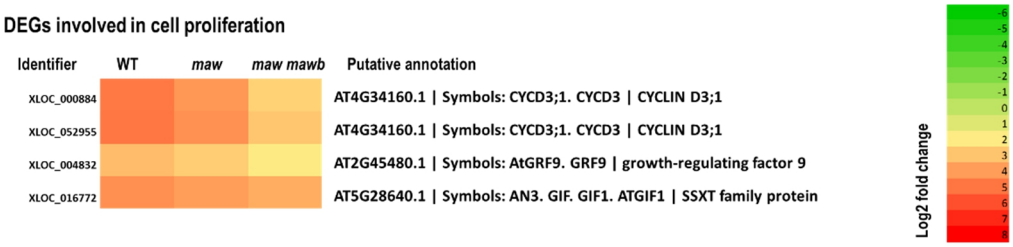

FIG. 8 Expression levels of cell proliferation related genes

Expression levels of cell-proliferation related DEGs are illustrated on a *log2* fold change basis.

The *miR156/SPL* genetic module is progressively affected in *maw* and *maw mawb*

We found that levels of *miR156/157* precursor are progressively upregulated in *maw* and *maw mawb* mutants (FIG. 9A). *miR156/157* is involved in several aspects of plant development, including vegetative to reproductive phase transition (Wu and Poethig 2006). Moreover, *miR156/157* is part of a genetic module including *SPL* (*SQUAMOSA-PROMOTER BINDING PROTEIN-LIKE*) genes, which are reported as typical targets of *miR156/157* (Wang and Wang 2015). SPLs are plant-specific transcription factors, firstly identified in Snapdragon as able to bind the promoter of the *SQUAMOSA* gene (Klein et al. 1996), and many of them are post-transcriptionally controlled by microRNAs and involved in pleiotropic effects in plant development (Chen et al. 2010). Interestingly,

*mi*R*156* targeted *SPLs* in Arabidopsis, such as *SPL9* and *SPL10*, are involved in plastochron length, with increased levels of *SPL9* and *SPL10* leading to increased plastochron length, whereas overexpression of *mi*R*156* leads to shortened plastochron length and overproduction of leaves (Wang et al. 2008). We found two *SPL*s orthologues in our data set correlating with the increased levels of *mi*R*156/157*: *SPL10* and *SPL1*3, displaying progressively decreased levels in the single and double mutant (FIG. 9A). These results match with the observation of a progressive increase in organ (leaf) number in *maw* and *maw mawb* at the rosette level (FIG. 9B), and it is further supported by statistical analysis, with significant differences in organ number among WTs and *maw*, and the single and the double mutant (FIG. 10). Organs produced by *maw* and *maw mawb* mutants include both normal size leaves, and smaller leaves (FIG. 9B, arrows), the latter absent in WT Petunias (FIG. 9B). *maw* and *maw mawb* mutants display an increasing number of small leaves (under 1.5 cm in length, as opposed to normal size leaves) which also account for the difference in total leaf number among the single and the double mutant (FIG. 10). Interestingly, in Arabidopsis, a compensatory mechanism has been proposed linking organ size and plastochron length: Shortened plastochron equals reduced leaf size; delayed plastochron equals larger leaves (Wang et al. 2008). This compensatory mechanism might explain the small size of leaves observed in *maw* and *maw mawb*.

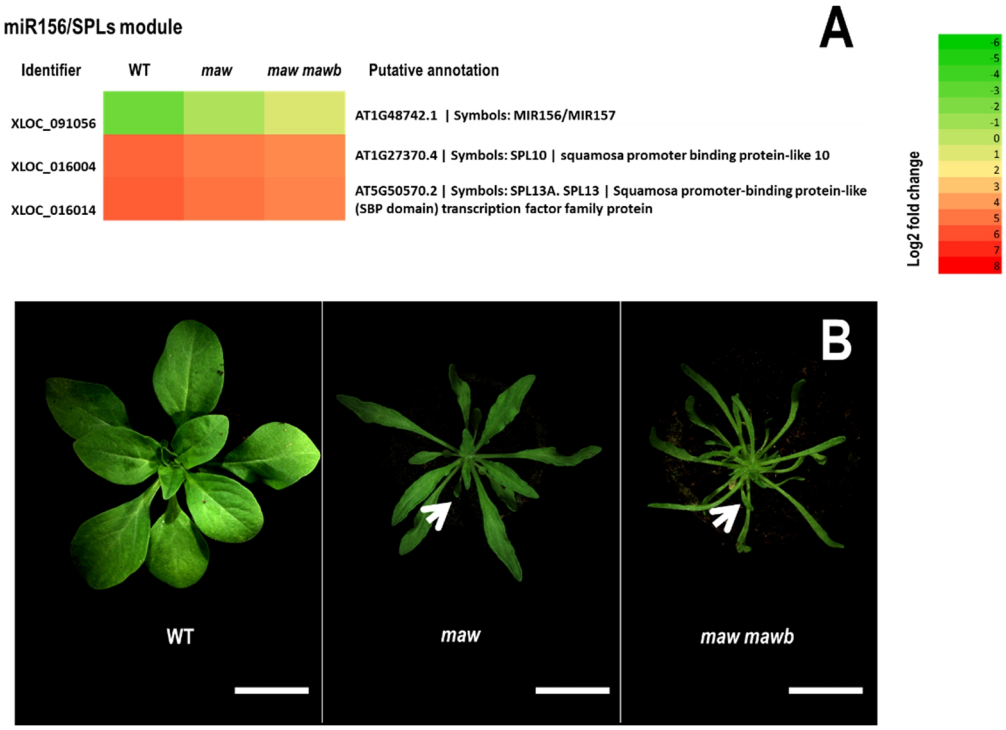

FIG. 9 *miR156/SPLs* genetic module is affected and correlates with supernumerary organs production in *maw* and *maw mawb* plants (aged of 5 weeks).

Genes from the miR156 genetic module (*miR156/157* precursor, *SPL10* and *SPL13*) are progressively affected in *maw* and *maw mawb* (**A**). Expression profiles reported as log2 fold change. Original FPKM values are as follows (ordered from WT to *maw mawb*): XLOC_091056 |0.177 < 0.716 < 1.837; XLOC_016004 |43.417 > 28.993 > 23.013; XLOC_016014 |50.128 > 33.822 > 25.422.

maw and *maw mawb* plants display more organs than WTs (**B**). Scale bars: 3 cm.

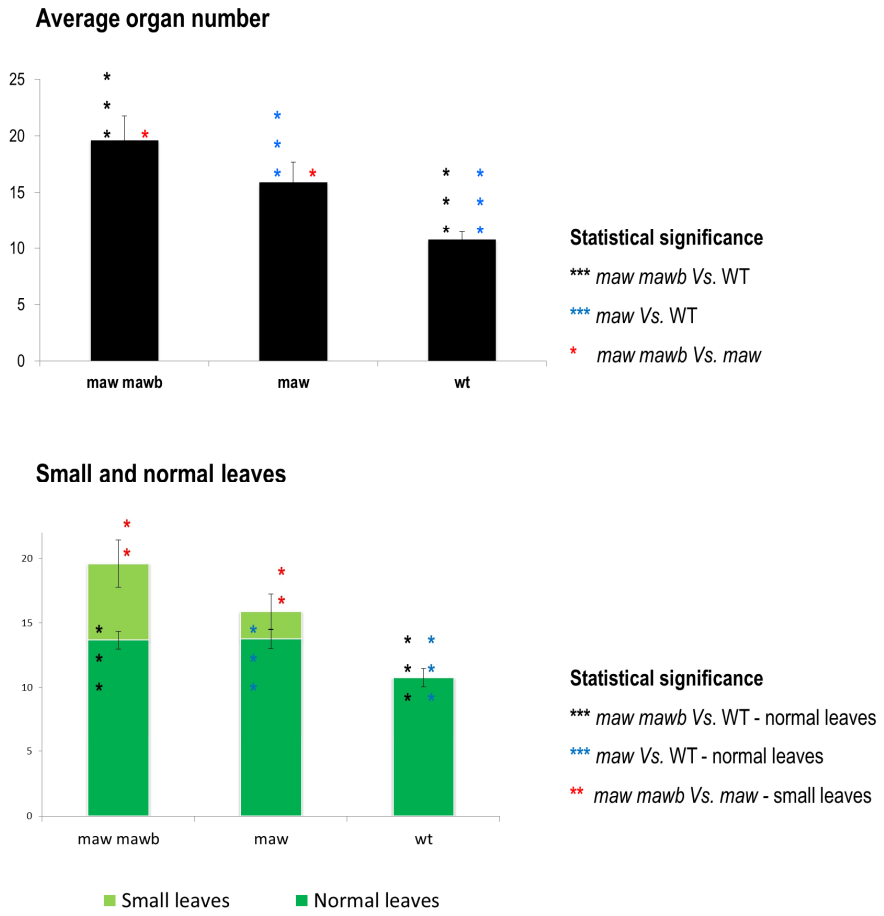

FIG. 10 Production of small organs in *maw* and *maw mawb* plants

Five week old plants were analyzed for leaf number. The total number of leaves is significantly higher in *maw* and *maw mawb* compared with WTs (top). Supernumerary organs produced by *maw* and *maw mawb* can be roughly divided into normal size and small size (under 1.5 cm) leaves. Normal leaves are significantly more in *maw* and *maw mawb*, compared to WT. Single and double mutants differ for the number of small leaves, significantly higher in the double mutant

A method for MAW/MAWB direct targets discovery

The second goal of our molecular analysis of the *maw* and *maw mawb* phenotypes was to identify the direct targets of the transcriptional activity of MAW. We opted for a RNA-Seq based method. For this, a construct carrying the promoter of *Ph-MAW* fused to the gluco-corticoid receptor (GR) from Mouse and to the genomic cds of *MAW* (FIG. 8A) was produced using the Gibson Assembly method. As the W138 line is not-genetically transformable, we introgressed our mutation into the V26 transformable background. Petunia plants (*maw -/+ mawb,* displaying a WT phenotype) derived from the W138 x V26 cross were transformed with the *pMAW::GR-MAW* construct using *A. tumefaciens,* by means of the leaf disc transformation method (FIG. 8A).

A parallel transformation of Arabidopsis *wox1 prs* plants was also performed with the same construct used in Petunia (FIG. 8B). As shown in Chapter III, genomic *MAW* from Petunia can rescue the *wox1 prs* phenotype in Arabidopsis. In this way, we were able to rapidly test the functionality of the construct: Grown on DEX plates, Arabidopsis seedlings displayed a WT phenotype (FIG. 8B).

Petunia plants derived from transformation and regeneration events were tested by PCR and selfed to select *maw mawb* double mutants carrying the transgene in the next generation. On the F_2, plants showing the *maw mawb* phenotype were tested by PCR for carrying the transgene (FIG. 8A). This line is intended for RNA-Seq analysis after DEX mediated activation of MAW (Schena et al. 1991), and CHX treatment to block protein turnover. The subsequent data analysis will likely identify a restricted pool of genes containing the direct targets of MAW/MAWB.

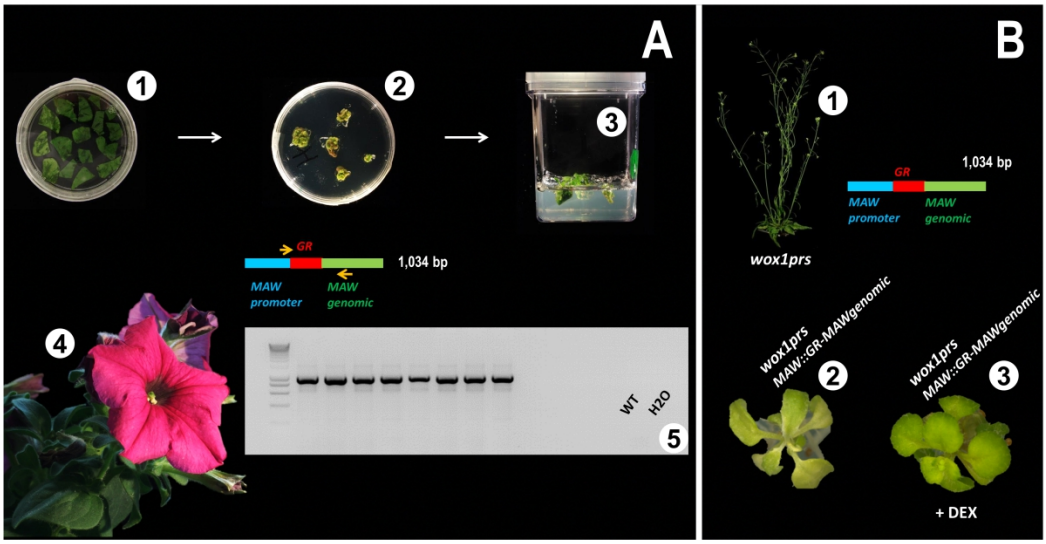

FIG. 11 Transformation of *Petunia* x *hybrida* (W138 in V26) and Arabidopsis using *Agrobacterium tumefaciens*

A – Petunia transformation with the *pMAW::GR-MAW* construct obtained by the Gibson Assembly method (construct cartoon shown in the middle). (**1**) Leaf discs from *maw* -/+ *mawb* plants (WT phenotype) were co-cultivated with *A. tumefaciens* on co-cultivation plates and callusing explants transferred to selective plates (**2**). Selected calli were transferred to rooting medium (**3**) for plant regeneration e transfer in soil. Regenerated plants (**4**) were tested by PCR (**5**) for the presence of the construct. These plants were selfed to obtain *maw mawb* mutant plants carrying the inducible *GR-MAW* construct.

B – *wox1 prs* plants (**1**) were transformed with the same construct used for Petunia. T_0 seeds were grown on MS medium (**2**), or MS medium supplied with DEX (**3**), resulting in narrow *wox1 prs* leaves (**2**) or complemented phenotype (**3**).

Discussion

RNA-Seq is a powerful method for transcriptome analysis and to discover affected genetic networks among different conditions. Here, we report preliminary results from an RNA-Seq analysis comparing WT, *maw*, and *maw mawb* mutants in Petunia, previously reported as affected in lamina outgrowth in lateral organs (Chapter III). Until recently Petunia was a non-sequenced model species. Then, draft genomes for *P. axillaris* and *P. inflata* became available ("Sequencing and Comparison of the Genomes of *Petunia inflata*

and *Petunia axillaris*", Conference paper, 2012). At the moment, no official release from the Petunia Consortium is available. However, selected labs already have the drafty genomes of *P. inflata* and *P. axillaris* (the two parental species of *P.* x *hybrida*). These genomes are available only as scaffold assembly, therefore lacking a GFF (coordinate) genome file. Because of these starting conditions, the RNA-Seq was performed as an almost *de novo* assembly. A basic GFF file was realized to help reads alignment, based on protein orthologues in Tomato. The two genomes of *P. inflata* and *P. axillaris* were merged together, obtaining a "synthetic" *P.* x *hybrida* genome. RNA samples were obtained from 9 biological samples, 3 per condition. Each biological sample was composed from a pool of vegetative apexes from the same condition (WT, *maw*, and *maw mawb*) and extracted using the Trizol method. Samples were sequenced on two lanes obtaining about 20 M reads of 100 bp per sample from each sequencing lane. After quality trimming using ERNE-Filter (Del Fabbro et al. 2013), libraries from the same sample were fused together and analyzed using the well described Tuxedo protocol (FIG. 3) (Trapnell et al. 2012). For our purposes, we considered the double mutant as a more dramatic phenotype than the single mutant. Given the high sensitivity of RNA-Seq and the consequent problem of data reproducibility, because of batch effects (Leek et al. 2010), we adopted a strong, radical filtering strategy to ensure the biological significance of our data. First, we have taken into account only DEGs shared by the 3 conditions, obtaining a common pool of 2650 DEGs. In order to find DEGs involved in lamina expansion, we applied a second strong filter, selecting only DEGs where *maw* expression levels were intermediate between WT and the double mutant (FIG. 4), obtaining 556 DEGs reflecting these criteria (133 upregulating, and 423 downregulating). The fact that the majority of DEGs are downregulating in the single and double mutant, is in accordance with previous studies concerning the mainly repressor activity of STF, the orthologue of MAW in Medicago (Tadege, Lin, Bedair, et al. 2011; Lin, Niu, McHale, et al. 2013; Lin, Niu, and Tadege 2013).

General analysis of RNA-Seq data

From a first GO analysis (FIG. 5), it appeared that almost half of the selected DEGs are involved in metabolic processes, and about 50 were automatically classified as involved in developmental processes. To refine this analysis, we focused our attention on the DEGs involved in DNA transcription (including transcription factor or co-factors). Given their broad role in plant development, *WOX* genes are likely to control other transcription pathways downstream of them. We performed such analysis manually, finding 36 DEGs involved in transcription (FIG. 6). These include a selected subset of transcription factors, compared to the distribution in a whole plant genome, such as the Arabidopsis genome (FIG. 6). In particular, *HOMEOBOXes*, *bHLHs*, and *ARFs* resulted particularly enriched in our data set, suggesting a potential role in biological processes affected in the single and in the double mutant.

Auxin plays an important role in *maw* and *maw mawb* phenotypes

Analyzing our RNA-Seq data set, we found several auxin-related DEGs (FIG. 7), the majority of which are downregulated in the single and double mutant. This result is interesting, and somehow expected, given the fundamental role of auxin in several aspects of plant development and the phenotype of the mutants, characterized by reduced leaf lamina. In fact, auxin is well known for its role in establishment of organ primordia, driven by formation of organ maxima (Benková et al. 2003). Finally, auxin is required for leaf blade outgrowth, as a symmetric distribution of auxin in the leaf, is required for symmetric cell division patterns and proper lateral expansion of the leaf lamina (Zgurski et al. 2005).

PIN1, auxin efflux carriers, are typically involved in auxin maxima establishment and in directing auxin fluxes through their localization in organ cells (Chen et al. 1998; Benková et al. 2003; Bohn-Courseau 2010; Luschnig and Vert 2014). We found 3 different sequences displaying the highest similarity wit At-PIN1 in Petunia (FIG. 7), all of which were progressively downregulated in *maw* and *maw mawb*. However, in our dataset we also

found auxin response factors (*ARFs*), as well as genes involved in auxin synthesis, such as *YUC4*, member of the *YUCCA* gene family. *YUCCA* genes are coding for flavin monooxygenases required for auxin biosynthesis (Mashiguchi et al. 2011). Moreover, in Arabidopsis, *YUC4* was shown to be required for leaf margin development, since corresponding local auxin biosynthesis is required for lamina expansion (Zgurski et al. 2005; W Wang et al. 2011). Tryptophan aminotransferases are another class of genes involved in auxin biosynthesis (Mashiguchi et al. 2011). We also found a tryptophan aminotransferase related gene downregulated in both the single and the double mutant (FIG. 7). Moreover, these findings are in accordance with previous studies in *stf* and *lam1* mutants in Medicago and *N. sylvestris*, respectively (Tadege, Lin, Bedair, et al. 2011) which, also by means of microarray analysis, pointed out that auxin related genes are affected in these mutants. In fact, several auxin related transcripts are affected in *stf* mutants in Medicago, whereas leaves from both *stf* and *lam1* displayed less free auxin as measured by GC-MS (Tadege, Lin, Bedair, et al. 2011).

An *ARF5* orthologue was downregulated in single and double mutants (FIG. 7 and FIG. 6). *ARF5* is positively controlling *At-HB8*, an homeobox gene involved in vein formation in Arabidopsis (Donner et al. 2009). We found that an *At-HB8* orthologue was also downregulated in the single and double mutant (FIG. 6). This is of interest because, given the lack of blade expansion, the corresponding vascular system crossing the leaf blade in the WT is also reduced in *maw* and *maw mawb*, where only the middle rib of the leaf is in place. Therefore, these observations well correlate with the described roles for *ARF5* and *AtHB8* and the phenotype in Petunia *maw* and *maw mawb*. Altogether, these data suggest that auxin biosynthesis and auxin distribution play a crucial role in leaf blade expansion defects observed in *maw* and *maw mawb*.

Cell-proliferation genes are affected in *maw* and *maw mawb*

The observed defects in lamina expansion in *maw* and *maw mawb* are likely due to less cell proliferation in the lateral direction (therefore, not forming the full lamina). To test this hypothesis, we analyzed cell-proliferation genes in our dataset. Two *CYCD3;1* orthologues, a cyclin directly involved in determining cell number in developing lateral organs in Arabidopsis (Dewitte et al. 2007), were downregulated in the single and double mutant (FIG. 8). Matching with this finding, an *At-GRF9* and an *At-GIF1/AN3* orthologue was progressively downregulated in *maw* and *maw mawb*. In Arabidopsis, *GRFs* form a nine-member gene family determining organ size by controlling cell proliferation (Kim et al. 2003; Kim and Kende 2004). *GRFs* have been shown to directly interact with *GIFs* and single as well as double mutants for *GRFs* and *GIFs* display narrower lateral organs than WTs (Kim and Kende 2004; Lee et al. 2009). *Gif1/an3* mutants in Arabidopsis display narrower leaves than WTs, and *GIF1/AN3* can directly interact with *GRF9* in this species (Horiguchi et al. 2005). Therefore, the same mechanism is likely responsible, at least in part, for the reduced leaf lamina observed in *maw* and *maw mawb*. As our RNA-Seq was intended as a preliminary analysis, further confirmation of *Ph-GIF1/AN3* and *Ph-GRF9* by qPCR is required. Based on this, it would be of interest to perform further functional analyses.

The *miR156/SPL* genetic module is affected in *maw* and *maw mawb*, and it likely accounts for supernumerary organs production

Single and double mutants display an increasing number of organs, additionally, small leaves are produced in *maw* and many more in *maw mawb* (FIG. 9B, FIG. 10). Interestingly, we found a possible explanation for this phenotype, since the genetic module of *mi*R*156/SPL*, reported to affect plastochron length and organ production in Arabidopsis (Wang et al. 2008; Chen et al. 2010; Wang and Wang 2015). The behavior of the

orthologues transcripts of a *mi*R*156* precursor, and *SPL10*, *SPL13* orthologues are in accordance with this model (FIG. 9A).

Perspectives

RNA-Seq analysis

Although the RNA-Seq previously reported was intended as a preliminary analysis, it already allowed the identification of relevant genetic pathways, which are likely to explain the observed phenotypes in *maw* and *maw mawb*. The analysis was performed following the reliable and widely used Tuxedo protocol (Trapnell et al. 2012). However, the actual state of the Petunia genome was challenging for RNA-Seq analysis. Therefore, different strategy might lead to more reliable results, and it might be of interest to compare different methods. Since RNA-Sequencing is a more and more used technique, even on non-model species, such a comparison might be technically interesting for other species in a similar situation. E. Bertolini (Pisa) performed a parallel RNA-Seq analysis in which reads were aligned separately on the two genomes of *P. axillaris* and *P. inflata*, and only in the very end a synthetic *P.* x *hybrida* transcriptome was reconstructed. We envisage providing a comparison of the two methods in the near future.

Validation of RNA-Seq data

In any case, data from RNA-Seq need to be further validated using a different method, typically qPCR. This validation step is generally required for publishing a consequent biological story. We plan to validate by qPCR the transcripts of interest previously reported.

Biological stories

After qPCR validation, the *mi*R*156*/*SPL* module and supernumerary organ production already represents a significant result on its own. As previously shown, we have identified

different genes which represent interesting targets for further functional analysis, after validation of RNA-Seq data by qPCR.

We have also identified auxin as a major player in *maw* and *maw mawb* phenotype. We are developing *maw mawb* plants expressing the *DR5::venus* construct [by crossings of *maw mawb* mutants with *DR5::venus* plants, previously obtained by Roeska Blankevoort at Ronald Koes lab (VU, Amsterdam)]. These plants could be used to compare the possibly different auxin patterns in WT and mutant plants, by means of confocal microscopy.

Implementation of a method for MAW/MAWB direct targets discovery

We also started implementing a method to discover the direct targets of MAW/MAWB. To this aim, we first produced a construct where genomic *MAW* is linked to the *GR* receptor sequence and expression placed under *MAW* promoter. Using this construct, we transformed Petunia plants in a way to obtain *maw mawb* mutants expressing *pMAW::GR-MAWgenomic*. In fact, GR can be activated by dexamethasone (DEX), and the linked MAW translocate to the nucleus (Schena et al. 1991). We first tested this construct transforming *wox1 prs* Arabidopsis mutants, which responded well to DEX treatment, complementing the phenotype (FIG. 11B). Petunia transformants were also obtained and tested by PCR. We eventually obtained F_2 plants *maw mawb* expressing *pMAW::GR-MAWgenomic*.. Before being used for the analysis, further tests to evaluate the efficacy of the DEX treatment are required.

Materials and Methods

RNA extraction - Total RNA was extracted from shoot apexes of W138 *P.* x *hybrida* plants grown under long day and stable environmental conditions in a growth chamber. Mutants were from the previously described *maw*-6 (Vandenbussche et al. 2009), and *maw*-4 *mawb* (Chapter III). We obtained 9 biological samples, 3 per condition (WT, *maw, maw mawb*). For each condition, biological samples were composed as follows: 10 apexes from WT plants; 7 apexes from *maw*-6 plants; 10 apexes from *maw*-4 *mawb* plants. RNA extraction was performed using the TRIzol® method and RNA quality assessed using an Agilent Bioanalyzer 2100. Samples displaying an RNA Integrity Number (RIN) > 8 were used for sequencing.

RNA sequencing - Samples were sequenced on a HiSeq 2500 Illumina machine by IGA Technology Services (Via J.Linussio, 51 Z.I.U. Udine 33100 – Italy). 1 x 100 bp reads were produced on a multiplexing lane (9 x 2), resulting in 18 libraries of ~20 M reads each.

Analysis of raw reads distribution - Raw reads distribution for each biological sample was analysed, showing the variability of depth of sequencing within each sample. Y axis indicates raw reads number in millions. Raw reads distribution is coherent within each condition.

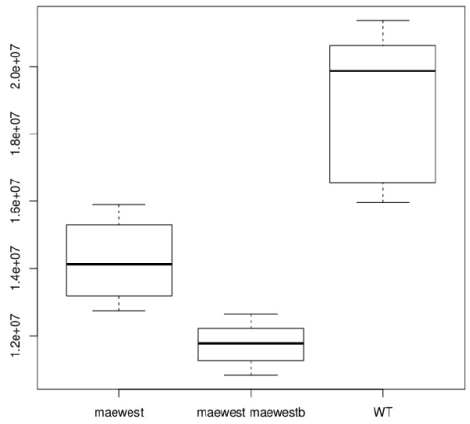

(Credit: E. Bertolini)

Quality trimming - Library trimming was performed with ERNE-Filter (Del Fabbro et al. 2013), producing trimmed read of min-mean-phred-quality 33 and minum size 90 bp. Trimmed reads from the two libraries derived from the same sample were fused together, obtaining 9 libraries.

Library name	Raw reads	Trimmed reads	Percentage
1A	21374674	18687202	0.8742
1B	20622968	18059393	0.8756
2A	16538825	14440538	0.8731
2B	15957426	13957004	0.8746
3A	20250360	17676825	0.8729
3B	19492276	17053260	0.8748
4A	15899131	13896420	0.8740
4B	15304528	13398512	0.8754
5A	13179757	11578847	0.8785
5B	12735309	11201811	0.8795
6A	14362644	12603430	0.8775

6B	13879837	12194177	0.8785
7A	12644967	11107849	0.8784
7B	12216930	10749956	0.8799
8A	11990403	10529268	0.8781
8B	11547290	10150695	0.8790
9A	11257009	9843690	0.8744
9B	10824700	9480924	0.8758
Total reads	**270079034**	**236609801**	**0.8760**

Data analysis - The two available genomes of *P. axillaris* and *P. inflata* were merged together, resulting in a "synthetic" *P.* x *hybrida* genome. Tomato based GFF files for the two genomes were also merged together. Following the Tuxedo package (Trapnell et al. 2012), reads alignment was performed using Bowtie2 (version 2.1.0), and TopHat2 (version 2.0.9).

TopHat2 alignment data for each sample (in number of reads)

Sample	**1**	**2**	**3**	**4**	**5**	**6**	**7**	**8**	**9**
Input	36746595	28397542	34730085	27294932	22780658	24797607	21857805	20679963	19324614
Mapped	31365782	24235145	29643529	23331798	19562393	21248464	18640699	17657821	16482000
Of these	20688224	15943440	19516457	15516916	13162191	14111501	12260234	11636341	10845946
Mapped %	85.4	85.3	85.4	85.5	85.9	85.7	85.3	85.4	85.3
Of these mult. align.%	66	65.8	65.8	66.5	67.3	66.4	65.8	65.9	65.8

Cufflinks, Cuffmerge, Cuffdiff - Isoform discovery and transcript quantification was performed using Cufflinks (version 2.1.1) followed by production of a merged GFF from all the three conditions with the sub-tool Cuffmerge (version 1.0.0). Quantification and statistical validation of differentially expressed genes was performed with Cuffdiff (version 2.1.1). Downstream analysis and graphs production was performed in Excel.

Blast, annotation, and GO terms analysis. We performed annotation of the selected DEGs by means of BlastX through the Bioedit software (Hall 1999) on the TAIR-10pep database for Arabidopsis thaliana. Non coding sequences were manually annotated through other TAIR databases. To perform GO terms analysis, we used the Blast2GO software (Conesa et al. 2005), after blasting sequences on the Blast2GO *Viridaeplantae* Pro database, and InterProScan analysis, following company's (Blast2GO) guidelines for data analysis and graphics production.

Statistical analysis of leaf number in WT, *maw*, and *maw mawb* plants - Leaves were counted manually on 5 weeks-old Petunia plants using the following samples: 8 WT plants, 8 *maw* plants, and 24 *maw mawb* plants. For small *Vs.* normal leaves counts, leaflets under 1.5 cm were considered as "small leaves". Data significance was assessed by heteroskedastic T-tests. Full data sets are available in Chapter VII.

Aknowledgements

RNA-Seq analysis was performed in collaboration with E. Bertolini and M. E. Pè (Istituto di Scienze della Vita, Scuola Superiore Sant'Anna, Pisa, Italy). J. Just (RDP UMR 5667, Lyon, France), provided Petunia GFF files, based on Tomato protein sequences, for Tophat2 analysis.

Chapter V cover - SEM picture (x 150) of a "trichome landscape" on a *wox3 wox3b* pedicel

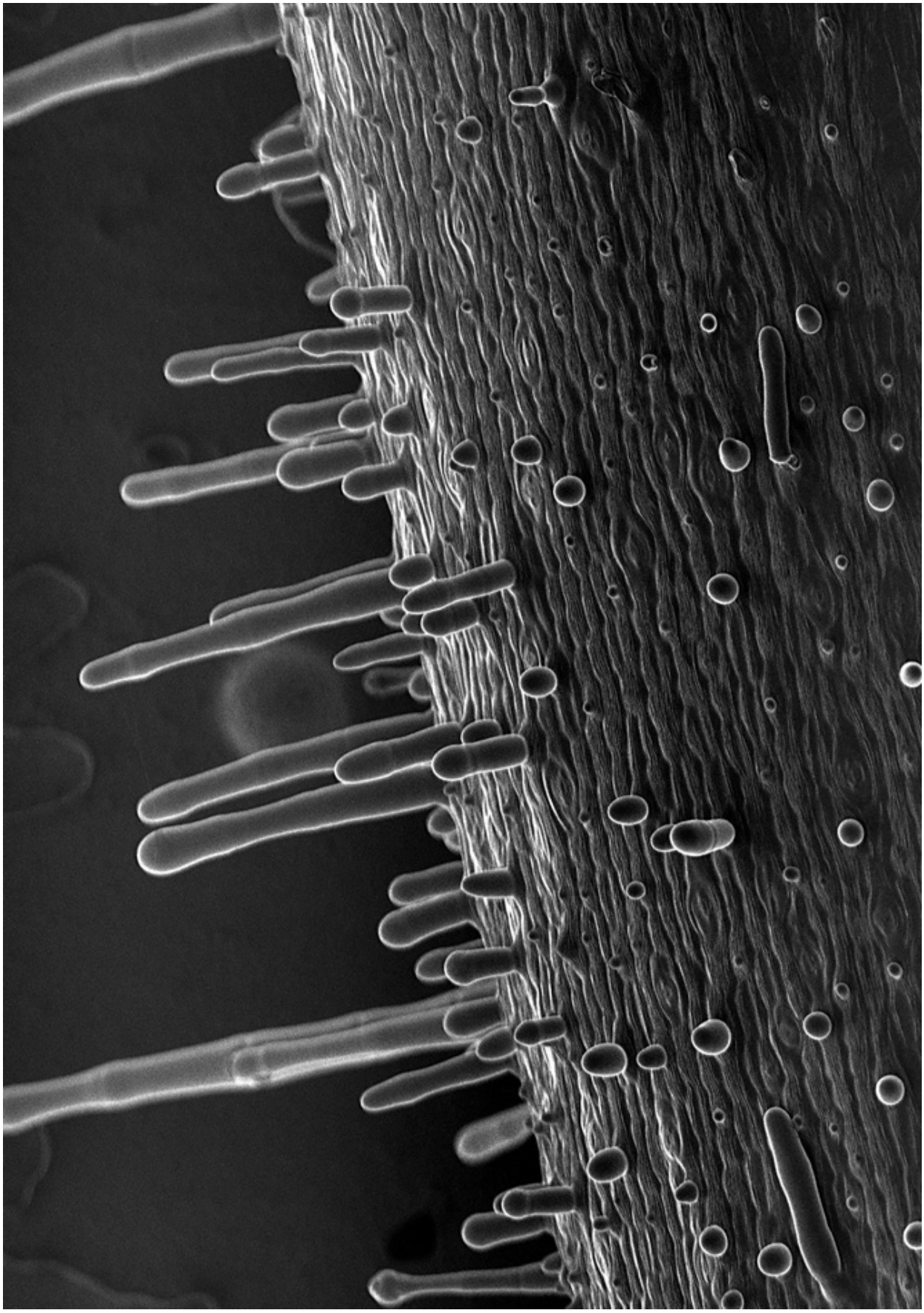

V. The two genes *WOX3* and *WOX3B* are involved in trichome development in Petunia

Enrico Costanzo[1,2], Patrice Morel[1] & Michiel Vandenbussche[1]

Abstract

In a comparative analysis of the functional role of *WOX* genes among Petunia (Asteridae) and Arabidopsis (Rosidae), we analyzed the role played by WOX3 subfamily genes in Petunia, through a reverse genetics approach. *WOX3* genes are typically involved in blade outgrowth in other species, including Arabidopsis, where the *WOX3* gene *PRS* genetically interacts with *WOX1* in blade outgrowth (Vandenbussche et al. 2009; Nakata et al. 2012). We have previously shown that the two *WOX1* genes in Petunia, *MAW* and *MAWB*, are redundantly involved in blade outgrowth in this species, questioning the role played by *WOX3* genes in Petunia. Unexpectedly, we found that WOX3 subfamily genes are involved in trichome development in Petunia (Asteridae). Molecular mechanisms leading to unicellular trichome development are nowadays well described in Arabidopsis (Rosidae), whereas little is known about the development of multicellular trichomes in Asteridae. Differently from Arabidopsis, we show that the two subfamilies WOX1 and WOX3 do not genetically interact in Petunia. The differential, functional recruitment of the WOX3 subfamily in Petunia highlights, once more, the evolutionary adaptability of this class of genes.

[1]*Laboratory of Reproduction and Development of Plants, UMR5667, Ecole Normale Supérieure de Lyon, Lyon, FRANCE*

[2]*Istituto di Scienze della Vita, Scuola Superiore Sant'Anna, Pisa, ITALY*

Introduction

We have previously shown that the two WOX1 subfamily genes, *MAW* and *MAWB,* are involved in lateral expansion of lateral organs in *Petunia* x *hybrida*, leaving open the question about the functional role of the WOX3 subfamily in this species.

In Arabidopsis, the only member of the WOX3 subfamily, *PRS*, was shown to have a unique function in lateral expansion of lateral sepals and in stipule development, although it was much broader expressed than just sepals and leaves, being also expressed at the lateral edges of petals and stamens, as well as in cotyledons during embryogenesis (Matsumoto and Okada 2001; Nardmann et al. 2004). In maize, the two *WOX3* genes *NS1 & NS2* are involved in lateral expansion of leaves (Nardmann et al. 2004). More recently, a broader developmental role for *PRS* was indeed revealed, since *PRS WOX1* genes in Arabidopsis functionally overlap in blade expansion in lateral organs (Vandenbussche et al. 2009). In Petunia, the two WOX1 members in Petunia are involved in blade expansion in lateral organs. In particular, the double mutant *maw mawb* already displayed a much stronger phenotype than *wox1 prs* in Arabidopsis, especially in leaves, questioning the role played by *WOX3* genes in Petunia. Here, we report for the first time that the WOX3 subfamily in Petunia comprises two genes which play a redundant role in multi-cellular trichome development.

Trichomes cover the epidermis of many plant species and are typically involved in processes such as plant defense, protection against water loss (Li et al. 2012), extreme temperature and other abiotic stresses (Levin 1973; Werker 2000; Wagner et al. 2004). Several different, analogous structures are reported as trichomes in botanical literature. Despite of that, trichomes can be generally defined as protuberances emerging from the epidermis and characterized by specific height/width ratios, roughly divided into simple trichomes and glandular, secreting trichomes (Wagner et al. 2004). Glandular trichomes

typically secrete complex secondary metabolite compounds, whereas simple trichomes are typically not secreting (Dai et al. 2010). *Arabidopsis thaliana* and *Petunia* x *hybrida* belong to the two distinct core-eudicots groups called Rosidae and Asteridae, respectively. Petunia is a member of the *Solanaceae* family, where different kinds of multicellular trichomes can be found (Adedeji O 2007). In contrast, Arabidopsis displays unicellular, three-branched trichomes (Hülskamp 2000) originating directly from the epidermis and characterized by four endoreduplication phases, therefore resulting in a 32C DNA content, on average (Hülskamp 2000; Schnittger and Hülskamp 2002). In Arabidopsis, trichomes are well studied structures and their underlying molecular pathways have been largely elucidated (Balkunde et al. 2010; Pattanaik et al. 2014). The *GL2* homeobox HD-Zip gene is involved in trichome cell differentiation in Arabidopsis leaves (Rerie et al. 1994), whereas the same gene acts as a suppressor of hairs at the root level, where it is expressed in hairless cells (Masucci et al. 1996). Instead, at the leaf level, trichomes are suppressed by TRY, a R3 single repeat MYB transcription factor (Hülskamp et al. 1994; Schnittger et al. 1998; Pesch and Hülskamp 2011). The MYB transcription factor CPC is also involved in trichome suppression (Schellmann et al. 2002). *try* mutants display trichome-clusters (Hülskamp et al. 1994), and TRY is acting by competing with GL1 for the same binding site on GL3 in cells not expressing trichomes (Marks and Esch 2003; Esch et al. 2003). *GL1* codes for a R2R3 MYB transcription factor (Herman and Marks 1989; Larkin et al. 1993), whereas *GL3* codes for a bHLH transcription factor (Payne et al. 2000). Along with TTG1, a WD40 repeat protein (Walker et al. 1999), and EGL3, another bHLH protein (Bernhardt et al. 2003), GL1 and GL3 are part of a TTG1-bHLH-MYB regulatory complex involved in trichome development in Arabidopsis (Zhao et al. 2008). Such a complex has been suggested to positively control *GL2* and *TTG2* (coding for a WRKY transcription factor (Johnson et al. 2002)) (Ishida et al. 2007; Morohashi et al. 2007; Yang and Ye 2013).

Therefore, this mechanism of single-cell trichome development in Rosidae is quite well understood nowadays.

Interestingly, the molecular components of the trichome developmental pathway in Arabidopsis represent a genetic module also involved in pigmentation. In fact, the MYB-bHLH-WD40 complex is involved in anthocyanin biosynthesis in many eudicots, including Arabidopsis, where different players of the trichome pathway are shared by the anthocyanin biosynthesis pathway (Robinson and Roeder 2015). In Asteridae, this complex is also involved in anthocyanin biosynthesis (Ramsay and Glover 2005; Robinson and Roeder 2015), but, apparently, not in trichome development (Yang and Ye 2013).

This is probably one of the main reasons why trichome development in Asteridae remains poorly understood. Moreover, different kind of trichomes can be found in this group (*e.g.*, seven types of trichomes have been described in Tomato, with type I, IV, VI, and VII being twisted glandular, and types II, III, and V defined as non-glandular (Tian et al. 2012)), and it has been proposed that different gene regulatory networks underlie different types of trichomes, despite the sharing of some common components (as suggested by overexpression experiments in *Nicotiana* (Payne et al. 1999)). The role of jasmonate and BAP in multicellular trichome development in Tomato (Asteridae) has also been reported (Li et al. 2004; Maes and Goossens 2010). Orthologues of *TRY* and *GL3* have been cloned from Tomato (*Solanum lycopersiocum, Sl*) and, whereas overexpression of *CPC::Sl-TRY* resulted in inhibition of trichome development in Arabidopsis (and in a corresponding root-hair enhancement), no effects were observed in *GL3::Sl-GL3* overexpressing plants (Tominaga-Wada et al. 2013). On the same line, overexpression of *GL1* from Arabidopsis in Tobacco didn't result in perturbation of trichome development in this species (Payne et al. 1999). Instead, overexpression of *MIXTA* (a *MYB* gene involved in conical cells development on petals (Noda et al. 1994)) from *Antirrhinum majus*

(another member of the Asteridae group) in Tobacco plants, resulted in supernumerary trichomes, as well as in conversion of conical cells into trichomes (Glover et al. 1998; Payne et al. 1999). Interestingly, overexpression of *MIXTA* in *gl1-1* Arabidopsis plants didn't rescue the glabrous phenotype (Payne et al. 1999).On the opposite, a *MIXTA* orthologue (*CotMYBA*) from Cotton, a member of the Order *Malvales* (part of the Rosidae (The Angiosperm Phylogeny Group 2009)), resulted in altered trichome patterns when overexpressed in Tobacco (Payne et al. 1999). These results are based on heterologous overexpression phenotypes. However, *RNAi* cotton for two *MIXTA-like* genes displayed shorter fibers and reduction in trichome number (Machado et al. 2009).

In tomato, the gene *WOOLLY* (*WO*) was firstly identified as a dominant mutation, producing abundant trichomes on tomato leaves (Shilling 1959; Yang, Li, Zhang, Wang, et al. 2011). Stable transformation of WT tomato plants with *WO* led to a woolly phenotype, due to increased trichomes (Yang, Li, Zhang, Wang, et al. 2011). *WO* codes for an orthologue of PDF2 in Arabidopsis (an HD-Zip transcription factor), and RNAi plants for *WO* display a glabrous phenotype (Yang, Li, Zhang, Luo, et al. 2011). In Arabidopsis, *PDF2* is involved in epidermal cell differentiation (Abe et al. 2003) and embryo development (Ogawa et al. 2015), whereas the *GL2* gene, coding for another HD-Zip transcription factor from a different sub-group than *PDF2* (Ariel et al. 2007), is involved in trichome development in Arabidopsis (Rerie et al. 1994). *WO* has been shown to physically interact with the cell-cycle related gene *CycB2* in Tomato, likely involved in development of multicellular trichomes (Yang, Li, Zhang, Luo, et al. 2011). Another HD-Zip transcription factor playing a role in trichome development is OCL4 from Maize, a Monocot. *RNAi OCL4* plants displayed ectopic macrohairs whereas, in Arabidopsis, *gl2-1* plants overexpressing *GL2::Zm-OCL4* displayed an even worse phenotype, suggesting the ability of *OCL4* to inhibit trichome development in both these two distantly related species (Vernoud et al. 2009). In another Monocot, Rice (*Oryza sativa*), a locus of agronomical

interest called Glabrous Rice 1 involved in trichome development has also been identified (Li et al. 2012). In fact, glabrous Rice (lacking trichomes) is relevant for Rice breeding, and most of cultivated Rice in the US is glabrous, as glabrous hulls have increased weight per unit volume compared to hairy ones, therefore reducing transportation costs (Hu et al. 2013). Moreover, glabrous rice varieties increase the efficiency of mechanical harvesting and further processing, therefore being of economical relevance (Nishikawa et al. 1992). The Glabrous Rice 1 locus codes for a WOX3 protein in (Os-WOX3B), *glr1* mutants are glabrous, RNAi plants for *GLR1* displayed reduced trichomes, and *GLR1* overexpressor partially complemented the *glr1* phenotype(Li et al. 2012). In Rice, the two paralog genes *NAL2 & 3* code for an identical transcription factor (Os-WOX3A) (Cho et al. 2013), which is involved in leaf lamina expansion in a similar way to its orthologues in Maize (*NS1 & 2*) and Arabidopsis (*PRS*) (Scanlon et al. 1996; Matsumoto and Okada 2001; Nardmann et al. 2004; Dai et al. 2007; Vandenbussche et al. 2009; Nakata et al. 2012; Cho et al. 2013; Yoo et al. 2013). Interestingly, whereas Os-WOX3B is involved in trichome development, Os-WOX3A has been shown to play a role also in root-hair development (Yoo et al. 2013), suggesting the same kind of trichome/root functional dichotomy already observed in Arabidopsis, but inside the same genetic subfamily: the WOX3 subfamily of *WOX* genes, homeobox genes related to *WUSCHEL* (*WUS*) (see (Costanzo et al. 2014)). In Arabidopsis, *PRS* is redundantly involved with *WOX1* in lateral expansion of leaf lamina and floral organs (Vandenbussche et al. 2009; Nakata et al. 2012; Nakata and Okada 2012;). In Medicago (Rosidae), the *WOX3* orthologue *LOOSE FLOWER* is involved in sepal and petal development but not in leaf blade outgrowth (Niu et al. 2015), where the *WOX1* gene *STF* plays an important role (Tadege, Lin, Bedair, et al. 2011). Differently from Arabidopsis, *LOOSE FLOWER* and *STF* do not genetically interact, even at the flower level (with the possible exception of carpel development), where *stf* single mutants alone already display narrow floral organs (Niu et al. 2015). Here we provide evidence for

differential functional recruitment of *WOX3* genes in Petunia in a completely different task to what has been previously shown in other eudicots: trichome development.

Results

The WOX3 subfamily is composed of two members in Petunia

Taking advantage of the availability of the two sequenced genomes from *P. inflata* and *P. axillaris*, in addition to the earlier described WOX3 member *Ph-WOX3*, we identified a second member of the WOX3 subfamily in Petunia, called *Ph-WOX3B* (FIG. 1). These two genes share a similar structure, formed by two exons (see FIG. 1B and C), a structural feature common to all members of the WOX3 subfamily (Vandenbussche et al. 2009). Both share the homeodomain and the WUSCHEL box (FIG. 1B and C), a domain required for proper activity of *WOX* genes from the recent WOX1-7 clade members (Lin, Niu, McHale, et al. 2013). To better understand the origin of the two WOX3 family members in Petunia, we screened the genomes of other sequenced *Solanaceae* species, finding different WOX3 sequences related to either *WOX3* or *WOX3B* (with the interesting exception of *N. benthamiana*, an allotetraploid (Bombarely et al. 2012), displaying in addition a WOX3 sequence quite distant related to the other ones). This indicates that the duplication leading to the two types of WOX3 proteins in Petunia happened before or at the basis of the *Solanaceae* radiation. Monocots also display more than one WOX3 sequence, whereas Rosidae seem to have only one copy. It will require the availability of genome data of a broader taxonomic range to assess whether or not Rosidae have lost a copy compared to other species.

To investigate the function of Petunia *WOX3* and *WOX3B*, we used a reverse genetics approach, screening our in-house *dTph1* transposon based mutant collection (Vandenbussche et al. 2008) for putative insertions in these genes. We identified three

putative insertions in exonic regions of *WOX3,* of which we further analyzed the insertions at positions 312 on the first exon and 439 on the second exon, in the coding sequence downstream of the start codon. In the case of *WOX3B*, we found, one insertion in the second exon at position 552 bp in the coding sequence downstream of the start codon. In *WOX3*, the 312 insertion is in located in the first exon, and because *dTph1* encodes multiple stop codons in all six possible reading frames, this most likely results in a truncated, non-functional protein. Also the second allele, *wox3*-439, is likely a null mutation. In fact, although in the second exon, the WUS box will be missing, a functional domain absolutely required for proper WOX activity (Lin, Niu, McHale, et al. 2013). For the same reason, also the *wox3B*-552 allele likely is also a null-mutant, as the transposon disrupts the WUS box (FIG. 1B and C).

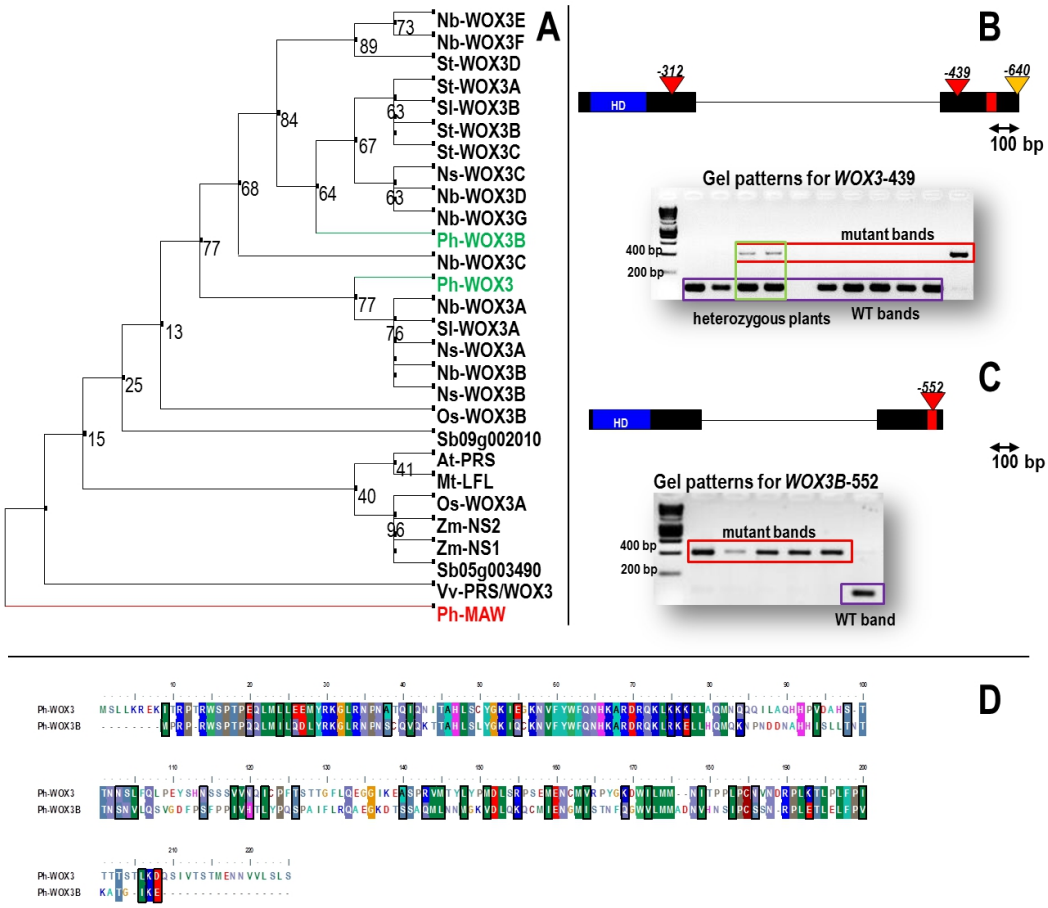

FIG. 1 Phylogenetic tree of WOX3 sequences, and characterization of Petunia *WOX3* and *WOX3B*

A – Phylogenetic tree of WOX3 sequences from different plant species, including Rosidae, Asteridae, and monocots. At – *Arabidopsis thaliana*, Mt – *Medicago truncatula*, Nb – *Nicotiana benthamiana*, Ns – *Nicotiana sylvestris*, Os – *Oryza sativa*, Ph – *Petunia* x *hybrida*, Sl – *Solanum lycopersicum*, St – *Solanum tuberosum*, Vv – *Vitis vinifera.*

B – Gene structure and gel patterns for *Ph-WOX3*. Insertion sites (triangles) of *dTph1* transposon available in our in-house collection are displayed on gene structure. Red triangles: alleles used in this study. Yellow triangle: allele available in our collection, not used in this study. Solid bars: exons. Line: intron. HD – homeodomain. Red box: WUSCHEL box.

WT gel bands are highlighted in blue (*wox3*-439 – 106 bp), mutant gel bands highlighted in red (*wox3*-439 – 390 bp). Two heterozygous plants are also shown, displaying both the WT and the mutant band (highlighted in green).

C – Gene structure and gel patterns for *Ph-WOX3B*. The insertion site of *dTph1* transposon available in our in-house collection is displayed (red triangle). Solid bars: exons. Line: intron. HD – homeodomain. Red box: WUSCHEL box.

WT gel bands are highlighted in blue (*wox3B*-552 – 114 bp), mutant gel bands highlighted in red (*wox3B*-552 – 398 bp).

D – Protein alignment of WOX3 and WOX3B. Conserved amino acids shaded in the same color.

Seeds from lines putatively carrying these insertions were germinated and plants were genotyped by PCR using primers flanking the insertion sites. All putative insertions could be identified *in planta*, and homozygous mutants were obtained in all cases. Although we paid special attention to sepal development, based on the phenotype of Arabidopsis *prs* mutants, no particular phenotype was observed in these plants, suggesting that, if these genes are involved in important (eye-visible) developmental processes and if the *dTph1* insertions indeed disrupt their gene-function, they are probably functionally redundant. To test this, we aimed to create *wox3 wox3b* double mutants. We crossed both *wox3-312* and *wox3-439* mutants with the *wox3b-552* mutant. In the first small F_2 populations resulting from these crosses, we found that homozygous mutants for *WOX3* were WT for *WOX3B*, and *vice versa*. However, we luckily identified one crossing-over event between *wox3-439* and *wox3B-552* in this population. Subsequent screening of larger populations (more than 200 plants) didn't provide other crossing-over events. These results suggest a close genetic linkage between *WOX3* and *WOX3B*. We tested the respective position of *WOX3* and *WOX3B* on the genomic sequence. Unfortunately, given the current scaffold assembly of the Petunia genome, the two genes resulted in two independent scaffolds and their real distance couldn't be assessed. Meanwhile, we searched for WOX3 subfamily genes in the tomato genome, finding two members as in Petunia, both located on chromosome11 (synthenic to chromosome 7 in Petunia), at a distance of less than 15 Kb. This doesn't

necessarily implies that *Ph-WOX3* and *Ph-WOX3B* have the same distance on chromosome 7 in Petunia but, along with results from population screening, it further suggests that they might be very close in Petunia as well. By selfing the *WOX3-439+/- wox3b-552* we identified, we subsequently obtained double homozygous *wox3 wox3b* mutant plants.

***wox3 wox3b* double mutants display a glabrous phenotype**

Analyzing *wox3 wox3b* double mutants, we could not notice any special effect on development of lateral organs, in contrast to what we expected based on previous findings in Arabidopsis and Maize. However, we noticed that plants were glabrous compared with WT, or *wox3* and *wox3b* single mutants (FIG. 2). We always found a correlation between the *wox3 wox3b* homozygous mutation and the glabrous phenotype in all the plants we analyzed. We observed that glabrousness was particularly evident at the stem level (compare FIG. 2J with FIG. 2A, G, and D). Accordingly, SEM analysis of the stem revealed that *wox3 wox3b* mutants display shorter, morphologically different trichomes (FIG. 2j) compared to WTs and single mutants (FIG. 2a, g, and d). A glabrous phenotype can be observed also in other trichome-bearing organs, such as sepals, leaves (data not shown) and bracts, especially on the adaxial side, with possible exclusion of the margin (FIG. 2K) compared to WT and single mutant bracts (FIG. 2B, H, and E). Petals (the abaxial side of petals, forming the petal tube) are less affected in *wox3 wox3b* mutants (FIG. 2L), compared to WTs and single mutants (FIG. 2, C, I, and F). This is an unexpected finding for the role of WOX3 subfamily genes in eudicots.

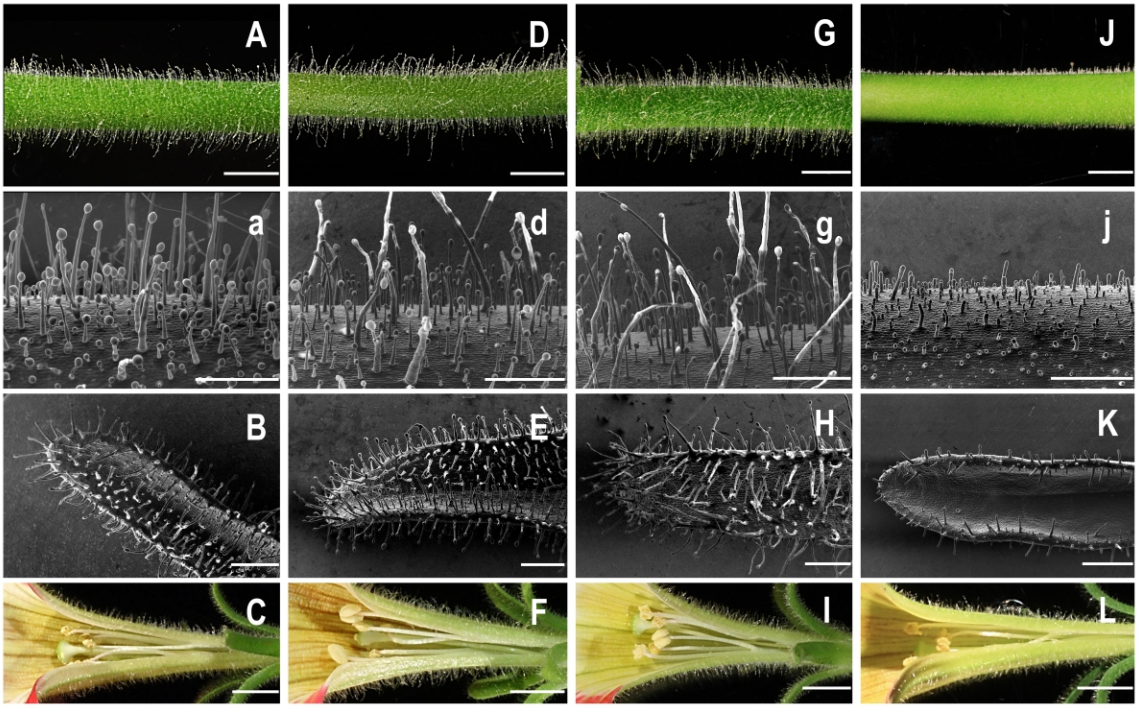

FIG. 2 Trichome phenotypes for WT, *wox3*-439, *wox3b* and *wox3*-439 *wox3b* mutants in Petunia W138

A, **a**, **B**, **C** – WT plants; (**A**) stem, (**a**) SEM close up of the stem, (**B**) SEM picture of a bract (adaxial side), (**C**) and flower tube lateral section.

D, **d**, **E**, **F** – *wox3b* plants; (**D**) stem, (**d**) SEM close up of the stem, (**E**) SEM picture of a bract (adaxial side), and (**F**) flower tube lateral section.

G, **g**, **H**, **I** – *wox3*-439 plants; (**G**) stem, (**g**) SEM close up of the stem, (**H**) SEM picture of a bract (adaxial side), and (**I**) flower tube lateral section.

J, **j**, **K**, **L** – *wox3*-439 *wox3b* plants; (**J**) stem, (**j**) SEM close up of the stem, (**K**) SEM picture of a bract (adaxial side), and (**L**) flower tube lateral section. Note that trichomes on the petal tube are less affected than elsewhere (**L**).

Scale bars: stems – 25 mm; SEM pictures: 500 μM; flowers 50 mm.

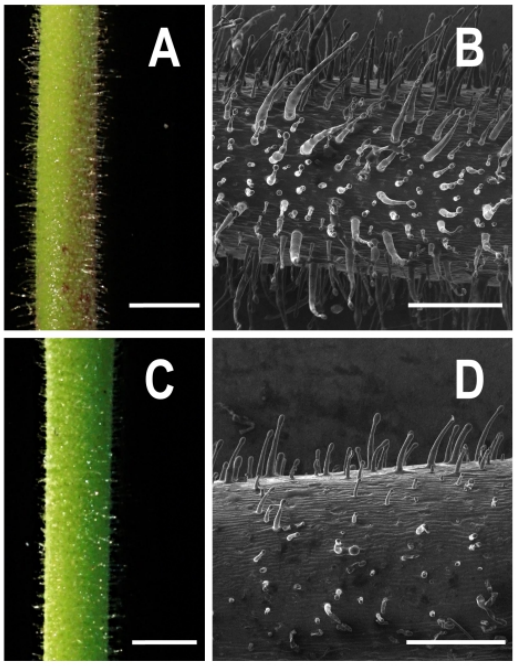

FIG. 3 *wox3*-439 *wox3b* mutants in Mitchell

Stems from WT Mitchell plants (**A**, **B**) are compared with stems from *wox3*-439 *wox3b* mutants in a Mitchell backgrounds (**C**, **D**). **A**, **B**: digital photos. Scale bars: 25 mm. **C**, **D**: SEM pictures. Scale bars: 500 μm.

The glabrous phenotype co-segregate with mutations in *WOX3* and *WOX3B* in the Mitchell background

To further support the linkage between the observed glabrous phenotype and the homozygous mutation in *WOX3* and *WOX3B*, we introgressed the *wox3 wox3b* double mutation in a different Petunia background (Mitchell). We also observed a full co-segregation between *wox3 wox3b* and the glabrous phenotype also in the Mitchell background (FIG. 3).

Phenotypic characterization of wild-type Petunia trichomes

Our findings suggest a role for *WOX3* and *WOX3B* in multicellular trichome development in Petunia. Therefore, we wanted to characterize wild-type trichomes in *Petunia* x *hybrida* from a morphological perspective. For instance, in the closely related

tomato, seven types of trichomes have been identified, classified accordingly to being glandular or non-glandular (that is, lacking a secretory cell at their tip), and according to their length. We characterized by SEM four different regions of Petunia: the stem, the floral tube, the leaf blade (adaxial) and the leaf margin. We roughly identified at least 4 different types of trichomes (FIG. 4 and FIG. 5), three of which are represented on all these structures. The last type consists of a single secretory/storage glandular cell emerging directly from the epidermis. From our morphological analysis, this structure was typically present on the leaf blade (FIG. 4C). All the trichomes we found can be classified as "glandular", because they are supporting a spherical cell at their tip (FIG. 5). We classified them as type I (FIG. 5A), long trichomes; type II (FIG. 5B), intermediate trichomes (see single cells composing this structures in FIG. 5B), type III, very short trichomes (formed of 3 to 5 cells, FIG. 5C, type IV, single glandular cells emerging from the epidermis (FIG. 5D).

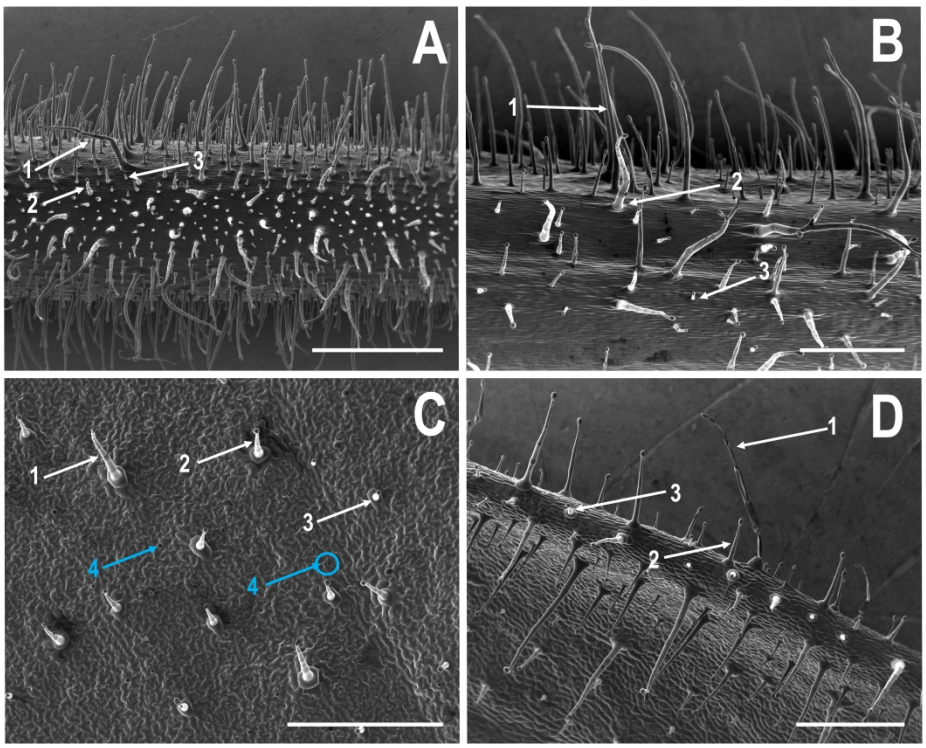

FIG. 4 Trichome organizations in Petunia

Trichomes on stem (**A**), petal tube (B), leaf blade (adaxial) (**C**), and leaf margin (**D**) were analyzed by SEM. Four different types of trichomes were identified: long (**1**), intermediate (**2**), short (**3**), and single-celled (**4**) (see light blue arrows). The last ones typically found on leaf blade (**C**). Scale bars: **A** – 1 mm; **B**, **C**, **D** – 500 μm.

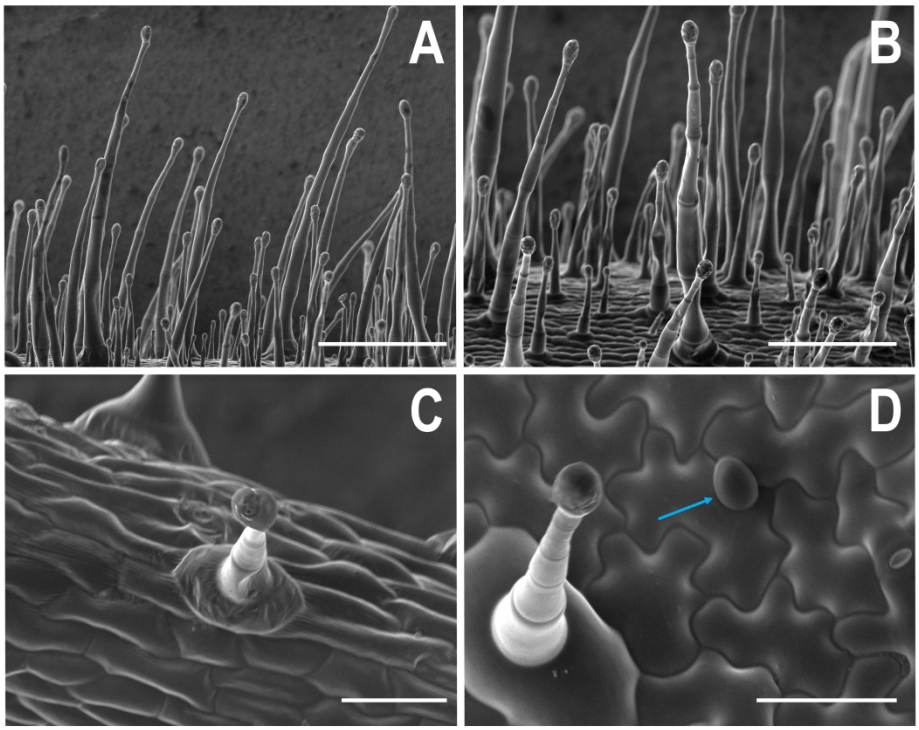

FIG. 5 Trichome classification in Petunia

A - Long trichomes (type I); **B** – intermediate trichomes (type II); **C** – short trichomes (type III); **D** - single-celled (type IV), see blue arrow. Scale bars: **A** – 300 μM; **B** – 200 μM; **C**, **D** – 50 μm.

Further phenotypic comparison of WT and *prs wox3b* mutants

We further compared the WT and the *wox3 wox3b* phenotype, looking for hints about the developmental and molecular mechanisms involved. We first compared conical cells on petal blades from WT and mutants. However, after SEM analysis (FIG. 6A and 6B), these cells appeared morphologically identical among these conditions. We also focused our attention on the general aspect of the epidermis, in order to test if the observed glabrous phenotype was specifically linked to trichome development, or if it has to be considered as a side-effect of distorted developmental programmes affecting epidermis as a whole. Beside

differences in trichome size and structure, we couldn't detect any specific epidermis alterations on *wox3 wox3b* mutants (FIG. 6D), compared with the WT epidermis (FIG. 6C). Trichome development is instead clearly affected in *wox3 wox3b* mutants, with multicellular trichomes reduced to just two or three cells, and even to a single cell. In this case, we observed the head trichome cell (a spherical cell typically at the top of secreting trichomes) directly emerging from the epidermis as a half-sphere (FIG. 6E and 6F). This observation is suggesting that the molecular pathways involved in trichome-cell differentiation are likely to be affected in *wox3 wox3b* plants.

In the end, we could not see any general alteration of leaf epidermis in *wox3 wox3b* mutants (FIG. 6). We might therefore conclude that the *wox3 wox3b* mutation is specifically linked to trichome development.

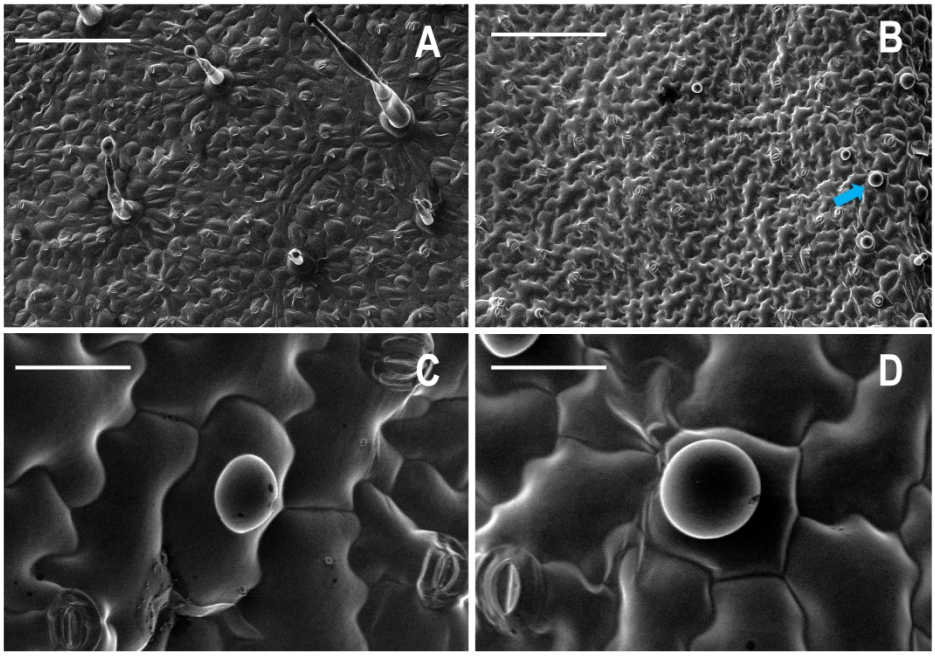

FIG. 6 Comparison of petal and leaf blades among WT and *wox3 wox3b* plants

Adaxial blades from young, developed leaves (in a position close to the tip of the leaf) are shown for WT (**A**) and *wox3 wox3b* plants (**B**). Scale bars: 200 μm.

Single-cell trichomes can be seen in **B** (one is highlighted by a blue arrow). These structures are already present in WT (FIG. 4C, 5D). Close up of these structures are shown in **C** and **D**. Scale bars: 30 μm.

Revertant analysis provides independent proof that trichome development is impaired because of mutations in *WOX3* and *WOX3B.*

In all plants analyzed, we observed a complete linkage between the glabrous phenotype and the *wox3 wox3b* genotype, strongly suggesting that trichome development is impaired because of mutations in *WOX3* and *WOX3B*. However, all double mutants we analyzed were derived from the progeny of a single *WOX3* +/- *wox3b* plant, resulting from the only cross-over event we identified in a large number of plants. Although unlikely, we could therefore not exclude that a novel mutation, unrelated to, but closely linked to *wox3*, had occurred in this *WOX3*+/- *wox3b* individual, and that was responsible for the glabrous

phenotype once in a homozygous state (Fig. 7). To discard this possibility, we screened for phenotypic revertants in the progeny of homozygous glabrous *wox3 wox3b* mutants.

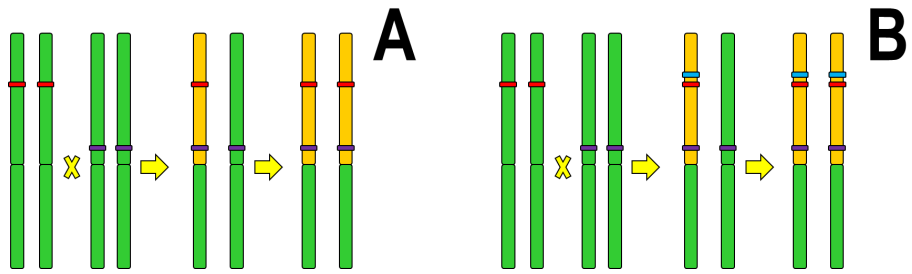

FIG. 7 Two possible mechanisms for crossing-over

A – Crossing over between *wox3* (**red**) and *wox3b* (**purple**) takes place as expected, resulting in a recombinant chromosome fragment (**orange**) which is duplicated in the next generation, leading to a homozygous state.

B – Another possibility, that we couldn't exclude *a priori*, was the occurrence of a new mutation in a different gene, close to *wox3-439* (**blue**) and actually responsible for the glabrous phenotype in the homozygous state.

We took advantage of the *dTph1* transposon system, in which the transposon after insertion can excise again, leaving a footprint in its original position. Upon perfect excision (which happens in the majority of the cases), a typical footprint of 8bp (originating from the 8 bp target site duplication upon insertion), is left behind, resulting in an out-of-frame insertion, which maintains the mutation. However, sometimes imperfect excision occurs, resulting in some cases in a footprint/deletion that is a multiple of 3 bp. In this case, the reading-frame is restored and, possibly, also the WT phenotype. Excision can occur in one layer only (e.g. L1 or L3), or in all layers. Since gametophytes are exclusively derived from the L2 layer, only revertant events that include this layer will be inherited into the progeny, all others are somatic. However, depending on the expression domain of the gene analyzed, somatic insertions may also give rise to phenotypically WT tissues. Progeny analysis is the most straightforward way to distinguish between somatic and germline revertants. In total,

we identified 6 revertants (Table 1), and genotyped the *wox3* and *wox3b* insertion loci in these revertants. In all revertants, we systematically found in-frame footprints/deletions in the *WOX3* gene. Transposon excisions took place also in *WOX3B*, but all the ones we observed were out-of-frame.

TABLE 1 List of footprints observed in revertants to WT phenotype

	Type of reversion	Revertant footprint in *WOX3*	Inheritance in the progeny
Revertant 1	Whole plant	excision with reversion to WT sequence	Yes
Revertant 2	Sector (branch)	excision with reversion to WT sequence	No
Revertant 3	Sector (branch)	3 bp footprint	No
Revertant 4	Sector (branch)	3 bp footprint	No
Revertant 5	Whole plant	9 bp deletion	Yes
Revertant 6	Whole plant	6 bp footprint	Yes

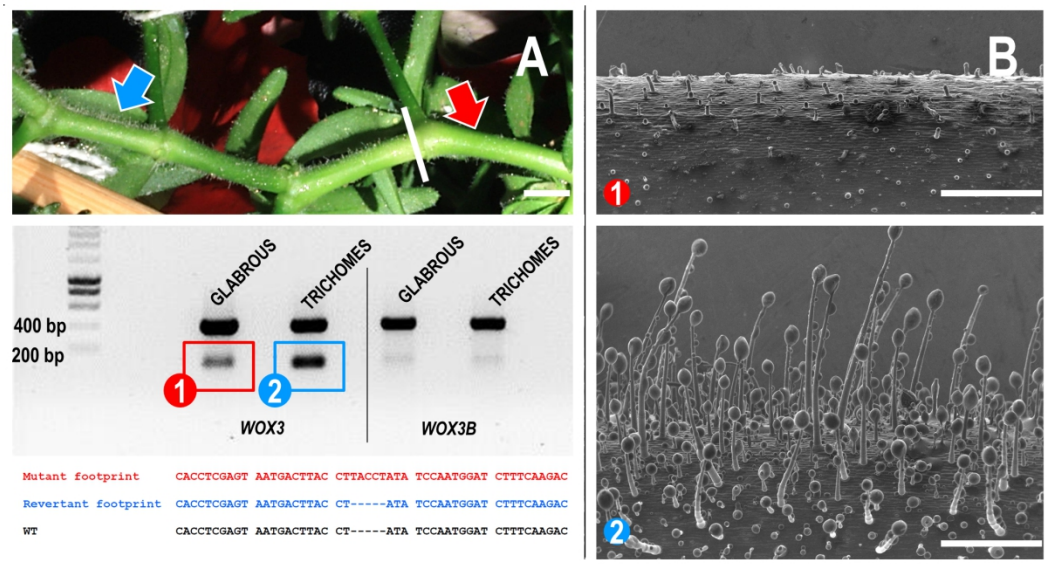

FIG. 8 *wox3*-439 *wox3b* glabrous mutant reverting to a WT trichome-rich phenotype, after excision of the transposon

A – Brach from a *wox3*-439 *wox3b* plant (Revertant 2, see Table 1) showing a reversion from glabrous (red arrow) to WT (trichome-rich) phenotype (blue arrow). The white bar indicates where the revertant sector starts. Gel analysis is shown for both *WOX3* and *WOX3B*. Whereas both the glabrous and the trichome-rich sectors appeared to be mutant for *WOX3B*, a heterozygous state was detected for *WOX3* in the glabrous and in the trichome-rich branch. After cloning and sequencing of the second band (**red** and **blue** squares numbered **1** and **2**, and corresponding **red** and **blue** sequences, bottom), the second band from the glabrous sector appeared to be an out-of-frame mutant footprint (5 bp) (**2**). Instead, the second band from the trichome-rich sector appeared to be a true WT band (true heterozygous), apparently derived from the excision with reversion to WT sequence (compare with the WT sequence in **black**, bottom). Scale bar: 50 mm.

B – SEM pictures of glabrous (**1**) and trichome-rich (**2**) sectors. Scale bars: 500 µm.

Different kinds of footprint can be observed: Full transposon excision (FIG. 8 and FIG. 9, plant (1); classical footprint with part of the transposon incorporated in the genomic sequence [FIG. 9, plant (6)]; deletions, as in FIG. 9 plant (5), where part of the genomic sequence has been eliminated by the transposon.

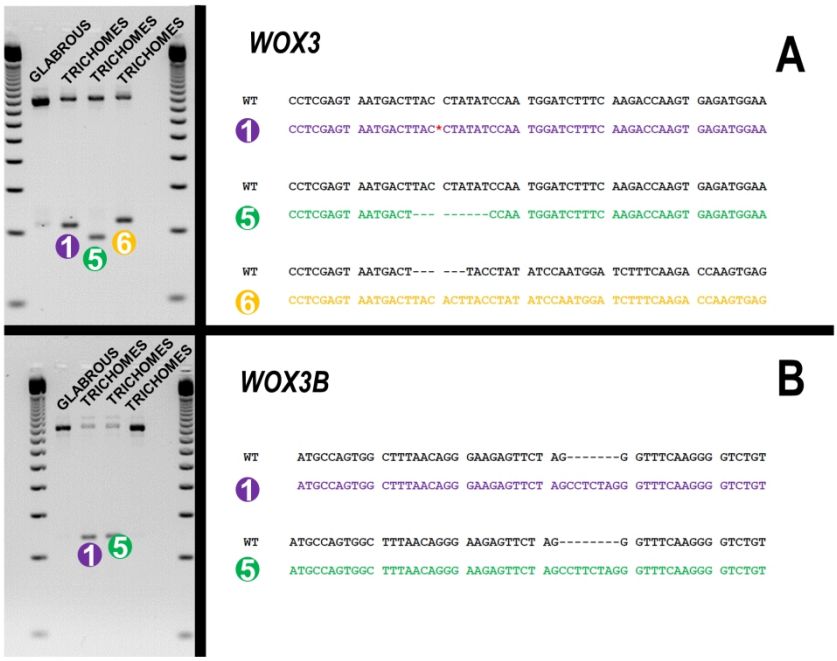

FIG. 9 Additional footprints from *wox3 wox3b* plants, showing a reversion from glabrous-to-trichome rich phenotype

Plants derive from the self-pollination of *wox3-439 wox3b* glabrous mutants. The whole F_1 plants displayed a WT trichome-rich phenotype. Gel analysis for *WOX3*-439 (**A**) and *WOX3B* (**B**), showed that different kinds of excisions restoring the reading frame occurred in *WOX3* (**A**): excision with reversion to WT sequence in (**1**) (**purple** sequence). The red * indicates the original insertion site of the transposon; a 9 bp *deletion* in (**5**) (**green** sequence); a 6 bp footprint from the *dTph1* transposon is left in (**6**) (**orange** sequence). Instead, *WOX3B* gel analysis (**B**) showed an out-of-frame *dTph1* footprint in plant (**1**) and (**5**) (7 bp and 8 bp, respectively), and a homozygous mutant band in (**6**).

We obtained plants from the self-pollination of the 6 revertants we analyzed. As shown in Table 1, only plants derived from whole revertants (and not from single revertant branches) displayed a revertant phenotype also in the progeny. In fact, plants derived from revertant branches were, again, only glabrous. This is matching with the fact that, as the whole plant was showing a revertant phenotype, the transposon excision likely took place also in the L2 layer from which the germline is originated and, as a consequence, the

excision could be passed to the progeny. Molecular segregation analysis of plants derived from revertants 1, 5 and 6 further confirm the link between the glabrous phenotype and mutations in *WOX3* and *WOX3B*. In fact, the transposon and the footprint will independently segregate and correlation with the phenotype can be established. As shown in FIG. 10, the transposon mutation for *WOX3* (1) and the revertant footprint (2)-a 6 bp footprint, or revertant footprint (4), a 9 bp deletion, different from the WT band (3), independently segregate in a Mendelian way in a *wox3b* background. In these progenies, we found that plants carrying only the mutant transposon fragment (*) displayed a glabrous phenotype, while all other plants carried normal trichomes. We thus may conclude that the glabrous phenotype is due the *wox3 wox3b* double mutation.

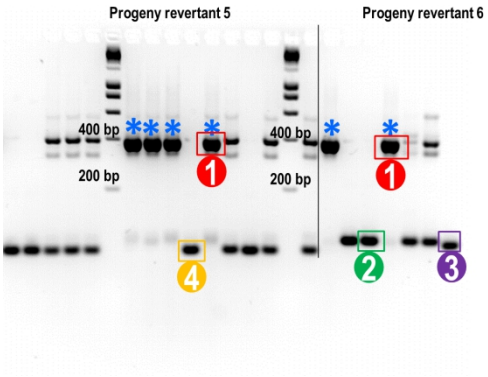

FIG. 10 Gel analysis of progeny from revertant 5 and revertant 6

Different bands are highlighted with different numbers and colours. *dTph1* mutant band is (**1**) in **red**. The WT band is (**3**) in **purple**. In progeny from revertant 6, the revertant footprint - (**2**) in **green** - is of 6 bp. In progeny from revertant 5, the revertant footprint (**4**) – **orange** – is 9 a bp deletion (therefore, its size is lower than the WT band). Plants (*) which are mutant for *WOX3* in a *wox3b* background displayed a glabrous phenotype. Gel: Patrice Morel.

The two subfamilies WOX1 and WOX3 are functionally independent in Petunia

In Arabidopsis, member of the Rosidae, it was previously shown that WOX1 genes and WOX3 subfamily genes functionally overlap in lateral expansion of lateral organs (Vandenbussche et al. 2009; Nakata et al. 2012). We tested if these two subfamilies are functionally linked also in Petunia, a member of the Asteridae. We obtained the quadruple mutant *maw mawb wox3 wox3b* where all the members from the WOX1 and WOX3 subfamilies were mutated (FIG. 11). However, differently from what observed in Arabidopsis, these two subfamilies didn't seem to interact in Petunia, since the phenotype of the quadruple mutant is the simple summary of the defects in lateral expansion of lateral organs observed in *maw mawb* mutants (FIG. 11D, E, and F), plus the glabrous phenotype observed in *wox3 wox3b* mutants (FIG. 11A, B, and C), as it can be seen in FIG. 11G, H, and I.

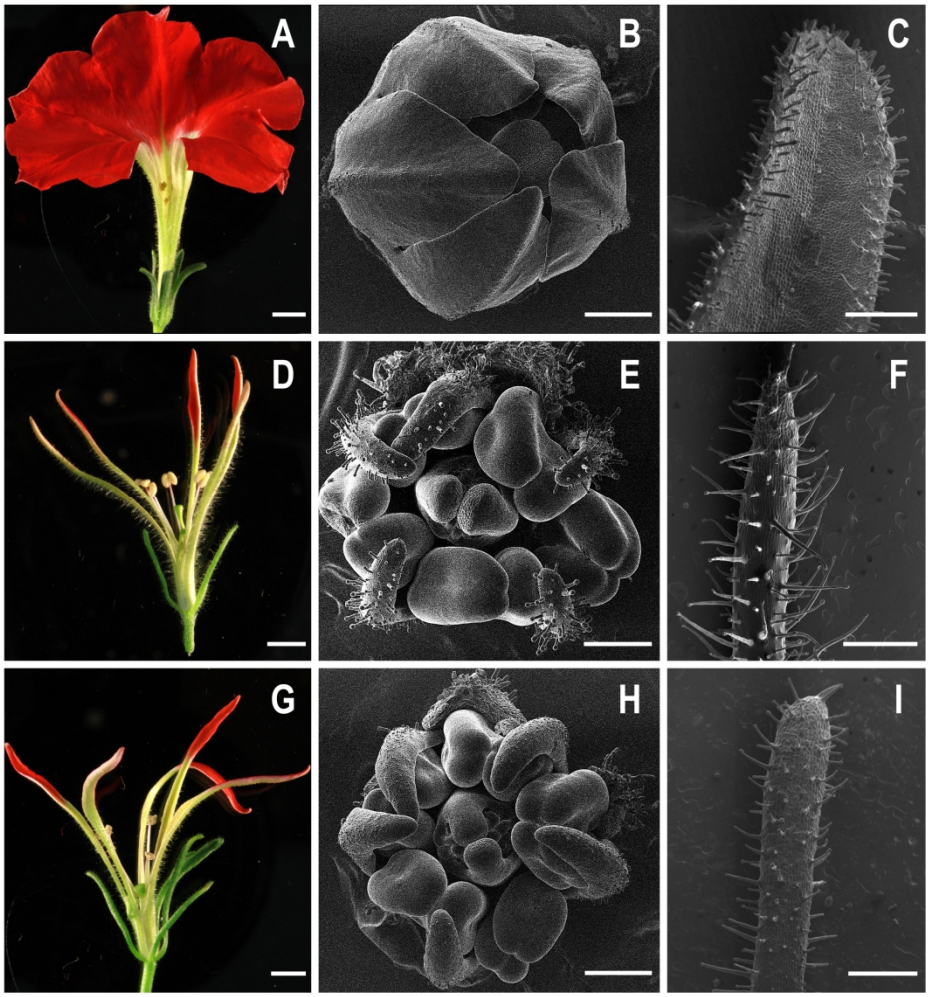

FIG. 11 Comparison of *wox3 wox3b*, *maw mawb* and *maw mawb wox3 wox3b* phenotypes

A – *wox3 wox3b* flower, lateral view. **B** – *wox3 wox3b* young floral bud, SEM picture. **C** – *wox3 wox3b* young bract, adaxial side. **D** – *maw mawb* flower, lateral view. **E** – *maw mawb* young floral bud, SEM picture. **F** - *maw mawb* young bract SEM picture, adaxial side. **G** – *maw mawb wox3 wox3b* flower, lateral view. **H** – *maw mawb wox3 wox3b* young floral bud, SEM picture. **I** - *maw mawb wox3 wox3b* young bract SEM picture, adaxial side. Scale bars: Flowers, lateral view - 50 mm; floral buds SEM – 250 μm; young bracts adaxial side, SEM – 500 μm.

Discussion

In this study we report the requirement of WOX3 subfamily genes for trichome development in Petunia. We uncovered this unexpected function during an evo-devo comparative study with Arabidopsis. In fact, the role played by the only *WOX3* gene in this species, *PRS*, is known, as it is involved in blade expansion in lateral organs along with *WOX1*, member of the WOX1 subfamily. We have previously reported (Chapter III), that the two WOX1 subfamily genes in Petunia, *MAW* and *MAWB*, are involved in blade expansion in this species, questioning the role of the WOX3 subfamily in Petunia. We identified *Ph-WOX3* and *Ph-WOX3B* as the two members of the WOX3 subfamily in this species, taking advantage of the sequenced genomes from *P. inflata* and *P. axillaris*. Thanks to the availability of an in-house *dTph1* mutant collection (Vandenbussche et al. 2008), we identified insertions in *Ph-WOX3* and *Ph-WOX3B* (see FIG. 1). We didn't observe any evident phenotype in *wox3* and *wox3b* single mutants (FIG. 2), which was suggesting possible functional redundancy with other genes. Therefore, we tested functional redundancy between *WOX3* and *WOX3B* by obtaining the double mutant *wox3 wox3b*. In the double mutant, we couldn't visually determine any specific defect going in the direction of *prs* in Arabidopsis (reduced expansion of lateral sepals), as expected. However, we found that colour of green parts was different from WT which appeared to be a result of the glabrousness appearance of mutants compared to WTs (FIG. 2). In fact, development of multicellular trichomes is seriously affected (FIG. 2) and evident on other green surfaces, such as leaves and bracts (FIG. 2), albeit less dramatically affected on the outside of the petal tube (FIG. 2). However, all the observed double mutants derived from only one recombination event between *wox3*-439 and *wox3b*-552. A great number of plants were screened to obtain other independent recombination events, and we also tried to obtain recombination events using a different *WOX3* allele, *wox3*-312, without success. Such a difficulty in obtaining crossing-over events between *WOX3* and *WOX3B* is probably due

to a close linkage between *WOX3* and *WOX3B loci* in Petunia. We couldn't test the exact position of these two genes on the genome, as the available genomes are composed only by unassembled scaffolds. However, we noticed that the close relative of Petunia, *Solanum lycopersicum*, also has two WOX3 subfamily genes, both located on the same chromosome (chromosome 11). To verify further that the observed phenotype is linked to mutations in *WOX3* and *WOX3B*, we introgressed *wox3 woxb* into a different Petunia background: Mitchell. Also in this case, we observed that glabrousness was linked to the *wox3 wox3b* genotype (FIG. 3). Since all the double mutants derived from a single crossing-over event between *wox3-439* and *wox3b-552* (producing a *WOX3* +/- *wox3b* plant), we wanted to exclude the possibility that another new mutation occurring close to *wox3-439* could be responsible for the glabrous phenotype (FIG. 7). We found that *dTph1* insertion in *wox3-439* is quite unstable, and the transposon is prone to excision, typically leaving an 8 bp footprint at the original locus. Since the 8 bp footprint is out-of-frame, the resulted phenotype is still a mutant phenotype. However, different kind of excision can also take place: excisions or deletions with a 3 (or multiple of 3) bp footprint can replace the reading frame and possibly result in a WT phenotype [FIG. 9, revertant (6)]. Other times, a full excision of the transposon can restore the WT sequence, as in FIG. 8 and FIG. 9 revertant (1). In these cases, we observed a reversion from glabrous to wild-type (with normal trichomes), and called these footprints "revertant footprints". Of the six revertants identified, three were in the germline, and thus were passed on to the progeny. In these progenies, all plants exhibited full restauration of trichome development, except plants that were homozygous mutant for the transposon insertion (around ¼ of the progeny in each case).

In Arabidopsis, WOX1 and WOX3 subfamily genes are cooperating in lamina outgrowth in lateral organs (Vandenbussche et al. 2009; Nakata and Okada 2012), questioning if a similar interplay between the two subfamilies is present also in Petunia. To

test this hypothesis, we obtained the quadruple mutant *maw mawb prs wox3b*, full mutant for the WOX1 and WOX3 subfamily. Interestingly, the resulting phenotype was the addition of single WOX1 and WOX3 subfamily phenotypes (blade restriction and affected trichome development), with no visible synergistic effects (FIG. 11). This, together with the observation that the blade development phenotype of *maw mawb* (WOX1 subfamily) is even more severe than the Arabidopsis *wox1 (wox6) prs* mutant, strongly suggests that the functions of *WOX1* and *WOX3* genes in Petunia have completely diverged.

Evo-devo of WOX3 subfamily genes

Taken together, our data show an interestingly, previously uncharacterized, differential functionalization of WOX3 subfamily genes in Petunia. Whereas WOX3 subfamily genes are involved in lamina expansion in lateral organs in Arabidopsis, they were recruited for trichome development in Petunia. In another *Rosida*, Medicago, the *WOX3* gene *LSF* is involved in flower development but, differently from Arabidopsis, it probably doesn't interact with the *WOX1* gene in this species, *STF* (Niu et al. 2015). Among Monocots, *WOX3* genes have also been shown to be involved in leaf lamina outgrowth (Scanlon et al. 1996; Nardmann et al. 2004; Dai et al. 2007) and, interestingly, Os-WOX3B in Rice is involved in trichome development (Li et al. 2012). Given the phylogenetic distance between Rice and Petunia, and the general widespread role of *WOX3* genes in lamina outgrowth, it could be that these functions in trichome development are new, independent acquisitions. We checked the number of *WOX3* genes in other species (FIG. 1), finding that other *Solanaceae* also have several *WOX3* genes, at least two (as in tomato). On the opposite, the Rosidae species taken into account (Arabidopsis, Medicago, Vitis) have just one WOX3 sequence.

WOX3 genes probably are another example of the evolutionary adaptability of *WOX* genes, whose roles spans from stem cells maintenance at different levels (*WUS* at the shoot

apical meristem (Laux et al. 1996), *WOX5* in the root (Gonzali et al. 2005; Ananda K. Sarkar et al. 2007), *WOX4* at the cambium level (Ji, Strable, et al. 2010)) till roles in flower and inflorescence architecture (see (Costanzo et al. 2014)). In any case, the common feature of *WOXes* seems to be their role in meristem formation and stem-cells maintenance through affecting cell proliferation mechanisms. This has been further shown by studies in the moss *Physcomitrella patens*, at the base of land plants, where the only two *WOX* genes have been knocked-out, resulting in mosses impaired in stem-cell formation, particularly because initiation of cell wall expansion is blocked by lack of cell-wall loosening (Sakakibara et al. 2014). In this light, the seriously impaired ability of *wox3 wox3b* Petunia plants to develop multicellular trichomes, might be another evolutionary declination of this basic role of *WOX* genes. Further evidence in this direction is given by Arabidopsis plants overexpressing *PRS*: Plants developed multicellular bulges at the stem level and on peduncles, and wrinkle structures on sepals (Matsumoto and Okada 2001). As for other *WOX* genes, this is suggesting a prominent (but not absolute) role for *cis* regulatory regions in determining the functional role of *WOX* genes [see also discussion in (Costanzo et al. 2014)]. Additionally, outside of angiosperms, recent analysis in Norway spruce (*Picea abies*) showed through *RNAi* lines that *PaWOX3* is involved in sawtooth hairs development (Alvarez et al. 2015) which, as trichomes in other species, are protuberances emerging from the epidermis. From an evo-devo perspective we can formulate the following model (FIG. 12). *WOX* genes were recruited in controlling cell proliferation already in basal land plants [e.g., *Physcomitrella* (Sakakibara et al. 2014)]. Subsequently to several duplication events, the main WOX groups appeared [the old, the intermediate, and the recent WUS group (van der Graaf et al. 2009)] all of them can be found in flowering plants. WOX3 subfamily genes can be found also in gymnosperms, in which they are involved in margin expansion in lateral organs, root elongation, and sawtooth hairs development (Alvarez et al. 2015). Monocots, as Gymnosperms, are lacking the WOX1 subfamily. Indeed, in different species

belonging to the Poaceae, such as Rice and Maize, processes in cell proliferation leading to blade expansion are controlled by *WOX3* genes instead (e.g., the *ns1*/*ns2* mutant in Maize (Scanlon et al. 1996; Nardmann et al. 2004). The lack of the WOX1 subfamily might also explain other specific characters of leaf development in Poaceae (monocots), such as parallel vasculature and elongated shape. Instead, we can find both WOX1 and WOX3 subfamilies in eudicots. In Arabidopsis, *WOX1* and *WOX3* genes are cooperating in blade expansion, such as (Vandenbussche et al. 2009; Nakata et al. 2012), and the *prs* mutant displays a phenotype (Matsumoto and Okada 2001). In Asteridae, *WOX*1 genes [*LAM1* in Tobacco, *MAW* and *MAWB* (Chapter III) in Petunia] already are deeply involved in blade expansion. Probably for this reason, *WOX3* genes could be recruited for a different role involving control of cell-proliferation, such as multicellular trichome development, at least in Petunia. The same kind of differential recruitment probably took place in a Monocot species like Rice, where cell proliferation activity of Os-WOX3A was recruited for lamina expansion (Dai et al. 2007), and Os-WOX3B for trichome development (Li et al. 2012).

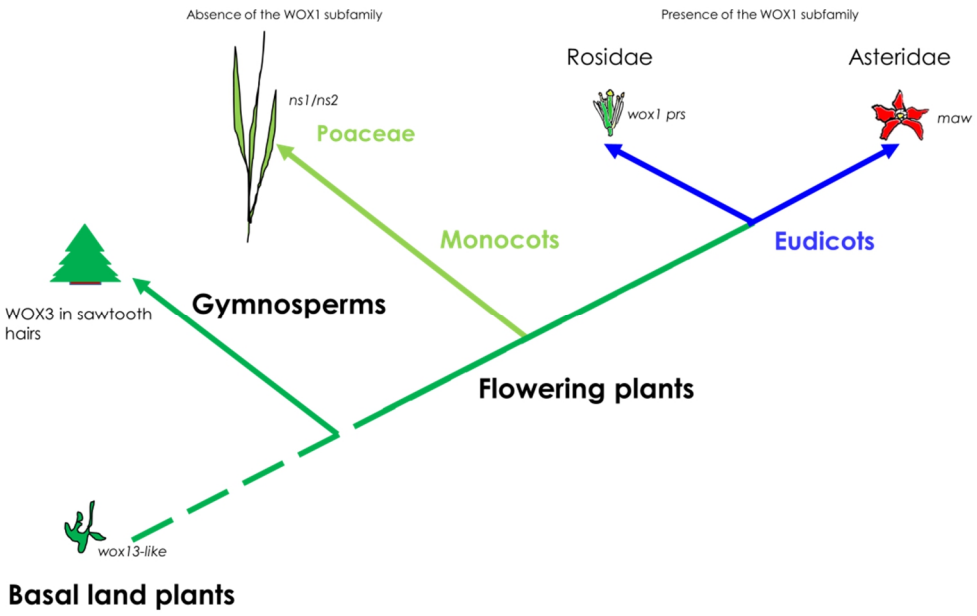

FIG. 12 evo-devo scenario for *WOX* genes

Perspectives

Investigating the gene regulatory network involved in trichome development in Asteridae

So far, little is known about the developmental, genetic pathways controlling trichome development in Asteridae. In fact, only one gene, *WOOLLY* in tomato (and the cell-cycle gene *CycB2* with which it is physically interacting), has been clearly shown to be involved in trichome development in Asteridae (Yang, Li, Zhang, Luo, et al. 2011). Another gene, *MIXTA*, has also been proposed as potentially involved in trichome development in Asteridae, but only based on heterologous overexpressor activity (Glover et al. 1998; Payne et al. 1999). WOOLLY is an HD-Zip IV transcription factor (as GL2 in Arabidopsis), with a maximum sequence similarity with PDF2 in Arabidopsis, which is involved in embryo development but not in trichome development in this species (Yang, Li, Zhang, Luo, et al. 2011; Ogawa et al. 2015). Homozygous mutants for *WO* couldn't be obtained because of embryo lethality, but *RNAi* plants, and consequent segregation analysis, showed a correlation between *WO* and trichome development (Yang, Li, Zhang, Luo, et al. 2011). We found at least 3 homologues of *WO* in the tomato genome, and 3 *WO* orthologues also in Petunia. We are going to test the expression levels of these genes in *wox3 wox3b* mutants, as well as the expression levels of the *CycB2* orthologue. If *WOX3* and *WOX3B* act upstream of *WO*, then we will have uncovered a small, but important fragment, of the gene regulatory network controlling trichome development in Asteridae.

Materials and Methods

Bioinformatics analysis and phylogeny – Sequence finding was performed trough BLAST search among different databases from Pubmed and the Solgenomics Consortium. Sequence alignment was performed using the BioEdit software (Hall 1999), and phylogenetic tree was drawn with the PhyML (Guindon et al. 2009) using an LG model. The tree was statistically supported by 1000 bootstrap replicates.

Materials and Methods are reported in full in **Chapter VII** (Materials and Methods).

VI. Conclusions

The results presented in this doctoral thesis add a new layer to the role of *WOX* genes in plant development. *WUS* is the founder member of the WOX family, a group of HOMEODOMAIN transcription factors involved in many aspects of plant development. Several studies have shown that different members of the WOX family were differentially recruited for different roles among different species and different organs along evolution, including at the flower level [see (Costanzo et al. 2014), Chapter II].

Here, the role of *WOX* genes in plant development has been further investigated by comparing the function of WOX1 and WOX3 subfamily members between Petunia and Arabidopsis, representatives of the two major eu-dicot groups called Asteridae and Rosidae. In Chapter III, the role of *MAW* and *MAWB* in blade outgrowth in lateral organs has been highlighted. Although the single mutant *mawb* is WT, the double mutant *maw mawb* displays extremely narrow leaves, sepals and petals, in addition to unfused and shorter carpels. A clear phenotypic gradient can be seen in WT > *maw* > *maw MAWB* +/- > *maw mawb*, which is suggesting that modulation of *MAW*/*MAW*B levels may be at the basis of the degree of lamina outgrowth, and thus may have been a selection target for plant architecture during evolution. Interestingly, a similar phenotype to the one of *maw mawb* in Petunia had been described earlier for the *lam1* mutant (McHale and Marcotrigiano 1998) in *Nicotiana sylvestris*, but at that time, the underlying mutation was not yet known. Later on, it was shown that *LAM1* was orthologous to *MAEWEST* (Tadege, Lin, Bedair, et al. 2011), despite that the *maw* phenotype was clearly much less severe compared to *lam1* mutants. With the current knowledge that *Nicotiana* contains only one WOX1 member, and Petunia two (*MAW* and *MAWB*), it is obvious now that the two members in Petunia have partly sub-functionalized and together encode the same function as *LAM1* in *Nicotiana*. In

both the *lam1* and the *maw mawb* mutant, only the midrib of the leaf develops, in which an adaxial and an abaxial side are still present showing that mainly mediolateral polarity is affected. Interestingly, whereas *WOX1* genes are absolutely required for lamina expansion in Asteridae, in monocots, such as rice and maize, this role is performed by *WOX3* genes. Studies in a gymnosperm (Norway spruce) suggest a similar role for the WOX3 subfamily also in this group (Alvarez et al. 2015). In Arabidopsis instead, a member of the Rosidae, blade outgrowth is only significantly affected when both *WOX1* and *WOX3* gene functions are compromised. We don't know if *WOX1* genes have been progressively recruited for this role in Asteridae, till completely replacing *WOX3* genes, or if functional redundancy between WOX3 and WOX1 subfamily members is a special feature of Rosidae. For this, *WOX* functional analysis of other members of the Rosidae (and eudicots in general) is required. Remarkably, *WOX1* genes are absent in all monocots for which a genome sequence is available (in particular, from Poaceae, see phylogenetic tree in FIG. 1, Chapter III), explaining the severe phenotype of *WOX3* mutants. Among monocots, Poaceae clearly display different leaf architecture than eudicots, characterized by parallel veins. Given the role of the WOX1 subfamily in leaf development in eudicots, the absence of *WOX1* genes might explain this peculiarity of the leaf in Poaceae. It is interesting to highlight that the mechanisms underlying lamina expansion are different between eudicots and Poaceae. In eudicots, founder cells of the blade are recruited from so-called marginal blastozones. It has been shown in different species belonging to the Poaceae that founder cells derive directly from the shoot apex (Hagemann and Gleissberg 1996; McHale and Marcotrigiano 1998; Scanlon 2000; Efroni et al. 2010). Therefore, *WOX* genes should act upon different kind of cells in order to provide lamina expansion in eudicots and Poaceae. The functionalization of *WOX1* and *WOX3* genes might mirror this difference in cell-types. In any case, the role played by *WOX* genes in blade expansion is in line with the previously hypothesized basic meristematic role of *WOXes*.

Moreover, in order to explain such a differential functional recruitment of *WOX* genes among different organs and species, it should be noticed that it likely is a result of different *cis* elements, rather than differences in protein sequence. This is shown by promoter swapping experiments (Lin, Niu, McHale, et al. 2013) in which members of the recent WUS subfamily were able to complement defects in blade expansion in *lam1* Tobacco mutants under the *STF* promoter. This is suggesting that the basic molecular activity is retained by different WOXes, whereas changes in expression patterns allow the implementation in different developmental processes among different species. An additional, unexpected finding was the involvement of *WOX1* genes in ovule development. *WOX1* genes cooperate with D lineage genes during ovule development. This highlights WOX1 subfamily genes as novel regulators of ovule identity, adding a new regulatory role to this class of genes.

We then investigated the downstream pathways controlled by MAW and MAWB in Petunia, by means of RNA-Seq (Chapter IV). We adopted a strategy aimed at identifying pathways commonly affected among the single *maw* and double *maw mawb* mutant. As a selection criterion, we considered the single *maw* mutant as intermediate between WTs and double mutants, to specifically identify biological processes involved in blade expansion. We found that DEGs involved in the auxin biosynthesis pathway are mainly downregulated, suggesting that also auxin levels do the same, in line with previous findings in *N. sylvestris* and Medicago (Tadege, Lin, Bedair, et al. 2011). This is of interest because auxin is involved in many aspects of organ development. Auxin maxima are known to determine the origin of organs at the shoot and root level (Benková et al. 2003). Moreover, auxin is involved in polarity establishment in lateral organs (Qi et al. 2014), and auxin fluxes pattern vein formation in leaves (Marcos and Berleth 2014). In line with the observed phenotype, we also found that cyclins and cell-proliferation transcription factors are downregulated, such as GRF and GIF, involved in leaf lamina expansion in

Arabidopsis (Horiguchi et al. 2005). We found that a genetic module involved in plastochron control in Arabidopsis, the *miR156/SPL* module (Wang et al. 2008) was also affected in the *maw* and *maw mawb* mutant. This probably explains the higher number of leaves and leaflets observed in the single and double mutant.

Finally, in Chapter V, we have shown another new role played by *WOX* genes in Petunia: Development of multicellular trichomes. To perform a comparison between the functional roles of the WOX1 and WOX3 subfamily between Petunia and Arabidopsis, we characterized the two members of the WOX3 subfamily in Petunia, *WOX3* and *WOX3B*. We were expecting for *Ph-WOX3* and *Ph-WOX3B* to find a similar role to Arabidopsis or Monocots, that is, a role in blade expansion in lateral organs. Instead, single and double mutants displayed normal sized organs. Blade development was not further affected even in *maw mawb wox3 wox3b* quadruple mutants, compared with *maw mawb* double mutants, therefore showing that no genetic interaction among WOX1 and WOX3 members take place in Petunia, in contrast to Arabidopsis. Unexpectedly, we observed a glabrous appearance in the double mutant *wox3 wox3b*. In fact, such a phenotype was due to extreme shortening of trichomes because of the fewer number of cells. We further confirmed the causal relationship between the phenotype and *wox3 wox3b* double mutation by revertant analysis. Components of the multicellular-trichome developmental pathways (typical of Asteridae) are almost unknown, with the exception of the gene *WO* in Tomato (Yang, Li, Zhang, Luo, et al. 2011). This is strikingly different from Arabidopsis (Rosidae), in which molecular pathways leading to unicellular trichome development (which have components in common with the anthocyanin production pathway) are very well characterized. The observed role of WOX3 subfamily genes in multicellular trichome development in Petunia probably is another example of the differential functional recruitment of *WOX* genes along evolution. We have shown that, in Petunia, WOX1 subfamily genes are in charge of blade outgrowth and WOX3 subfamily genes are involved in trichome development. The

common ground probably is the ability of *WOX* genes to control cell proliferation, here to extend organ blade, there to produce the cells forming the trichome.

Experiments in mosses (Sakakibara et al. 2014), are pointing to the possibility that the very first role of *WOX* genes was in stem-cell formation and cell wall loosening. Probably because of this basic role, *WOXes* resulted useful every time a new stem-cell niche was required during evolution: Shoot and root meristems (Laux et al. 1996; Ananda K. Sarkar et al. 2007), and the cambium meristem (Ji et al. 2010 p. 4). In Petunia, the *WOX9* orthologue *EVG*, and *COMPOUND INFLORESCENCE* in Tomato, have been recruited for inflorescence development (Rebocho et al. 2008; Lippman et al. 2008). Moreover, *WOX* genes are also known to pattern embryo development (Haecker et al. 2004). In fact, this was among the first roles assigned to *WOX* genes, just after discovery of *WUS* involvement in the shoot apical meristem. For instance, *WOX9* and *WOX8* (from the same genetic subfamily), are overlapping at the embryo level in promoting cell division in Arabidopsis (Wu et al. 2007; Breuninger et al. 2008). This highlights, once more, how such a basic role of *WOX* genes at cell level has probably been recruited in different organs, species, and even developmental programs (embryonic *vs.* adult) during evolution. The case of *WOX9* in Arabidopsis is even more telling. In fact, *WOX9* is an "old WOX", not a member of the recent WUS lineage. Despite of that, *WOX9* has probably retained some of its ancient functions in promoting growth of the shoot apical meristem and in promoting *WUS* expression at the shoot level (Skylar et al. 2010). Probably *WOX9* underwent functional degeneration in Arabidopsis, and its fundamental role has been progressively substituted by *WUS*. The fact that simple addition of sucrose can rescue the *wox9* phenotype in Arabidopsis (Wu et al. 2005), is a further sign of its ancient role in basic cellular processes.

In conclusion, this work clearly illustrates the need for multiple plant model systems, not only for comparative analyses and to better understand evolution, but also to uncover the full plethora of functions performed by master regulators of plant development, such as the WOX family. *WOX* genes might well support and further extend the view of plant evolution based on the central role of modularity and differential genetic recruitment. In the very end, *WOX* genes probably represent an excellent example of evolution's playground.

VII. Materials and Methods

In this section, laboratory protocols and supporting information (Appendix I & II) are reported.

Plant material and growth conditions

The comparative study among Rosidae and Asteridae was performed by means of two representative species of these main groups of core-eudicots (representing, together, more than 65 % of flowering plants): *Arabidopsis thaliana* and *Petunia* x *hybrid,* respectively. Additionally, these two species have different floral structures, as pointed out by their classical botanical fomulas: $Ca_4Co_4A_{4+2}G_{(2)}$ for Arabidopsis (*Brassicaceae, Brassicales,* Rosidae), and $Ca_5Co_{(5)}A_5G_{(2)}$ for Petunia (*Solanaceae, Solanales,* Asteridae). (Ca=calyx, Co=corolla, A=androecium and G=gynoecium).

Arabidopsis thaliana

Arabidopsis plants (Columbia 0 genotype) were sown and grown in pots (compost ARGIL10 - FAVORIT®) and a two days 4 °C chilling performed before moving seeds under short days conditions (8 h light, 16 h dark) for the first weeks (allowing rosette expansion). Later, plants were moved to long day conditions (16 h light, 8 h dark).

wox1 prs mutants for transformation, as well as mutant combinations for statistical analysis (see below), derive from the following lines: *wox1* line 8AAJ85 (En205 transposon); *prs* line SALK_127850; *wox6* - pfs2-2 line SALK_033323, as in (Vandenbussche et al. 2009).

Petunia x *hybrida*

We used three different *Petunia* x *hybrida* lines: The high-copy number *dTph1* transposon W138 line (Gerats et al. 1990), the V26 line (van der Meer 2006), and the Petunia Mitchell line [*e.g.*, (McLean et al. 1988)]. For germination, Petunia seeds were sown in pots (compost ARGIL 10 - FAVORIT®) and sprayed with a 30 μM GA_3 solution.

Plants were grown in a growth chamber under long day conditions (16 h light, 8 h dark) for the first weeks, and then moved to greenhouse conditions. Mutant plants carrying the *dTph1* transposon (T) or footprint (ft) were obtained from the in-house W138 seed collection, based on methods described in (Vandenbussche et al. 2008, 2013a; b).

N.B. Plant lines listed in this chapter have a serial number where the first letters (*e.g.* 'LY' for Petunia plants, or 'ATLY' for Arabidopsis plants) unequivocally refer to a common list adopted by our team in Lyon, allowing progeny (and parents) tracking over time.

DNA extraction (Edwards' method)

DNA extraction from plant material (Petunia and Arabidopsis) was performed using the following method, based on (Edwards et al. 1991).

Young plant material (vegetative apexes or young leaves) was harvested in 1 ml collection tubes (96 wells), each tube containing one grinding ball made of stainless steel (ø 4 mm). Samples were frozen in liquid nitrogen. Grinding of samples was performed two times at 30 Hz for 30" using a TissueLyser II machine (Qiagen). 400 µl of extraction buffer (Tris 0.1 M pH 8.0, NaCl 0.5 M, EDTA 50 mM, SDS 0.7%) were added to each sample. After mixing, DNA extraction was performed at 60 °C for 60'. Tubes were centrifuged at 4,000 rpm for 15' at room temperature and 300 µl of supernatant were transferred to new 1 ml tubes (96 wells). To each sample, 300 µl of isopropanol were added. Tubes were inverted ten times for mixing, and samples centrifuged at 4,000 rpm for 15' at room temperature. The supernatant was eliminated, keeping the DNA pellet. 200 µl of ethanol 70% were added to each sample. Samples were centrifuged at 4,000 rpm for 15' at room temperature, and supernatant eliminated. DNA pellet was air-dried overnight at room temperature. DNA was dissolved in 500 µl of water. Samples were incubated one night at 4 °C. Before use (*e.g.*, PCR) samples are centrifuged 10' at 4,000 rpm at room temperature.

Polymerase Chain Reactions (PCRs)

PCRs were performed on DNA samples extracted as previously described. For each reaction, 5 µl of DNA solution were mixed with 4 µl of 5x Go Taq® buffer (Promega), 0.2 µl of dNTPs 20 µM, 0.1 µl of Taq Polymerase (Promega), 1 µl of forward primer 10 µM, 1 µl of reverse primer 10 µM and water to a final volume of 20 µl. Samples were incubated in a 96 wells plate (or, alternatively, PCR tubes) and reactions performed in a thermocycler. For example, in Petunia genotyping the following thermal cycle was typically used:

95 °C x 2'; {95 °C x 30"; 60°C x 30"; 72°C x 30" x $kb_{product}$} x 40; 72 °C x 7'; 18 °C x ∞.

Table of primers for mutant screening in *Petunia* x *hybrida*

Mutant allele	Transposon insertion	Primer fw	Primer rv	WT fragment size	Footprint
maw-4	2054 bp after ATG genomi**c sequence**	MLY0158	MLY0159	110 bp	ft analysis: EL300: 110 min
maw-6	601 bp after ATG on genomique	MLY0780	MLY0781	138 bp	
mawb-788	788 bp after ATG on cDNA	MLY0491	MLY0492	120 bp	ft analysis: EL300: 125 min
wox3-312	312 bp after ATG on cDNA	MLY0494	MLY0495	121 bp	
wox3-439	439 bp after ATG on cDNA	MLY0496	MLY0497	106bp	
wox3-640	640 bp after ATG on cDNA	MLY0722	MLY0723	108 bp	
wox3b-552	552 bp after ATG on cDNA	MLY0499	MLY0437	114 bp	

fbp7	**(Heijmans et al. 2012a)**	MLY1094	MLY1095	125 bp
fbp11-1	**(Heijmans et al. 2012a)**	MLY1033	MLY1034	148 bp

List of primers for mutant screening in *Petunia* x *hybrida*

Primer	Sequence (5'-3')
MLY0158	AGAAAGATGGATACCATTCGATGAG
MLY0159	GTGGTGAACAAGACAAATGCATCA
MLY0780	TGAACAAATTCAGCACATTACTGC
MLY0781	AGCGGCATTGGATTCAAGTTGAC
MLY0491	TCTTCGAACATGCCTCTCAATCAG
MLY0492	CCTTTCATTTTCAACATTTCTTGCTAG
MLY0494	CCTGTTGATGCTCATAGTACTACC
MLY0495	CTTGTAGAAACCCTGTAGTAGAAG
MLY0496	GGTGGAATCAAAGAGGCCTCAC
MLY0497	CTTTTCCATAAGGTCTTACCATGC
MLY0722	ATTACAACTACAAGTACCCTCAAGG
MLY0723	ATGACTTTCCCGACGAGTTAACTG
MLY0499	TCTTGATGATGGCAGACAATGTTC
MLY0437	TCGGTCCCTATTCCTTAATGCCAG
MLY1094	CAGGAATATTATATTGTGAGATGG
MLY1095	AGTTCATATGCCTTTTTCAGCAATC
MLY1033	TATATAGGAAAGTGAGATCATTATGG
MLY1034	GCATCACAAAGAACTGAAAGTTCG

List of primers for mutant screening in *Arabidopsis thaliana*

Primer	Original name*	Sequence (5'-3')	Notes
MLY0089	*At-WOX1-2* fw	CACAGCAGTGGTGACGATGACG	segregation analysis, 8AAJ85
MLY0090	*At-WOX1-2* rv	CTTCAAGAACCCTTAACTGATCTGGTG	segregation analysis, 8AAJ85
MLY0097	En205 Transposon	AGAAGCACGACGGCTGTAGAATAGGA	For *At-WOX1-2* screening
MLY0093	*At-PRS* fw	GGGAACTGGAGTAGGAGAAGCTC	For *At-PRS* screening
MLY0094	*At-PRS* rv	CATCCAATCTCGACCGTACGATGAG	For *At-PRS* screening
MLY0091	*At-WOX6* fw	TAAAGACGTCAAGGATTCATCATCAG	For *At-WOX6* screening
MLY0092	*At-WOX6* rv	GAGCTTTGTCTGATCAACTCGATG	For *At-WOX6* screening
MLY0099	T-DNA LEFT border	GAACAACACTCAACCCTATCTCG	For mutant screening in lines *prs* SALK_127850 and *wox6* - *pfs2-2* line SALK_033323

*see reference papers in 'Notes' column.

Elchrom™ electrophoresis

For screening of Petunia transposon (T) mutants, normal gel electrophoresis was performed on agarose-TAE gels. Elchrom™ Spreadex® EL300 gels were used for screening of Petunia footprints (ft) mutants. In some cases, Elchrom™ Spreadex® EL500 gels were also used. Elchrom gels were run in an Elchrom™ Origins machine, loaded with TAE

buffer preheated at 55 °C. Gels were stained in TAE-ethidium bromide before UV detection.

DNA extraction from agarose gels

Low percentage agarose (1-2%)-TAE gels were used for electrophoresis. After UV detection, gel bands were rapidly excised from gels and purified using the NucleoSpin® Gel and PCR Clean-up kit (Macherey-Nagel), following producer's instructions. The Macherey-Nagel protocol is based upon the method from (Vogelstein and Gillespie 1979).

Competent cells transformation (heat-shock)

50 µl of competent *E. coli* cells (DH5α strain) were thaw on ice. 2 µl of transformation plasmid were added. Cells were incubated on ice for 30' and heat shock performed at 42°C for 30", followed by rapid ice incubation. To each vial of transformant cells, 250 µl of SOC medium were added. Cells were incubated (225 rpm) at 37°c for 1 to 2 hours under shaking. 250 µl and 50 µl of culture were separately plated on different selective LB agar plates, containing the suitable antibiotics, and incubated overnight at 37 °C.

Colony PCRs

Colony PCRs on *Escherichia coli* were set up using the following method (Michiel Vandenbussche, personal communication). Sterilised wooden-tips were used to gently scrape the selected bacterial colonies from growth plates. Using sterile PCR tubes, reflecting the order of colony PCR reactions, the wooden-tip bringing the colony was first immersed in 50 µl of LB, and then moved to the PCR reaction tubes, to let the remaining cells to work as DNA template for PCR. PCRs were performed in 20 µl volume (see above). A 5' hot-start step at 95 °C was added to the thermal cycle. PCR tubes containing LB inoculated with the bacterial colonies were incubated at 37 °C under shaking. After gel analysis of PCR products, the suitable LB tubes were used as *inoculum* for overnight liquid cultures and subsequent plasmid extraction.

Plasmid extraction from bacterial cell cultures (miniprep)

Overnight *E. coli* liquid cells cultures were performed at 37 °C (cultures provided with selective antibiotics, depending on plasmid construct – typically: Carbenicillin 20 μg/ml; kanamycin 50 μg/ml; streptomycin 50 μg/ml). Minipreps were performed from these cultures, using the Nucleospin® Plasmid kit (Macherey-Nagel), accordingly to manufacturer's instructions. The Macherey-Nagel protocol is based upon the method from (Birnboim and Doly 1979).

RNA extraction (TRIzol® method)

RNA EXTRACTION – Plant material was collected in 2 ml tubes containing two grinding balls (stainless steel, ø 4 mm) and rapidly frozen in liquid nitrogen. A TissueLyser II machine (Qiagen) for grinding (two times at 30 Hz for 30"). RNA extraction was performed using the TRIzol® method (Thermo-Scientific), as described by the manufacturer. TRIzol is a commercial product containing guanidinium thiocyanate and phenol. Eventually, RNA samples were re-suspended in 40 μl of MilliQ water and stored at -80 °C. For RNA concentration, a NanoDrop 1000 Spectrophotometer (Thermo Scientific™) was used. RNA quality was assessed on 1% agarose-TAE gels by electrophoresis.

DNase TREATMENT - DNA removal from RNA samples was performed using the Ambion® TURBO DNA-*free*™ DNase kit, accordingly to the following manufacturer's protocol (optimized for removal of 1 μg of DNA from a reaction volume 25 – 100 μl).

cDNA synthesis

REVERSE TRANSCRIPTION – For each sample, 1 μg of RNA was treated in 1.5 test tubes (RNase-free) adding 1 μl primer Smart Race CDS-A 20 μM (AAGCAGTGGTATCAACGCAGAGTTTTTTTTTTTTTTTTTTTTTTTTTTTTTV N) and MilliQ water to a final volume of 11 μl. Samples were incubated at 70 °C for 5' and

transferred to ice. RT reaction: Buffer Fermentas 5x (4 µl), dNTPs 20 mM (1 µl), RNasine 40 U – Fermentas (0.5 µl), MilliQ water (1.5 µl) and added (8 µl) to each tube. Samples were incubated at 37 °c for 5'. 1 µl of reverse transcriptase (RevertAid M-MuLV 200 U/µl – Fermentas) was added to each sample. Reactions were incubated at 42 °C for 1h, and stopped by incubation at 70 °C for 10'.

Phusion® PCR (High-Fidelity)

Phusion® PCR for high-fidelity products was performed based on the protocol from the manufacturer (Thermo Scientific™).

Reaction setup

Component	Final volume 50 µl	Final Concentration
Nuclease-free water	to 50 µl	
5x Phusion HF	10 µl	1X
10 mM dNTPs	1 µl	200 µM
10 µM Forward Primer	2.5 µl	0.5 µM
10 µM Reverse Primer	2.5 µl	0.5 µM
Template DNA	5 µl	< 100 ng
DMSO (optional)	1.5 µl	3%
Phusion DNA Polymerase	0.5 µl	

Thermal cycle: 98 °C x 30"; {98 °C x 8"; 70 °C -> 60°C x 30" –touchdown- ; 72°C x 30" x $kb_{product}$} x 10; {98 °C x 8"; 60°C x 30"; 72°C x 30" x $kb_{product}$} x 40; 72 °C x 7'; 18 °C x ∞.

Cloning and sequencing of *WOX3* footprints in Petunia – *WOX3* footprints were amplified by touchdown PCR from genomic DNA using the following primer combination:

Fw primer MLY0496	GGTGGAATCAAAGAGGCCTCAC
Rv primer MLY0497	CTTTTCCATAAGGTCTTACCATGC

After colony PCR, and plasmid preparation, purified plasmids were sent for sequencing to GATC Biotech (GATC Biotech SARL, 4 rue des Bonnes Gens, 68100 Mulhouse, France). Sequence alignment was performed using the BioEdit package (Hall 1999).

In situ hybridization

In situ hybridization was performed on different Petunia tissues and organs. Probes were produced by PCR Phusion® amplification (see above) from genomic DNA, using the following primers:

Primer	Target gene	Type	Sequence
MLY1654	Ph-MAWB	fw	CTGATGAATTTAATTCATATGCATGCTC
MLY1557	Ph-MAWB	Rv + T7	TGTAATACGACTCACTATAGGGCAACACAGATCAGAAGACTCATCTATAC
MLY1019	Ph-*PRS*	fw	CACCATGTCTCTTTTGAAAAGAGAAAAAATTACAAGAC
MLY1528	Ph-*PRS*	rv + T7	TGTAATACGACTCACTATAGGGCAGTACACACTGAAACAGTTGAACTAC
MLY1021	Ph-*WOX3B*	fw	CACCATGCCTCGACCAAGATG
MLY1530	Ph-*WOX3B*	rv + T7	TGTAATACGACTCACTATAGGGCACTAGAAGTCAGCTGTTTTACAAATC

PCR products were purified from agarose gels and analyzed using a NanoDrop 1000 Spectrophotometer (Thermo Scientific™).

PROBE TRANSCRIPTION – For probe transcription, 200 ng of PCR product were used. In a final volume of 20 µl, the following reagents were mixed: 4 µl Transcription Optimized 5x Buffer (Promega®), 2 µl DIG RNA labeling mix 10x (Promega®), 1 µl Ribo-block (Thermo Scientific™), 1.5 µl T7 RNA polymerase (Promega®). Reactions were incubated 1 h at 37 °C. 1 µl of reaction product was loaded on agarose gel for analysis. Unincorporated nucleotides were eliminated by EtOH precipitation: Precipitation solution (NaAc 1 volume+ EtOH 2.5 volumes) was supplied with 2 µl glycogen (2 mg/ml) and incubated 1h at – 80°C, then centrifuged 30' at 4°C. Pellet was resuspended in 25 µl H_2O.

PROBE HYDROLYSIS – Hydrolysis time was estimated as follows: (Initial length – Final length) / (K*initial length*final length), where K = 0.1 kb/mn. Hydrolysis was performed at 60°C adding 25 µl of carbonate buffer 2x (see solutions).

RNA PRECIPITATION – 2 µl of glycogen [2 µg/ml], 19 µl of NaAc solution and 47.5 µl of EtOH were added to the transcription product. The reaction was incubated at -80 °C for 1 h and then centrifuged at > 16,000 g for 30', 4 °C. Pellet was dissolved in 25 µl of formamide:H_2O (1:1) and stored at -80 °C.

DOT BLOT TEST – *In situ* probes in formamide:H_2O (1:1) were tested on nitrocellulose membrane. For each probe, 4 dilutions were used (1, 1:10, 1:100, 1:1,000), blotting 1 µl of each dilution. The membrane was incubated as follows. Tp2 for 30', Tp2 supplemented with antibody anti-DIG 1:2,000 (Anti-Digoxigenin-AP Fab fragments 150 U [200 µl], Roche®), Tp2 for 5', Tp1 for 5' (x 3 times), Tp4 for 5', coloring solution. The last step was performed in the dark. N.B. The colorimetric reaction is time and probe concentration dependent.

Solutions:

Tp1 – Tris 100 mM pH 7.5, NaCl 150 mM

Tp2 – Tp1, blocking reagent 0.5%. Heated 5" in the microwave after preparation.

Tp3 – Tp1, BSA 1%, Triton X100 0.5%

Tp4 – Tris 100 mM pH 9.5, NaCl 100 mM, MgCl2 50 mM

Staining solution – Tp4, 4.5 µl of NBT [75 mg/ml dimethylformamide], 3.5 µl XP [50 mg/ml dimethylformamide].

Carbonate buffer. For 10 ml H2O, 127.2 mg sodium carbonate, 67.2mg sodium, pH 10.2 with NaOH.

SAMPLE PREPARATION FOR *in situ* HYBRIDIZATION – Plant material from Petunia plants was included in paraffin accordingly to the following protocol.

Samples were fixed in FAA solution (EtOH 50%, acetic acid 5%, formaldehyde 3.7%) and incubated on ice. Vacuum infiltration was performed 2 times for 15' at -0.6 bars. Overnight incubation at 4 °C, in FAA solution. Samples dehydratation: 1 h in EtOH 70%, 1 h in EtOH 95%, 1 h in EtOH 100%, 1 h in EtOH 100% and 1 h in methanol 100%. Samples were incubated two days at -20 °C and then embedded in Paraplast Plus® (Sigma-Aldrich®) using a Roboplast TP 1020 machine (Leica), following producer's instructions.

SAMPLE SECTIONS - Samples were sectioned using a HM 355 S microtome (Microm/Zeiss) at 9 µm width. Sections were deposited on Superfrost UltraPlus® (Thermo Scientific™) slides and incubate at 37 °C overnight. Slides were stored at 4 °C.

FORMALDEHYDE IMPREGNATION AND DEHYDRATATION –Different washing steps were performed, to eliminate paraffin: 10' in Histo-Clear® 100% (National Diagnostic) for 2 times, 5' in EtOH 100% for 2 times, 30" in EtOH 95%, 30" in EtOH 85%, 30" in EtOH 70%, 30" in EtOH 50%, 30" in EtOH 30%, and 15' in H_2O. Samples were incubated in HCl 0.2 M for 20' at RT, 5' in H_2O, 5' in SSC 2x for two times, and 15' in a proteinase K solution at 37 °C (Tris pH 8 100 mM, EDTA 50 mM, proteinase K 1

μg/ml) (this step is needed to expose endogenous RNAs), 2' in glycin solution 2 mg/ml at RT, 4' in PBS 1x, 10' in formaldehyde 4% in PBS 1x, 10' in PBS 1x. Samples were dehydrated throughout the following steps: 30" in EtOH 30%, 30" in EtOH 50%, 30" in EtOH 70%, 30" in EtOH 85%, 30" in EtOH 95%, 1' in EtOH 100%, and 1' in EtOH 100%.

HYBRIDIZATION – For each slide, 1 μl of probe was combined with 75 μl of DIG Easy Hyb buffer (Roche) (working on ice). The diluted *in situ* probe was denatured for 2' at 80°C and incubated on ice. Slides from EtOH 100% were dried and placed in a humid chamber. Slides were covered with 76 μl of diluted probe and a 60 μm cover slip was placed over each slides. Humid chambers were sealed with parafilm and incubated overnight at 50 °C.

Slides were incubated with SSC 0.1x + SDS 0.5% for 2' at 50 °C in order to detach cover slips. A preheated solution (50 °C) of SSC 2x + formamide 50% was used for two washing steps of 60' and 90' respectively, always at 50 °C. At RT, slides were incubated 5' in TBS 1x and 60' in blocking solution (blocking reagent 0.5 % - Roche – TBS 1x). This step was performed under gentle shaking. Slides were incubated 30' with BSA solution (BSA 1%, Triton X100 3%, TBS 1x) under gentle shaking. Slides were placed in light-opaque humid chambers and covered with 500 μl of Anti Digoxigenin AP fab fragments (Roche) diluted 1:3000 in BSA solution. Incubation was performed with the anti-DIG antibody for 1 h and half. 3 washing steps of 20' each with BSA solution followed, under gentle agitation. Slides were incubated 5' with Tp5 (Tris pH 9 100 mM, NaCl 100 mM, $MgCl_2$ 50 mM) and then moved in dark chambers containing the detection solution (NBT 250 μl –Roche-, BCIP 200 μl –Roche-, Tp5 50 ml). 24 h incubation (minimum) away from light was required prior to microscope observation.

Ph-MAW **cloning and Arabidopsis transformation**

Genomic *Ph-MAW* was cloned into a pENTR™/D-TOPO® vector (Invitrogen) by means of the pENTR™ Directional TOPO® cloning kit (Invitrogen) and thermo-competent *E. coli* cells (DH5α strain) were transformed by heat-shock with the recombinant plasmid. The KAN resistance cassette from the recombinant plasmid was removed by restriction reaction (Nci I enzyme), and restriction products purified by electrophoresis and gel extraction. LR reaction between the restricted plasmid and the destination vector pMDC123 (accession number Tair: 1009003750) performed by means of the Gateway® LR Clonase™ II Enzyme Mix kit (Invitrogen). Competent *E. coli* cells (DH5α) were transformed by heat-shock and plasmid purified from liquid culture. *A. tumefaciens* electro-competent cells (C58::pMp90 strain) were transformed by electroporation. Arabidopsis *wox1 prs* plants were transformed following the method of (Logemann et al. 2006).

DEX inducible ***pMAW::GR-MAW*** **Petunia line**

To identify direct targets of MAW and MAWB by RNA-seq analysis, we set up a system consisting of mutants *maw mawb* plants carrying the construct *pMAW::GR-MAEWEST*. Here, the genomic sequence of *MAW* is fused with the sequence coding for the rat glucocorticoid receptor (*GR*), under the control of the same *MAEWEST* promoter. In this way, it is possible to activate MAEWEST after treating transgenic mutant plants dexamethasone. As additional advantage, mutant *maw mawb* plants expressing *pMAW::GR-MAEWEST* can restore WT phenotype after DEX treatment, allowing seed production by self-pollination.

CONSTRUCT PRODUCTION - The construct *pMAW::GR-MAEWEST* to be inserted into Agrobacterium was produced using the Gibson Assembly method for large contructs (Gibson et al. 2009), using the Gibson Assembly® Cloning kit (New England

Biolabs). As a first step, all the components of the construct need to be amplified at high fidelity using a proof-reading taq polymerase (such as Phusion®, see above). Primers must be designed so that neighbouring fragments have a 15-25 nucleotides overlap. We amplified fragments from appropriate templates using the following primers:

List of primers for Phusion® amplification and Gibson Assembly method

MLY1288	pENTR fw for Gibson GR-MAW	AGATCAATTCCGATAATATCAAGGGTGGGCGCGCCGACCCAGCTTTC
MLY1289	pENTR rev for Gibson GR-MAW	CATTCTACTCTTATAACTAATTGGGTGAAGGGGGCGGCCGCGGAGCCTGCT
MLY1290	MAW PROMOTER fw for Gibson GR-MAW	GCCGCCCCCTTCACCCAATTAGTTATAAGAGTAGAATGAACAAAC
MLY1291	MAW PROMOTER rev for Gibson GR-MAW	GTTTTTCGAGCTTCCATTTTGTGTTTTACTTAGTGGGGCACGTAC
MLY1292	GR+ATG no STOP fw for Gibson GR-MAW	CAAAATGGAAGCTCGAAAAACAAAGAAAAAAATCAAAGGGATTCAG
MLY1293	GR+ATG no STOP rev for Gibson GR-MAW	TGTCATTGTAACCCATCATCCATTTTTGATGAAACAGAAGCTTTTTGATATTTCC
MLY1294	MAEWEST cds no ATG fw for Gibson GR-MAW	CAAAAATGGATGATGGGTTACAATGACAGTG
MLY12	MAEWEST	CGCGCCCACCCTTGATATTATCGGAATTGATCTGCAGTC

95	cds rev no ATG for Gibson GR-MAW

From the GR fragment we eliminated the STOP codon and added the ATG to allow its positioning in 5' to the *MAEWEST* genomic sequence. The PCR products amplified with these primers were used for the assembly reaction (after gel purification), in combination with the linearized vector pENTR™.

Total amount of fragments	0.2 – 1 pmols (50-100 ng of vector with 2-3 fold inserts) – x µl
Gibson Assembly master mix (2x)	10 µl
MilliQ H2O	10 – x µl
Total volume	20 µl

The reaction was incubated for 1 h at 50 °C and reaction product used for transformation of *E. coli* competent cells by heat-shock method. Colony-PCR, colny culture and miniprerps followed, to obtain the recombinant plasmid.

By LR recombination (see above), the *pMAW::GR-MAEWEST* insert obtained by Gibson Assembly was cloned into two different vectors suitable for Agrobacterium transformation: The (pKGW0) carrying the KANAMYCIN resistance in plants, and the (pMDC123) carrying the BASTA resistance in plants. Recombinant plasmids were used for transformation of electro-competent *Agrobacterium tumefaciens* cells, strain EHA105, by electroporation. Transformed Agrobacteria were plated on selective medium and grown for 3 days. The Agrobacterium film was collected to set up an overnight 5 ml LB liquid culture (containing selective media), suitable for leaf-discs transformation.

PLANT MATERIAL - Since the W138 plants from the transposon collection are untransformable with Agrobacterium, we first crossed mutant W138 *maw mawb* plants with the more easily transformable line V26. *MAW* +/- *mawb* in the F_2 were used for transformation.

PETUNIA LEAF-DISCS TRANSFORMATION – Young leaves (2 to 5 cm in length) from 4 to 6 weeks-old Petunia plantlet (*mawb maw* -/+ genotype in the W138 x V26 background) were used for leaf discs production and consequent transformation. About 30 leaves from six to ten different plants were harvested and washed with demineralized. Under a sterile hood, leaves were immersed in a NaClO solution (0.5% of active Cl) under agitation for 10'. This step was followed by 5 washing steps, each of five 5', in sterile water.

Leaves were sectioned in several squares of 0.5 x 0.5 cm, obtaining about 90-100 leaf-discs. The overnight Agrobacterium culture was dilute 1:10 and used for leaf-discs infection in a 50 ml sterile Falcon® tube. Leaf-discs were co-incubated with Agrobacterium for 15'. The Agrobacterium solution was removed and leaf-discs dried with sterile filter-paper. Leaf discs were incubated on selective plates (50 mg/ml kanamycin, or 2.5 mg/ml basta) for 1 week in the dark.

During the following weeks, explants were continuously transferred to fresh selective medium, till emergence of shoots. Newly formed explants where excided and transferred on rooting medium (supplied with 50 mg/ml kanamycin or 2.5 mg/ml basta). Several transfers to new rooting medium were performed in the following weeks, till complete rooting. Plants were transferred in soil under appropriate moisture conditions. Plants were tested by PCR for the presence of the transgene. The whole protocol takes about 4 months.

Media

Standard plant medium

900 ml H2O, 30 g sucrose, MS provided with Gamborg B5 vitamins 4.4 g, pH 5.7, 4 g phytagel.

In vitro media

Standard medium provided with:

- mg/l BAP, 0.1 mg/l NAA **co-cultivation medium**;
- mg/l BAP, 0.1 mg/l NAA and 50 mg/l kanamycin or 2.5 mg/ml basta **selective medium**
- 50 mg/l kanamycin or 2.5 mg/ml basta **root medium**

This protocol is derived from the protocol of Anneke Rijpkema (RU Nijmegen), based on protocol of Peter de Groot (RU Nijmegen), adapted from VU protocol A'dam, and on transformation protocol of Dave Clark lab (University of Florida).

Statistical analysis of Arabidopsis carpels

Columbia-0 WT plants and mutants for *prs, wox1 prs, wox1 wox6, prs wox6, wox1 prs wox6* were obtained from crossings of plants analyzed in (Vandenbussche et al. 2009) (and associated Supplementary Materials; *wox1* line 8AAJ85; *prs* line SALK_127850; *wox6* - pfs2-2 line SALK_033323). Plants were grown for 3 weeks under short day conditions, and then moved to long days for bolting.

For statistical analysis, 4 plants per genotype were taken into account. From each plant, 25 flowers were visually screened for carpel defects at the microscope, giving a total number of 100 flowers screened per genotype. Two different classes were established: Perfectly WT stigma on one side, and altered (mutant) stigmas on the other.

Raw data (average) from stigma screening from different genotypes (4 plants per genotype, 25 flowers per plant).

WT Col-0	WT stigma	Affected stigma
Value	25	0
Error	0	0
prs	WT stigma	Affected stigma
Value	25	0
Error	0	0
wox1 prs	WT stigma	Affected stigma
Value	25	0
Error	0	0
wox1 wox6	WT stigma	Affected stigma
Value	24.25	0.75
Error	1.5	1.5
prs wox6	WT stigma	Affected stigma
Value	24	1
Error	2	2
wox1 prs wox6	WT stigma	Affected stigma
Value	19.75	5.25
Error	1.258	1.258

T test among different genotypes

t test 99%		**p<0.01**	***
t test 95%		**p<0.05**	**
wox1prswox6 vs..	WT	0.0002	***
wox1prswox6 vs.	*prs*	0.0002	***
wox1prswox6 vs.	*wox1 prs*	0.0002	***
wox1prswox6 vs.	*wox1 wox6*	0.0037	***
wox1prswox6 vs.	*prs wox6*	0.0114	**
WT *vs.*	*wox1 wox6*	0.3559	ND
WT *vs.*	*prs wox6*	0.3559	ND
wox1 wox6 vs.	*prs wox6*	0.8481	ND

ND in all other cases

Statistical analysis of organ number in WT, *maw*, and *maw mawb* Petunia plants

Lateral organs were manually counted on 5 weeks-old Petunia W138 plants, grown under greenhouse conditions. 8 plants from WT, 8 from *maw* and 24 from *maw mawb* were used.

Table reporting the average number of leaves per genotype

	maw mawb	*maw*	wt
total leaves	19,58333	15,875	10,75
dev. St	5,380453	2,587746	1,035098
conf.	2,15259	1,793183	0,717273

Heteroskedastic T-tests

maw mawb vs maw - total leaves	0,015	*
maw mawb vs wt - total leaves	3,082 E-08	***
maw vs wt - total leaves	0,001	***

Normal leaves and small leaves

		maw mawb	*maw*	WT
Average	Small leaves	5.92	2.13	0
	Normal leaves	13.67	13.75	10.75

		maw mawb	*maw*	WT
St. dev.	Small leaves	4.59	1.96	0
	Normal leaves	1.76	1.04	1.04

		maw mawb	*maw*	WT
Conf.	Small leaves	1.83	1.36	0
	Normal leaves	0.70	0.72	0.72

Heteroskedastic T-tests

maw mawb Vs. maw - normal leaves	0.873	no difference
maw mawb Vs. WT - normal leaves	1.199 E -05	***
maw Vs. WT - normal leaves	4.631 E -05	***
maw mawb Vs. maw - small leaves	0.003	**

Annex III: Protein alignment of WOX1 sequences

Full protein alignments for different WOX1 sequences (including *Petunia* x *hybrida* MAEWEST and MAEWESTB) are shown (next page). Displayed sequences belong to the following species: At, *Arabidopsis thaliana*; Ph, *Petunia* x *hybrida*; Pt, *Populus trichocarpa*; Vv, *Vitis vinifera*.

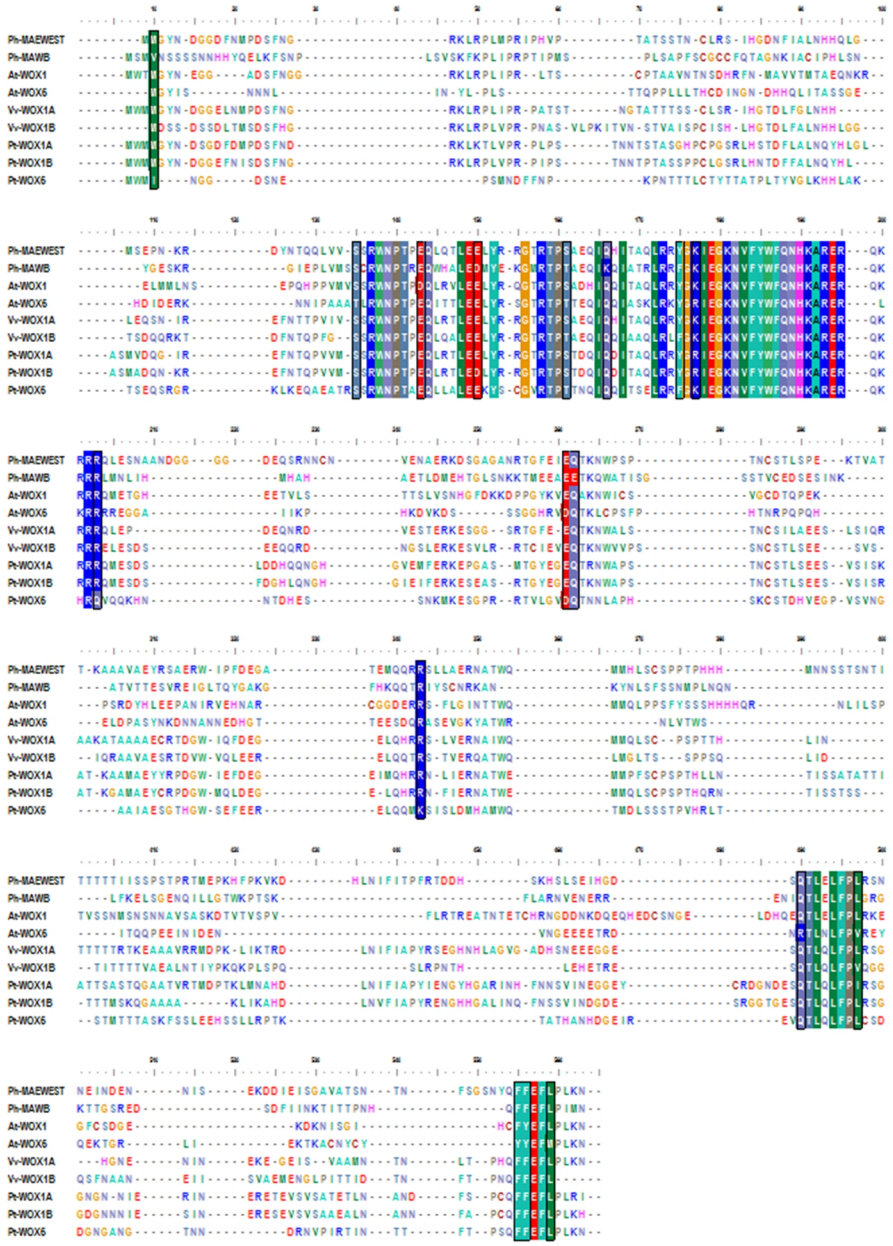

Alignment of different WOX1 aminoacidic sequences

Annex IV: Bioinformatics and phylogenetic analysis

Sequence search and cDNA prediction

The BioEdit package (Hall 1999), the Wise2 tool ("WISE2 Online Tool"), the NCBI databases ("NCBI database"), and the Sol Genomics database ("Sol Genomics Network Database") were adopted for sequence search, sequence alignment and cDNA prediction.

Phylogenetic analysis

The homeodomain regions WOX proteins were aligned and used for drawing the phylogenetic tree (reported in FIG. 1, Chapter III), as described in (Vandenbussche et al. 2009). To support inferred phylogeny, 1000 bootstrap samples were generated. The tree was drawn using the Treecon software (Van de Peer and De Wachter 1994), as described in (Vandenbussche et al. 2009). Homedomain WOX sequences from the following species were used (see the HOMEODOMAIN alignment below): At, *Arabidopsis thaliana*; Os, *Oryza sativa*; Ph, *Petunia* x *hybrida*; Pt, *Populus trichocarpa*; Sb, *Sorghum bicolor*; Vv, *Vitis vinifera*; Zm, *Zea mays*. Only bootstrap values above 65% were shown in the resulting tree.

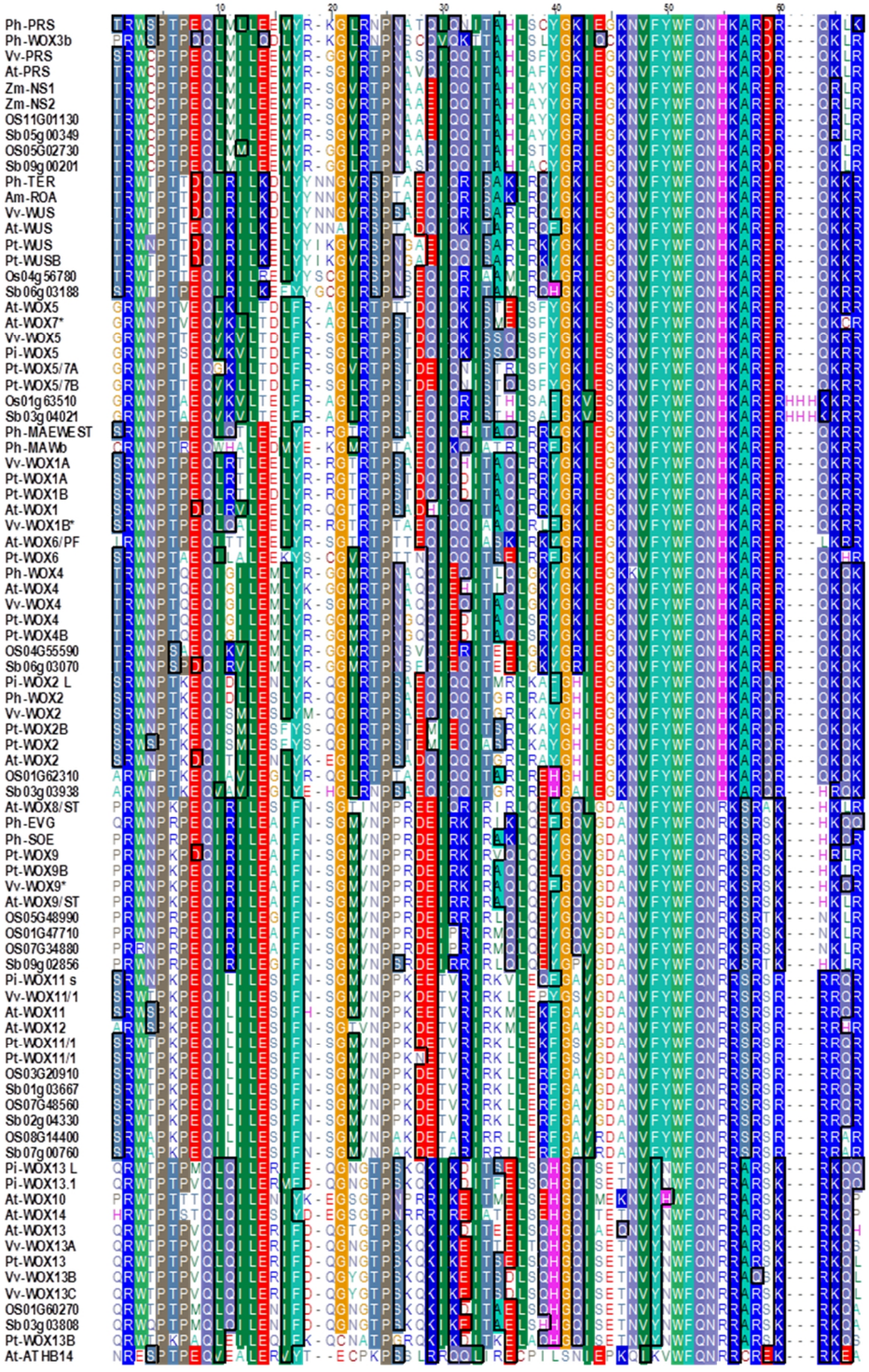
Ph-PRS
Ph-WOX3b
Vv-PRS
At-PRS
Zm-NS1
Zm-NS2
OS11G01130
Sb05g00349
OS05G02730
Sb09g00201
Ph-TER
Am-ROA
Vv-WUS
At-WUS
Pt-WUS
Pt-WUSB
Os04g56780
Sb06g03188
At-WOX5
At-WOX7*
Vv-WOX5
Pi-WOX5
Pt-WOX5/7A
Pt-WOX5/7B
Os01g63510
Sb03g04021
Ph-MAEWEST
Ph-MAWb
Vv-WOX1A
Pt-WOX1A
Pt-WOX1B
At-WOX1
Vv-WOX1B*
At-WOX6/PF
Pt-WOX6
Ph-WOX4
At-WOX4
Vv-WOX4
Pt-WOX4
Pt-WOX4B
OS04G55590
Sb06g03070
Pi-WOX2 L
Ph-WOX2
Vv-WOX2
Pt-WOX2B
Pt-WOX2
At-WOX2
OS01G62310
Sb03g03938
At-WOX8/ST
Ph-EVG
Ph-SOE
Pt-WOX9
Pt-WOX9B
Vv-WOX9*
At-WOX9/ST
OS05G48990
OS01G47710
OS07G34880
Sb09g02856
Pi-WOX11 s
Vv-WOX11/1
At-WOX11
At-WOX12
Pt-WOX11/1
Pt-WOX11/1
OS03G20910
Sb01g03667
OS07G48560
Sb02g04330
OS08G14400
Sb07g00760
Pi-WOX13 L
Pi-WOX13.1
At-WOX10
At-WOX14
At-WOX13
Vv-WOX13A
Pt-WOX13
Vv-WOX13B
Vv-WOX13C
OS01G60270
Sb03g03808
Pt-WOX13B
At-ATHB14

RNA-sequencing

RNA SEQUENCING ON W138 SAMPLES - RNA samples were obtained by TRIzol method (see above). For each condition (WT, *maw*-6 and *maw*-4 *mawb* mutants), 3 biological samples were used. Each biological sample was composed of vegetative apexes in a variable number comprised between 7 to 10, per biological sample.

Samples	Genotype	Comments
Sample 1	WT	10 apexes (6 from line LY1502 et 4 from line LY1503)
Sample 2		
Sample 3		
Sample 4	*maw*-6	7 apexes (LY1504/LY1506)
Sample 5		
Sample 6		
Sample 7	*maw*-4 *mawb*	10 apexes (6 de LY1502 et 4 de LY1503)
Sample 8		
Sample 9		

Sample quality was assessed accordingly to sequencing platform specifications: 4 micrograms in 100 µl of MilliQ water (40 ng/µl); 260/280 ratio >1.8; gel analyzed RNA displayed two prominent bands; after Agilent Bioanalyzer 2100 analysis, RNA samples displayed an RNA Integrity Number (RIN) > 8.

Samples were sent to IGA Technology Services (Via J.Linussio, 51 Z.I.U. Udine 33100 – Italy) and sequenced on a HiSeq 2500 Illumina machine. A single-end (unstranded) sequencing on two lanes, producing 100 bp fragments, was performed (meaning that each

sample was run two times, each time producing ~20 M fragments). In total, 18 FASTQ library files (2 files per sample) were obtained.

The bio-informatics work was performed in collaboration with Edoardo Bertolini (Institute of Life Sciences, Scuola Superiore Sant'Anna, Pisa, Italy).

Library trimming

Libraries were quality trimmed using the ERNE-FILTER software (IGA Technology Services) (Del Fabbro et al. 2013):

```
for i in {1..18}; do erne-filter --query1 $i.gz --gzip --min-
mean-phred-quality 33 --min-size 90 --threads 8 --output-prefix
$i-trimmed; done
```

Quality assessed libraries were unzipped and fused together accordingly to sample origin (information from each biological sample contained into two different fastq files):

```
cat Na-trimmed_1.fastq Nb-trimmed_1.fastq >
sample_N_trimmed.fastq
```

merged libraries were then saved in a new folder called "`copy_database`".

As described in Chapter IV, the bioinformatics analysis was set up as a *pseudo de novo* analysis. The two genomes of *P. axillaris* and *P. inflata* were merged in a single file, obtaining a synthetic *P.* x *hybrida* genome (called "`P.hybridasynth.fasta`", for code reasons, a symbolic link, "`Phybrida.fa`" to the original file "`P.hybridasynth.fasta`" was created). GFF files for *P. axillaris* and *P. inflata* based on annotation in Tomato were created by Jeremy Just (INRA, Laboratory of Reproduction and Development of Plants, UMR5667, Ecole Normale Supérieure de Lyon, Lyon, France).

The following GFF combinations were obtained, to be used in the analysis:

`tomato_prot_on_Pehybrida_synth_genome.gff`, containing coding sequences in Petunia (*P.axillaris* + *P.inflata*) based on Tomato;

`Pehybrida_synth.rRNA.gff`, containing rRNA sequences in Petunia (*P.axillaris* + *P.inflata*) based on Tomato;

`tomato_prot_on_Pehybrida_synth_genome_with_rRNA.gff`, containing both coding and rRNA sequences in (*P.axillaris* + *P.inflata*) based on Tomato.

BIO-INFORMATICS ANALYSIS USING THE "TUXEDO" PACKAGE

(Trapnell et al. 2012)

For bio-informatics analysis of RNA-seq data, we relied on the "Tuxedo" package (Roberts et al. 2011; Trapnell et al. 2012; Kim et al. 2013).

The bowtie2 (bowtie2_align version 2.1.0 - 64 bit) software was run to create an indexed version of our synthetic *P.* x *hybrida* genome:

```
bowtie2-build P.hybridasynth.fasta
```

Tophat2 (TopHat v2.0.9) was used to align reads on the genome, using the GFF file tomato_prot_on_Pehybrida_synth_genome_with_rRNA.gff containing both coding and rRNA sequences. Tophat2 was launched using the following bash script:

```
#!/bin/bash

#

tophat2 -o ./tophat_sampleN_phybrida -p 10 -i 10 -I 500000 --
library-type fr-unstranded -G
tomato_prot_on_Pehybrida_synth_genome_with_rRNA.gff
./Genome/Phybrida ./copy_database/sample_N_trimmed.fastq.gz
```

```
#'nohup' command

$ nohup ./script.sh > script.out2> script.err &
```

```
#Tophat2 produces aligned hits (accepted_hits.bam) for Cufflinks.
Cufflinks (cufflinks v2.1.1) is used to assemble transcript
derived from Tophat2. Cufflinks was launched using the following
script in bash:

#!bin/bash

#

cufflinks -o ./cufflinks/cufflinks_sample_N_pehybrida -p 5 --
library-type fr-unstranded -G
```

```
tomato_prot_on_Pehybrida_synth_genome.gff -g
tomato_prot_on_Pehybrida_synth_genome.gff -M
Pehybrida_synth.rRNA.gff
./tophat_sampleN_phybrida/accepted_hits.bam



#'nohup' command:

$ nohup sh script.sh >script.log &
```

Before running Cuffmerge, a list containing the path that Cuffmerge will follow for each sample is created: "assembly_list_pehybrida.txt".

Containing the following list:

```
./cufflinks/cufflinks_sample_1_pehybrida/transcripts.gtf
./cufflinks/cufflinks_sample_2_pehybrida/transcripts.gtf
./et cetera.
```

Cuffmerge (merge.cuff.asms v1.0.0) was used for merging transcripts from all the nine samples producing a GTF file as baseline for transcripts quantification. All the nine conditions are taken into account for the production of the GTF file, so that even low expressed transcripts are taken into account.

The output from cuffmerge was organized into a new folder: "merged_asm_pehybrida_synth".

```
$ cuffmerge -s ./Genome/P.hybridasynth.fasta -g
./tomato_prot_on_Pehybrida_synth_genome.gff -o
./merged_asm_pehybrida_synth ./assembly_list_pehybrida.txt
```

The output gtf file, called "merged.gtf" can be converted into a FASTA file using "gffread".

```
$ gffread -w reference_pehybrida_transcriptome.fa -g
Genome/Phybrida.fa merged_asm_pehybrida_synth/merged.gtf
```

Conditions (WT, *maw*, *maw mawb*) were compared in pairs using CuffDiff (cuffdiff V2.1.1), obtaining FPKM (Fragments Per Kilobase of transcript per Million fragments mapped) values of differentially expressed genes.

```
$ cuffdiff -o CuffDiff/mawmawb_vs_wt --compatible-hits-norm --
multi-read-correct --upper-quartile-norm -b
```

```
./Genome/P.hybridasynth.fasta -p 7 -L wt,mawmawb -u
./merged_asm_pehybrida_synth/merged.gtf
./tophat_sample1_phybrida/accepted_hits.bam,./tophat_sample2_phyb
rida/accepted_hits.bam,./tophat_sample3_phybrida/accepted_hits.ba
m
./tophat_sample7_phybrida/accepted_hits.bam,./tophat_sample8_phyb
rida/accepted_hits.bam,./tophat_sample9_phybrida/accepted_hits.ba
m
```

```
$ cuffdiff -o CuffDiff/maw_vs_mawmawb --compatible-hits-norm --
multi-read-correct --upper-quartile-norm -b
./Genome/P.hybridasynth.fasta -p 7 -L mawmawb,maw -u
./merged_asm_pehybrida_synth/merged.gtf
./tophat_sample7_phybrida/accepted_hits.bam,./tophat_sample8_phyb
rida/accepted_hits.bam,./tophat_sample9_phybrida/accepted_hits.ba
m
./tophat_sample4_phybrida/accepted_hits.bam,./tophat_sample5_phyb
rida/accepted_hits.bam,./tophat_sample6_phybrida/accepted_hits.ba
m
```

```
$ cuffdiff -o CuffDiff/maw_vs_wt --compatible-hits-norm --multi-
read-correct --upper-quartile-norm -b
./Genome/P.hybridasynth.fasta -p 7 -L wt,maw -u
./merged_asm_pehybrida_synth/merged.gtf
./tophat_sample1_phybrida/accepted_hits.bam,./tophat_sample2_phyb
rida/accepted_hits.bam,./tophat_sample3_phybrida/accepted_hits.ba
m
./tophat_sample4_phybrida/accepted_hits.bam,./tophat_sample5_phyb
rida/accepted_hits.bam,./tophat_sample6_phybrida/accepted_hits.ba
m
```

The output tables were exported in Excel (Office Suite – Microsoft) for downstream analysis.

Production of a transcriptome assembly for downstream analysis and primer design in *P.* x *hybrida*

A simplified "Tuxedo" protocol (see above) was used to obtain a *de novo* transcriptome. In particular, no GFF file was provided, in order to allow the software to not be misguided in the assembly process.

```
#!/bin/bash

#

tophat2 -o
./tophat_for_transcriptome_de_novo_assembly/tophat_denovo_sampleN
_phybrida -p 10 -i 10 -I 500000 --library-type fr-unstranded
./Genome/Phybrida ./copy_database/sample_N_trimmed.fastq.gz
```

```
#!bin/bash

#

cufflinks -o ./denovocufflinks/denovocufflinks_sample_N_pehybrida
-p 5 --library-type fr-unstranded
./tophat_sampleN_phybrida/accepted_hits.bam
```

List: denovo_assembly_list_pehybrida.txt

```
./denovocufflinks/denovocufflinks_sample_1_pehybrida/transcripts.
gtf
./denovocufflinks/denovocufflinks_sample_2_pehybrida/transcripts.
gtf ./et cetera.
```

```
$cuffmerge -s ./Genome/P.hybridasynth.fasta -o
./denovomerged_asm_pehybrida_synth
./denovo_assembly_list_pehybrida.txt
```

```
$gffread -w denovo_reference_pehybrida_transcriptome.fa -g
Genome/Phybrida.fa denovomerged_asm_pehybrida_synth/merged.gtf
```

Appendix I

Chronostratigraphic Chart

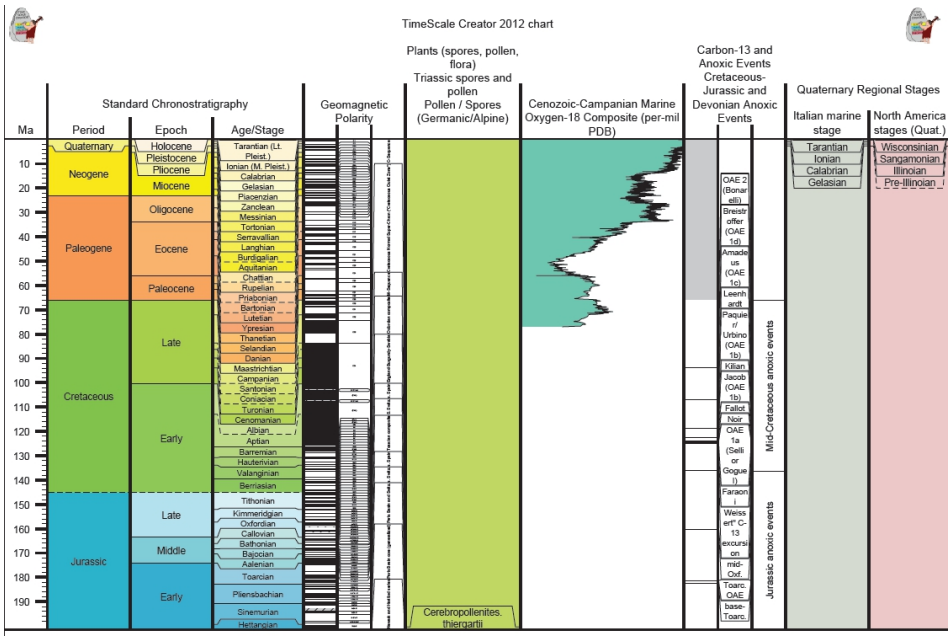

Appendix II

Data sets from RNA-Seq Analysis

Original FPKM values (not log2) for differentially expressed genes (DEGs) reported from heat-maps in Chapter IV.

DEGs involved in transcription

Identifier	WT	*maw*	*maw mawb*	Scaffold
XLOC_041435	3.439	0.865	-0.895	Peaxi162Scf00705:10676-14621
XLOC_010740	1.546	0.686	-0.068	Peaxi162Scf00071:229280-232779
XLOC_086126	3.280	1.758	1.217	Peinf101Scf01368:385922-390456
XLOC_044833	-1.122	0.459	1.325	Peaxi162Scf00875:160201-162010
XLOC_032717	-0.816	0.446	1.439	Peaxi162Scf00418:784360-787239
XLOC_042581	0.243	0.898	1.531	Peaxi162Scf00756:238582-243574
XLOC_022995	-0.451	0.910	1.631	Peaxi162Scf00226:143274-145621
XLOC_049562	0.635	1.190	1.734	Peaxi162Scf01306:60107-63892
XLOC_045999	-0.514	0.981	1.834	Peaxi162Scf00939:372964-373892
XLOC_004832	3.214	2.759	1.981	Peaxi162Scf00021:1288348-1292905
XLOC_039966	3.254	2.677	2.154	Peaxi162Scf00654:189690-198727
XLOC_030956	4.480	4.026	2.329	Peaxi162Scf00380:175815-193413
XLOC_013509	1.285	1.774	3.087	Peaxi162Scf00098:598565-602829
XLOC_047061	1.809	2.719	3.257	Peaxi162Scf01006:367466-368054
XLOC_031992	1.385	2.103	3.289	Peaxi162Scf00401:84633-86799
XLOC_044976	1.389	2.549	3.383	Peaxi162Scf00882:220039-220486
XLOC_037144	2.314	2.903	3.421	Peaxi162Scf00546:112259-113677
XLOC_069003	2.325	2.974	3.503	Peinf101Scf00500:299826-300328
XLOC_016772	4.347	3.968	3.595	Peaxi162Scf00135:1083975-1087869
XLOC_084095	4.812	4.185	3.624	Peinf101Scf01208:506175-508369
XLOC_095215	4.951	4.426	3.707	Peinf101Scf02757:412771-414420
XLOC_034619	2.917	3.445	3.841	Peaxi162Scf00465:570952-572879
XLOC_047703	3.037	3.704	4.189	Peaxi162Scf01064:29927-31787
XLOC_026314	5.437	4.826	4.291	Peaxi162Scf00287:1900666-1907293
XLOC_009116	2.654	3.254	4.333	Peaxi162Scf00055:1935487-1938124
XLOC_047468	5.330	4.857	4.377	Peaxi162Scf01044:218342-221589
XLOC_012239	5.369	4.987	4.414	Peaxi162Scf00083:1645457-1647077

XLOC_073172	2.397	3.332	4.525	Peinf101Scf00661:180334-180823
XLOC_039307	3.121	3.906	4.703	Peaxi162Scf00624:652952-658242
XLOC_071013	5.961	5.418	4.748	Peinf101Scf00576:359452-360584
XLOC_070477	6.551	5.668	5.191	Peinf101Scf00559:1363672-1390738
XLOC_059332	6.388	5.684	5.341	Peinf101Scf00184:90365-91609
XLOC_042000	2.602	4.169	5.391	Peaxi162Scf00732:231933-234101
XLOC_029167	6.600	6.021	5.557	Peaxi162Scf00345:215389-220956
XLOC_026002	1.931	2.701	6.223	Peaxi162Scf00284:779318-781137
XLOC_037580	2.402	3.714	6.312	Peaxi162Scf00560:255874-256309

Auxin-related DEGs

Identifier	WT	*maw*	*maw mawb*	Scaffold
XLOC_001236	5.16494	3.72536666	1.80734	Peaxi162Scf00003:4971688-4974533
XLOC_063950	5.20554	3.46942052	1.1845	Peinf101Scf00335:1091683-1095352
XLOC_085252	21.7526	14.6612644	7.62887	Peinf101Scf01294:525501-528794
XLOC_026314	43.3249	28.3623759	19.5766	Peaxi162Scf00287:1900666-1907293
XLOC_029167	97.0342	64.9339478	47.0909	Peaxi162Scf00345:215389-220956
XLOC_029938	13.2805	9.65167715	4.05724	Peaxi162Scf00362:884789-888495
XLOC_087092	44.4308	32.6460666	13.58	Peinf101Scf01468:28155-32150
XLOC_034619	7.55234	10.8919727	14.335	Peaxi162Scf00465:570952-572879
XLOC_046604	1.25318	2.14700715	4.77453	Peaxi162Scf00976:88676-92325
XLOC_047468	40.2233	28.9736288	20.7737	Peaxi162Scf01044:218342-221589
XLOC_084095	28.0818	18.1896863	12.3292	Peinf101Scf01208:506175-508369
XLOC_011420	6.62671	4.23471302	2.23243	Peaxi162Scf00075:2290593-2293392
XLOC_012901	2.91755	1.62818186	0.82086	Peaxi162Scf00089:1521276-1526815
XLOC_026216	2.88801	4.25165297	21.5731	Peaxi162Scf00286:1029572-1030994
XLOC_028163	0.87047	1.9078239	3.31758	Peaxi162Scf00325:76311-77031
XLOC_028911	2.06661	1.07027288	0.128225	Peaxi162Scf00339:1173385-1177246

XLOC_023577	19.1519	11.3862293	4.26066	Peaxi162Scf00235:772404-775909
XLOC_095215	30.9225	21.4956681	13.0575	Peinf101Scf02757:412771-414420

DEGs involved in cell proliferation

Identifier	WT	*maw*	*maw mawb*	Scaffold
XLOC_000884	30.6122	17.86700554	6.25221	Peaxi162Scf00003:2407558-2409240
XLOC_052955	31.3152	19.68724886	7.81057	Peinf101Scf00019:116538-119101
XLOC_004832	9.28162	6.770467309	3.94852	Peaxi162Scf00021:1288348-1292905
XLOC_016772	20.3525	15.65075462	12.0838	Peaxi162Scf00135:1083975-1087869

miR156/SPLs module

Identifier	WT	*maw*	*maw mawb*	Scaffold
XLOC_091056	0.176599	0.71602566	1.83733	Peinf101Scf01889:60268-62529
XLOC_016004	43.4172	28.99338893	23.0128	Peaxi162Scf00128:1314265-1319766
XLOC_016014	50.1275	33.82232076	25.4217	Peaxi162Scf00128:1473754-1477676

References

Abe M, Katsumata H, Komeda Y, Takahashi T. **2003**. Regulation of shoot epidermal cell differentiation by a pair of homeodomain proteins in Arabidopsis. *Development (Cambridge, England)* **130**: 635–643.

Adedeji O AOY. **2007**. Foliar Epidermal Studies, Organographic Distribution and Taxonomic Importance of Trichomes in the Family Solanaceae. *International Journal of Botany*.

Alvarez JM, Sohlberg J, Engström P, Zhu T, Englund M, Moschou PN, von Arnold S. **2015**. The WUSCHEL-RELATED HOMEOBOX 3 gene PaWOX3 regulates lateral organ formation in Norway spruce. *The New Phytologist*.

Ando T, Kokubun H, Watanabe H, Tanaka N, Yukawa T, Hashimoto G, Marchesi E, Suárez E, Basualdo IL. **2005**. Phylogenetic analysis of Petunia sensu Jussieu (Solanaceae) using chloroplast DNA RFLP. *Annals of Botany* **96**: 289–297.

Andriankaja M, Dhondt S, De Bodt S, Vanhaeren H, Coppens F, De Milde L, Mühlenbock P, Skirycz A, Gonzalez N, Beemster GTS, Inzé D. **2012**. Exit from proliferation during leaf development in Arabidopsis thaliana: a not-so-gradual process. *Developmental Cell* **22**: 64–78.

Angeles-Shim RB, Asano K, Takashi T, Shim J, Kuroha T, Ayano M, Ashikari M. **2012**. A WUSCHEL-related homeobox 3B gene, depilous (dep), confers glabrousness of rice leaves and glumes. *Rice* **5**: 28.

Angenent GC, Franken J, Busscher M, van Dijken A, van Went JL, Dons HJ, van Tunen AJ. **1995**. A novel class of MADS box genes is involved in ovule development in petunia. *The Plant Cell* **7**: 1569–1582.

Aoyama T, Chua NH. **1997**. A glucocorticoid-mediated transcriptional induction system in transgenic plants. *The Plant Journal: For Cell and Molecular Biology* **11**: 605–612.

Ariel FD, Manavella PA, Dezar CA, Chan RL. **2007**. The true story of the HD-Zip family. *Trends in Plant Science* **12**: 419–426.

Avila EM, Day A. **2014**. Stable plastid transformation of petunia. *Methods in Molecular Biology (Clifton, N.J.)* **1132**: 277–293.

Van Bakel H, Nislow C, Blencowe BJ, Hughes TR. **2010**. Most "dark matter" transcripts are associated with known genes. *PLoS biology* **8**: e1000371.

Balkunde R, Pesch M, Hülskamp M. **2010**. Trichome patterning in Arabidopsis thaliana from genetic to molecular models. *Current Topics in Developmental Biology* **91**: 299–321.

Barrett PM, Willis KJ. **2001**. Did dinosaurs invent flowers? Dinosaur—angiosperm coevolution revisited. *Biological Reviews* **76**: 411–447.

Beemster GTS, De Veylder L, Vercruysse S, West G, Rombaut D, Van Hummelen P, Galichet A, Gruissem W, Inzé D, Vuylsteke M. 2005. Genome-wide analysis of gene expression profiles associated with cell cycle transitions in growing organs of Arabidopsis. *Plant Physiology* **138**: 734–743.

Benková E, Michniewicz M, Sauer M, Teichmann T, Seifertová D, Jürgens G, Friml J. 2003. Local, efflux-dependent auxin gradients as a common module for plant organ formation. *Cell* **115**: 591–602.

Bernhardt C, Lee MM, Gonzalez A, Zhang F, Lloyd A, Schiefelbein J. 2003. The bHLH genes GLABRA3 (GL3) and ENHANCER OF GLABRA3 (EGL3) specify epidermal cell fate in the Arabidopsis root. *Development (Cambridge, England)* **130**: 6431–6439.

Besnard F, Vernoux T, Hamant O. 2011. Organogenesis from stem cells in planta: multiple feedback loops integrating molecular and mechanical signals. *Cellular and molecular life sciences: CMLS* **68**: 2885–2906.

Birnboim HC, Doly J. 1979. A rapid alkaline extraction procedure for screening recombinant plasmid DNA. *Nucleic Acids Research* **7**: 1513–1523.

Bohmert K, Camus I, Bellini C, Bouchez D, Caboche M, Benning C. 1998. AGO1 defines a novel locus of Arabidopsis controlling leaf development. *The EMBO journal* **17**: 170–180.

Bohn-Courseau I. 2010. Auxin: a major regulator of organogenesis. *Comptes Rendus Biologies* **333**: 290–296.

Bombarely A, Rosli HG, Vrebalov J, Moffett P, Mueller LA, Martin GB. 2012. A draft genome sequence of Nicotiana benthamiana to enhance molecular plant-microbe biology research. *Molecular plant-microbe interactions: MPMI* **25**: 1523–1530.

Bowman JL. 2004. Class III HD-Zip gene regulation, the golden fleece of ARGONAUTE activity? *BioEssays: News and Reviews in Molecular, Cellular and Developmental Biology* **26**: 938–942.

Bowman JL, Drews GN, Meyerowitz EM. 1991. Expression of the Arabidopsis floral homeotic gene AGAMOUS is restricted to specific cell types late in flower development. *The Plant cell* **3**: 749–758.

Bowman JL, Smyth DR, Meyerowitz EM. 2012. The ABC model of flower development: then and now. *Development (Cambridge, England)* **139**: 4095–4098.

Brambilla V, Battaglia R, Colombo M, Masiero S, Bencivenga S, Kater MM, Colombo L. 2007. Genetic and molecular interactions between BELL1 and MADS box factors support ovule development in Arabidopsis. *The Plant Cell* **19**: 2544–2556.

Brambilla V, Kater M, Colombo L. 2008. Ovule integument identity determination in Arabidopsis. *Plant Signaling & Behavior* **3**: 246–247.

Brand U, Fletcher JC, Hobe M, Meyerowitz EM, Simon R. **2000**. Dependence of stem cell fate in Arabidopsis on a feedback loop regulated by CLV3 activity. *Science (New York, N.Y.)* **289**: 617–619.

Breuninger H, Rikirsch E, Hermann M, Ueda M, Laux T. **2008**. Differential expression of WOX genes mediates apical-basal axis formation in the Arabidopsis embryo. *Developmental cell* **14**: 867–876.

Broderick SR, Jones ML. **2014**. An Optimized Protocol to Increase Virus-Induced Gene Silencing Efficiency and Minimize Viral Symptoms in Petunia. *Plant molecular biology reporter / ISPMB* **32**: 219–233.

De Bruijn S, Angenent GC, Kaufmann K. **2012**. Plant "evo-devo" goes genomic: from candidate genes to regulatory networks. *Trends in Plant Science* **17**: 441–447.

Busch W, Miotk A, Ariel FD, Zhao Z, Forner J, Daum G, Suzaki T, Schuster C, Schultheiss SJ, Leibfried A, Haubeiss S, Ha N, Chan RL, Lohmann JU. **2010**. Transcriptional control of a plant stem cell niche. *Developmental cell* **18**: 849–861.

Byrne ME, Barley R, Curtis M, Arroyo JM, Dunham M, Hudson A, Martienssen RA. **2000**. Asymmetric leaves1 mediates leaf patterning and stem cell function in Arabidopsis. *Nature* **408**: 967–971.

Carroll SB. **1995**. Homeotic genes and the evolution of arthropods and chordates. *Nature* **376**: 479–485.

Castelli-Gair J. **1998**. Implications of the spatial and temporal regulation of Hox genes on development and evolution. *The International journal of developmental biology* **42**: 437–444.

Chen R, Hilson P, Sedbrook J, Rosen E, Caspar T, Masson PH. **1998**. The arabidopsis thaliana AGRAVITROPIC 1 gene encodes a component of the polar-auxin-transport efflux carrier. *Proceedings of the National Academy of Sciences of the United States of America* **95**: 15112–15117.

Chen X, Zhang Z, Liu D, Zhang K, Li A, Mao L. **2010**. SQUAMOSA promoter-binding protein-like transcription factors: star players for plant growth and development. *Journal of Integrative Plant Biology* **52**: 946–951.

Cho S-H, Yoo S-C, Zhang H, Pandeya D, Koh H-J, Hwang J-Y, Kim G-T, Paek N-C. **2013**. The rice narrow leaf2 and narrow leaf3 loci encode WUSCHEL-related homeobox 3A (OsWOX3A) and function in leaf, spikelet, tiller and lateral root development. *The New phytologist* **198**: 1071–1084.

Clark SE, Williams RW, Meyerowitz EM. **1997**. The CLAVATA1 gene encodes a putative receptor kinase that controls shoot and floral meristem size in Arabidopsis. *Cell* **89**: 575–585.

Coen E. **2001**. Goethe and the ABC model of flower development. *Comptes rendus de l'Académie des sciences. Série III, Sciences de la vie* **324**: 523–530.

Colombo L, Battaglia R, Kater MM. **2008**. Arabidopsis ovule development and its evolutionary conservation. *Trends in plant science* **13**: 444–450.

Colombo L, Franken J, Koetje E, van Went J, Dons HJ, Angenent GC, van Tunen AJ. **1995**. The petunia MADS box gene FBP11 determines ovule identity. *The Plant Cell* **7**: 1859–1868.

Conesa A, Götz S, García-Gómez JM, Terol J, Talón M, Robles M. **2005**. Blast2GO: a universal tool for annotation, visualization and analysis in functional genomics research. *Bioinformatics* **21**: 3674–3676.

Costa V, Angelini C, De Feis I, Ciccodicola A. **2010**. Uncovering the complexity of transcriptomes with RNA-Seq. *Journal of Biomedicine & Biotechnology* **2010**: 853916.

Costanzo E, Trehin C, Vandenbussche M. **2014**. The role of WOX genes in flower development. *Annals of Botany*.

Dai M, Hu Y, Zhao Y, Liu H, Zhou D-X. **2007**. A WUSCHEL-LIKE HOMEOBOX gene represses a YABBY gene expression required for rice leaf development. *Plant physiology* **144**: 380–390.

Dai X, Wang G, Yang DS, Tang Y, Broun P, Marks MD, Sumner LW, Dixon RA, Zhao PX. **2010**. TrichOME: a comparative omics database for plant trichomes. *Plant Physiology* **152**: 44–54.

D'Amato, F. **1952**. Polyploidy in the differentiation and function of tissues and cells in plants. *Caryologia: International Journal of Cytology, Cytosystematics and Cytogenetics* **4:3, 311-358**.

Darwin Correspondence Project » letter: 12167.

Dewitte W, Scofield S, Alcasabas AA, Maughan SC, Menges M, Braun N, Collins C, Nieuwland J, Prinsen E, Sundaresan V, Murray JAH. **2007**. Arabidopsis CYCD3 D-type cyclins link cell proliferation and endocycles and are rate-limiting for cytokinin responses. *Proceedings of the National Academy of Sciences of the United States of America* **104**: 14537–14542.

Dkhar J, Pareek A. **2014**. What determines a leaf's shape? *EvoDevo* **5**: 47.

Dobzhansky T. **1973**. Nothing in Biology Makes Sense except in the Light of Evolution. *The American Biology Teacher* **35**: 125–129.

Donnelly PM, Bonetta D, Tsukaya H, Dengler RE, Dengler NG. **1999**. Cell cycling and cell enlargement in developing leaves of Arabidopsis. *Developmental Biology* **215**: 407–419.

Donner TJ, Sherr I, Scarpella E. **2009**. Regulation of preprocambial cell state acquisition by auxin signaling in Arabidopsis leaves. *Development (Cambridge, England)* **136**: 3235–3246.

Dreni L, Pilatone A, Yun D, Erreni S, Pajoro A, Caporali E, Zhang D, Kater MM. **2011**. Functional analysis of all AGAMOUS subfamily members in rice reveals their roles in

reproductive organ identity determination and meristem determinacy. *The Plant cell* **23**: 2850–2863.

Edwards K, Johnstone C, Thompson C. **1991**. A simple and rapid method for the preparation of plant genomic DNA for PCR analysis. *Nucleic Acids Research* **19**: 1349.

Efroni I, Eshed Y, Lifschitz E. **2010**. Morphogenesis of Simple and Compound Leaves: A Critical Review. *The Plant Cell* **22**: 1019–1032.

Esch JJ, Chen M, Sanders M, Hillestad M, Ndkium S, Idelkope B, Neizer J, Marks MD. **2003**. A contradictory GLABRA3 allele helps define gene interactions controlling trichome development in Arabidopsis. *Development* **130**: 5885–5894.

Del Fabbro C, Scalabrin S, Morgante M, Giorgi FM. **2013**. An extensive evaluation of read trimming effects on Illumina NGS data analysis. *PloS One* **8**: e85024.

Friedman WE. **2009**. The meaning of Darwin's "abominable mystery." *American journal of botany* **96**: 5–21.

Friedman WE, Diggle PK. **2011**. Charles Darwin and the origins of plant evolutionary developmental biology. *The Plant Cell* **23**: 1194–1207.

Frohlich MW. **2003**. An evolutionary scenario for the origin of flowers. *Nature Reviews. Genetics* **4**: 559–566.

Frohlich MW, Chase MW. **2007**. After a dozen years of progress the origin of angiosperms is still a great mystery. *Nature* **450**: 1184–1189.

Fu X, Fu N, Guo S, Yan Z, Xu Y, Hu H, Menzel C, Chen W, Li Y, Zeng R, Khaitovich P. **2009**. Estimating accuracy of RNA-Seq and microarrays with proteomics. *BMC genomics* **10**: 161.

Garcia D, Collier SA, Byrne ME, Martienssen RA. **2006**. Specification of leaf polarity in Arabidopsis via the trans-acting siRNA pathway. *Current biology: CB* **16**: 933–938.

Gerats AG, Huits H, Vrijlandt E, Maraña C, Souer E, Beld M. **1990**. Molecular characterization of a nonautonomous transposable element (dTph1) of petunia. *The Plant Cell* **2**: 1121–1128.

Gerats T, Vandenbussche M. **2005**. A model system for comparative research: Petunia. *Trends in Plant Science* **10**: 251–256.

Gerats T, Zethof J, Vandenbussche M. **2013**. Identification and applications of the Petunia class II Act1/dTph1 transposable element system. *Plant Transposable Elements - Methods in Molecular Biology*. Humana Press, 223–237.

Gibson DG, Young L, Chuang R-Y, Venter JC, Hutchison CA, Smith HO. **2009**. Enzymatic assembly of DNA molecules up to several hundred kilobases. *Nature Methods* **6**: 343–345.

Glover BJ, Perez-Rodriguez M, Martin C. **1998**. Development of several epidermal cell types can be specified by the same MYB-related plant transcription factor. *Development (Cambridge, England)* **125**: 3497–3508.

Goethe JW von. **1790**. *Versuch die Metamorphose der Pflanzen zu erklären*. Gotha: C.W. Ettinger.

Goethe JW, Turpin PJF, Martins C. **1837**. *Oeuvres d'histoire naturelle de Goethe: Avec un atlas in-fol. ... enrichi... d'un texte explicatif sur la métamorphose des plantes : comprenant divers mémoires d'anatomie comparée, de botanique et de géologie*.

Gonzali S, Novi G, Loreti E, Paolicchi F, Poggi A, Alpi A, Perata P. **2005**. A turanose-insensitive mutant suggests a role for WOX5 in auxin homeostasis in Arabidopsis thaliana. *The Plant Journal: For Cell and Molecular Biology* **44**: 633–645.

(Van der) Graaff E, Laux T, Rensing SA. **2009**. The WUS homeobox-containing (WOX) protein family. *Genome biology* **10**: 248.

Grimaldi D. **1999**. The Co-Radiations of Pollinating Insects and Angiosperms in the Cretaceous. *Annals of the Missouri Botanical Garden* **86**: 373–406.

Gross-Hardt R, Lenhard M, Laux T. **2002**. WUSCHEL signaling functions in interregional communication during Arabidopsis ovule development. *Genes & Development* **16**: 1129–1138.

Guindon S, Delsuc F, Dufayard J-F, Gascuel O. **2009**. Estimating maximum likelihood phylogenies with PhyML. *Methods in Molecular Biology (Clifton, N.J.)* **537**: 113–137.

Haecker A, Gross-Hardt R, Geiges B, Sarkar A, Breuninger H, Herrmann M, Laux T. **2004**. Expression dynamics of WOX genes mark cell fate decisions during early embryonic patterning in Arabidopsis thaliana. *Development (Cambridge, England)* **131**: 657–668.

Hagemann W, Gleissberg S. **1996**. Organogenetic capacity of leaves: The significance of marginal blastozones in angiosperms. *Plant Systematics and Evolution* **199**: 121–152.

Hall TA. **1999**. BioEdit: a user-friendly biological sequence alignment editor and analysis program for Windows 95/98/NT. *Nucleic Acids Symp. Ser.* **41**: 95–98.

Hedman H, Zhu T, von Arnold S, Sohlberg JJ. **2013**. Analysis of the WUSCHEL-RELATED HOMEOBOX gene family in the conifer picea abies reveals extensive conservation as well as dynamic patterns. *BMC plant biology* **13**: 89.

Heijmans K, Ament K, Rijpkema AS, Zethof J, Wolters-Arts M, Gerats T, Vandenbussche M. **2012a**. Redefining C and D in the petunia ABC. *The Plant Cell* **24**: 2305–2317.

Heijmans K, Morel P, Vandenbussche M. **2012b**. MADS-box genes and floral development: the dark side. *Journal of experimental botany* **63**: 5397–5404.

Herman PL, Marks MD. **1989**. Trichome Development in Arabidopsis thaliana. II. Isolation and Complementation of the GLABROUS1 Gene. *The Plant Cell* **1**: 1051–1055.

Holland PWH. **2013**. Evolution of homeobox genes. *Wiley interdisciplinary reviews. Developmental biology* **2**: 31–45.

Horiguchi G, Kim G-T, Tsukaya H. **2005**. The transcription factor AtGRF5 and the transcription coactivator AN3 regulate cell proliferation in leaf primordia of Arabidopsis thaliana. *The Plant Journal* **43**: 68–78.

Huang T, Harrar Y, Lin C, Reinhart B, Newell NR, Talavera-Rauh F, Hokin SA, Barton MK, Kerstetter RA. **2014**. Arabidopsis KANADI1 Acts as a Transcriptional Repressor by Interacting with a Specific cis-Element and Regulates Auxin Biosynthesis, Transport, and Signaling in Opposition to HD-ZIPIII Factors. *The Plant cell* **26**: 246–262.

Hülskamp M. **2000**. Cell morphogenesis: How plants split hairs. *Current Biology* **10**: R308–R310.

Hülskamp M, Misŕa S, Jürgens G. **1994**. Genetic dissection of trichome cell development in Arabidopsis. *Cell* **76**: 555–566.

Hunter C, Sun H, Poethig RS. **2003**. The Arabidopsis heterochronic gene ZIPPY is an ARGONAUTE family member. *Current biology: CB* **13**: 1734–1739.

Hunter C, Willmann MR, Wu G, Yoshikawa M, de la Luz Gutiérrez-Nava M, Poethig SR. **2006**. Trans-acting siRNA-mediated repression of ETTIN and ARF4 regulates heteroblasty in Arabidopsis. *Development (Cambridge, England)* **133**: 2973–2981.

Hu B, Wan Y, Li X, Zhang F, Yan W, Xie J. **2013**. Phenotypic Characterization and Genetic Analysis of Rice with Pubescent Leaves and Glabrous Hulls (). *Crop Science* **53**: 1878–1886.

Ikeda M, Mitsuda N, Ohme-Takagi M. **2009**. Arabidopsis WUSCHEL is a bifunctional transcription factor that acts as a repressor in stem cell regulation and as an activator in floral patterning. *The Plant cell* **21**: 3493–3505.

Ishida T, Hattori S, Sano R, Inoue K, Shirano Y, Hayashi H, Shibata D, Sato S, Kato T, Tabata S, Okada K, Wada T. **2007**. Arabidopsis TRANSPARENT TESTA GLABRA2 is directly regulated by R2R3 MYB transcription factors and is involved in regulation of GLABRA2 transcription in epidermal differentiation. *The Plant Cell* **19**: 2531–2543.

Ishiwata A, Ozawa M, Nagasaki H, Kato M, Noda Y, Yamaguchi T, Nosaka M, Shimizu-Sato S, Nagasaki A, Maekawa M, Hirano H-Y, Sato Y. **2013**. Two WUSCHEL-related homeobox genes, narrow leaf2 and narrow leaf3, control leaf width in rice. *Plant & cell physiology* **54**: 779–792.

Iwasaki M, Takahashi H, Iwakawa H, Nakagawa A, Ishikawa T, Tanaka H, Matsumura Y, Pekker I, Eshed Y, Vial-Pradel S, Ito T, Watanabe Y, Ueno Y, Fukazawa H, Kojima S, Machida Y, Machida C. **2013**. Dual regulation of ETTIN (ARF3) gene expression by AS1-AS2, which maintains the DNA methylation level, is

involved in stabilization of leaf adaxial-abaxial partitioning in Arabidopsis. *Development (Cambridge, England)* **140**: 1958–1969.

Jackson D, Veit B, Hake S. **1994**. Expression of maize KNOTTED1 related homeobox genes in the shoot apical meristem predicts patterns of morphogenesis in the vegetative shoot. *Development* **120**: 405–413.

Ji L, Liu X, Yan J, Wang W, Yumul RE, Kim YJ, Dinh TT, Liu J, Cui X, Zheng B, Agarwal M, Liu C, Cao X, Tang G, Chen X. **2011**. ARGONAUTE10 and ARGONAUTE1 regulate the termination of floral stem cells through two microRNAs in Arabidopsis. *PLoS genetics* **7**: e1001358.

Jin J, Zhang H, Kong L, Gao G, Luo J. **2014**. PlantTFDB 3.0: a portal for the functional and evolutionary study of plant transcription factors. *Nucleic Acids Research* **42**: D1182–1187.

Ji J, Shimizu R, Sinha N, Scanlon MJ. **2010**. Analyses of WOX4 transgenics provide further evidence for the evolution of the WOX gene family during the regulation of diverse stem cell functions. *Plant signaling & behavior* **5**: 916–920.

Johnson JM, Edwards S, Shoemaker D, Schadt EE. **2005**. Dark matter in the genome: evidence of widespread transcription detected by microarray tiling experiments. *Trends in genetics: TIG* **21**: 93–102.

Johnson CS, Kolevski B, Smyth DR. **2002**. TRANSPARENT TESTA GLABRA2, a trichome and seed coat development gene of Arabidopsis, encodes a WRKY transcription factor. *The Plant Cell* **14**: 1359–1375.

Katsir L, Davies KA, Bergmann DC, Laux T. **2011**. Peptide signaling in plant development. *Current biology: CB* **21**: R356–364.

Kidner CA, Martienssen RA. **2004**. Spatially restricted microRNA directs leaf polarity through ARGONAUTE1. *Nature* **428**: 81–84.

Kieffer M, Stern Y, Cook H, Clerici E, Maulbetsch C, Laux T, Davies B. **2006**. Analysis of the transcription factor WUSCHEL and its functional homologue in Antirrhinum reveals a potential mechanism for their roles in meristem maintenance. *The Plant cell* **18**: 560–573.

Kim JH, Choi D, Kende H. **2003**. The AtGRF family of putative transcription factors is involved in leaf and cotyledon growth in Arabidopsis. *The Plant Journal: For Cell and Molecular Biology* **36**: 94–104.

Kim JH, Kende H. **2004**. A transcriptional coactivator, AtGIF1, is involved in regulating leaf growth and morphology in Arabidopsis. *Proceedings of the National Academy of Sciences of the United States of America* **101**: 13374–13379.

Kim D, Pertea G, Trapnell C, Pimentel H, Kelley R, Salzberg SL. **2013**. TopHat2: accurate alignment of transcriptomes in the presence of insertions, deletions and gene fusions. *Genome Biology* **14**: R36.

Klein J, Saedler H, Huijser P. **1996**. A new family of DNA binding proteins includes putative transcriptional regulators of the Antirrhinum majus floral meristem identity gene SQUAMOSA. *Molecular & general genetics: MGG* **250**: 7–16.

Kole C. **2011**. *Wild Crop Relatives: Genomic and Breeding Resources: Plantation and Ornamental Crops*. Springer Science & Business Media.

Korbie DJ, Mattick JS. **2008**. Touchdown PCR for increased specificity and sensitivity in PCR amplification. *Nature Protocols* **3**: 1452–1456.

Kumar R, Kushalappa K, Godt D, Pidkowich MS, Pastorelli S, Hepworth SR, Haughn GW. **2007**. The Arabidopsis BEL1-LIKE HOMEODOMAIN proteins SAW1 and SAW2 act redundantly to regulate KNOX expression spatially in leaf margins. *The Plant Cell* **19**: 2719–2735.

Kurakawa T, Ueda N, Maekawa M, Kobayashi K, Kojima M, Nagato Y, Sakakibara H, Kyozuka J. **2007**. Direct control of shoot meristem activity by a cytokinin-activating enzyme. *Nature* **445**: 652–655.

Langmead B, Trapnell C, Pop M, Salzberg SL. **2009**. Ultrafast and memory-efficient alignment of short DNA sequences to the human genome. *Genome Biology* **10**: R25.

Larkin JC, Oppenheimer DG, Pollock S, Marks MD. **1993**. Arabidopsis GLABROUS1 Gene Requires Downstream Sequences for Function. *The Plant Cell* **5**: 1739–1748.

Laux T, Mayer KF, Berger J, Jürgens G. **1996**. The WUSCHEL gene is required for shoot and floral meristem integrity in Arabidopsis. *Development (Cambridge, England)* **122**: 87–96.

Lee BH, Ko J-H, Lee S, Lee Y, Pak J-H, Kim JH. **2009**. The Arabidopsis GRF-INTERACTING FACTOR gene family performs an overlapping function in determining organ size as well as multiple developmental properties. *Plant Physiology* **151**: 655–668.

Leek JT, Scharpf RB, Bravo HC, Simcha D, Langmead B, Johnson WE, Geman D, Baggerly K, Irizarry RA. **2010**. Tackling the widespread and critical impact of batch effects in high-throughput data. *Nature Reviews. Genetics* **11**: 733–739.

Leibfried A, To JPC, Busch W, Stehling S, Kehle A, Demar M, Kieber JJ, Lohmann JU. **2005**. WUSCHEL controls meristem function by direct regulation of cytokinin-inducible response regulators. *Nature* **438**: 1172–1175.

Lenhard M, Bohnert A, Jürgens G, Laux T. **2001**. Termination of stem cell maintenance in Arabidopsis floral meristems by interactions between WUSCHEL and AGAMOUS. *Cell* **105**: 805–814.

Lenhard M, Laux T. **2003**. Stem cell homeostasis in the Arabidopsis shoot meristem is regulated by intercellular movement of CLAVATA3 and its sequestration by CLAVATA1. *Development (Cambridge, England)* **130**: 3163–3173.

Levin DA. **1973**. The Role of Trichomes in Plant Defense. *The Quarterly Review of Biology* **48**: 3–15.

Levin HL, Moran JV. **2011**. Dynamic interactions between transposable elements and their hosts. *Nature Reviews Genetics* **12**: 615–627.

Lie C, Kelsom C, Wu X. **2012**. WOX2 and STIMPY-LIKE/WOX8 promote cotyledon boundary formation in Arabidopsis. *The Plant journal: for cell and molecular biology* **72**: 674–682.

Li W, Jaroszewski L, Godzik A. **2001**. Clustering of highly homologous sequences to reduce the size of large protein databases. *Bioinformatics (Oxford, England)* **17**: 282–283.

Lincoln C, Long J, Yamaguchi J, Serikawa K, Hake S. **1994**. A knotted1-like homeobox gene in Arabidopsis is expressed in the vegetative meristem and dramatically alters leaf morphology when overexpressed in transgenic plants. *The Plant Cell* **6**: 1859–1876.

Lindberg J, Lundeberg J. **2010**. The plasticity of the mammalian transcriptome. *Genomics* **95**: 1–6.

Lin H, Niu L, McHale NA, Ohme-Takagi M, Mysore KS, Tadege M. **2013**. Evolutionarily conserved repressive activity of WOX proteins mediates leaf blade outgrowth and floral organ development in plants. *Proceedings of the National Academy of Sciences of the United States of America* **110**: 366–371.

Lin H, Niu L, Tadege M. **2013**. STENOFOLIA acts as a repressor in regulating leaf blade outgrowth. *Plant Signaling & Behavior* **8**: e24464.

Lippman ZB, Cohen O, Alvarez JP, Abu-Abied M, Pekker I, Paran I, Eshed Y, Zamir D. **2008**. The making of a compound inflorescence in tomato and related nightshades. *PLoS biology* **6**: e288.

Liu X, Kim YJ, Müller R, Yumul RE, Liu C, Pan Y, Cao X, Goodrich J, Chen X. **2011**. AGAMOUS terminates floral stem cell maintenance in Arabidopsis by directly repressing WUSCHEL through recruitment of Polycomb Group proteins. *The Plant cell* **23**: 3654–3670.

Li J, Yuan Y, Lu Z, Yang L, Gao R, Lu J, Li J, Xiong G. **2012**. Glabrous Rice 1, encoding a homeodomain protein, regulates trichome development in rice. *Rice (New York, N.Y.)* **5**: 32.

Li L, Zhao Y, McCaig BC, Wingerd BA, Wang J, Whalon ME, Pichersky E, Howe GA. **2004**. The Tomato Homolog of CORONATINE-INSENSITIVE1 Is Required for the Maternal Control of Seed Maturation, Jasmonate-Signaled Defense Responses, and Glandular Trichome Development. *The Plant Cell* **16**: 126–143.

Logemann E, Birkenbihl RP, Ulker B, Somssich IE. **2006**. An improved method for preparing Agrobacterium cells that simplifies the Arabidopsis transformation protocol. *Plant methods* **2**: 16.

Lohmann JU, Hong RL, Hobe M, Busch MA, Parcy F, Simon R, Weigel D. **2001**. A molecular link between stem cell regulation and floral patterning in Arabidopsis. *Cell* **105**: 793–803.

Long JA, Moan EI, Medford JI, Barton MK. **1996**. A member of the KNOTTED class of homeodomain proteins encoded by the STM gene of Arabidopsis. *Nature* **379**: 66–69.

Long JA, Ohno C, Smith ZR, Meyerowitz EM. **2006**. TOPLESS regulates apical embryonic fate in Arabidopsis. *Science (New York, N.Y.)* **312**: 1520–1523.

Luschnig C, Vert G. **2014**. The dynamics of plant plasma membrane proteins: PINs and beyond. *Development (Cambridge, England)* **141**: 2924–2938.

Lynn K, Fernandez A, Aida M, Sedbrook J, Tasaka M, Masson P, Barton MK. **1999**. The PINHEAD/ZWILLE gene acts pleiotropically in Arabidopsis development and has overlapping functions with the ARGONAUTE1 gene. *Development (Cambridge, England)* **126**: 469–481.

Machado A, Wu Y, Yang Y, Llewellyn DJ, Dennis ES. **2009**. The MYB transcription factor GhMYB25 regulates early fibre and trichome development. *The Plant Journal: For Cell and Molecular Biology* **59**: 52–62.

Maes L, Goossens A. **2010**. Hormone-mediated promotion of trichome initiation in plants is conserved but utilizes species- and trichome-specific regulatory mechanisms. *Plant Signaling & Behavior* **5**: 205–207.

Magnani E, Hake S. **2008**. KNOX lost the OX: the Arabidopsis KNATM gene defines a novel class of KNOX transcriptional regulators missing the homeodomain. *The Plant Cell* **20**: 875–887.

Mallory AC, Reinhart BJ, Jones-Rhoades MW, Tang G, Zamore PD, Barton MK, Bartel DP. **2004**. MicroRNA control of PHABULOSA in leaf development: importance of pairing to the microRNA 5' region. *The EMBO journal* **23**: 3356–3364.

Marcos D, Berleth T. **2014**. Dynamic auxin transport patterns preceding vein formation revealed by live-imaging of Arabidopsis leaf primordia. *Plant Systems and Synthetic Biology* **5**: 235.

Marks MD, Esch JJ. **2003**. Initiating inhibition. *EMBO reports* **4**: 24–25.

Mashiguchi K, Tanaka K, Sakai T, Sugawara S, Kawaide H, Natsume M, Hanada A, Yaeno T, Shirasu K, Yao H, McSteen P, Zhao Y, Hayashi K, Kamiya Y, Kasahara H. **2011**. The main auxin biosynthesis pathway in Arabidopsis. *Proceedings of the National Academy of Sciences of the United States of America* **108**: 18512–18517.

Masucci JD, Rerie WG, Foreman DR, Zhang M, Galway ME, Marks MD, Schiefelbein JW. **1996**. The homeobox gene GLABRA2 is required for position-dependent cell differentiation in the root epidermis of Arabidopsis thaliana. *Development (Cambridge, England)* **122**: 1253–1260.

Mathews S, Kramer EM. **2012**. The evolution of reproductive structures in seed plants: a re-examination based on insights from developmental genetics. *The New Phytologist* **194**: 910–923.

Matsumoto N, Okada K. **2001**. A homeobox gene, PRESSED FLOWER, regulates lateral axis-dependent development of Arabidopsis flowers. *Genes & development* **15**: 3355–3364.

Mayer KF, Schoof H, Haecker A, Lenhard M, Jürgens G, Laux T. **1998**. Role of WUSCHEL in regulating stem cell fate in the Arabidopsis shoot meristem. *Cell* **95**: 805–815.

McConnell JR, Emery J, Eshed Y, Bao N, Bowman J, Barton MK. **2001**. Role of PHABULOSA and PHAVOLUTA in determining radial patterning in shoots. *Nature* **411**: 709–713.

McHale NA, Marcotrigiano M. **1998**. LAM1 is required for dorsoventrality and lateral growth of the leaf blade in Nicotiana. *Development (Cambridge, England)* **125**: 4235–4243.

McLean M, Baird WV, Gerats AG, Meagher RB. **1988**. Determination of copy number and linkage relationships among five actin gene subfamilies in Petunia hybrida. *Plant Molecular Biology* **11**: 663–672.

Van der Meer IM. **2006**. Agrobacterium-mediated transformation of Petunia leaf discs. *Methods in Molecular Biology (Clifton, N.J.)* **318**: 265–272.

Magallon S, Gomez-Acevedo S, Sanchez-Reyes LL, Hernandez-Hernandez T. 2015. A metacalibrated time-tree documents the early rise of flowering plant phylogenetic diversity. *New Phytologist* **207**(2):437-53.

Mercer TR, Gerhardt DJ, Dinger ME, Crawford J, Trapnell C, Jeddeloh JA, Mattick JS, Rinn JL. **2012**. Targeted RNA sequencing reveals the deep complexity of the human transcriptome. *Nature Biotechnology* **30**: 99–104.

Merelo P, Xie Y, Brand L, Ott F, Weigel D, Bowman JL, Heisler MG, Wenkel S. **2013**. Genome-wide identification of KANADI1 target genes. *PloS one* **8**: e77341.

Minelli A. **2009**. *Forms of Becoming: The Evolutionary Biology of Development*. Princeton University Press.

Mizukami Y, Ma H. **1995**. Separation of AG function in floral meristem determinacy from that in reproductive organ identity by expressing antisense AG RNA. *Plant molecular biology* **28**: 767–784.

Morohashi K, Zhao M, Yang M, Read B, Lloyd A, Lamb R, Grotewold E. **2007**. Participation of the Arabidopsis bHLH factor GL3 in trichome initiation regulatory events. *Plant Physiology* **145**: 736–746.

Mortazavi A, Williams BA, McCue K, Schaeffer L, Wold B. **2008**. Mapping and quantifying mammalian transcriptomes by RNA-Seq. *Nature Methods* **5**: 621–628.

Mukherjee K, Brocchieri L, Bürglin TR. **2009**. A comprehensive classification and evolutionary analysis of plant homeobox genes. *Molecular biology and evolution* **26**: 2775–2794.

Müller R, Borghi L, Kwiatkowska D, Laufs P, Simon R. **2006**. Dynamic and compensatory responses of Arabidopsis shoot and floral meristems to CLV3 signaling. *The Plant cell* **18**: 1188–1198.

Mutz K-O, Heilkenbrinker A, Lönne M, Walter J-G, Stahl F. **2013**. Transcriptome analysis using next-generation sequencing. *Current Opinion in Biotechnology* **24**: 22–30.

Nakata M, Matsumoto N, Tsugeki R, Rikirsch E, Laux T, Okada K. **2012**. Roles of the middle domain-specific WUSCHEL-RELATED HOMEOBOX genes in early development of leaves in Arabidopsis. *The Plant cell* **24**: 519–535.

Nakata M, Okada K. **2012**. The three-domain model: a new model for the early development of leaves in Arabidopsis thaliana. *Plant signaling & behavior* **7**: 1423–1427.

Nardmann J, Ji J, Werr W, Scanlon MJ. **2004**. The maize duplicate genes narrow sheath1 and narrow sheath2 encode a conserved homeobox gene function in a lateral domain of shoot apical meristems. *Development (Cambridge, England)* **131**: 2827–2839.

Nardmann J, Werr W. **2006**. The shoot stem cell niche in angiosperms: expression patterns of WUS orthologues in rice and maize imply major modifications in the course of mono- and dicot evolution. *Molecular biology and evolution* **23**: 2492–2504.

Nardmann J, Werr W. **2012**. The invention of WUS-like stem cell-promoting functions in plants predates leptosporangiate ferns. *Plant molecular biology* **78**: 123–134.

Nardmann J, Werr W. **2013**. Symplesiomorphies in the WUSCHEL clade suggest that the last common ancestor of seed plants contained at least four independent stem cell niches. *New Phytologist* **199(4)**: 1081–1092.

Nardmann J, Zimmermann R, Durantini D, Kranz E, Werr W. **2007**. WOX gene phylogeny in Poaceae: a comparative approach addressing leaf and embryo development. *Molecular biology and evolution* **24**: 2474–2484.

Nimchuk ZL, Tarr PT, Meyerowitz EM. **2011**. An evolutionarily conserved pseudokinase mediates stem cell production in plants. *The Plant cell* **23**: 851–854.

Nishikawa A, Yamamoto T, Tuji S, Sakano H, Hirohara H. **1992**. Process for breeding a glabrous variety of rice crop and a glabrous plant.

Niu L, Lin H, Zhang F, Watira TW, Li G, Tang Y, Wen J, Ratet P, Mysore KS, Tadege M. **2015a**. LOOSE FLOWER, a WUSCHEL-like Homeobox gene, is required for lateral fusion of floral organs in Medicago truncatula. *The Plant Journal: For Cell and Molecular Biology* **81**: 480–492.

Noda K, Glover BJ, Linstead P, Martin C. **1994**. Flower colour intensity depends on specialized cell shape controlled by a Myb-related transcription factor. *Nature* **369**: 661–664.

Nolte C, Staiger D. **2015**. RNA around the clock - regulation at the RNA level in biological timing. *Frontiers in Plant Science* **6**: 311.

Ogawa E, Yamada Y, Sezaki N, Kosaka S, Kondo H, Kamata N, Abe M, Komeda Y, Takahashi T. **2015**. ATML1 and PDF2 Play a Redundant and Essential Role in Arabidopsis Embryo Development. *Plant & Cell Physiology*.

Ohmori Y, Tanaka W, Kojima M, Sakakibara H, Hirano H-Y. **2013**. WUSCHEL-RELATED HOMEOBOX4 is involved in meristem maintenance and is negatively regulated by the CLE gene FCP1 in rice. *The Plant cell* **25**: 229–241.

Okazaki, Furuno, et al., FANTOM Consortium, **RIKEN Genome Exploration Research Group Phase I & II Team**. **2002**. Analysis of the mouse transcriptome based on functional annotation of 60,770 full-length cDNAs. *Nature* **420**: 563–573.

Otsuga D, DeGuzman B, Prigge MJ, Drews GN, Clark SE. **2001**. REVOLUTA regulates meristem initiation at lateral positions. *The Plant Journal: For Cell and Molecular Biology* **25**: 223–236.

Pattanaik S, Patra B, Singh SK, Yuan L. **2014**. An overview of the gene regulatory network controlling trichome development in the model plant, Arabidopsis. *Frontiers in Plant Science* **5**: 259.

Payne T, Clement J, Arnold D, Lloyd A. **1999**. Heterologous myb genes distinct from GL1 enhance trichome production when overexpressed in Nicotiana tabacum. *Development (Cambridge, England)* **126**: 671–682.

Payne CT, Zhang F, Lloyd AM. **2000**. GL3 encodes a bHLH protein that regulates trichome development in arabidopsis through interaction with GL1 and TTG1. *Genetics* **156**: 1349–1362.

Van de Peer Y, De Wachter R. **1994**. TREECON for Windows: a software package for the construction and drawing of evolutionary trees for the Microsoft Windows environment. *Computer applications in the biosciences: CABIOS* **10**: 569–570.

Pesch M, Hülskamp M. **2011**. Role of TRIPTYCHON in trichome patterning in Arabidopsis. *BMC plant biology* **11**: 130.

Picard D. **1993**. Steroid-binding domains for regulating the functions of heterologous proteins in cis. *Trends in Cell Biology* **3**: 278–280.

Ponting CP, Belgard TG. **2010**. Transcribed dark matter: meaning or myth? *Human Molecular Genetics* **19**: R162–168.

Prunet N, Morel P, Negrutiu I, Trehin C. **2009**. Time to stop: flower meristem termination. *Plant physiology* **150**: 1764–1772.

Qin Y-M, Hu C-Y, Pang Y, Kastaniotis AJ, Hiltunen JK, Zhu Y-X. **2007**. Saturated very-long-chain fatty acids promote cotton fiber and Arabidopsis cell elongation by activating ethylene biosynthesis. *The Plant Cell* **19**: 3692–3704.

Qi J, Wang Y, Yu T, Cunha A, Wu B, Vernoux T, Meyerowitz E, Jiao Y. **2014**. Auxin depletion from leaf primordia contributes to organ patterning. *Proceedings of the National Academy of Sciences* **111**: 18769–18774.

Ramsay NA, Glover BJ. **2005**. MYB-bHLH-WD40 protein complex and the evolution of cellular diversity. *Trends in Plant Science* **10**: 63–70.

Rebocho AB, Bliek M, Kusters E, Castel R, Procissi A, Roobeek I, Souer E, Koes R. **2008**. Role of EVERGREEN in the development of the cymose petunia inflorescence. *Developmental cell* **15**: 437–447.

Reddy ASN, Marquez Y, Kalyna M, Barta A. **2013**. Complexity of the Alternative Splicing Landscape in Plants. *The Plant Cell* **25**: 3657–3683.

Reinhardt D, Pesce E-R, Stieger P, Mandel T, Baltensperger K, Bennett M, Traas J, Friml J, Kuhlemeier C. **2003**. Regulation of phyllotaxis by polar auxin transport. *Nature* **426**: 255–260.

Reinhart BJ, Liu T, Newell NR, Magnani E, Huang T, Kerstetter R, Michaels S, Barton MK. **2013**. Establishing a framework for the Ad/abaxial regulatory network of Arabidopsis: ascertaining targets of class III homeodomain leucine zipper and KANADI regulation. *The Plant cell* **25**: 3228–3249.

Rerie WG, Feldmann KA, Marks MD. **1994**. The GLABRA2 gene encodes a homeo domain protein required for normal trichome development in Arabidopsis. *Genes & Development* **8**: 1388–1399.

Ribone PA, Capella M, Chan RL. **2015**. Functional characterization of the homeodomain leucine zipper I transcription factor AtHB13 reveals a crucial role in Arabidopsis development. *Journal of Experimental Botany*.

Robert JS. **2001**. Interpreting the homeobox: metaphors of gene action and activation in development and evolution. *Evolution & Development* **3**: 287–295.

Roberts A, Pimentel H, Trapnell C, Pachter L. **2011**. Identification of novel transcripts in annotated genomes using RNA-Seq. *Bioinformatics (Oxford, England)* **27**: 2325–2329.

Robinson DO, Roeder AH. **2015**. Themes and variations in cell type patterning in the plant epidermis. *Current Opinion in Genetics & Development* **32**: 55–65.

Sakakibara K, Reisewitz P, Aoyama T, Friedrich T, Ando S, Sato Y, Tamada Y, Nishiyama T, Hiwatashi Y, Kurata T, Ishikawa M, Deguchi H, Rensing SA, Werr W, Murata T, Hasebe M, Laux T. **2014**. WOX13-like genes are required for reprogramming of leaf and protoplast cells into stem cells in the moss Physcomitrella patens. *Development (Cambridge, England)* **141**: 1660–1670.

Sarkar AK, Luijten M, Miyashima S, Lenhard M, Hashimoto T, Nakajima K, Scheres B, Heidstra R, Laux T. **2007**. Conserved factors regulate signalling in Arabidopsis thaliana shoot and root stem cell organizers. *Nature* **446**: 811–814.

Sarkar AK, Luijten M, Miyashima S, Lenhard M, Hashimoto T, Nakajima K, Scheres B, Heidstra R, Laux T. **2007**. Conserved factors regulate signalling in Arabidopsis thaliana shoot and root stem cell organizers. *Nature* **446**: 811–814.

Scanlon MJ. **2000**. NARROW SHEATH1 functions from two meristematic foci during founder-cell recruitment in maize leaf development. *Development (Cambridge, England)* **127**: 4573–4585.

Scanlon MJ, Chen KD, McKnight CC IV. **2000**. The narrow sheath duplicate genes: sectors of dual aneuploidy reveal ancestrally conserved gene functions during maize leaf development. *Genetics* **155**: 1379–1389.

Scanlon MJ, Schneeberger RG, Freeling M. **1996**. The maize mutant narrow sheath fails to establish leaf margin identity in a meristematic domain. *Development (Cambridge, England)* **122**: 1683–1691.

Schellmann S, Schnittger A, Kirik V, Wada T, Okada K, Beermann A, Thumfahrt J, Jürgens G, Hülskamp M. **2002**. TRIPTYCHON and CAPRICE mediate lateral inhibition during trichome and root hair patterning in Arabidopsis. *The EMBO journal* **21**: 5036–5046.

Schena M, Lloyd AM, Davis RW. **1991**. A steroid-inducible gene expression system for plant cells. *Proceedings of the National Academy of Sciences* **88**: 10421–10425.

Schnittger A, Hülskamp M. **2002**. Trichome morphogenesis: a cell-cycle perspective. *Philosophical Transactions of the Royal Society of London. Series B, Biological Sciences* **357**: 823–826.

Schnittger A, Jürgens G, Hülskamp M. **1998**. Tissue layer and organ specificity of trichome formation are regulated by GLABRA1 and TRIPTYCHON in Arabidopsis. *Development (Cambridge, England)* **125**: 2283–2289.

Schoof H, Lenhard M, Haecker A, Mayer KF, Jürgens G, Laux T. **2000**. The stem cell population of Arabidopsis shoot meristems in maintained by a regulatory loop between the CLAVATA and WUSCHEL genes. *Cell* **100**: 635–644.

Scutt CP, Vinauger-Douard M, Fourquin C, Finet C, Dumas C. **2006**. An evolutionary perspective on the regulation of carpel development. *Journal of Experimental Botany* **57**: 2143–2152.

Semiarti E, Ueno Y, Tsukaya H, Iwakawa H, Machida C, Machida Y. **2001**. The ASYMMETRIC LEAVES2 gene of Arabidopsis thaliana regulates formation of a symmetric lamina, establishment of venation and repression of meristem-related homeobox genes in leaves. *Development (Cambridge, England)* **128**: 1771–1783.

Shilling PR. **1959**. An Investigation of the Hereditary Character, Woolly, in the Tomato.

Shimizu R, Ji J, Kelsey E, Ohtsu K, Schnable PS, Scanlon MJ. **2009**. Tissue specificity and evolution of meristematic WOX3 function. *Plant physiology* **149**: 841–850.

Sinha N. **1999**. LEAF DEVELOPMENT IN ANGIOSPERMS. *Annual Review of Plant Physiology and Plant Molecular Biology* **50**: 419–446.

Skylar A, Hong F, Chory J, Weigel D, Wu X. **2010**. STIMPY mediates cytokinin signaling during shoot meristem establishment in Arabidopsis seedlings. *Development (Cambridge, England)* **137**: 541–549.

Smaczniak C, Immink RGH, Muiño JM, Blanvillain R, Busscher M, Busscher-Lange J, Dinh QDP, Liu S, Westphal AH, Boeren S, Parcy F, Xu L, Carles CC, Angenent GC, Kaufmann K. **2012**. Characterization of MADS-domain transcription factor complexes in Arabidopsis flower development. *Proceedings of the National Academy of Sciences of the United States of America* **109**: 1560–1565.

Song S-K, Lee MM, Clark SE. **2006**. POL and PLL1 phosphatases are CLAVATA1 signaling intermediates required for Arabidopsis shoot and floral stem cells. *Development (Cambridge, England)* **133**: 4691–4698.

Souer E, van der Krol A, Kloos D, Spelt C, Bliek M, Mol J, Koes R. **1998**. Genetic control of branching pattern and floral identity during Petunia inflorescence development. *Development (Cambridge, England)* **125**: 733–742.

Souer E, Rebocho AB, Bliek M, Kusters E, de Bruin RAM, Koes R. **2008**. Patterning of inflorescences and flowers by the F-Box protein DOUBLE TOP and the LEAFY homolog ABERRANT LEAF AND FLOWER of petunia. *The Plant cell* **20**: 2033–2048.

Stehmann JR, Lorenz-Lemke AP, Freitas LB, Semir J. **2009**. The Genus Petunia. In: Gerats T, Strommer J, eds. *Petunia*. Springer New York, 1–28.

Strickler SR, Bombarely A, Mueller LA. **2012**. Designing a transcriptome next-generation sequencing project for a nonmodel plant species1. *American Journal of Botany* **99**: 257–266.

Stuurman J, Hoballah ME, Broger L, Moore J, Basten C, Kuhlemeier C. **2004**. Dissection of Floral Pollination Syndromes in Petunia. *Genetics* **168**: 1585–1599.

Stuurman J, Jäggi F, Kuhlemeier C. **2002**. Shoot meristem maintenance is controlled by a GRAS-gene mediated signal from differentiating cells. *Genes & development* **16**: 2213–2218.

Sun X, Feng Z, Meng L, Zhu J, Geitmann A. **2013**. Arabidopsis ASL11/LBD15 is involved in shoot apical meristem development and regulates WUS expression. *Planta* **237**: 1367–1378.

Sun G, Ji Q, Dilcher DL, Zheng S, Nixon KC, Wang X. **2002**. Archaefructaceae, a new basal angiosperm family. *Science (New York, N.Y.)* **296**: 899–904.

Sun B, Xu Y, Ng K-H, Ito T. **2009**. A timing mechanism for stem cell maintenance and differentiation in the Arabidopsis floral meristem. *Genes & development* **23**: 1791–1804.

Tadege M, Lin H, Bedair M, Berbel A, Wen J, Rojas CM, Niu L, Tang Y, Sumner L, Ratet P, McHale NA, Madueño F, Mysore KS. **2011**. STENOFOLIA regulates blade outgrowth and leaf vascular patterning in Medicago truncatula and Nicotiana sylvestris. *The Plant cell* **23**: 2125–2142.

Tadege M, Lin H, Niu L, Mysore KS. **2011**. Control of dicot leaf blade expansion by a WOX gene, STF. *Plant signaling & behavior* **6**: 1861–1864.

Takahashi H, Iwakawa H, Ishibashi N, Kojima S, Matsumura Y, Prananingrum P, Iwasaki M, Takahashi A, Ikezaki M, Luo L, Kobayashi T, Machida Y, Machida C.

2013. Meta-analyses of microarrays of Arabidopsis asymmetric leaves1 (as1), as2 and their modifying mutants reveal a critical role for the ETT pathway in stabilization of adaxial-abaxial patterning and cell division during leaf development. *Plant & cell physiology* **54**: 418–431.

The Angiosperm Phylogeny Group. **2009**. An update of the Angiosperm Phylogeny Group classification for the orders and families of flowering plants: APG III. *Botanical Journal of the Linnean Society* **161**: 105–121.

Tian D, Tooker J, Peiffer M, Chung SH, Felton GW. **2012**. Role of trichomes in defense against herbivores: comparison of herbivore response to woolly and hairless trichome mutants in tomato (Solanum lycopersicum). *Planta* **236**: 1053–1066.

To JPC, Haberer G, Ferreira FJ, Deruère J, Mason MG, Schaller GE, Alonso JM, Ecker JR, Kieber JJ. **2004**. Type-A Arabidopsis response regulators are partially redundant negative regulators of cytokinin signaling. *The Plant cell* **16**: 658–671.

Tomescu AMF. **2009**. Megaphylls, microphylls and the evolution of leaf development. *Trends in Plant Science* **14**: 5–12.

Tominaga-Wada R, Nukumizu Y, Sato S, Wada T. **2013**. Control of plant trichome and root-hair development by a tomato (Solanum lycopersicum) R3 MYB transcription factor. *PloS One* **8**: e54019.

Traas J, Monéger F. **2010**. Systems biology of organ initiation at the shoot apex. *Plant Physiology* **152**: 420–427.

Trapnell C, Hendrickson DG, Sauvageau M, Goff L, Rinn JL, Pachter L. **2013**. Differential analysis of gene regulation at transcript resolution with RNA-seq. *Nature Biotechnology* **31**: 46–53.

Trapnell C, Roberts A, Goff L, Pertea G, Kim D, Kelley DR, Pimentel H, Salzberg SL, Rinn JL, Pachter L. **2012**. Differential gene and transcript expression analysis of RNA-seq experiments with TopHat and Cufflinks. *Nature Protocols* **7**: 562–578.

Tsukaya H. **2013**. Leaf Development. *The Arabidopsis Book*: e0163.

Vandenbussche M, Horstman A, Zethof J, Koes R, Rijpkema AS, Gerats T. **2009**. Differential recruitment of WOX transcription factors for lateral development and organ fusion in Petunia and Arabidopsis. *The Plant cell* **21**: 2269–2283.

Vandenbussche M, Janssen A, Zethof J, van Orsouw N, Peters J, van Eijk MJT, Rijpkema AS, Schneiders H, Santhanam P, de Been M, van Tunen A, Gerats T. **2008a**. Generation of a 3D indexed Petunia insertion database for reverse genetics. *The Plant Journal: For Cell and Molecular Biology* **54**: 1105–1114.

Vandenbussche M, Zethof J, Gerats T. **2013a**. Massive indexed parallel identification of transposon flanking sequences. *Methods in Molecular Biology (Clifton, N.J.)* **1057**: 251–264.

Vandenbussche M, Zethof J, Gerats T. **2013b**. Transposon display: a versatile method for transposon tagging. *Methods in Molecular Biology (Clifton, N.J.)* **1057**: 239–250.

Vernoud V, Laigle G, Rozier F, Meeley RB, Perez P, Rogowsky PM. **2009**. The HD-ZIP IV transcription factor OCL4 is necessary for trichome patterning and anther development in maize. *The Plant Journal: For Cell and Molecular Biology* **59**: 883–894.

Vogelstein B, Gillespie D. **1979**. Preparative and analytical purification of DNA from agarose. *Proceedings of the National Academy of Sciences of the United States of America* **76**: 615–619.

Wagner GJ, Wang E, Shepherd RW. **2004**. New approaches for studying and exploiting an old protuberance, the plant trichome. *Annals of Botany* **93**: 3–11.

Waites R, Hudson A. **1995**. phantastica: a gene required for dorsoventrality of leaves in Antirrhinum majus. *Development* **121**: 2143–2154.

Walker AR, Davison PA, Bolognesi-Winfield AC, James CM, Srinivasan N, Blundell TL, Esch JJ, Marks MD, Gray JC. **1999**. The TRANSPARENT TESTA GLABRA1 locus, which regulates trichome differentiation and anthocyanin biosynthesis in Arabidopsis, encodes a WD40 repeat protein. *The Plant Cell* **11**: 1337–1350.

Wang Z, Gerstein M, Snyder M. **2009**. RNA-Seq: a revolutionary tool for transcriptomics. *Nature Reviews. Genetics* **10**: 57–63.

Wang Y, Ghaffari N, Johnson CD, Braga-Neto UM, Wang H, Chen R, Zhou H. **2011**. Evaluation of the coverage and depth of transcriptome by RNA-Seq in chickens. *BMC bioinformatics* **12 Suppl 10**: S5.

Wang C, Gong B, Bushel PR, Thierry-Mieg J, Thierry-Mieg D, Xu J, Fang H, Hong H, Shen J, Su Z, Meehan J, Li X, Yang L, Li H, Łabaj PP, Kreil DP, Megherbi D, Gaj S, Caiment F, van Delft J, Kleinjans J, Scherer A, Devanarayan V, Wang J, Yang Y, Qian H-R, Lancashire LJ, Bessarabova M, Nikolsky Y, Furlanello C, Chierici M, Albanese D, Jurman G, Riccadonna S, Filosi M, Visintainer R, Zhang KK, Li J, Hsieh J-H, Svoboda DL, Fuscoe JC, Deng Y, Shi L, Paules RS, Auerbach SS, Tong W. **2014**. The concordance between RNA-seq and microarray data depends on chemical treatment and transcript abundance. *Nature Biotechnology* **32**: 926–932.

Wang W, Li G, Zhao J, Chu H, Lin W, Zhang D, Wang Z, Liang W. **2014**. Dwarf Tiller1, a Wuschel-related homeobox transcription factor, is required for tiller growth in rice. *PLoS genetics* **10**: e1004154.

Wang J-W, Schwab R, Czech B, Mica E, Weigel D. **2008**. Dual effects of miR156-targeted SPL genes and CYP78A5/KLUH on plastochron length and organ size in Arabidopsis thaliana. *The Plant Cell* **20**: 1231–1243.

Wang H, Wang H. **2015**. The miR156/SPL Module, a Regulatory Hub and Versatile Toolbox, Gears up Crops for Enhanced Agronomic Traits. *Molecular Plant* **8**: 677–688.

Wang W, Xu B, Wang H, Li J, Huang H, Xu L. **2011**. YUCCA genes are expressed in response to leaf adaxial-abaxial juxtaposition and are required for leaf margin development. *Plant Physiology* **157**: 1805–1819.

Werker E. **2000**. Trichome diversity and development. In: Research B-A in B, ed. Academic Press, 1–35.

Wijsman HJW. **1982**. On the Interrelationships of Certain Species of Petunia. *Acta Botanica Neerlandica* **31**: 477–490.

Wolberger C. **1996**. Homeodomain interactions. *Current opinion in structural biology* **6**: 62–68.

Wu X, Chory J, Weigel D. **2007**. Combinations of WOX activities regulate tissue proliferation during Arabidopsis embryonic development. *Developmental biology* **309**: 306–316.

Wu X, Dabi T, Weigel D. **2005**. Requirement of homeobox gene STIMPY/WOX9 for Arabidopsis meristem growth and maintenance. *Current biology: CB* **15**: 436–440.

Wu G, Poethig RS. **2006**. Temporal regulation of shoot development in Arabidopsis thaliana by miR156 and its target SPL3. *Development (Cambridge, England)* **133**: 3539–3547.

Xi Z, Rest JS, Davis CC. **2013**. Phylogenomics and coalescent analyses resolve extant seed plant relationships. *PloS One* **8**: e80870.

Yadav RK, Perales M, Gruel J, Girke T, Jönsson H, Reddy GV. **2011**. WUSCHEL protein movement mediates stem cell homeostasis in the Arabidopsis shoot apex. *Genes & development* **25**: 2025–2030.

Yang C, Li H, Zhang J, Luo Z, Gong P, Zhang C, Li J, Wang T, Zhang Y, Lu Y, Ye Z. **2011**. A regulatory gene induces trichome formation and embryo lethality in tomato. *Proceedings of the National Academy of Sciences of the United States of America* **108**: 11836–11841.

Yang C, Li H, Zhang J, Wang T, Ye Z. **2011**. Fine-mapping of the woolly gene controlling multicellular trichome formation and embryonic development in tomato. *TAG. Theoretical and applied genetics. Theoretische und angewandte Genetik* **123**: 625–633.

Yang C, Ye Z. **2013**. Trichomes as models for studying plant cell differentiation. *Cellular and molecular life sciences: CMLS* **70**: 1937–1948.

Yanofsky MF, Ma H, Bowman JL, Drews GN, Feldmann KA, Meyerowitz EM. **1990**. The protein encoded by the Arabidopsis homeotic gene agamous resembles transcription factors. *Nature* **346**: 35–39.

Yoo S-C, Cho S-H, Paek N-C. **2013**. Rice WUSCHEL-related homeobox 3A (OsWOX3A) modulates auxin-transport gene expression in lateral root and root hair development. *Plant Signaling & Behavior* **8**: doi: 10.4161/psb.25929.

Yu LP, Simon EJ, Trotochaud AE, Clark SE. **2000**. POLTERGEIST functions to regulate meristem development downstream of the CLAVATA loci. *Development (Cambridge, England)* **127**: 1661–1670.

Zeng L, Zhang Q, Sun R, Kong H, Zhang N, Ma H. **2014**. Resolution of deep angiosperm phylogeny using conserved nuclear genes and estimates of early divergence times. *Nature Communications* **5**: 4956.

Zgurski JM, Sharma R, Bolokoski DA, Schultz EA. **2005**. Asymmetric auxin response precedes asymmetric growth and differentiation of asymmetric leaf1 and asymmetric leaf2 Arabidopsis leaves. *The Plant Cell* **17**: 77–91.

Zhang F, Tadege M. **2015**. Repression of AS2 by WOX family transcription factors is required for leaf development in Medicago and Arabidopsis. *Plant Signaling & Behavior*: 0.

Zhang F, Wang Y, Li G, Tang Y, Kramer EM, Tadege M. **2014**. STENOFOLIA Recruits TOPLESS to Repress ASYMMETRIC LEAVES2 at the Leaf Margin and Promote Leaf Blade Outgrowth in Medicago truncatula. *The Plant Cell* **26**: 650–664.

Zhang Z, Zhang X. **2012**. Argonautes compete for miR165/166 to regulate shoot apical meristem development. *Current Opinion in Plant Biology* **15**: 652–658.

Zhao M, Morohashi K, Hatlestad G, Grotewold E, Lloyd A. **2008**. The TTG1-bHLH-MYB complex controls trichome cell fate and patterning through direct targeting of regulatory loci. *Development (Cambridge, England)* **135**: 1991–1999.

Zhuang L-L, Ambrose M, Rameau C, Weng L, Yang J, Hu X-H, Luo D, Li X. **2012**. LATHYROIDES, encoding a WUSCHEL-related Homeobox1 transcription factor, controls organ lateral growth, and regulates tendril and dorsal petal identities in garden pea (Pisum sativum L.). *Molecular plant* **5**: 1333–1345.

Zhu T, Moschou PN, Alvarez JM, Sohlberg JJ, von Arnold S. **2014**. Wuschel-related homeobox 8/9 is important for proper embryo patterning in the gymnosperm Norway spruce. *Journal of Experimental Botany* **65**: 6543–6552.

ÉCOLE
NORMALE
SUPÉRIEURE
DE LYON

ENS DE LYON

Sant'Anna
School of Advanced Studies – Pisa